THE DIVERSITY AND INTERACTIONS OF FUNGI FROM THE PALEOZOIC AND MESOZOIC OF ANTARCTICA

By

Carla Jane Harper

Submitted to the graduate degree program in Ecology and Evolutionary Biology and the Graduate Faculty of the University of Kansas in partial fulfillment of the requirements for the degree of Doctor of Philosophy.

_____

Chairperson Thomas N. Taylor

_____

Daniel J. Crawford

_____

Stephen T. Hasiotis

_____

Robert W. Lichtwardt

_____

Alison Olcott Marshall

_____

Edith L. Taylor

Date Defended: May 1, 2015

The Dissertation Committee for Carla Jane Harper

certifies that this is the approved version of the following dissertation:

THE DIVERSITY AND INTERACTIONS OF FUNGI FROM THE PALEOZOIC AND MESOZOIC OF ANTARCTICA

_____

Chairperson Thomas N. Taylor

Date approved: May 1, 2015

ABSTRACT

Fungi are ubiquitous in all ecosystems and are the driving force in many types of interactions, such as mutualists, saprotrophs, parasites, and necrotrophs. Fungi are equally as integral in extant ecosystems as they certainly were in paleoecosystems. Paleomycology, the study of fossil fungi, is an emerging field of paleontology. Most fossil fungi are found in or in close association with plants and thus, paleomycology is also considered a sub-discipline of paleobotany. Therefore when plants are well preserved there is the increase potential to examine their fungal associates. Permineralized material is a preservation type that offers the opportunity to study plants, fungi, and other microorganisms anatomically and morphologically. Prior research suggested that fungi were too fragile and delicate to be structurally preserved in the fossil record; however, fungi have been described in some early paleobotanical studies as dispersed fragments, spores, and other remnants. The taxonomic and ecological affinities of many of these fungi, however, were not described in great detail. The objective of this study is to investigate the fungal components and plant-fungal associations of the Permian, Triassic, and Jurassic of Antarctica. The Paleobotanical Collections at the University of Kansas (KU) house the largest collection of Antarctic permineralized peat deposits in the world. To date, the majority of reports on Antarctic fossil fungi are found in Triassic peat material, with fewer reports on Permian fungi, and are most sparse on Jurassic fungi. These contributions utilized the acetate peel technique, a traditional method of studying permineralized material in paleobotany, and provided a platform for the investigation of microorganisms in ancient Antarctic environments. It has been demonstrated that paleontological thin sections of permineralized peat yields more information on fossil microbes because the fine details of the microorganisms are not etched away as they would be in the acetate peel technique. This study will fully exploit the use of paleontological thin section techniques, as well as preliminary studies using analytical

techniques, to discover and describe new fossil fungi and plant-fungal interactions from the Antarctic paleobotanical collections at KU. Despite the large number of fungal remains in the fossil record, including those that provide direct or indirect evidence of an association or interaction with land plants, the discipline of paleomycology is at a relatively early stage of development. As more information is obtained about fossil fungi, including those from Antarctic permineralized peat deports, it will be increasingly possible to present more detailed hypotheses that can be used in association with those described from modern communities, to more accurately depict the role of these organisms in the functioning of early continental ecosystems. Therefore, this study adds new information to our understanding of the diversity of fungi in the Permian, Triassic, and Jurassic of Antarctica, and thus contributes to a more focused concept of the complexity of late Paleozoic and Mesozoic ecosystems.

ACKNOWLEDGEMENTS

Although a dissertation has one author, it is an embodiment of work building upon the extensive research of others before me and would not be possible without the help of many colleagues.

I am forever indebted and thankful to my advisor, Dr. Thomas N. Taylor, and Dr. Edith L. Taylor for their continuous help, mentorship, support, and encouragement throughout this work, as well as for fostering my passion in paleobotany and paleomycology. A special thank you goes to Dr. Michael Krings who has been incredibly helpful in answering questions and providing advice with many of my projects since the start of my graduate career. To Dr. Rudolph Serbet, whose friendship, helpful discussions, and unabating help with technical assistance made many of these projects achievable since my first day in the lab. As well as an important thank you and recognition to Ms. Jeannie Houts, whose friendship, support, and vital help in everything and anything behind the scenes made the Taylor lab run and this dissertation possible.

Thank you to my committee members: Drs. Edith L. Taylor, Daniel J. Crawford, Robert W. Lichtwardt, Alison Olcott Marshall, and Stephen T. Hasiotis for their support, patience, and help with this study. Thanks also to Dr. Prem Thapa Chetri, and Ms. Heather Shinogle for assistance on analytical microscopy. Special thanks goes to Drs. Alison Olcott Marshall and Craig P. Marshall for their mentorship and fostering an interest in geochemistry and analytical techniques. I gratefully acknowledge Dr. Robert A. Blanchette for helpful discussions on wood decay fungi. To all of the staff of the Ecology and Evolutionary Biology (EEB) Department, with special recognition and appreciation to Ms. Jaime Keeler, Dorothy Johanning, and Aagje K. Ashe for all of their help with the administrative work and paperwork throughout grad school.

I have had the great fortunate of working with many esteemed paleobotanists as my fellow lab members, current and past, who served as mentors, friends, and colleagues throughout

graduate school and beyond. I am forever grateful and appreciative for their help, support, and friendship: Julie A. Bergene, Benjamin Bomfleur, Anne-Laure Decombeix, Abby L. Glauser, Timothy J. Hieger, Ashley A. Klymiuk, Patricia E. Ryberg, Andrew B. Schwendemann.

I am also thankful to the 2014 Antarctic austral summer G-496 team members: Andrew Brown, David Buchanan, Charles P. Daghlian, Anne-Laure Decombeix, Ignacio H. Escapa, Erik L. Gulbranson, Lauren A. Michel, Rudolph Serbet, and Anna Zajicek for a wonderful and productive field season. Thank you for making Antarctica a reality beyond the University of Kansas (KU) collections or descriptions in papers, and putting much of this research into context.

I would also like to gratefully acknowledge the multiple funding resources that made this research possible: NSF EAR-0949947 to T.N.T. and M.K.; NSF OPP-0943934 to E.L.T. and T.N.T.; Alexander von Humboldt Foundation V-3.FLF-DEU/1064359 to M.K.

KU Graduate Studies Doctoral Research Funds, KU Endowment Fund Ida H. Hyde Scholarship, KU EEB Summer Research Funds, Botanical Society of America Graduate Research Award, Association for Women in Geosciences-Osage Chapter Research Award, Triarch Botanical Image Award, KU Graduate Studies Travel Award, Mycological Society of America, Mike Boulter award from IOP, Botanical Society of America-Mycological Section, KU Botany Endowment Fund, Donald J. Obee Botany Dissertation Fellowship to C.J.H. Special thanks and appreciation to Dr. Christopher H. Haufler for support in securing funding and continuous encouragement throughout my duration at KU.

I want to dedicate this work to my dad, James E. Harper, “the chief,” who always led by example and taught me to embrace all challenges in life with dedication, determination, self-confidence, optimism, and strength. Thank you dad for your unconditional support and believing in me.

Love Carla

TABLE OF CONTENTS

Chapter 1

The importance of permineralized floras in the study of fossil fungi: A case study from the Paleozoic and Mesozoic of Antarctica

1. Introduction

1.1 Importance of fungi in ancient and modern ecosystems

Plant–fungal interactions occur at multiple ecosystem levels and help to shape plant communities and the environment that they comprise. Fungi are integral to modern and past ecosystems by filling many fundamental niches, e.g., mutualists, parasites, saprotrophs, necrotrophs, in rare instances, as carnivores. In fact, it is hypothesized that a mutualistic symbiosis between an alga and fungal partner may have been the necessary prerequisite to the establishment of plants on early continental terrains (Pirozynski and Malloch, 1975; Pirozynski, 1976; Raven, 1977; Selosse and Le Tacon, 1998). Many of these fundamental interactions have been documented in the fossil record; however, it is only recently that fossil fungi have been placed in a paleoecological context.

2. Fossil preservation: permineralization

In general, fossils are extremely rare and represent far less than 1% of life that occurred throughout geologic time (Jablonski, 2004). Organisms can only be preserved as fossils under a unique combination of circumstances with abiotic and biotic influences: proximity to water, temperature, chemical composition of the ambient environment, atmospheric conditions, microbial community present, etc. Plant fossils can be preserved in a variety of different ways, e.g., compression, impression, coal and charcoal, casts, molds (Schopf, 1975). Each of these

preservational modes offers a different set of information about the organism, however and usually without exception, there are only two types of preservation that offer structurally preserved cellular detail of fossils: petrification and permineralization (Taylor et al., 2009). Petrification occurs when the cell lumina and walls have been completely replaced by minerals. In contrast, permineralization is a rare form of preservation in which minerals have replaced the internal contents of cells, but the cell walls are not completely replaced by minerals and are composed of highly alternated organic matter. This difference between the cell lumina and wall can also be differentiated chemically via X-ray spectroscopy (Boyce et al., 2002). The significant benefit of this type of preservation is that it offers the opportunity to study the cellular anatomy and morphology of structurally preserved plants. Additionally, investigators can make serial sections of permineralized material in order to reconstruct and study specimens within a three-dimensional context.

3. Permineralized deposits of the world

Although permineralized floras are rare, there are multiple examples of these permineralized deposits worldwide from various points in geologic time. For example, late Devonian of southern Morocco contains large permineralized trunks of the arborescent progymnosperm, *Callixylon* (Meyer-Berthaud et al., 1997). The Carboniferous is well known for permineralized material in the form of calcium carbonate coal balls from North America and Europe (e.g., Williamson, 1882; Stopes and Watson, 1909; Andrews, 1951; Scott and Rex, 1985, Galtier, 1997). There is more information known about the plants from the Carboniferous based on the anatomical and morphological details preserved in the coal balls than any other time period. Multiple Permian permineralized plant assemblages in volcaniclastic tuffs occur in China (e.g., Hilton et al., 2001; 2004; Wang et al., 2006), as well as examples of *in situ* forests from

Germany and Brazil (Rössler, 2006). Triassic permineralized deposits are exceptionally rare and only a few exist in the world that yield plant fossils, such as the Arctic Svalbard Archipelago (Strullu-Derrien et al., 2012; Pott, 2014). There are multiple Jurassic permineralized deposits in Argentina, including the famous Cerro Cuadrado in Santa Cruz Province, southern Argentina (Patagonia), which has exquisitely preserved conifer seed cones (e.g., Stockey, 1994; Escapa et al., 2013). Recently, new deposits described from the North American Pacific northwest contain carbonate concretions with a diverse range of anatomically preserved fossils such as conifer cones, shoots, leaves (e.g., Atkinson et al., 2014a; 2014b). Cenozoic permineralized deposits include the Eocene Princeton Chert, British Colombia, Canada that contains one of the most diverse assemblages of Tertiary plants, e.g., ferns, *in situ* aquatic plants, seeds, fruits, flowers, ferns (e.g., Cevallos-Ferriz et al., 1991; Stockey and Pigg, 1991; Stockey et al., 1999; Little and Stockey, 2003; Smith and Stockey, 2003) and the middle Miocene Yakima Canyon floras from Washington, United States which also includes several examples of flowers, fruits, seeds, and ferns (Pigg and Rothwell, 2000; Pigg and DeVore, 2004).

Even fewer of the permineralized deposits have been systematically studied or surveyed for fossil microorganisms, including fungi. Only a few geologic deposits have yielded fungal fossils preserved in sufficient detail to permit assignment to any one of the major lineages of fungi with any degree of confidence. In is important to note that the famous Rhynie Chert *Konservat-Lagerstätten* (Early Devonian, Rhynie, Scotland, UK) which is well known for microorganism diversity and plant-fungal interactions will not be discussed in this report because it is considered a silicified *in situ*, petrified sinter deposit and not a permineralized site (Rice et al., 2002; Trewin et al., 2003). For discussion on Rhynie Chert fungal and microorganism diversity the reader is referred to several review articles on the subject, e.g., Remy et al., 1996; Taylor et al., 2007; Berbee and J. Taylor, 2007; Krings et al., 2012. Recently, i.e., within the last

couple of decades, there has been increased interest in surveying permineralized deposits for microorganisms. For example, historic slide collections of Carboniferous (Pennsylvanian) coal balls from North America (i.e., Illinois, Indiana, Kentucky, Ohio) and Europe (i.e., Great Britain, France) have been extensively reexamined for fossil microbes. Multiple reports on the microbial diversity that includes mycorrhizal associations, evidence of basidiomycete clamp connections, enigmatic "sporocarps" that have been recently reinterpreted as zygomycetes (see Taylor et al., 2015), chytrid communities, and fungal-like organisms such as Peronosporomycetes, add a new dimension to understanding plant-fungal interactions in coal swamp ecosystems (e.g., Stubblefield and Taylor, 1983a; Stubblefield et al., 1983b; Taylor et al., 1994; Strullu-Derrien et al., 2009; Krings et al., 2010b; Krings and Taylor, 2010; Krings et al., 2011). Additionally, the permineralized calcium carbonate concretions from the North American Pacific northwest (Vancouver Island, British Columbia, Canada) have also yielded examples of fungi and other microorganisms such as ascomycetes and lichens (Bronson et al., 2013; Matsunaga et al., 2013). The Eocene Princeton Chert (British Columbia, Canada) contains numerous examples of fungi and fungal interactions, such as ectomycorrhizal associations, ascomycetes, poroid hymenophores, dark-septate endophytes, examples of hyphomycetes, (e.g., Currah et al., 1998; Klymiuk et al., 2013a; 2013b; Lepage et al., 1997; 1994; Smith et al., 2004).

The co-occurrence of permineralized deposits that span multiple intervals of time are exceptionally rare. One of the best and well known examples of this phenomenon are the permineralized peat deposits of Antarctica, e.g., the Permian, Triassic, and Jurassic localities (e.g., Taylor et al., 1988; Taylor and Taylor, 1990; Bomfleur et al., 2014c). Plant-bearing Permian, Triassic, and Jurassic continental deposits from the Central Transantarctic Mountains are a unique source of information about the biology and ecology of these past high-latitude ecosystems (Figure 1). Although fossil floras from the Central Transantarctic Mountains have

been intensively studied during the last several decades, many questions crucial for a better understanding of Antarctic paleoecosystems still remain unsolved; this combination of deposits with exquisite anatomical preservation provides a unique experimental setting to address specific scientific inquiries about the evolutionary history of fossil fungi in high latitude polar paleoecosystems such as: (1) how microbes influenced plants that lived in an environment with extreme light regimes (i.e., 4 months of complete darkness, 4 months of 24-hour day light, and 4 months of transitionary periods of light), (2) did the microbial diversity change or remain static during floral turnover events and (3) climate change, (4) which plant lineages had symbiotic relationships with fungi, (5) do ancient plants employ the same defense strategies or host responses to parasitic forms of microorganisms, (6) what mechanisms do saprotrophic fungi use and have these biochemical pathways evolved over time or remained resilient, and many more. In this contribution, the current state of fungal diversity, plant-fungal interactions, and gaps in the fungal fossil record from the Late Permian through Early Jurassic of Antarctica (Table 1) is critically reviewed.

4. Late Paleozoic and Mesozoic climate and environments of Antarctica

4.1 The Early to Late Permian Environment and Plant Diversity

In contrast to the harsh environment of Antarctica today, favorable climatic conditions existed during warmer periods of Earth history supporting rich vegetation in South Polar latitudes. The Late Carboniferous to Early Permian floras are reflective of the latest phases of glaciation as a result of the Earth rising out of one of the great ice ages, or icehouse condition (Isbell et al., 2003). Early Permian palynomorphs and microfossils from the central Transantarctic Mountains indicate a low diversity assemblage, e.g., ferns, lycophytes, sphenopsids, rich in *Gangamopteris* or *Noeggerathiopsis*, with a scarce presence of glossopterid

plants reflective of last phase of a glaciation period (Masood et al., 1994; Miller and Isbell, 2010). Macrofossils from the Early Permian are comprised of a similar post-glacial flora, which includes lycophytes, possible fern fragments, *Gangamopteris* seed plants, *Noeggerathiopsis*, rare *Glossopteris*, and possible conifer axes (i.e., *Walkomiella transvaalensis*)(Plumstead 1962; 1975; Taylor et al. 1989; McLoughlin et al., 2005). It has been suggested by some authors that plants rapidly colonized Early Permian continental Antarctica as the ice sheets retreated in an environment with continuous permafrost, which meant that the trees had to have shallow root systems (Krull, 1999; Taylor et al., 1996). In modern ecosystems, fungi are abundant in tundra and taiga biomes, as well as permafrost soils (Treseder et al., 2004; Talbot et al., 2008; Ozerskaya et al., 2009). To date, no fungi have been described from the Early Permian of Antarctica; possibly owing in part to the fact that no permineralized deposits have yet been found and not a result of paleoclimatic conditions.

Evidence for climate amelioration from the late Early Permian through to the latest Permian can be found within the Transantarctic Mountains in the transition from glacial-influenced fluvial systems to fluvial systems lacking evidence for glacial influence (Cantrill and Poole, 2012). Although still considered an icehouse condition relative to other geologic periods, this increase in temperature from the Early to Late Permian provides one explanation for glossopterid dominance during the Late Permian. The macrofossil floral diversity of the Late Permian was fairly homogenous dominated by *Glossopteris* spp., but also included, based mostly on permineralized floras, one example each of a bryophyte and lycophyte, sphenophytes, a fern, *Noeggerathiopsis,* rarely *Gangamopteris*, walchian conifer seeds (*Samaropsis*), multiple examples of *Glossopteris* leaf spp., reproductive organs (e.g., *Arberiella, Eretmonia, Lakkosia, Plumsteadia, Rigbya*), wood (*Dadoxylon, Australoxylon*), and rooting structures (*Vertebraria*) (Cridland, 1963; Rigby, 1969; Schopf, 1976; Lacey and Lucas 1981; Smoot and Taylor, 1985;

Taylor and Taylor, 1992; Galtier and Taylor, 1994; McLoughlin and Drinnan, 1996; Weaver et al., 1997; McLoughlin, et al., 2005; Ryberg, 2009; Schwendemann et al., 2010). Also reported is an *in situ* preserved fossil forest on Mount Achernar with 15 tree stumps (Taylor et al., 1992). The palynofloras, in contrast to the macrofossils, suggest a much greater diversity in vegetation but also show the dominant role of the glossopterids (e.g., Lindström and McLoughlin, 2007).

Late Permian permineralized peat horizons occur in the central Transantarctic Mountains and Prince Charles Mountains, East Antarctica. These deposits have been suggested as rafts of peat mire that eroded into river channels and once entombed in sand, silica rich water initiated the permineralization process (Taylor et al., 1989). There are two key Permian permineralized peat deposits from the central Transantarctic Mountains: Skaar Ridge (Schopf, 1970; Taylor et al., 1986) and Collinson Ridge (McManus et al., 2002). Each of these deposits has multiple examples of anatomically preserved plants such as a bryophyte, fern, *Vertebraria* roots, *Glossopteris* leaves, wood, and numerous ovulate structures (Schopf, 1970; Smoot and Taylor, 1986; Taylor and Taylor, 1987; Pigg, 1990; Zhao et al., 1995; Taylor and Ryberg, 2007). The Prince Charles Mountains has one significant permineralized deposit from the Toploje Member of the lower Bainmedart Coal Members. The sequences were not as thermally altered as the central Transantarctic Mountains and provide a different view into Late Permian landscapes (Lindström and McLoughlin, 2007). The majority of the biomass within the Prince Charles Mountains permineralized deposits is glossopterids, but also includes small lycophyte axes and megaspores, *Noeggerathiopsis*, wood (*Australoxylon* spp.), and *Vertebraria* roots (McLoughlin and Drinnan, 1996; Weaver et al., 1997; Slater et al., 2011). The vast majority of reports focused on the plants but few have concentrated on the fungi and fungal-like organism diversity. To date, microorganisms have been described from two Permian permineralized deposits: Skaar Ridge

and from the Prince Charles Mountains. These will be discussed in detail in later sections (see *Permian* roots; stems; leaves; matrix sections).

4.2 Permian–Triassic Crisis and Vegetation Turnover: Icehouse to Greenhouse

The transition from the Permian into the Triassic is an important point in geologic time. It includes the Permian-Triassic (P-T) mass extinction, which led to 90% extinction rates in marine environments and 80-85% extinction rates in terrestrial environments (Song et al., 2013; Benton and Newell, 2014). In addition to animal and arthropod turnover, there is evidence of major floral turnover events as well, especially in the Southern Hemisphere. The P-T transition marks the change from paleophytic (e.g., *Glossopteris* dominated) to more modern and highly diversified floral components based on the drastic change in physical environment and global temperature (Iglesias et al., 2011). Southern Gondwana had a generally warmer and less seasonal climate after the end-Permian event, which marked the passage from a global icehouse condition that characterized the Early Permian to the hothouse state of the Early Triassic, and eventually to the greenhouse climate which persisted throughout the Triassic (Kidder and Worsley, 2004; Lindström and McLoughlin, 2007; Preto et al., 2010). The Middle Triassic marked the peak of global extension of climate zones, which is reflected by the floras from this time, i.e., the equator was arid and warm-temperate to temperate zones were at the high polar latitudes (Ziegler et al., 1993; Cúneo et al., 2003). The Late Triassic was a period of climate stability with warm temperate climate and abundant water supply that also promoted favorable growing conditions and species diversification of the vegetation (Cantrill and Poole, 2012). It is interesting to note, however, that fungi remain highly conserved and therefore show great resilience during times of global climate change. The interactions and types of fungi present in the Antarctic ecosystem

spanning the P-T boundary, for the most part, remain static and similar groups of fungi and interactions can be found in each time period with different major plant groups.

The Early Triassic vegetation is known predominately from palynomorphs and palynodebris remains. Taxa found within these assemblages include bryophytes (but only as a minor component), peltasperms, corystosperms, lycophytes, several fern taxa (e.g., *Lophotriletes, Osmundacidites*), and some seed plants (e.g., *Guttulapollenites*) (McLoughlin et al., 1997; Lindström and McLoughlin, 2007). The floras increase in abundance and diversity into the Middle Triassic, especially in the central Transantarctic Mountains, such as several examples of impression floras from the Lashly Formation, members A and B (Kyle and Schopf, 1982; Escapa et al., 2011). Two examples of silicified, permineralized fossil forests have been discovered in Antarctica from this time: (1) Gordon Valley with 99 tree stumps of *Jeffersonioxylon gordonense* (Cúneo et al., 2003) and (2) recently, a second *in situ* early succession forest that contains approximately 37 trees, each with attached stem to root interfaces at Roscolyn Tor (Allan Hills, southern Victoria Land) discovered during the 2014 austral summer Antarctic field season. The majority of floral diversity from the Middle Triassic of Antarctica is known from a well-known permineralized deposit, Fremouw Peak (Upper Fremouw Formation), that includes Equisetales (*Spaciinodum collinsonii*), several pteridophytes (e.g., Gleicheniaceae, Cyatheaeceae, Matoniaceae, Osmundaceae, Marattiales, *Hapsidoxylon terpsichorum, Schleporia incarcerata)*, cycad, multiple corystosperms and their reproductive structures (e.g., *Rhexoxylon, Kykloxylon, Petriellaea, Dicroidium, Umkomasia, Pteruchus*), *Voltzialean* conifers (*Telemachus*), and several reproductive remains (e.g., *Igonotospermum, Probolosperma*) (Schopf, 1978; Smoot et al., 1985; Osborn and Taylor, 1989; Millay and Taylor, 1990; Pigg, 1990; Delevoryas et al., 1992; Meyer-Berthaud et al., 1992; Yao et al., 1995; Phipps et al., 2000; McManus et al., 2002; Rothwell et al., 2002; Klavins et al., 2004; Bomfleur et al.,

2013; 2014a; Decombeix et al., 2014). Floras from the Late Triassic were equally diverse and based almost exclusively on compression, impression, and cuticle remains from the Falla Formation (central Transantarctic Mountains), Lashly Formation Members C and D, Allan Hills (southern Victoria Land), Section Peak Formation at Timber Peak (northern Victoria Land), and the Flagstone Bench Formation (Prince Charles Mountains) (e.g., Townrow, 1967; Boucher et al., 1995; Cantrill et al., 1995; Bomfleur and Kerp, 2010). Many of the Late Triassic localities provide insight into the spatial heterogeneity of the plant communities, examples of the floras present include *Dejerseya*, voltzialean conifers, *Dicroidium* foliage-types and numerous corystosperm reproductive structures, *Cladophlebis*, *Lepidopteris* cuticles, lycophytes megaspores, and conifers (*Pagiophyllum*), as well as examples of algae and bryophytes (e.g., Cantrill and Drinnan, 1994; Cantrill et al., 1995; Boucher et al., 1995; Phipps et al., 1998; Bomfleur and Kerp, 2010a; Bomfleur et al., 2011c; 2014b).

The vast majority of what is known about Triassic fungi and plant-fungal interactions is from the Middle Triassic permineralized peat deposits of Fremouw Peak. In contrast to the Early and Late Triassic floras of Antarctica, which are based predominately on compression, impression, and palynological samples, anatomically preserved specimens from the Middle Triassic provide a unique insight into the fungal diversity and ecological interactions of these peat ecosystems. Each of the fungi and fungal interactions will be described in detail below in the following sections (see *Triassic* roots; stems; leaves; matrix; reproductive structures). There is one exception, however, to this trend of only permineralized fungi from a compression flora from the Late Triassic Allan Hills. The single example of what may be fungal hyphae on leaf compressions (*Heidiphyllum*) indicates the preservation potential of fungi on Antarctic compression material as well as their presence in Late Triassic ecosystems. (see Fig. 6C, Bomfleur et al., 2013).

4.3 The Triassic-Jurassic Transition, Volcanism, and the Break-Up of Gondwana

The break up of the southern hemisphere supercontinent Gondwana marks the transition from the Triassic to Jurassic. This time period is characterized by increased activity in volcanism that is reflected in the geologic record. Tholeitic magmatic rocks are widespread from southern Africa (i.e., Karoo Dolerite, volcanic Drakensberg Group) and along the length of the Transantarctic Mountains (i.e., Ferrar Dolerite, Kirkpatrick Basalt), through the southern and northern Victoria Land (Ferrar Dolerite, Kirkpatrick Basalt), as well as into southern Australia (Riley et al., 2006; Hergt and Brauns, 2001; Bromfield et al., 2007; Elliot and Fleming, 2008). The warm and wet greenhouse conditions of the Late Triassic also extended into the Jurassic; however, temperatures and atmospheric CO_2 continued to increase throughout the Jurassic (e.g., McElwain et al., 1999; Huber et al., 2000; Ruhl and Kürschner, 2011; Pálfy and Kocsis, 2014). The climate of the Early Jurassic is further complicated by the earth continuously going through phases of warming and cooling, with shifting climatic belts, as well as episodic periods of extreme warmth or "hothouse" conditions (Kidder and Worsley, 2010). The Early to Middle Jurassic plant fossil record is extremely scarce and limited to a few localities in Antarctica, i.e., in northern and southern Victoria Land, as well as a recent site in West Antarctica (e.g., Plumstead, 1962; Townrow 1967a; 1967b; Yao et al., 1991; Rees and Cleal, 2004; Garland et al., 2007; Bomfleur et al., 2011b).

In northern Victoria Land, individual silicified conifer trees engulfed in lava flows have been found in the Mesa Range (Jefferson et al., 1983). Other floras from the Mesa Range area include ferns, *Isoetites, Equisetites*, Bennettitales, as well as other conifers. Deposits of the Shafer Peak Formation yield well-preserved plants and cuticle remains (Bomfleur et al., 2007; Bomfleur and Kerp, 2010b; Bomfleur et al., 2011a). In southern Victoria Land, localities such as

Carapace Nunatak yield floras that include charcoalified ferns, benettitaleans, and conifers, including well-preserved pollen cones (Plumstead, 1962; 1964; Townrow 1967a; 1967b; Schwendemann et al., 2007; Hieger et al., 2015). Additional deposits include trees entombed in lava from Coombs Hills (Garland et al., 2007) and silicified dipterid ferns from Storm Peak (Yao et al., 1991). In West Antarctica, Early and Middle Jurassic are sequences in the Antarctic Peninsula area that include the Sweeney Formation, which includes silicified wood and leaf material of sphenopsids and conifers and the Anderson Formation, that contains horsetails, ferns, cycadophytes, cycads, other seed plants, and conifers (Cantrill and Hunter, 2005; Hunter et al., 2006). Other examples of West Antarctica Jurassic deposits include the palynoflora from Botany Bay, which is highly diverse relative to other Antarctic Jurassic localities (see taxa list(s) in Rees, 1990; 1993a; 1993b; Rees and Cleal, 2004; Cantrill and Hunter, 2005; Hunter et al., 2005). There is even less known about Early Jurassic fungi and microorganisms, especially from Antarctica. Worldwide Jurassic permineralized deposits are exceptionally rare; therefore, the few silicified deposits in Antarctica provide a unique view into a time period where there is virtually nothing known about the microbial components of ecosystems. See *Jurassic* stems; matrix sections for discussion on these reports. Therefore, it is necessary to survey and document the types of fungi present during each of these time intervals and transitionary periods, i.e., Permian through Jurassic, in order to understand how fungi played a role in the success or detriment of certain plant groups.

5. Preservational and technique biases

Documenting the evolutionary history of fungi based on fossils is generally hampered by the incompleteness of the fungal fossil record. Initially fossil fungi were thought to be too delicate to be preserved as fossils. In addition many paleontologists lack the training and

background in mycology necessary to identify fungal fossils (Taylor et al., 2015). Additionally, it has only been recently that fossil fungi have been the focus of many paleobotanical studies; typically investigators reported on fungi in passing or they were a minor component of the overall study. Preservational biases have also played an important role in paleomycological studies; only the most pristine and well preserved specimens were used for anatomical or morphological studies, while specimens with fungal signs or symptoms, e.g., poorly preserved, degradation, were disregarded. Perhaps the most important of these is the small size of most fungal fossils and the lack of specific diagnostic features that can be sufficiently resolved with transmitted light. The increasing amount of new material and the advancements in paleobotanical and paleomycological research methodology offer great potential for future, innovative paleobiological and paleoecological research (see Chapter 2 Materials and Methods for discussion).

Technique and preparation bias also plays a crucial role in the study of paleomycology. During the late 1800s and early 1900s, paleobotanical studies utilized paleontological thin sections of permineralized material, such as historic slide collections of Bernard Renault of material from the Carboniferous of France (e.g., Renault, 1896). The time-consuming preparation of conventional paleontological thin-sections for plant-fossil analysis was considered obsolete after the introduction of the easier and more rapid acetate peel technique in the mid-1950s. It has been demonstrated, however, that the fine anatomical detail crucial for the description of fossil (micro)fungi is inevitably lost during the etching process that uses dilute acid in the preparation of acetate peels of permineralized remains.

Preparation of conventional thin-sections therefore plays a vital role in the accurate documentation and interpretation of fossil fungi (Taylor et al., 2011). The thin-section technique involves adhering a sectioned specimen to a glass slide and subsequently grinding it with varying

grades of carborundum until it can be examined in transmitted light. Extensive loss of material during thin section preparation, the three-dimensionality of the specimens can be examined. Images can be taken at multiple focal planes and then focal stacked to create a composite image of the specimen of interest. Results from thin sections and focal stacking techniques, especially from Antarctic peats, have already yielded an abundance of definitive morphological characters that can be used to expand the biodiversity of the Paleozoic and Mesozoic fungi (e.g., Harper et al., 2012; 2013; 2015).

6. Beyond descriptive studies: Ecological niches, associations and interactions

Plants are not solitary organisms; they host and are associated with multiple types of organisms, e.g., bacteria, viruses, basal eukaryotes, fungi, invertebrates, and vertebrates. Of these, fungi have a significant impact and multiple types of interactions with plants, especially dependent on the plant organ, e.g., roots, stems, leaves, reproductive structures, and surrounding soil matrix. Root-fungal interactions include the mutualistic relationship of mycorrhizal fungi. Fungi act as the principal decomposers and degradational agents in lignified stems or wood. The leaf microbial phyllosphere may contain commensalistic, parasitic endophytes, or epiphyllous fungi, whereas pathogenic fungi often affect the reproductive structures in plants, e.g., spores, pollen, seeds, cones, flowers, and fruits. In all plant organs fungi can act as parasites or saprobes. Fungi and other microorganisms comprise the majority of biomass in the surrounding soil matrix, or rhizosphere.

Each of these examples of plant-organ-specific fungal interactions can be found throughout the fossil record, including the Late Paleozoic and Mesozoic of Antarctica. The remainder of this chapter will provide a critical review of the reports to date on fungi and fungal-like organisms from permineralized deposits of the Permian through Jurassic of Antarctica. This

is organized by the plant organ that the fungus was associated or found in association with, and further subdivided by the time period, i.e., Permian, Triassic, or Jurassic. Some of these reports describe a specific type of plant-fungal interaction when possible, e.g., mycorrhizal associations or wood decay, whereas other reports describe the fungus only, i.e., strictly as a descriptive study and/or the possible taxonomic fungal affinity, and organs that it is found in association with but do not discuss any interaction type (see also Table 1).

7. Roots

7.1 Mycorrhizal associations

Plants are limited by the bioavailability of many essential macro- and micronutrients in the rhizosphere, e.g., phosphorous, nitrogen, potassium, copper, and zinc (Marschner and Dell, 1994). Plants overcome this by forming mycorrhizal associations that are generally mutualistic, but occasionally weakly parasitic between a fungus and the roots or thalli of a plant (Kirk et al., 2008). The fungal component of the mycorrhiza can alter its ambient environment in the rhizosphere through the secretion of acids, which allow specific minerals to become available to the plant in order to uptake as nutrients. Mycorrhizal associations occur in approximately 92% of all extant plant groups, including the bryophytes, lycophytes, sphenophytes, pteridophytes, gymnosperms, and angiosperms (Wang and Qiu, 2006).

7.2 Permian mycorrhizal association

The Glossopteridales are an extinct group of Paleozoic seed ferns that dominated Gondwana during the Middle to Late Permian, including Antarctica. Surprisingly and despite this dominance of the landscape, it is only recently that reports of mycorrhizae do occur in in the small rootlets of *Vertebraria*, the rooting organ of the glossopterids (Harper et al., 2013; Chapter

3 of this dissertation) from the Skaar Ridge locality. This fungus is also a *Paris*-type mycorrhizae and is the oldest representative of this morphological type. This association may have helped the glossopterids thrive in peat forming environments, as well as survive the extreme light regimes in the high paleolatitudes in the Permian forests of Antarctica.

7.3 Triassic mycorrhizal associations

Multiple examples of mycorrhizal associations have been described in two taxa from the Middle Triassic locality, Fremouw Peak. It is common today for plants to possess multiple types of mycorrhizal fungi within the same plant. Two distinct species of co-occurring mycorrhiza have been described in the cycad, *Antarcticycas schopfii* (Stubblefield et al., 1987a; 1987b; Phipps and Taylor, 1996). The initial description by Stubblefield et al. (1987a; 1987b) is one of the best representatives of mycorrhizal fungi in the fossil record, and the first description of mycorrhizae from ancient Antarctica. Phipps and Taylor (1996) described *Glomites cycestris*, a mycorrhiza with similar features of the extant *Glomus* spp., the most common and abundant type of modern mycorrhizal association, and *Gigasporites myriamyces*, which shares features and is one of the only fossil representatives of *Gigaspora* spp. Additional reports of this mutualistic association occurs in *Notophytum krauselii,* a voltzialean conifer, sometimes termed "transitional conifers." Schwendemann et al. (2011) reported preserved mycorrhizal nodules in *N. krauselii*, which are a common occurrence in the soil subsurface in some modern conifers, e.g., Podocarpaceae (Dickie and Holdaway, 2011). Recently, Harper et al. (2015) reported on a second type of mycorrhizal association, an endo-vesicular arbuscular mycorrhizae, within the young rootlets of *N. krauselii* (Chapter 4 of this dissertation). These two different mycorrhizal fungi within *N. krauselii* are significant because they do not co-occur within the same root because one is a nodular type and the other newly found fungus is an endo-vesicular mycorrhizal

fungus. From these findings, one can infer that different types of mycorrhizal fungi co-occurred within the same plant at perhaps different soil levels, i.e., subsurface (nodules) and at the tips of young meristematic rootlets. Additionally, to date, all mycorrhizal fungi reported from Fremouw Peak are of the *Arum*-type a morphological form characterized by extensive dichotomies of the arbuscule.

7.4 Other Permian root associated fungi

Non-mutualistic fungi associated and in close proximity with roots also occur within the Skaar Ridge peats. García Massini (2007) described a cluster of terminal and intercalary chlamydospores with extensive hyphal attachment, *Glomorphites intercalaris*, which occurs within highly degraded tissue, possibly roots and suggested possible affinities with *Glomus*-type chlamydospores based on their morphology. Additional Permian root fungi include wood rotting fungi of glossopteridalean roots, *Vertebraria* (Schopf, 1970; Stubblefield and Taylor, 1985; 1986). Mature, lignified *Vertebraria* roots with secondary growth have been identified with white pocket rot, a type of wood decay common in modern ecosystems. It is important to note that in the initial reports of pocket rot in *Vertebraria*, fungal remains are limited to poorly preserved hyphae that show little detail, and irregularly shaped pockets. See *Stems* section for detail on wood decay in the fossil record.

8. Stems

8.1 Wood decay

In modern ecosystems, the most recognized ecological role of fungi is the degradation of organic material. The nutrients of the organisms being decayed can be recycled back into the soil for use by other organisms, such as plants and soil microorganisms. Woody plants are one of the

most prevalent hosts for fungal degradation (Laiho and Prescott, 2004). There are three principal types of wood rot (or fungal decay): white, brown, and soft. The delineating characteristics between the three rots include the presence or absence of delignified cell wall material by specific enzymes, patterns of degradation in the S_1-S_3 walls, the type of fungi (e.g. basidiomycetes, ascomycetes, or the former deuteromycetes), and the type of wood (e.g. gymnosperms or angiosperms type wood) (Schwarze et al., 2000).

8.2 Permian stem wood decay

Specimens of *Australoxylon bainii* from the Prince Charles Mountains exhibit patterns of wood decay, such as irregular cavities that lack sharp margins, gradational decay patterns that extend in to the surrounding xylem tissues, tracheids with small holes in the cell walls near edge of the cavities, and appositions within cell lumina (a common host response) (Weaver et al., 1997). The causative agent for the decay was not determined, but Weaver et al. (1997) suggested it as fungal decay, although no fungal remains, vegetative or reproductive, were found in the specimens. Other species of *Australoxylon*, such as *A. mondii* from this study also exhibit signs of decay including spindle shaped cavities that lack any fungal remains; these cavities can occur within individual ring boundaries, across tree rings, as well as localized into specific regions of the wood or randomly dispersed throughout the specimen. Similar to *A. bainii*, appositions do occur in the cell lumina, but *A. mondii* also contained unidentified filamentous structures.

8.3 Triassic stem wood decay

To date, the description of white pocket rot and white rot fungi in the fossil record is restricted to reports of Triassic wood-type *Araucarioxylon* and Permian *Vertebraria* from Antarctica (Stubblefield and Taylor, 1985; 1986). In this report, the vast majority of decay sign

and symptoms occur in *Araucarioxylon* wood such as pocket distribution ranging from isolated areas on specimens (within ring boundaries, segment of specimen) to crossing ring boundaries, circular to irregularly shaped pocket in transverse section and spindle shape in longitudinal planes. Fungal remains associated with the decay include hyphae within the pockets, tracheids, and ray parenchyma. Morphological aspects of the hyphae consist of septate, branching, and production of clamp-connections. Detailed analysis of the cell wall layer degradation indicates that the corner areas between four adjacent cells contain the thickest portion of the middle lamella and distinct separation patterns within the cell walls. Appositions, possibly corresponding to the S_3 cell wall layer, were also described in *Araucarioxylon.* Overall, the high frequency and proliferation of pocket rot in Triassic woods (and to a lesser extent Permian woods) suggest that wood-decaying fungi played a major role as decomposers in Permian and Triassic peat forming environments.

8.4 Jurassic fungal-wood interactions

Saprotrophic fungi represent only a fraction of the microbial biodiversity that can occur within and interact with trees (Scotland et al., 2012). An example of a possible parasitic fungus and induced host response via tylosis formation in Jurassic trees is reported from Antarctica (Harper et al., 2012; Chapter 7 of this dissertation). The authors describe extensive hyphal proliferation throughout a conifer axis with numerous examples of tylosis, a suberized structure and common host response elicited by lignified by trees to occlude cell lumina to prevent water loss or fungal infections (Pearce, 1996). In this study, the investigators were able to map out the interaction between the fungal hyphae and tylosis formation; and suggested that the tyloses were a host response as a result of fungal infection.

8.5 Other Permian stem fungi

Other studies that include evidence of fungi associated with stems include a report by Slater et al. (2012) that described fungi-rich coprolites, some within galleries of *Australoxylon* or *Vertebraria*, which contain broken fungal spores and crushed hyphae. The authors suggested that these coprolites were produced by fungivorous arthropods, such as oribatid mites, rather than the fungus secondarily infecting the coprolites. More recently, axes of the lycophyte *Paurodendron stellatum* from the Prince Charles Mountains have been described with cross sections of hyphae in the lumina of metaxylem tracheids (McLoughlin et al., 2015). Portions of the lycophyte have thin-walled tissues, which suggests moderate signs of aerobic decay attributing that these fungi may represent saprotrophs in the Toploje Member peat.

8.6 Other Triassic stem fungi

Examples of possible stem-associated fungi include an example of two large spheroidal structures ("sporocarps"?) with mycelia surrounding the petriellalean stem, *Rudixylon serbetianum* (see Fig. 4J in Bomfleur et al., 2014a). Although the authors did not describe the fungi in the study, these structures are morphologically similar to "sporocarps", which are typically associated with the matrix and not specific organs, the mycelia surrounding the stem deserves recognition. It is inconclusive if the fungal mycelia penetrated the surface of *R. serbetianum* or is just restricted to the surrounding matrix. Studies on petriellalean-fungal interactions are unknown and would be an interesting component to understanding the ecology of these enigmatic Triassic seed plants.

9. Leaves

Although leaves constitute a harsh habitat for fungi due to temporary nutrient availability, extreme fluctuations in humidity, temperature, gas exchange gradients, and ultraviolet radiation (Goodman and Weisz 2002), leaf endophytes and epiphytes represent a major component of fungal associations with plants (Krings et al., 2012). To date there is little evidence of pre-Cretaceous fungal endophytes and epiphytes on leaves, with the exception of well-preserved leaf endophytes from the Carboniferous. Examples of permineralized endophytes found in Carboniferous foliage types within coal swamp environments include: fern pinnules with hyphae of unknown affinity within hypodermal cells (Krings et al., 2009a), fungal spores and hyphae within vascular and parenchymatous tissues (Barthel, 1961; Krings, 2001), and possible fungal microsclerotia, resting spores, and hyphae within fern pinnule hypodermal cells (Krings et al., 2010a).

9.1 Permian leaf fungi

Reports on permineralized Permian leaf fungi from Antarctica are restricted to a single study from the Prince Charles Mountains (Holdgate et al., 2005). There is evidence for filamentous hyphae ramifying through the mesophyll tissues of *Noeggerathiopsis* leaves. There was no discussion of the potential ecological affinity of the fungus, but it may represent a saprotrophic fungus within the peat. One explanation for this paucity maybe the low potential for leaves to be permineralized and be recognized within Antarctic peat deposits. Another hypothesis for the absence of Antarctic Paleozoic and Mesozoic leaf endophytes may be due to the physiology of these high-paleolatitude plants and the ability for these plants to support leaf endophytes despite polar light regimes. For further discussion see Chapter 8 of this dissertation. Although the affinities of these fungi are currently unknown, it is important to document these occurrences in order to increase our knowledge of these foliar types of fungal associations.

10. Reproductive structures

Plant reproductive structures include spores, pollen, ovules, seeds, strobili, cones, flowers, and fruits. Each of these structures are susceptible to fungal infection and to other fungal-like organisms, as well as each structure has developed specific defense mechanisms against fungi, such as biochemical, e.g., pollen (Char and Bhat, 1975), or structural (Freeman and Beattie, 2008). Many plant reproductive structures are the target for host specific fungal diseases, such as modern agricultural plant pathogens (e.g., Oliver and Solomon, 2008). Reports on fossil microbial interactions and plant reproductive units are increasing, however, there are only a limited number of these reports on permineralized material from Antarctica.

10.1 Permian pollen-fungal interactions

The comprehensive study of the peat biodiversity of the Prince Charles Mountains by Slater et al. (2014) notes several examples of fungi, including ten different fungal morphotypes. Among these is Fungal Morphotype 7, or fungi associated with pollen grains, with suggested affinities to Chytridiomycota and saprotrophic. Pollen grains infected and degraded by chytrids in extant ecosystems is common occurrence (e.g., Goldstein, 1960). The co-occurrence is also noted in the fossil record such as in the Carboniferous, the Permian of India, Early Cretaceous, and other Tertiary deposits (Elsik, 1966; Millay and T. N. Taylor, 1978; Aggarwal et al., 2015). Studies of pollen and chytrid interactions are important to note as they may provide insight into building complete life history biology of these microbes.

10.2 Triassic reproductive structures with fungi

Two reproductive structures with fungal interactions have been described from permineralized material of Antarctica. An exquisitely preserved specimen of *Parasciadopitys aequata,* the seed containing a well-preserved embryo of the voltzialean *Telemachus*-type conifer from the Middle Triassic Fremouw Peak locality has been reported with fungal endophytes (Schwendemann et al., 2010). The endophytes are *Mycocarpon asterineum* "sporocarps" that occupy the space between the nucellus and megagametophyte tissue. *M. asterineum* has been recently reinterpreted to share affinities with zygomycetous fungi and the ecological affinity suggested by Schwendemann et al. (2010) was either as a saprotroph or parasite. However, the authors concluded that there was not enough evidence to support either association. But due to lack of any host response by *P. aequata* and the zygomycetous affinity of *M. asterineum*, it is most likely a saprotroph, but more evidence and studies of this association are needed.

Additional evidence of reproductive structure and fungal interaction comes from the Middle Triassic Mount Falla locality in an enigmatic gymnospermous ovulate structure, *Dordrechtites arcanus* (Bergene et al., 2013). This report is based on a rare type of preservation combination of compression-impression and permineralized material. The authors of this report describe high proliferation of fungal colonization with multiple specimens and tissues of the ovule, including within the megaspore membrane and transfusion parenchyma. It is difficult to know the taxonomic affinity of the fungus because only vegetative mycelia was reported. Similar to the report of fungi within *Parasciadopitys aequata,* Bergene et al. (2013) were unable to conclude the ecological affinities of the fungus as either a saprotroph or parasite. Based on the poor preservation of some specimens and lack of host-response, it is most likely also a saprotroph. Due to the diversity of reproductive structures of the Triassic of Antarctica, more work is needed in this area of reproductive unit and fungal interactions in order to resolve the ecological interactions and specific groups of fungi that colonized these structures.

11. Matrix

Fungi and fungal-like organisms constitute a large portion of the total biodiversity within soil communities (Baldrian et al., 2013; Wardle and Lindahl, 2014). Therefore, it is not surprising that the vast majority of fungi and fungal-like organisms described from the Antarctic permineralized peats are found within the matrix. Many of these reports are strictly descriptive studies and do not provide discussion or have enough evidence to confidentially assign any degree of ecological association. Other reports concentrate on the taxonomic affinity of the fungus or fungal-like organism. In the following section, discussion of the microbial organisms from the permineralized peats are organized by geologic time of Peronosporomycetes, "sporocarps", and all other reported fungal types, i.e., fungal morphotypes, specific fungal taxa that occur within the peat matrix.

11.1 Fungal-like organisms, *Peronosporomycetes*

One of the more prevalent groups of fungal-like organisms in the fossil record are the Peronosporomycetes (formally: Oomycota). In modern ecosystems, this group of aquatic and terrestrial microorganisms function as saprotrophs and facultative or obligate parasites of plants, animals, and other fungi. The Peronosporomycetes (Phylum: Stramenopila, Patterson 1999, emend. Adl et al. 2005), however, are not true fungi and are more closely related to brown alga, but are sometimes termed fungal-like organisms (Taylor et al., 2015). Although this group of fungal-like organisms has been documented as occurring in the Carboniferous–Triassic, the majority of the life cycle of the Peronosporomycetes is lacking. Characters that can unequivocally and positively identify these organisms include: biflagellate zoospores and oogonium-antheridium complex (Dick, 2001). Specimens that have been described in the

Antarctic permineralized peats are of the *Combresomyces* spp. and to date have not been found with either biflagellate zoospores or associated oogonium-antheridium complexes. Interestingly, *Combresomyces* spp. are characterized by the oogonia possessing complex, compound surface ornaments (sometimes termed "antler-like" extensions) of hollow papillations of the oogonial wall (Dotzler et al., 2008; Taylor et al., 2015).

11.2 Permian Peronosporomycetes

Two distinct species of *Combresomyces* spp. have been described by Slater et al. (2013) from the Middle to Late Permian of the Prince Charles Mountains. Each species has prominent ornamentation and occur within the matrix. *C. caespitosus* is characterized by having long, hollow, slender, conical papillae with at least two orders of strongly divergent, sharply pointed, apical branches. It was noted that *C. caespitosus* was found in association in matrices near *Vertebraria* roots and leaves of *Glossopteris* and *Noeggerathiopsis*. In contrast, *C. rarus* is characterized by spherical oogonia bearing long, hollow, broad, conical papillae that terminate in at least one bifurcation producing a pair of, generally acutely divergent, sharply pointed branches. *C. rarus* is relatively less abundant, i.e., present in 25% of peat samples studied, than *C. caespitosus,* i.e., present in 50% of total peat sample examined. Both species were noted to have a short truncate extension, likely where the parent hyphal attachment occurred. Slater et al. (2014) suggested that the *Combresomyces* spp. likely played a significant role in degradation of organic matter or perhaps existed as a parasite to plants and/or animals.

There is also a figure of a reported fungal zoosporangium in the Schopf (1970) that superficially looks like an ornamented peronosporomycete attached to a parental hypha. Although the author did not discuss the affinities or ecological habit of the specimen, it is important to note that these organisms were also present in the Late Permian, Skaar Ridge

locality. It is without question that more data is needed to further resolve the affinities of the Peronosporomycetes within the Late Permian peats of Antarctica.

11.3 Triassic Peronosporomycetes

Another report of *Combresomyces cornifer* has been described in the matrix and near a well-preserved seed with embryo from the Triassic of Antarctic, and may represent a possible parasite (Schwendemann et al., 2009; 2010). These specimens are morphologically similar to the type specimen from the Carboniferous, but are much larger in diameter. The persistence of *Combresomyces* spp. in the Permian and Triassic Antarctic suggest that these organisms are quiet resilient during times of global climate change and floral turnover, as well as their possible role as generalists in high latitude peat forming environments.

11.4 "Sporocarps"

Several spherical microfossils have been described in Carboniferous coal balls and especially the Triassic of Antarctica as fungal sporocarps. These structures range in diameter from 100–500 μm, typified by the morphology of surface ornamentation, can occur singularly or in clusters, and include a central cavity (with or without contents) surrounded by an investment or mantle with particular hyphal arrangement (Taylor et al., 2015). Collectively, these structures have been termed sporocarps, but Krings et al. (2011) suggested that since this term is possibly inaccurate relative to modern fungal sporocarps, it should be placed in quotation marks, i.e., "sporocarps". Interestingly, the life history and biology of these microfossils is relatively unknown and have been typically interpreted as some type of resting structure. Different morphotypes and species have been described in detail from the Fremouw Peak locality of

Antarctica. To date, “sporocarps” have not been described from the Permian or Jurassic deposits, leaving a large gap in the fossil record in the transition from the Paleozoic to the Mesozoic.

11.5 Triassic “sporocarps”

Two species of “sporocarps” have been described from the matrix of the Middle Triassic permineralized peats, i.e., *Endochaetophora antarctica* (White and Taylor, 1988; 1989a) and *Mycocarpon asterineum* (Taylor and White, 1989). *E. antarctica* was described as having a tripartite layer envelopment, with an acellular middle layer that developed secondarily after the outer and inner cell wall layers. Additionally, the “sporocarp” contains numerous appendages arising from the inner layer, and some specimens can contain as ostiole or opening. In contrast, *M. asterineum* are morphologically similar to *Mycocarpon* spp. from the Carboniferous (e.g., (Stubblefield et al., 1983) but differ due to an outer investment composed of an outer hyphal portion and an inner non-hyphal component, with some specimens containing interwoven hyphae. The authors were able to determine the developmental stages of the investment based on these Antarctic specimens and discussed the ecological association as saprotrophs in the peat. Other examples of *M. asterineum* have been described as endophytes within a well-preserved embryo (see *Triassic reproductive structures with fungi* section for discussion; Schwendemann et al., 2010). Many of these “sporocarps” have been interpreted as having affinities with zygomycetous fungi but structural features have not been conclusively documented. One example of zygomycetous fungi with possible association with a “sporocarp” includes *Jimwhitea circumtecta* (Endogonaceae) (Krings et al., 2012). *J. circumtecta* was formally described as an endogonalean zygosporagium with prominent hyphal mantle, and attached megagametangium, microgametangium, and microsuspensors. Additionally, there is a “sporocarp” co-occurring within the peat matrix with *J. circumtecta,* which shares many of the same morphological

features. These shared characters suggest that the "sporocarp" likely belongs to *J. circumtecta* and provides insight into the biology as well as the developmental parental status of "sporocarp" biology, which is an important contribution since these enigmatic structures are typically described as resting structures. The remaining "sporocarps" from the Triassic peats are purely descriptive studies of several different morphotypes of these microfossils. For example, White and Taylor (1989c) described two differing "sporocarp" specimens (Fungal types 2 and 3 in paper) each with a mycelial peridium with internal spores within and with a mantle respectively. Another comprehensive study Taylor and White (1991) described multiple examples of "sporocarps" (Fossils 1–4; 6–10 in paper) ranging from "sporocarps" with some of the following characters irregularly thick interwoven hyphae, multiple layer investment, and some with spores or without spores.

11.6 Other Permian matrix fungi

The peat matrix of the Prince Charles Mountains is rich in fungal remains (Slater et al., 2014). Among these, include ten distinct fungal morphotypes, including: septate and non septate hyphae, hyphae with swellings, multiple examples of ornamented spores, disc-like structures, possible fungal sclerotia, and specimens of complex fruiting bodies with and without contents (Holdgate et al., 2005). The systematic affinities or ecological association for all of these morphotypes could not be confidently concluded. It is important to continue to document these occurrences, as more data is collected from the peats, this will likely yield increased resolution on many of these morphotypes. Matrix fungi are also reported from the Skaar Ridge locality; including possible members of the Chytridiomycota, interpreted as *Synchytrium*-like fungus: *Synchytrium permicus* (Garcia Massini, 2007a). The author of this report was able to determine a proposed life cycle based on various developmental stages within the peat. This fungus was

interpreted as a parasite with roots, leaves, and stems, and certain tissues exhibited a hypertrophic host-response.

11.7 Other Triassic matrix fungi

Many of the matrix fungi within the Triassic exhibit well-preserved characters similar to extant fungi, and when possible, even to the genus level. One example include the *Sclerocystis*-like fungus reported by Stubblefield et al. (1987c). Modern phylogenies indicate that *Sclerocystis* spp. are related to the Glomeromycota and have been suggested to be saprotrophic organisms. Additional fungi include *Palaeofibulus antarctica*, which is an example of a clamp producing fungus with septate hyphae with definitive affinities to basidiomycete fungi based on the presence of the clamp connection (Osborn et al., 1989). Other studies such as an example of possible arthropod-fungal interaction, include the Trichomycete-like fungus of hyphal thalli attached to a putative insect cuticle is (White and Taylor, 1989b). Trichomycete fungi today exist only in the gut of certain arthropods and are host-specific, thus suggesting the possible diversity of certain insect groups within the peat deposits. The remaining reported matrix fungi from the Triassic are fungal morphotypes and are only descriptive studies: globose spores in clusters, possible chlamydospores with a mycoparasite, and subglobose sporangia (White and Taylor, 1989c; 1991). Continued surveys of Triassic permineralized peats will undoubtedly yield more examples of fossil fungi, including increased resolution of groups already known and possible examples of fungal phyla not known from the Triassic (i.e., Blastocladiomycota, Ascomycota), as well as insight into the life history and biology of these groups.

11.8 Other Jurassic matrix fungi

Reports of Jurassic matrix microorganisms from Antarctica are almost absent with the exception of one brief note by Bomfleur et al. (2007) of fungal remains possibly within a microbial mat from Mount Carson. This area of Jurassic microorganism studies is a completely new avenue of research that requires investigation into a time period in which there are limited reports of fossils.

12. Considerations when studying fossil fungi

Overall, deposits that yield anatomically preserved plants, such as permineralized peat, offer one of the best opportunities to study ancient plant-fungal interactions. And based on the previously mentioned studies, an overall theme or set of criteria are necessary to consider while studying fungi in permineralized material. Permineralized peat, which is the conglomeration of many different plant, parts and the same type of plant can be preserved in multiple planes of section, which is an important attribute for studying fossil fungi. Investigators can study how the fungus traverses the plant in multiple planes, i.e., transverse vs. longitudinal. This can provide insight into the type of symbiotic interaction between the fungus and plant. For example, if the fungus is found in multiple tissues such as the epidermis, cortex, and vasculature, the fungus may be a generalist; in contrast, if the fungus is restricted to a specific tissue, then it may be a specialist. Additional benefits of anatomically preserved material include the ability to make serial sections of a particular specimen. This is crucial for studying the fungus throughout the entirety of a plant or within the matrix, and for clarification of the taxonomic affinity of the plant organ. This is an important point for researchers examining historic slide collections, where typically there is only one slide per specimen and no opportunity to make serial sections. It is critical that investigators identify the plant organ in question that is associated with a fungal partner, in order to accurately study plant-fungal interactions in the fossil record. Furthermore,

taxonomic or systematic affinity of said organ will provide the foundation for understanding plant-fungal relationships in that particular lineage of plants. Any paleobotanist who has worked on permineralized material can testify that each of these points of recognizing the correct plant organ type and identify the affinity of the organ is not always intuitive, therefore it will be important for investigators to look at organ specific fungal interactions with caution. For example, not all root endophytes will be involved in mycorrhizal association, or fungi in woody axes are degradation fungi. Also, two plant axes that co-occur or are grouped together in a deposit, with no obvious organic connection, may not be from the same parent plant. Roots are especially difficult to identify to a taxonomic level, especially without organic connection, but the overall composition of the peat matrix may provide insight into the affinities, e.g., a heterogeneous matrix of organs of all of the same taxon (e.g., Harper et al., 2015). Other considerations while studying fossil fungi include knowing and understanding the ontogenetic stage of the plant organ, e.g., a young rootlet with intact cortex and no secondary or woody tissues will show a mycorrhizal association versus a mature root with secondary growth that will not contain mycorrhizae. Because paleomycology is not necessarily an experimental science, a salient point in paleomycology is having multiple examples of the same plant-fungal interaction in different specimens, so that the interaction is not just a single occurrence. For example as the majority of a certain species of fossil leaves has a specific type of epiphyllous fungus consistently associated with it, this provides greater confidence that the fungal interaction is host specific or is an interaction to the plant lineage. Finally, the absence or presence of host responses by plant organs can be an indicator if the plant was alive at the time of infection and provide an important line of evidence for the type of interaction that the fungus had with the plant, i.e., no host response is evidence for a mutualistic or commensalistic relationship for a living plant, or the plant was not alive at the time of the interaction and the fungus may be a

saprotroph, whereas presence of host reposes indicates the plant was alive at the time of fungal infection and was possibly a parasite. Adding to this level of complexity of interpreting host-fungal interactions is that although a host response may indicate the possible presence of a parasite, certain parasites do not elicit a host response (Taylor et al., 1992; Hass et al., 1994; Krings et al., 2009b; 2010c). Each of these areas was considered while conducting the research for the following dissertation chapters. This adds a greater degree of confidence to the analyses and interpretations of the results.

13. Conclusions

Despite the large number of fungal remains in the fossil record, including those that provide both direct and indirect evidence of an association or interaction with land plants, the discipline of paleomycology is at relatively early stage of development. The study of fungal relationships adds a new perspective to the Permian, Triassic, and Jurassic floras as biological entities in their past environment. In combination with a large dataset of information about the anatomy and physiology of these plants, fungal associations offer new paleoecological insights as how such relationships may have promoted the dominance of certain plant groups in Gondwanan ecosystems. Furthermore, these findings continue to add to our knowledge of the complex interactions in paleoenvironments and evolutionary interactions between fungi and plants.

Chapter 2

Materials and methods: Thin sections, focal stacking, and analytical techniques in paleomycology

1. Introduction

Plant fossils can be preserved in a variety of different modes, e.g., compression, impression, casts, molds, petrification, etc. (Schopf, 1975). Each of these different preservational types offers a level of detail and information specific to the type of preservation of the fossil specimen (Taylor et al., 2009). One such preservational type, permineralization, is a rare type of preservation in which a majority of the specimen has been replaced by minerals, except the cell walls are still (highly altered) organic matter (Dietrich et al., 2001). Permineralized material offers a unique source of information due to the structurally preserved anatomy and morphology of the organism, and is process that likely happens so rapidly that fine, micro-details of cells and cell contents can be preserved and studied (Bomfleur et al., 2014d; Hellawell et al., 2015).

The plant-bearing Permian to Jurassic continental deposits of the Transantarctic Mountains of Antarctica are a unique source of information about the biology and ecology of these past high-latitude ecosystems (Taylor et al., 1989a; Bomfleur et al., 2014c). Of special importance are permineralized peat deposits that contain anatomically preserved plants. Although fossil floras from the Transantarctic Mountains have been intensively studied during the last decades (e.g., Taylor and Taylor, 1990; Cantrill and Poole, 2013), many questions for a better understanding of Antarctic paleoecosystems, such as the role of fungi in ecosystem functioning, still remain unsolved. The widespread occurrences of permineralizations in the Transantarctic Mountains offer tremendous potential to document fungal diversity and study the

ecology of Antarctic fossil plant-fungal interactions. Of particular importance are the Permian and Triassic silicified peat deposits from the central Transantarctic Mountains (Schopf, 1971). The exquisite preservation of these plant remains is similar or even better than that in the well-known Carboniferous coal balls (Scott and Rex, 1985; Scott et al., 1996). The ever-increasing amount of new material and paleobotanical research methods such as petrographic thin sections and advancements in the use of analytical techniques offer great potential for future, innovative paleobiological and paleoecological research with fossil fungi.

Traditionally, early paleobotanical studies of permineralized material utilized petrographic thin sections (e.g., Renault, 1894). The time-consuming preparation of conventional petrographic thin-sections for plant-fossil analysis has historically been regarded to generally replaced by the introduction of the acetate peel technique in the mid- 1950s (Joy et al., 1956). It has been shown, however, that fine anatomical detail crucial for the description of fossil (micro)fungi is inevitably lost during the etching process when preparing acetate peels (Taylor et al., 2011). The preparation of conventional thin-sections therefore continues to play an accurate role and interpretation of fossil fungi. This technique involves adhering a piece of permineralization to a glass slide and subsequently grinding it down with varying grades of silicon carbide until the specimen is thin enough to be studied in transmitted-light.

As paleobiological techniques have advanced, several analytical methods are emerging that hold promise in the study of fossil fungi. Such techniques include Raman spectroscopy and biomarker analysis using gas chromatography-mass spectrometry (GC-MS), and Fourier transform infrared spectroscopy (FTIR) spectroscopy. Such methods can yield results of direct and indirect evidence of fungal interactions with ancient plants. One of benefits of these analytical techniques is that they can each be used on permineralized material, and thus are ideal for studying fossil fungi.

This chapter is divided into four parts: (1) geologic setting, localities, and ages of fossil material; University of Kansas (KU) specimen and slide numbers (2) petrographic thin section preparation and protocol, (3) microscopic image processing, i.e., focal stacking techniques, and (4) analytical methods for studying fossil fungi.

2a. Geologic setting, localities, and ages of fossil material

2a.1 Permian locality, Skaar Ridge, Antarctica

Permineralized material is known from Skaar Ridge, 840 49' 11.8" S, 1630 20' 37.0" E, (2300 m, 8600 ft.) locality within the Buckley Formation near the Beardmore Glacier Area, Queen Alexandra Range, central Transantarctic Mountains, Antarctica. The Permian Buckley Formation, which consists of coal measures that crop out extensively throughout the central Transantarctic Mountains, is at least 745 m thick (Barrett et al., 1986) (Figure 2a). The formation has a lower arkosic (i.e., a sandstone with at least 25% feldspar) member and an upper volcaniclastic member (Barrett et al., 1986; Isbell, 1990). Similar coal measures characterize the Permian throughout the Transantarctic Mountains and Ellsworth Mountains, although those in the Victoria Land sector do not contain volcanic detritus (Collinson et al., 1994). At this locality, the stratigraphy of the Permian plant deposits is characterized by permineralized peat containing ecotype floras, such as *Glossopteris* leaves, *Australoxylon* type wood, *Vertebraria* root systems, and several reproductive structures such as *Plumsteadia* Rigby (Figures 2b, 2c).

2a.1.1 Chapter 3: Vertebraria *mycorrhizae*

At this site, deposits include permineralized (silicified) peat containing typical glossopterid elements, including *Glossopteris* leaves, wood traditionally assigned to the

Australoxylon (see Decombeix et al., 2014) several reproductive structures (Taylor and Taylor, 1987; Cúneo et al., 1993; Ryberg, 2009; Ryberg et al., 2012), and *Vertebraria* root systems. To date, there have been no leaves or reproductive structures of non-glossopterid gymnosperms described from the Skaar Ridge peat. There are, however, some gymnosperm roots with an anatomy different from *Vertebraria*; these are similar to what Neish et al. (1993) described as "solid-cylinder *Vertebraria*." It is impossible to determine whether they represent a variation in root system anatomy within the glossopterids, or if they are the roots of a different group (Decombeix et al., 2009). As noted by Neish et al. (1993), the very young developmental stages of these roots do look very similar to the young stages of the *Vertebraria* roots that have only two protoxylem strands. However, in the present case we are confident that the roots in which the fungi are described are indeed *Vertebraria* and not the "solid-cylinder" type of roots. This is partly due to evidence that the "solid-cylinder" roots are very rare (only a few occurrences in the peat blocks from Skaar Ridge) and they occur in small distinct clusters of a few roots (i.e., not inter-mixed with *Vertebraria*) p. 655 in Decombeix et al. (2009).

2a.1.2 Chapter 6: Permian wood fungi

Specimens of stem and root wood were collected over several field seasons from Skaar Ridge. Specimens used in this study can either be assigned to the glossopteridalean stem wood, *Australoxylon* (Marguerier, 1973) or lignified root wood, *Vertebraria* (Schopf, 1982), both characterized by pycnoxylic wood. All specimens lack preserved primary vascular anatomy, and therefore affinities are based on wood morphogenera characters. Stem characters share closest affinities with *Australoxylon* spp., which are morphologically similar to *Araucarioxylon* (Philippe, 2011). *Australoxylon* spp. have generally been regarded as a morphogenera for Permian Gondwanan woods (Marguerier, 1973; Prasad, 1982; Pant and Singh, 1987; Weaver et

al., 1997) and are closely associated with *Glossopteris* flora (e.g., Merlotti and Kurzawe, 2006; Philippe, 2011). Further support for *Glossopteris* affinity includes the anatomical attachment of *Glossopteris skaarensis* leaves to wood (Pigg and Taylor, 1993). Characters of *Australoxylon* include: individual and distinct wood rings, square to rectangular tracheids in transverse section, multiple types of radial pitting (e.g., abietinean, araucariod, conspicuous arrangements of independent and spaced radial files or circular pitting), and groups of 2–3 or 4–5 pits (typically small, <15 μm in diameter) that are distinct from each other in clusters. One of the key distinguishing characteristics of *Australoxylon* wood that all specimens in this study share are mixed-type pitting on the tracheid radials.

Specimens of *Vertebraria* were identified by the presence of the characteristic radiating wedges of secondary wood separated by lacunae rather than a solid axis. Certain specimens that lack the characteristic wedges were not included in this study as specimens of *Vertebraria,* although portions of wood axes may also represent portions of *Vertebraria*. It is also important to note that there are rare types of *Vertebraria* spp., i.e., the "solid cylinder" type (Neish et al., 1993) that lack lacunae and were also not included in this study. *Vertebraria* axes from the Bowen Basin, Australia, Permian of Brazil, Skaar Ridge of Antarctica (this study), and the Prince Charles Mountains, East Antarctica have been reported with *Australoxylon* type wood (Mussa, 1978; Neish et al., 1993; Weaver et al., 1997; Decombeix et al., 2009) due to the characteristic opposite or mixed pitting in these *Vertebraria* specimens (Pant and Singh, 1968; Beeston, 1972; Gould, 1975).

2a.1.3 Chapter 8: Glossopteris *leaf fungi*

Skaar Ridge: *Glossopteris* leaf mats are comprised of highly degraded, poorly preserved leaves. Many of the leaves are lacking diagnostic characters that render it impossible to assign

species. Paradermal sections of *Glossopteris* leaves are characterized by large meshes and a more prominent midrib. In transverse sections, the bundle sheath, when preserved, is composed of thin-walled cells that sometimes include dark contents. Stomata are rarely preserved, but are sunken. Typically the only remaining component of the leaf that is consistent are the parallel, thick walled vascular bundles (i.e., Plate 16, Fig. 183).

Collinson Ridge: Specimens were collected during the 1995–1996 field season from a lens of silicified peat, 6 m across and 0.6 m thick, within a medium-grained sandstone on Collinson Ridge (85º13'S, 175º21'W), in the central Transantarctic Mountains, Shackleton Glacier area (Collinson and Hammer, 1996). On top of Collinson Ridge, above a thick dolerite sill, is a 90-m-thick section of cyclical ledge-forming medium- to coarse- grained sandstone and slope-forming greenish-gray mudstone. The silicified peat is dominated by *Glossopteris* flora, but also includes *Vertebraria* and *Australoxylon*-type wood (McManus et al., 2002) occurs in the lower part of the Fremouw Formation (Collinson and Hammer, 1996).

2a.2 Triassic locality, Fremouw Peak, Antarctica

The fossils occur in permineralized (silicified) peat from the Fremouw Formation in the central Transantarctic Mountains of Antarctica (Taylor et al., 1986; Cúneo et al., 2003; Faure and Mensing, 2010). The Fremouw Formation is a 620–750 m thick siliclastic succession deposited by low sinuosity, braided streams (Faure and Mensing, 2010). The fossils occur within several allochthonous clasts that are at approximately the same stratigraphic level within a trough-crossbedded, medium-grained, greenish-gray volcaniclastic sandstone. Permineralized peat is found at a single level at the Fremouw Peak locality, approximately 30 m below the top of the formation (Figure 2a). Blocks of peat were likely rafted into their current position during a flooding event that caused them to be stranded on sand bars prior to permineralization (Taylor et

al., 1989a) and isolated into individual lenses within the outcrop. The peat was silicified after burial in its current position and the age of the fossil plants within the peat is equivalent to the surrounding clastic sediments, i.e., fluvial sandstone, which also contains trunks of wood of equivalent age to the peat (Decombeix et al., 2014). The silica source for the permineralization is interpreted to be the result of the dissolution of siliceous, volcanic detritus that was abundant in the upper Fremouw Formation. The peat and surrounding material has been dated as early Middle Triassic (Anisian) based on palynomorphs and nearby vertebrate fossils (Farabee et al., 1990; Hammer, 1990; Sidor et al., 2008; Faure and Mensing, 2010) (Figures 2b, 2d).

2a.2.1 Chapter 4: Notophytum *mycorrhizae*

Fossil specimens were initially prepared according to standard acetate peel techniques utilizing hydrofluoric acid to survey the material for fungi, including roots that may show evidence of mycorrhizal colonization. The peat blocks used in this study contain abundant components attributable to the voltzialean conifers, including axes of *Notophytum krauselii* (Meyer-Berthaud et al., 1991), e.g., characterized by eustelic woody stems, roots of *N. krauselii* characterized by a distinctive *phi* layer suggesting the plants may have grown in a fluctuating water table environment (Millay et al., 1987; Taylor and Ryberg, 2007), permineralized *N. krauselii* leaves, numerous *Alisporites* pollen grains, and ovules of *Parasciadopitys*.

Fossil roots in general are difficult to identify at any systematic level because the characters used to define them are relatively uniform. However, *Notophytum krauselii* roots and aerial axes/stems do share several anatomical features that make it possible to assign the roots with confidence to the stems, which in turn are correlated with other vegetative and reproductive organs (e.g., Meyer-Berthaud and Taylor, 1991; Escapa et al., 2011).

2a.2.2 Chapter 5: Ashicaulis *microorganisms*

This study is concentrated on a single, large permineralized osmundaceous fern root ball with dimensions, approximately 40 cm (length) x 37 cm (width) x 30 cm (height) found at Fremouw Peak (Plate 6, Figs. 46-48), which shares anatomical features and characters with *Ashicaulis wolfeii* Rothwell et al. (2002). Morphospecies of permineralized osmundaceous plants include stems 5–7.5 mm wide with a heterogeneous pith with sclerenchyma and interspersed parenchymatous cells. The xylem cylinder, when preserved is on average, 1.3mm wide, 0.2–0.3 mm thick with 8–9 xylem segments separated by distinct leaf gaps. The inner cortex is parenchymatous and is 0.5–0.6 mm thick, while the outer cortex is about 0.8 mm thick and composed of homogeneous sclerenchyma fibers. The frond trace is C-shaped with one endarch protoxylem strand proximally which divides in two in outer cortex, developing enrolled margins distally. Based on multiple sections and peels, 25 frond traces have been found. Additionally, annuli attached to sporangia devoid of contents are common. Other degraded tissues are found throughout the matrix and a single seed has been observed. The fern root ball is composed primarily of small rootlets typically 1-3 mm in diameter interspersed with numerous arthropod coprolites.

2a.2.3 Chapter 9: Endochaetophora *leaf litter fungi*

The peat blocks are a combination of material collected during the 2010-2011 austral summer Antarctic field season and specimens collected from previous field seasons from Fremouw Peak locality. This study contains abundant partially degraded leaves, many of which are attributable to the *Dicroidium* sp. (Pigg, 1990) and *Notophytum krauselii* leaves (Axsmith et

al., 1998), together with unidentifiable axes. These silicified blocks represent leaf litter mats based on the large number of compacted leaves axes, and degraded plant matter. The leaf litter matrix lacks roots and reproductive organs. A considerable portion of the peat blocks contain areas of greater than 1-2 mm by 500 µm–1 mm in diameter of a white matrix made up of fungal sporocarps.

2a.3 Jurassic locality, Suture Bench, Antarctica

2a.3.1 Chapter 7: Jurassic tyloses

The studied specimens were collected from slope debris directly underneath the base of the lava flows. The three permineralized axes used in this study were collected during the Ninth German Antarctic North Victoria Land Expedition (GANOVEX IX 2005/2006) on Suture Bench, a small bench east of the Gair Mesa in northern Victoria Land, Transantarctic Mountains, East Antarctica. At this site, *in situ* tree trunks occur within the early Toarcian (late Early Jurassic) Kirkpatrick lavas of the Ferrar Group (Figure 3) (Bomfleur et al., 2011).

2b. KU specimen and slide numbers used in this study

2b.1 Chapter 3: Vertebraria *mycorrhizae*

Specimens and slides are deposited in the Paleobotanical Collections, Natural History Museum and Biodiversity Institute, University of Kansas (KUPB), under specimen accession numbers 15491G bot, 15685 A, slide accession numbers 23172 and 23214, and thin section slide accession numbers 26831–26385. Slides of extant *Metasequoia glyptostroboides* specimens used for comparison are housed in the University of Alberta Paleobotanical Collections (UAPC-ALTA).

2b.2 Chapter 4: Notophytum *mycorrhizae*

Specimens and slides are deposited in the Paleobotanical Collections, Natural History Museum and Biodiversity Institute, University of Kansas (KUPB) under specimen accession numbers 26590, 30000-30007.

2b.3 Chapter 5: Ashicaulis *microorganisms*

Specimens and slides are deposited in the Paleobotanical Collections, Natural History Museum and Biodiversity Institute, University of Kansas (KUPB) under specimen accession numbers 17608 A-DD. 30626-30658.

Extant *Osmunda* slides: Acknowledgement and thanks to M. A. Gandolfo Nixon and J. L. Svitko (Ithaca, New York) for permission to use images from the Cornell University Plant Anatomy Collection (CUPAC; http://cupac.bh.cornell.edu/) of *Osmunda* rootlets (619-621).

2b.4 Chapter 6: Permian wood fungi

Specimens and slides are deposited in the Paleobotanical Collections, Natural History Museum and Biodiversity Institute, University of Kansas (KUPB) under specimen accession numbers 30659-30712.

2b.5 Chapter 7: Jurassic tyloses

Specimens and slides are currently deposited in the Paleobotanical Collections, Natural History Museum and Biodiversity Institute, University of Kansas, under specimen accession numbers GIX-SB-007; GIX-SB-014; GIX-SB-036, acetate peel slide accession number AP-GIX-SB-007-CT2-01, and thin section slide accession numbers TS-GIX-SB-007-01; TS-GIX-SB-

036-01; TS-GIX-SB-036-02. Additional specimens used in this study but not figured in this report are under the thin section slide accession number TS-GIX-SB-014-01.

2b.6 Chapter 8: Glossopteris *leaf fungi*

Specimens and slides are deposited in the Paleobotanical Collections, Natural History Museum and Biodiversity Institute, University of Kansas (KUPB) under specimen accession numbers: This study also utilized slides from H. A. McManus thesis, 15312-15375 and 19967-19969. 30713-30745.

2b.7 Chapter 9: Endochaetophora *leaf litter fungi*

Specimens and slides are deposited in the Paleobotanical Collections, Natural History Museum and Biodiversity Institute, University of Kansas (KUPB) under specimen accession numbers: 11521 C bot, C top, D bot; 11891 B1 base; 17683 C bot, C top, D bot, D top, E bot, H bot; 17695 C bot, D top; 17729 E bot, E top, F top; 17738 B top, D top; 17779 E bot; 17892 E top, G top, J top; 18021 B bot, C top; 18026 A, B bot, B top, C bot, C top, D bot, D top, E top, F top, G; 18041; 18042; 18043; 18044; 18084 A, B top, E bot, F1 bot, F2 bot, F2 top, F4 bot, F5 top, G1 bot, G2 bot, G2 top, G3 top, H1, H2, H4. Slides: 30746-30761.

3. Petrographic thin section preparation and protocol

3.1.1 Acetate peels vs. thin sections

Thin sections have been extensively used in geological studies, specifically mineralogy, petrography, etc. (Williams et al., 1982) The process of producing a thin section is arduous, but often produces a rewarding result. In recent years the study of permineralized fossilized plant material using paleontological thin sections has gone through a period of resurgence. Original

descriptions of permineralized plant specimens was based initially on paleontological thin sections (e.g., Williamson, 1874; Hick and Cash, 1884), and later generally replaced by the cellulose acetate peel technique (Joy et al., 1956). The process of permineralization is so rapid in certain deposits, such as Antarctica, that even ephemeral structures (e.g., some extant arbuscules last only 4-5 days, (Tooth and Miller, 1984; Bouffant et al., 2009) such as arbuscules are preserved.

Cellulose acetate peels utilize far less of the fossil plant specimen and can be rapidly produced. Historically, fungi and other microorganisms were thought to be too delicate and fragile to be sufficiently preserved (Taylor and Krings, 2010). This resulted in a form of preparation and technique bias that has masked the actual diversity of fungi that is present in the fossil record. More recently, however, it has been shown that the acid etching process sometimes destroys the fine microstructure of fungi and other microbial organisms (Taylor et al., 2011). Of perhaps more importance is the fact that when using acetate peels fungi and other microorganisms present in the matrix, as well as in the lumen of cells, are simply lost in etching process involved in the preparation of peels further reducing the opportunity to examine the potential diversity.

One of the most important uses of thin sections in paleobotanical studies is the unique investigative use of three-dimensionality with minimum specimen loss. This is extremely advantageous when studying fungi, including hyphae. It is possible to view how the hyphae extend through cells, both intra- and intercellularly. This is in contrast with acetate peels, whereas in peels, one is typically limited to a two-dimensional structure. While looking through the microscope, one can focus through the specimen and see anatomical and morphological features that may have been lost in the etching process. However, there are many trade offs to this method. First, thin-sections are extremely labor intensive compared to acetate peels. Second,

specimen loss, depending on the thickness of the blade, approximately 1 to 1.5 mm of material can be lost through the kerf of the saw blade. In addition, in order to allow transmitted light through on a microscope, one must grind away micrometers and even millimeters of rocks in order to achieve the desired thickness. Third, if a thin section is damaged, i.e., dropped, epoxy begins to dissolve over time, the thin section of the specimen is broken, etc., these specimens are irreplaceable. Unlike acetate peels which can be easily fixed to slides again.

3.1.2 Acetate peel protocol

Blocks permineralized by silica were sectioned into slabs using a conventional geologic rock saw. The cut surfaces of the slabs were then hand-polished smooth using an aluminosilicate grit on a piece of glass. The smooth surfaces were then etched 49% hydrofluoric acid for 1-5 minutes depending on the rock and strength on the acid. The slabs were then neutralized in a concentrated solution of aqueous sodium bicarbonate for approximately one hour. Slabs were then transferred to a warm water bath to remove any of the sodium bicarbonate that remained after the neutralizing phase. After drying, the etched surface of a slab was flooded with acetone and a sheet of cellulose acetate was rolled onto this surface. The acetone was allowed to dissolve the cellulose acetate sheet, causing the sheet to surround the plant remains standing in relief on the rock surface. After 15–20 minutes, the cellulose acetate sheet harden around the plant remains. The sheet can then be removed from the rock for analysis in reflected light (e.g., Joy et al., 1956; Galtier and Phillips, 1999).

3.2. Petrographic thin section protocol

The following section can be used as a protocol and guide for petrographic thin section preparation. Although it is written specifically for paleobotanical and paleomycology specimens,

it can be used for standard geological or mineralogical studies. It is also specifically written for use on a Buehler Petrothin® Thin Sectioning machine.

3.2.1 Selection of fossil material

During the early stages of this project the focus was directed at the mycoflora of the Permian and Triassic of Antarctica. Thus, small portions of larger blocks that had fallen off while being cut and processed were used for thin section preparation. Although there is an abundance of fungal fossils within the peat material, this "blind search" approach does not necessarily guarantee that an investigator will find or identify any fungi. It is recommended to look through acetate peels of cut blocks first to locate specific plant organs (e.g., one has an idea of what fungi they are looking for such as stem specific fungi or root specific fungi) different matrices, or target areas of study first before investing the time into making a thin section. Peels do not typically have the appropriate resolution needed for fossil fungi studies, but is an addition record of the specimen if the rock is damaged during the thin sectioning process. One point to keep in mind is that the area of interest must fit on a microscope slide, thus if it a large target area, then multiple slides must be used. It may be necessary to make preparation that utilize larger slides (>5.08 x >7.62 cm), but they are difficult to prepare to achieve a consistent thickness.

3.2.2 Size and types of rocks

The size of the rock prepared for thin section is initial and important step. It is obvious that the rocks have to fit on the microscope slide glass, however preservational type, shape and height are also other important factors. The type of rock used in this study is permineralized peat. Other types of preservation, such as compressions, may be thinned to prepare sections. However, one

should embed compression type material in epoxy before thin sectioning due to the fragility of the sample. Shape is another important factor for specimen selection. A rock with numerous jagged edges and uneven features will take longer to prepare. Thus, a specimen that is flat on the side of desired study would be ideal.

Finally, height is another important, yet seemly trivial, consideration. This is especially important for use of the Buehler Petrothin® machine used to make the initial section. The maximum height for a specimen (not including glass) is 3.5 cm. Otherwise, the sample will not make the necessary clearance between the saw blade and grinding wheel. If this height limit is unavoidable, then one is limited to absolute maximum height of 4 cm, one can set the saw increment gauge to the lowest setting 0.00. Then, it can cut the section to have a thick wafer of ~4-5 mm, and then subsequently cut the thick wafer to ~100 μm. This process will require two cuts and one will lose additional material through these multiple cuts. However, you are left with two wafers for additional sectioning, both with a flat surface and will make the clearance of the Buhler Petrothin®.

3.2.3 Size and types of glass

The type and size of glass is another significant consideration for the preparation of thin sections, as the glass microscope slides will be the platform for the thin section. Thick glass slides, i.e., those with a thickness of 0.5 mm or greater, have both positive and negative limits. Benefits of using thick glass slides include the fact that thicker glass is less likely to break during the initial cutting of the wafer stage. However, the cons greatly out-weigh the pros. Thick glass microscope slides are extremely uneven, and it takes a lot more grinding to produce a level, even surface. The gradients on thick glass slides can range up -/+ 400 μm, which would inevitably result in an uneven thin-section. In addition, the thick glass sections need additional preparation

for thin section use, such as beveling the sides of the glass. Custom microscope slides from a glass company are typically unbeveled and one can bevel the sides on the Hilquist machine, however, this takes additional time and effort. One can request the sides of the glass to be beveled but this is at an additional cost. The thick glass microscope slides can only be used on the Hilquist thin sectioning machine and thus restrict the type of thin section machine which can be used. Lastly, the microscope slides are very difficult for collections and archival proposes because the slides are too thick for typical slide boxes, and thus custom boxes must be produced.

It is clear that normal, thin microscope slides are the best choice for thin sections. There is less depth, and a lesser chance for gradients from end to end. The thin glass slides can also be used on virtually all thin sectioning machines. Finally, thin glass slides are easy to archive and manage in a paleontological collection. All microscope slides are inherently uneven with gradients from +/- 5-15 μm, thus "frosting" the glass is recommended (see section 3.2.6).

3.2.4 Hilquist vs. Buehler Petrothin machine

Thin sections are prepared on specialized instruments. Two of the most common are Hilquist and Buehler Petrothin®. There are numerous differences between the Hilquist and Buehler, each share commonalities as well as advantages and disadvantages. The Hilquist machine can grind both thick glass and thin (or normal) microscope slides. The Hilquist is also good for grinding down the edges of glass. In addition there is more flexibility on the Hilquist machine that allows one to readjust the slide horizontally or vertically in the chuck in order to cut or grind specific areas of the sample. However, the Hilquist system lacks precision and thus cannot give precise incremental adjustments for cutting and grinding. In addition, there is no secure locking mechanism for the glass slide, and thus during grinding the slides can easily slip out and break, not only damaging the specimen but potentially also the person working on the machine.

The Buehler Petrothin®, is a highly sophisticated thin-sectioning machine. It is made specifically for thin-glass microscope slides, but can accommodate many sizes and variations, such as 2x3", 1x3", 1x2" slides based on the alignment of pins in the chuck. It also has a micrometer for precise cuts and measurements on the saw and grinding wheel. This is an invaluable feature because this gives the machine user precise measurements and even surfaces when cutting. In addition, the vacuum on the chuck is also extremely helpful, because it not only keeps the slide on the chuck but when the glass does break, the glass does not shatter everywhere. Disadvantages of the Buhler Petrothin include limited height of the sample due to the distance between the chuck and the blades, difficulty seeing progress of the specimen (i.e., no internal light source to monitor thin section in preparation), and lack of orientation on the chuck, where one cannot turn the section vertically or horizontally.

3.2.5 Preparation of rocks

The most important aspect of rock selection for thin section preparation the rocks are small enough to fit the microscope slide used, i.e., between 2.54 to 5 cm by 5 to 7.6 cm, as well as have enough clearance for the blades on the Buehler Petrothin, less than 3.5 cm in height (Figure 4a). Specimens can be cut down to desired size using the table handsaw or the Buehler Isomet low speed saw, 11-1180-160. It is important to take note of any fractures within the rock because these cannot only break while initially sizing the rock, but more importantly while cutting the rock on the thin section machine, which will damage or destroy the thin section.

Once the specimen is cut to the desired size, the surface of the specimen that will be studied or adhered to the glass must be a smooth and even surface. In order to achieve this even surface, the rock must be either ground down by hand or on a circulating wheel with grit, e.g., a pottery wheel. If the surface is severely uneven, then it is recommend to use 100 grit, i.e., silicon

carbide or carborundum, on a circulating wheel or by hand on a glass plate. However, it is recommended to finish the surface of the rock with either 600 or 1200 carborundum grit in order to have as smooth of surface as possible. It is also imperative to clean or remove all of the grit from the sample because it will obscure the view through light microscopy, or not allow the epoxy to set fully, thus damaging the thin section while cutting the specimen on the thin section machine.

3.2.6 Preparing the microscope slides and frosting the glass

One step that is optional but also recommended when preparing microscope slides is removing a corner of the slide for orientation purposes (see Figure 4b inset). This can be achieved by grinding down a corner of the glass on the Hilquist lapping wheel. This step is helpful for orienting the slide during "frosting" on the chuck on the Buehler Petrothin, as well as keeping the same position for the slide for working on the specimen, as well as for orientation on while studying the finished slide on the microscope and is crucial for maintaining the coordinate system (see section 4.2).

"Frosting" or grinding the glass to make it a rough surface serves two purposes: (1) it creates a uniform and even surface because microscope slides when manufactured are uneven, even small variances in the glass, e.g., -/+ 5 μm variation, can greatly affect the finished thin section, (2) it creates a semi-rough plane that allows more surface area for the epoxy to adhere between the sample and the glass. It is highly recommended to frost the glass on the thin section machine, specifically the Buehler Petrothin. Using the micrometer, set it to where the grinding cup wheel is barely touching the surface of the glass. Because all microscope glass slides have slightly different surface, this micrometer setting will be different depending on the thickness of the glass. Once the machine is set to where it is barely touching the surface of the glass, it is

recommend to increase the setting between 10-20 μm in order to grind or frost the glass. Be sure to record this number for the set of microscope slides because this will be tarred-out or 0.00 point for when the specimen is in the finishing steps of grinding it on the cup wheel (Figure 4b).

After the glass is frosted, it is suggested that when marking or labeling the slide to match the specimen number. The easiest place to mark or label the slide is on the opposite or unfrosted side with a diamond tip tool. It is often difficult to discern any markings on the frosted side of the glass, as well as impacts the adhering the specimen to the glass step.

3.2.7 Adhering rock specimen to glass

During the initial stages of this study, Ward's Bio-Plastic® was used as the epoxy for thin sections using thick glass. However, after continuous grinding it was noticed that not only did the epoxy begin to separate from the sample during the final grinding stages on glass as well as during storage of the specimen. Therefore, Ward's Bio-Plastic® discontinued because it was not archival and also not intended for use of thin sectioning. It is useful for embedding specimens and keeping specimens intact that will not be thin sectioned.

To date, Hilquist thin section epoxy A-B has been found to be the most effective adhesive for thin sectioning. It is a high bond strength epoxy used for cementing rock chips to slides. It is a two part epoxy that uses 7:3 ratio, A:B.

Once rock specimens are initially prepared, cleaned, and microscope slides are frosted and labeled, the rock specimen can be adhered to the glass. One of the problems with Hilquist A-B epoxy is the number of bubbles that are produced while mixing the epoxy together. Incorporating air into the epoxy creates bubbles which obscures the view of specimens under high magnification in transmitted light. Therefore to eliminate such bubbles, we have heated up the slides and rock specimens on a heat plate at approximately 100º F. The specimens and frosted

portion of the slides are wiped down and cleaned with ethyl alcohol, pure (200 proof, anhydrous, ≥99.5%; CH_3CH_2OH) and placed area of interest down on the heating plate, and the frosted side of the glass face up. After approximately 10 min on the heating plate, a thin layer of epoxy applied to the rock specimen and then immediately placed on the frosted portion of the slide. Best results are attained by holding the specimen in place on the slide (caution, it will be hot, so wear gloves) until it is set and does not move, ~30 seconds. The heat from the rock and the slide will make the epoxy much more viscous, and the rock samples will move easily. If desired and possible, place lead weights on top of the specimens in order to eliminate micro bubbles. For the next 1 to 2 hours, monitor the newly adhered samples to make sure the rock specimen does not slide off of the microscope slide. The epoxy takes approximately 2-3 days to fully set and cemented at room temperature, or but this process is typically expedited using higher temperatures such as the heat plate (Figure 4b).

3.2.8 Cutting the rock specimen on the Buehler Petrothin thin section machine

Due to the hardness of the peat blocks, the amount of time to cut these rocks can range from 30 min to 2 hours, with the average rock size in length ~2 inches and height of ~1 inch. Rock hardness will greatly affect the time it takes to cut and grind rock samples, for example silicified cherts such as Rhynie Chert or Skaar Ridge material can take up to 2 hours for cuts on the Hillquist, but typically 30 minutes on the Buehler Petrothin. In contrast, other silicified cherts such as Fremouw Peak take about 5-10 min on the Buehler Petrothin, while calcium carbonate coal balls only take 2-5 min for initial cuts.

After placing the specimen now adhered to the slide into the vacuumed pressured chuck on the Buehler Petrothin, the micrometer must be set before the initial cut. The initial cut typically results in the rock sample at a ~250 μm thickness (Figure 4c). The setting on the micrometer is

dependent on the thickness of the glass, however, it is important to note that the micrometer measurement on the cup wheel (or the initial tarred out number for the glass). Typically, a setting of "3.0" on the diamond blade micrometer yields a ~250 µm measurement. Also, it is imperative to factor in the thickness of the glass, thus a "2.5" setting will not yield 250 µm wafer, but possibly a 150 µm wafer (i.e., depending on the thickness of the microscope slide); as well as the kerf of the diamond blade. Also, do not make the initial cut the final cut. Set the micrometer for a final 50-65 µm thickness; the diamond cutting blade is not as accurate as the cup wheel and will likely result in a complete loss of the specimen. Speed is also an important factor while cutting a large portion of the specimen off; a slow steady speed is best. Cutting too rapidly will result in placing too much strain on the diamond blade and will crack or break the thin section. The reader is referred to the Buehler Petrothin instruction manual for how each of these micrometers function.

3.2.9 Grinding the thin section on the cup wheel

The resulting thickness of a thin section is largely dependent on the grinding the section on the cup wheel. The micrometer should be tarred or zeroed out based on the thickness of the glass, i.e., the same measurement as the frosting of the glass. After the micrometer is set for the baseline of the glass, the micrometer should then be reset so that the cup wheel is barely touching the surface of the thin section; this should be a negative number. From this micrometer setting, then the subsequent, slow grinding process can begin. It is recommended to decrease the micrometer measurements by 30 µm at each pass, thus each pass of the cup wheel, you are removing 30 µm of material. The slower that the process takes place, the better the outcome and result of the thin section; depending on the hardness of the rock, a faster pass with the cup wheel will likely result in an uneven thin section or a "wedge" in the middle of the specimen. The

resulting thickness of the thin section is dependent on the area of study. Certain fungal specimens require thicker sections, i.e., studying the mantle or hyphal networks surrounding sporocarps, such specimens require a thickness of 150-200 μm. In contrast, other fungal specimens require thinner thin sections to study structures, such as mycorrhizal associations, i.e., arbuscules, hyphal networks within roots or fungal infections within wood, thus a section of 50-60 μm (Figure 4d). These sizes are in contrast to petrographic thin sections for geological studies which are usually ground down to a desired thickness of 30 μm, while paleontological thin section are thicker, typically 50 μm or greater. As a rule, as the thin section is ground down via the cup wheel to a thickness of 200 μm, it is imperative to remove the section from the machine and constantly check thickness using a microscope. This is the most difficult step in the thin section process because it is easy to damage a thin section by grinding down on the cup wheel too rapidly, thus either resulting in a wedge, or complete loss of the thin section.

3.2.10 Final steps - grinding and polishing by hand

Finishing thin sections by hand is usually an essential step (Figure 4e), especially if a "wedge" or uneven thin section has been produced while using the machine (Figure 4f). If there is an area of the thin section that is thicker than the majority of the section, polishing or grinding by hand is the best method to rectify this problem. Using 600 silicon carbide grit on a glass plate, with the thin section (i.e., sample side down), and putting pressure on the particular area that is thick will eventually thin the section to an overall thickness (Figure 4g). This can be a laborious process, thus the slower the better. It is also imperative to continuously check the thickness of the thin section, because similar to the Buehler Petrothin, it is easy to have complete loss of a specimen. The "wedge" is one of the most difficult obstacles to overcome and eliminate while

making thin sections; practice and a slower pace, i.e., the slower the better, with thin sectioning techniques will reduce the likelihood of a resulting “wedge” in the thin section.

This process can either be completely done by hand or with the use of a specially manufactured acrylic slide holder for the KU Paleobotany Lab. Benefits of this slide holder is the even distribution while grinding and ease of holding the slide while grinding. Negatives include that if there is a specific area that requires pressure while grinding, the slide holder cannot be used. Additionally at this final step of thin section processing, is not recommended to use the rotating wheel or pottery wheel for final grinding steps; due to the speed of the pottery wheel, it will crack or break the slide, and/or grind the slide to complete specimen loss.

4. Microscope image processing techniques

Images of thin section, fungal specimens require attention to a variety of different factors due to the variation of thickness of the thin sections, including lighting and location of the organisms in study. Many of the microorganisms can range in size from 1 to 500 μm, and the smaller organisms are difficult to relocate on a slide, thus diligent notes and location information is crucial. Due to this variation of thickness and the three-dimensionality of fungi and fungal-like organisms within these sections, post image processing is often required.

4.1 Lighting and filters

Due to the variation of thickness of an individual thin section as well as the ample presence of minerals (in contrast to acetate peels where the mineral content was dissolved during the etching process), lighting and filters should be taken into consideration while examining in transmitted light. Digital images can be taken with a Leica DC500 digital camera attachment. Using a white filter while taking images of thin sections is essential. If a proper filter is not

available, then a sheet a plain white paper can be used as a substitute. The paper can be placed under the slide on the stage of the microscope. The filter or white paper is useful in avoiding a vignetting effect while focal stacking images (see section 4.3.1) (Figure 4h).

4.2 Coordinate system

Because of the variability in the size, microorganisms are often difficult to relocate on a thin section or slide. Thus, one of the most beneficial and crucial steps in documenting fossil fungi is using a standard x-axis and y-axis coordinate system on a microscope stage. This practice is commonly used in palynological studies where similar to fossil microorganisms, small microscopic objects such as pollen and spores are difficult to find again (e.g., Holt et al., 2011). Therefore, through the use of the coordinate system on the microscope stage, one is able to find and locate the desired object again without delay even at high magnification. It is also recommended to either write the coordinates down for specific specimens in a lab notebook or within the file name of the image taken.

4.3.1 Focal stacking techniques

All digital images in this study were taken with a Leica DC500 digital camera attachment and minimally processed using Adobe Photoshop CS6 Version 13.0 x64 (1990-2012, Adobe Systems). Multiple micrographs of the same specimen at different focal planes were compiled to produce composite images (e.g., Bercovici et al., 2009). The images were stacked in Adobe Photoshop CS4 and specific areas were erased to reveal the full three-dimensional view that can be seen through the thin sections. Measurements were taken using ImageJ 1.43u software (Abràmoff et al., 2004).

When taking multiple images at different focal planes, it is important to maintain the same magnification and not to move the stage in the x-axis or y-axis direction. The only difference for focal planes is using the z-axis setting. Additionally, all of the light setting for the microscope must be consistent and all of the images must be the same pixel dimensions. Last, the order that the images taken is important; thus when naming the digital images, label them in a sequential order from the begging (lowest z-axis plane) to the end of the focal plane sequence (highest z-axis plane).

When importing images into Adobe Photoshop, using the example of 6 images to be focal stacked, import all 6 images into one file but with each individual image as a separate layer; with the first image in the focal stack sequence as the first layer, and the last image in the sequence as the last layer (Figure 5a). Hiding the 3rd through 6th layer (and all other layers not in use), there should be only two open or active layers while processing an area (Figure 5b). Selecting the second image/layer, one can either decrease the opacity of the layer by selecting "Opacity" and decreasing it using the slider arrows, or the preferred method of changing back and forth between layers by making this visible or invisible. Open the layer that is higher in sequential order, or the second layer in this example and select the eraser tool. The eraser tool should be an appropriate diameter for the area of interest and most importantly, should be: Brush mode, "Hard Round" with 53% Opacity and 57% Flow, these are all options that can be selecting using the eraser tool. This will provide a blurred eraser tool that is best used for blending two or more layers together. Then working on the second layer, begin erasing areas that are visible in the previous layer but not the in second layer, thus revealing the full three-dimensionality through all focal planes (Figures 6a, 6b). When finished with the second layer, make the third layer visible and repeat the previous steps until the last and final layer is finished. Eventually, the full effect of focal stacking will be revealed and a more complete image will be produced

(Figures 7a, 7b). It is important while focal stacking images, to only stitch together images from a sequence of images within a different focal planes of the same object, and not to change the object completely through too much image manipulation or processing.

4.3.2 Adobe Photoshop vs. Helicon Focus

There are specific programs that will automatically stack images together to make composite image results. One of these is the Helicon Focus 4.2.9 x64. Once a sequence of images at different focal planes is imported this program will digitally stitch them together to create a complete composite image. Several images are digitally focal stacked using Helicon Focus software (e.g., Method B, Radius 8, Smoothing 4) in order to study intricate areas of the specimens (e.g., Saupe and Selden, 2009). The positives with this program include the process is automated and quick, thus saving time as compared to stacking by hand in Adobe Photoshop. There are however, many negative aspects to using Helicon Focus. Unless each image is manipulated before being imported into Helicon, the user is unable to specifically target an area of interest. Thus other aspects of an image that are not desired would be incorporated into the final product. Additionally, due to variation in lighting between individual images, areas that are vignetted, especially images taking at high magnification, are often highlighted in the final result. Overall, although Helicon Focus is a useful program for the automated, quick process, and for areas of interest that are not complex, it is not recommended for the study of microorganisms that have a high level of detail in a particular area of study.

5. Analytical techniques and protocols

Paleomycological studies are in the early stages of integrating analytical techniques and new systems of methodology. One such analytical technique includes biomarker analysis.

Biomarkers can be any type of molecule indicating the existence, past or present, of living organisms (Olcott, 2005). Biomarker analysis can be useful when there is no detectable signs or symptoms of microorganisms on or in a specimen. In order to determine if a specimen is suitable for biomarker analysis, Raman spectroscopy can be conducted on a sample to detect if a specific highly modified type of carbon is present, which is required for samples to use in biomarker analysis. Raman spectroscopy is a non-destructive vibrational spectroscopy used to study the structure and composition of compounds; it relies on inelastic or Raman scattering of a monochromatic light, typically a laser in either the visible, near infrared or near ultraviolet range (Nasdala et al., 2012). Raman spectroscopy can be used a screening method to see if geologic material is suitable for biomarker analysis. Other spectroscopic techniques include Fourier transform infrared spectroscopy (FTIR) analysis, a technique widely used in the study of extant wood decay by fungi (e.g., Pandey and Pitman, 2003; 2004). FTIR is a technique typically used to obtain infrared spectra of absorption, emission, photoconductivity or Raman scatting of a solid, liquid, or gas (Marshall et al., 2005). One of the major advantages of FTIR is that the spectra is produced are organic compounds which have well defined frequency valves, which can easily discerned and referenced in a organic chemistry FTIR table (e.g., Lin-Vien et al., 1991).

5.1 Biomarker protocol

Numerous permineralized samples were prepared from Permian sites. All samples were processed serially, rather than in parallel, to avoid cross-contamination. About 50 g of rock was washed then sonicated in distilled water for ~10 s. Samples were air-dried at room temperature and crushed into <5 cm pieces with a jaw-type rock crusher that had been cleaned 4x each with acetone then dichloromethane (DCM). These large pieces were then sonicated with ~250 ml 9:1 DCM:MeOH for 2 minutes. Solvent was collected and rock pieces were crushed to <1 cm on a

smaller rock crusher cleaned as before. Ultrasonic extraction was repeated, and the sample was powdered in a shatter box that was cleaned by grinding quartz sand followed by 4x acetone and DCM cleaning.

The powdered rock was extracted in a microwave-accelerated reaction system (MARSXpress): 20 g of rock was split equally between 5 clean Teflon vessels, 25 ml of 9:1 DCM/MeOH was added to each vessel, and the samples were extracted at 100°C for 15 minutes with stirring. Extracts were filtered through combusted glass-fiber filters to remove particulates, and solvent was evaporated to ~30ml under nitrogen at 35°C, taking care not to allow samples to completely dry. Elemental sulfur was removed by filtration through activated copper (~3.5g, -40+100 mesh), and the S°-free extract was evaporated to near-dryness under N_2. Extract was transferred to a vial with hexane, solvent volume was reduced under N_2 to 100µl, and then analyzed by gas chromatography/mass spectrometry (GC/MS). Extracts from the two preliminary extractions were prepared and analyzed following the same procedures. All samples were analyzed on a ThermoFinnigan Trace GC-DSQ quadrupole MS equipped with a DB-5MS capillary column (30 m x 0.25 mm x 0.25 µm film thickness). 1 µl aliquots were injected into a PTV injector (35°C hold for 3 min, 14.5°C/s to 200°C then 12°C/s to 350°C with a 3 minute hold). The column oven was programmed at 20°C/min to 130°C, then 5°C/min to 320°C with a 20 minute hold.

After initial GC/MS analyses, each of the final extracts was separated into fractions by column chromatography. Polar compounds (mainly phthalates and other plasticizers) were first separated from hydrocarbons on 1.0g silica gel (100-200 mesh, 5% deactivated) dry-packed into Pasteur pipettes. Hydrocarbons were eluted with 3.75 ml 8:2 Hexane:DCM (F1) and polar compounds were eluted with 6ml 7:3 DCM:MeOH (F2). Saturates and aromatics were then separated on silica gel with 10% $AgNO_3$ dry-packed into Pasteur pipettes. Aliphatic compounds

were eluted with 5ml hexane (F1a) and aromatic compounds were eluted with 4ml DCM (F1b). The three fractions (polar, aromatic, aliphatic) were concentrated under N_2, and analyzed by GC-MS using the same conditions as above.

Laboratory blanks of the solvents, copper, silica gel, silver-impregnated silica gel and MARS vessels were analyzed, and a block of pre-baked basalt was spiked with a standard lipid solution and then subjected to the entire analytical procedure. No hydrocarbons, oil residues or UCM were observed in any of the blanks. Biomarker yields were confirmed with replicate extractions of several samples.

5.2 Raman spectroscopy

Raman spectra were acquired from each Permian wood sample using a Renishaw *inVia* Reflex Raman microprobe. A 325 nm wavelength line of an air-cooled Kimmon HeCd 20 mW laser was used to excite the samples, with a beam measuring 1 μm in diameter. UV excitation was used rather than green excitation at 514.5 or 532 nm, which is typically used for carbonaceous materials, in order to mitigate autofluorescence emission from such thermally immature organic matter. The Raman scattered light was dispersed with a 3600 mm/line diffraction grating, and the signal was analyzed with a Peltier cooled charge-coupled device (CCD) camera at room temperature (1,024×256 pixels). A Leica DMLM microscope coupled to the system, and two UV objectives (LMU x15/NUV 0.32 and LMU x40/NUV 0.50) were used to view and analyze the samples. A diamond sample was used to calibrate Raman shift at one accumulation for 10 seconds using the F_{2g} mode at 1332 cm^{-1}. Spectra were acquired using 100% laser power for one accumulation at an exposure time of 30 seconds. Spectra were collected from three areas of the spores and pollen grains (intracellular inclusion, cell lumen, and surrounding matrix) of three cells from each taxon. Raman spectra were normalized using Renishaw software

(e.g., Olcott Marshall and Marshall, 2015), converted to SPC files using Batch File Converter, and analyzed using GRAMS/32 software to obtain I_D and I_G values, as well as carbonate band positions. Additionally, GRAMS/32 software was used for the removal of cosmic rays, and several spectra were baseline corrected using Renishaw WiRE 3.3™ 158 software.

5.3 FTIR spectroscopy

Specimens of permineralized wood with signs of pocket rot, based on reports of previously described signs of fungal infected woods, were selected for analysis (Stubblefield and Taylor, 1986a; Stubblefield and Taylor, 1986b) were approximately 1 to 2 cm in width, by 2 to 4 cm in length, and 1 to 3 cm in depth and had clear signs of pocket rot 2 to 5 mm in diameter throughout the entire specimen. The samples were initially cut on a Buehler Isomet low speed saw, 11-1180-160 saw into wafers approximately ~2 mm in thickness. Wafers were then subsequently ground to desired thickness on a glass plate with 600 carborundum grit by hand. Measurements of wafer thickness were taken by a Mitutoyo Digital Micrometer H-2780. Due to the delicate nature of the wafers measurements were taken by: (1) recording the thickness of a standard transmittance light microscope slide, (2) placing the wafers on standard transmittance light microscopy slides, (3) then recording the thickness of the wafer and the glass slide together, (4) and finally subtracting the initial glass slide measurement. Using this method results in an accurate measurement of the wafer without damage to it by the micrometer accidentally crushing or chipping the sample. The wafers were ground unevenly on one side to produce a "wedge" shape on the specimen. The "wedge" or gradient of thickness from 2 μm at the thinnest point to 15 μm at the thickest portion, made it possible to examine and analyze different thickness of sample using FTIR analysis of the same specimen in order to compare and contrast which is the optimal thickness for a wafer for FTIR analysis.

Measured wafers were carefully placed via forceps into a beaker of DI water in order to clean and remove all dust and carborundum grit particles. Samples were removed from the beaker and subsequently placed in a desiccation chamber for three days to eliminate and evaporate all residual water. The wafers were then placed on an IR microscope slide and washed with ethanol as an additional cleaning step, but to also help adhere the specimen to the IR slide. Once the ethanol evaporated, the wafer was analyzed with FTIR spectroscopy.

5.3.1 FTIR spectroscopy protocol

IR spectra were measured using a Smiths Detection IlluminatIR IITM Infrared Microprobe coupled to a Leica DM 2500 microscope. The spectrometer uses a mercurycadmium-telluride (MCT) photoconductive liquid nitrogen–cooled detector and contains a KBr beamsplitter with a spectral range of 4000 to 650 cm21. FTIR microspectroscopic measurements were made using the reflection-absorption ARO objective (315, 0.88 NA). The aperture controls the size and shape of the region to be analyzed by the IR beam. An aperture area of 20 x 20 mm was used to collect the IR spectra, which gave adequate signal to noise ratios. The inferogram for the background and the microfossils were collected for 256 to 2000 scans over a spectral region from 4000 to 650 cm21 at 4 cm^{-1} spectral resolution. The spectrometer is controlled by SynchronizIRTM software. The spectra were exported into GRAMS/AITM software for further processing. Processing included converting the spectra into absorbance and baseline correcting them using a fifth-order polynomial.

5.4 Scanning Electron Microscopy (SEM)

A Versa 3D dual beam Scanning Electron Microscope/ Focused Ion Beam (FEI, Hillsboro, OR, USA) with a silicon drift EDX detector (Oxford Instruments, X-Max, UK) was

used to measure the surface morphology, elemental composition, and distribution of elements. All the SEM data reported were obtained at low vacuum of 0.53 Torr, acceleration voltage of 15kV, spot size 4.0 and the images were collected with a Low Vacuum Secondary Electron detector (LVSED). The elemental mapping and energy spectrums were acquired with Aztec tools (Oxford Instruments, UK).

Chapter 3

Mycorrhizal symbiosis in the Paleozoic seed fern *Glossopteris* from Antarctica

1. Introduction

1.1. Importance of mycorrhizal associations

Fungi are critical in modern ecosystems, where they fill many fundamental niches, e.g., as biotrophs, mutualists, saprotrophs, necrotrophs, and parasites (Dighton et al., 2005). All major phyla of fungi (i.e., Ascomycota, Basidiomycota, Blastocladiomycota, Chytridiomycota, Glomeromycota, and Zygomycota) occur in the fossil record and appear to be morphologically conserved organisms (Lucking et al., 2009). Moreover, paleontological evidence indicates many fossil fungi performed similar roles in the bio- and geosphere as they do today, including as key associates of photosynthetic organisms ranging from microalgae to Embryophyta (e.g., Pirozynski and Malloch, 1975; Selosse and Le Tacon, 1998; Krings et al., 2012). For example, extant plants are nutritionally limited by the bioavailability of many essential macro- and micronutrients in the rhizosphere, e.g., phosphorous, nitrogen, potassium, copper, and zinc (Marschner and Dell, 1994; Peterson and Farquhar, 1994). The availability of these nutrients is strongly dependent on the chemical state that can be readily metabolized by the plant and the pH of the soil. Fungal hyphae can secrete acids, thus chemically reducing the surrounding soil, which transforms nutrients into a useable form for the plant. Additionally, fungal partners are beneficial because they can explore surrounding soil at reduced carbon cost for the plant due the small size of hyphae in contrast to roots (Toljander et al., 2006). By definition, mycorrhizae are symbiotic (generally mutualistic) associations between a fungus and the roots (or thalli) of a

plant (Dickson, 2004; Kirk et al., 2008). The designation paramycorrhizae for colonization of thalli and shoot systems, and eumycorrhizae for colonization of roots has been introduced by paleontologists as a means to distinguish where colonization occurs in the plant since various organs containing symbionts pre-date the evolution of true roots (Strullu-Derrien and Strullu, 2007). Para- and eumycorrhizal associations occur in all extant plant groups, which include bryophytes, lycophytes, sphenophytes, pteridophytes, gymnosperms, and angiosperms (Wang and Qiu, 2006). The most widespread mycorrhizal type, the arbuscular form, involves the fungal group Glomeromycota, a phylum that comprises about 200 morphospecies within 26 genera (Oehl et al., 2011; Stürmer, 2012); traditionally these fungi have been distinguished by features of the spore wall, mode of spore formation (Morton, 1988), and the use of molecular markers. This group of obligate mutualists is characterized by the presence of coenocytic mycelia, asexual reproduction through sporogenesis at the hyphal tip, and the production of arbuscules (Redecker and Raab, 2006; Schüssler and Walker, 2011). *Glomus* is the largest genus in the phylum with more than 70 species formally described to date (Schwarzott et al., 2001; Schüssler and Walker, 2011). One of the most distinct morphological features of *Glomus* sp. is the production of vesicles (lipid storage) and arbuscules within roots; other genera, such as *Gigaspora* and *Scutellospora*, form arbuscules within roots but lack vesicles (Redecker and Raab, 2006). In the glomeromycetes, the arbuscule is the point of physiological exchange between the plant and fungus, i.e., the plant receives the accessible form of nutrients and the fungus receives carbohydrates (hexoses) that are then converted into glycogen (Peterson and Farquhar, 1994; Smith and Read, 2008).

Arbuscules can be further divided into two morphologic groups: the *Arum*- and *Paris*-types. *Arum*-type arbuscules are highly dichotomized structures that are produced via the trunk hyphae in the lumen of a cell. Conversely, *Paris*-type arbuscules are coiled structures that grow

in the root cortex intercellularly (Dickson, 2004); however, it has been demonstrated that the same fungus can produce either morphology depending upon on the host plant (Gerdemann, 1965; Brundrett and Kendrick, 1988, 1990). The term arbuscule literally translates to "small tree." Since the *Paris*-type morphology is represented by hyphae that do not dichotomize, we will refer to the *Paris*-type as mycorrhizal hyphae rather than arbuscules, although they are functionally equivalent to highly branched arbuscules.

1.2. Glossopteridales — Vertebraria

The Glossopteridales are a group of late Paleozoic seed ferns that were the dominant floral component of the Permian in Gondwana. *Vertebraria*, the anatomically distinctive root of *Glossopteris*, consists of a central zone of exarch primary xylem surrounded by two to eight radiating arms of wood, each separated by distinct lacunae (McLoughlin, 1992; Neish et al., 1993; Decombeix et al., 2009). The secondary xylem can be continuous near the periphery of the axis and typically contains distinct growth rings; a narrow band of periderm surrounds the zone of secondary xylem. In longitudinal section, the secondary xylem wedges are connected at varying intervals by transverse segments of wood that have been termed platforms, and these commonly contain a trace to a lateral root (Decombeix et al., 2009). A few crushed parenchyma cells have been identified in the hollow areas between the xylem arms and the platforms; cells are only present at early stages of development, and are essentially empty during later stages (Neish et al., 1993). Young *Vertebraria* rootlets are distinguished by the presence of an intact cortical layer and lack of secondary xylem (Neish et al., 1993; Decombeix et al., 2009). Although the vegetative and some of the reproductive organs of the Glossopteridales from Antarctica have been described (e.g., Taylor et al., 1989b; Pigg and Taylor, 1993; Ryberg, 2009;

Ryberg et al., 2012), the fungal associations with these plants have not been studied in great detail (see below).

1.3. Antarctic Permian fungi

There have been a few reports of fungal remains from the Permian of Antarctica (e.g., Schopf, 1970; see Fig. 4. Permian Fungi in Taylor and Taylor (1997); Holdgate et al., 2005; Slater et al., 2012; 2013; 2014), including forms interpreted as parasitic chytrids and Glomeromycota-like chlamydospores (García Massini, 2007a, 2007b). To date, the only accounts of fungi associated with the Glossopteridales are three reports of wood-decaying fungi, in the form of fungal fragments such as hyphae in the secondary xylem of mature *Vertebraria* roots (Stubblefield and Taylor, 1986; expanded upon in Chapter 6 of this dissertation), and stem wood attributed to *Araucarioxylon* (McLoughlin, 1992) or *Australoxylon* (Weaver et al., 1997). The present paper expands the current knowledge of fungi associated with the Glossopteridales with the description of the first mycorrhizal association in roots of *Vertebraria*. Additionally, it provides the first evidence of mycorrhizal associations in Paleozoic seed ferns and the earliest account of *Paris*-type mycorrhizae in the fossil record.

2. Systematic paleomycology

Phylum: Glomeromycota C. Walker et Schüssler 2001.

Genus: *Glomites* Taylor, Remy, Hass et Kerp emend.

Type species: *Glomites rhyniensis* Taylor, Remy, Hass et Kerp 1995. MycoBank number: MB17290.

Emended diagnosis: Fossil mycorrhizal fungi similar in basic morphology to modern Glomus; vegetative hyphae aseptate to (sparsely) septate, with H-, Y- or right-angle branches; spores glomoid, occurring singly, in loose aggregates or dense clusters (possibly sporocarps?), usually within the roots or rhizomes of plants; vesicles and arbuscules may be present.

Remarks: As was often the practice in the past for fossil diagnoses, there is no separate diagnosis of the genus in the original account on *Glomites* (Taylor et al., 1995). Rather, the diagnosis for *Glomites* is indicated as being the same as the diagnosis for the type species *G. rhyniensis*. This, however, makes it impossible to describe additional species for *Glomites*. Moreover, the diagnosis for *G. rhyniensis* includes such precise indications as spore size, hyphal diameter and features of the arbuscular structures, which are too detailed for an adequate generic diagnosis. We, therefore, have provided a broader generic diagnosis for *Glomites* in this paper.

Species: *Glomites vertebrariae* C.J. Harper, T.N. Taylor, M. Krings et E.L. Taylor nov. sp.

MycoBank number: MB803219.

Species diagnosis: Endomycorrhizal fungus; hyphae knobby, intra-cellular, serpentine to helical, in some cases sinuous; transverse septa present; branching dichotomous, sporadically with swellings; within individual cells serpentine to helical hyphae ~4–5.5 μm in diameter, forming structures similar in morphology to the physiological exchange structure seen in some extant

Paris-type mycorrhizal fungi; intracellular vesicles ~10–30 μm in diameter, pyriform to globose, terminal, septum absent at base of vesicle.

Etymology: The specific epithet "*vertebrariae*" refers to the plant (*Vertebraria*) hosting the new fungal species.

Holotype (hic designatus): Slide 26831, Plate 1, Figs. 5–7; Plate 2, Figs. 8–12 this paper.

Repository: Paleobotanical Collections, Natural History Museum and Biodiversity Institute, University of Kansas (KUPB), Lawrence, Kansas, United States.

Locality: Skaar Ridge, Beardmore Glacier area, Queen Alexandra Range, central Transantarctic Mountains, Antarctica; 84° 49' 11.8" S, 163° 20' 37.0" E.

Age: Late Permian.

Stratigraphy: Upper Buckley Formation, Victoria Group, Beacon Supergroup.

Plant host: *Vertebraria* (Glossopteridales, Pteridospermophyta).

Description: The matrix containing the *Vertebraria* rootlets is a highly heterogeneous assemblage of permineralized peat. As noted above, the silicified peat contains numerous anatomically preserved specimens including various parts of the *Glossopteris* plant. Mature *Vertebraria* roots are easily recognizable by their characteristic air spaces; many

developmentally younger *Vertebraria* rootlets grow through these air spaces. We hypothesize that the mature, fully developed *Vertebraria* root was in place first, perhaps moribund or partially degraded, with the young *Vertebraria* roots growing through the air spaces secondarily. Rootlets range from 300 μm to 1 mm in diameter with an average of 800 μm (Plate 1, Fig. 1). Evidence of fungal colonization is visible in a majority of the rootlets, and only within the cortex, where they appear in both cross and longitudinal section (Plate 1, Figs. 2–4). A particularly conspicuous type of fungal hypha is found approximately between 3 and 4 cell layers below the epidermis and 2–3 cell layers from the vascular cylinder. These hyphae range from 3.5 to 5.5 μm in diameter and contain irregularly spaced, perpendicular septa. They typically extend through the cortical cells intracellularly (rarely intercellularly). Intracellular hyphae are typically of ubiquitous diameter on opposite sides of host cell wall; when constricted, hyphal diameter is ~3 μm. Some locally produce H branches (Plate 1, Fig. 5), but more commonly, they produce Y branches (Plate I, 6); all lack septa at the points of division (Plate 1, Fig. 7). Longitudinal sections also show evidence of the hyphae in the young cortical cells (Plate 2, Fig. 8). Cells containing the fungus are rectangular with rounded edges and approximately 50 μm long by 25 μm wide. These fungi are characterized by thick hyphae that average 5 μm in diameter (range = 4–5.5 μm; Plate 2, Fig. 9) and are often confined to a mycorrhizal zone that is 2–3 cell layers thick. They extend from cell to cell intracellularly, with no visible host responses at the point where the fungus penetrates the cell wall. Hyphae also produce numerous knobs and variously shaped swellings with no septum at the base of these structures (arrow in Plate 2, Fig. 9). The hyphae fill the cell lumen, by initially following the inner periphery of the cell and then forming large, loop-like coils in the interior of the cell prior to penetrating the adjacent cell (Plate 2, Fig. 10). These hyphae can occur singularly and tightly coiled (Plate 2, Fig. 11) within the cortical cells of the rootlets. Additionally, the hyphae that produce the coils also produce vesicles ranging from 10 to

30 μm long, and are typically oblong, elongate, and rarely globose. We have been unable to find distinct septa at the base of attached vesicles, although Plate 2, Fig. 12 (arrow) attachment site may also represent septa. Vesicles are typically found degraded and either attached to hyphae or isolated in the matrix (Plate 2, Figs. 12–14). The cell wall of these vesicles is thin, smooth, and shows no external ornamentation.

3. Discussion

The seed ferns, or pteridosperms, are an artificial, highly diverse group of vascular plants that spanned the Late Devonian to possibly the Eocene (McLoughlin et al., 2008; Taylor et al., 2009). Although many seed ferns have been studied in great detail based on impression/compression specimens and/or structurally preserved fossils, and are therefore well-understood today with regard to morphology and internal organization, there are few reports on interactions of these plants with fungi, specifically mycorrhizal fungi. At this stage we are uncertain as to whether this absence is the result of a failure to adequately appreciate the occurrence of fungal endophytes in roots, or simply that these organs have not been critically examined for these associations.

3.1. Justification of new species

To date, three other species of *Glomites* have been described, i.e., *Glomites* rhyniensis Taylor, Remy, Hass et Kerp (Taylor et al., 1995), *Glomites cycestris* Phipps et Taylor (Phipps and Taylor, 1996), *Glomites sporocarpoides* Karatygin, Snigirevskaya, K. Demchenko et Zdebska (Karatygin et al., 2006). Among these, *Glomites vertebrariae* is the only specimen that

does not have the *Arum*-type arbuscule morphology, and is instead characterized by hyphal loops similar to *Paris*-type morphology. The host plant is not in the species diagnosis because such fungi are morphologically indistinguishable between a range of hosts.

3.2. Comparisons with extant fungi

Paris-type mycorrhizal associations are broadly distributed among land plants including several groups of bryophytes and pteridophytes, Ginkgo, cycads, the conifers Podocarpaceae, Taxaceae, Cupressaceae sensu lato, and most flowering plant families (Simon et al., 1993; Taylor et al., 1995; Phipps and Taylor, 1996; Smith and Smith, 1997). There is also a wide range of variation in the degree of development of arbuscules from species to species (Smith and Smith, 1997). Studies of modern fungi suggest that arbuscule morphology is dependent upon the host plant; however, there are no modern analogs of seed ferns in extant ecosystems.

The morphology of the arbuscules and vesicles in the glossopteridalean *Vertebraria* roots described in this paper is strikingly similar to the *Paris*-type mycorrhizal fungus found in both fossil and extant *Metasequoia* roots (Konoe, 1957; Böcher, 1964; Rothwell and Basinger, 1979; Stockey et al., 2001). In extant *Metasequoia glyptostroboides* Hu and Cheng, 1948 (Hu and Cheng, 1948), *Paris*-type mycorrhizal hyphae occur in cortical cells but do not encompass the entire length of the root (Noldt et al., 2004), being restricted to a defined band at a specific level with the cortex longitudinally and radially (Plate 3, Fig. 15). These hyphae are morphologically similar to those found in *Vertebraria* relative to hyphal diameter, degree of coiling, and the presence of knobs (Plate 3, Fig. 16). Extant *Paris*-type mycorrhizal hyphae can also be found isolated and in very tight coils throughout the cortex (Plate 3, Fig 17). These extant fungi also

produce elongated vesicles of similar dimensions and shape to those of the Permian fungus (Plate 3, Fig. 18).

Like in the roots of modern and fossil *Metasequoia*, hyphae of the mycorrhizal fungus in *Vertebraria* appear to be primarily intracellular and are of the *Paris*-type morphology. Hyphal coils generally fill cells or are confined to the inner periphery of the cell wall, and arbuscules or mycorrhizal hyphae are both numerous and well developed. In extant *M. glyptostroboides*, *Paris*-type mycorrhizal hyphae can be found singly as in *Glomites vertebrariae* and do not appear to occupy a concise mycorrhizal zone. This is likely due to the ephemeral nature of arbuscules (Bonfante and Perotto, 1995) as these structures persist for only about a week at a time. Cross sections of the root at varying levels indicate that the *Paris*-type mycorrhizal hyphae are widely dispersed and may or may not be in close contact with vesicles. The hyphae of *Glomites vertebrariae* and the *Paris*-type mycorrhizal fungi of *M. glyptostroboides* are similar in having transverse septa. Although not common for glomalean fungi, it has been demonstrated that under certain conditions (e.g., damage, age, pre-penetration stages of colonization) both the intra- and extra-radical hyphae can become septate, (Gerdemann, 1955; Kinden and Brown, 1976; Giovannetti et al., 1993; Smith and Smith, 1997). Additional similarities include the production of hyphal knobs on the mycorrhizal fungi in both extant *M. glyptostroboides* and fossil *G. vertebrariae*. In extant fungi, such hyphal knobs have been hypothesized to represent the points of early branching. Other possible functions for these structures include increasing the surface area within a single cell, or perhaps representing the region of the hypha that will ultimately penetrate the cell wall. It is important to note that *Gigaspora* and *Scutellospora* sp. also produce hyphal coils and knob-like structures; however, those genera do not produce vesicles. Thus, as *G. vertebrariae* contains vesicles and hyphal knobs, we hypothesize that this may represent either a

fungus that does not show these morphological characters in extant material or may represent an intermediate form among genera, i.e., *Glomus, Gigaspora, or Scutellospora*.

3.3. Exclusion of dark septate endophytes (DSE) affinity

Dark septate endophytes (DSE) are a diverse group of ascomycetous anamorphic fungi that colonize root cells and tissues (Jumpponen, 2001). Based on the presence of the sparsely septate hyphae, *G. vertebrariae* superficially resembles extant DSE. Certain *Paris*-type mycorrhizal fungi, consequently, can produce sparsely septate intracellular hyphae (e.g., Bedini et al., 2000; Matekwor Ahulu et al., 2004; Wu et al., 2004). Additionally, due to an absence of several diagnostic morphological DSE characters as suggested by Jumpponen and Trappe (1998), we reject the hypothesis that the fungus in this study is a DSE. These characters include a superficial net in the root cylinder; *G. vertebrariae* is restricted to a specific zone in the root cylinder and does not produce a highly extensive hyphal net. The fungal hyphae are exclusively intracellular and typically hyphal diameters are consistent on either side of cell wall penetration (see Plate 1, Fig. 5) and therefore lack appressoria preceding penetrating hyphae in host cell walls as seen in DSE and penetration tubes. Finally, DSE commonly form microsclerotia and have not observed in the young *Vertebraria* rootlets to date. It is important to note that DSE and *Paris*-type mycorrhizal fungi can co-occur in host plants (e.g., Wubet et al., 2003; Kubota et al., 2004; Muthukumar et al., 2006; Dolinar and Gaberščik, 2010; Stevens et al., 2010), at this time there is no evidence for the DSE. Future studies of *Vertebraria* may elucidate multiple levels of plant–fungal interactions, including DSE.

3.4. Additional fungi in Vertebraria

There are several other types of fungal remains associated with the *Vertebraria* rootlets, including hyphae and spores. Hyphae are intracellular, occur within root cortical tissue, and do not appear to form coils like the hyphae described above; some of the hyphae are up to 9 μm in diameter (Plate 3, Fig. 19). The morphology of these structures is highly variable, ranging from upright hyphal branches (3–5 μm) to truncated, enlarged vase-like units (Plate 3, Fig. 20). We are uncertain as to the exact biological affinities of these hyphae; perhaps they represent some stage in the formation of coils, structures leading to the formation of mature vesicles, or some other type of reproductive stage. It is important to note that these structures are remarkably similar to the fan-shaped structures found in pteridophytes produced by certain endophytes (Fig. 38, Bonfante-Fasolo, 1984). The mycorrhizal status of these fungi remain unknown in extant studies. At this time we are uncertain if these morphologies are produced by the *G. vertebrariae* fungus. In addition, asexual spores, like those of certain glomeromycetes, are dispersed throughout the matrix, including some in close association with young *Vertebraria* rootlets. These spores range from 100 to 177 μm in diameter and are typically globose. A thick outer opaque wall, 5 to 7 μm thick, characterizes the spores. A few spores are pyriform with a blunt end—the likely site of hypha attachment. Rarely, do these spores contain a subtending hypha (Plate 3, Fig. 21). Generally these spores are devoid of contents; however, one specimen contains many spherical structures with an average diameter of 23 μm that are enclosed in a larger sphere (120 μm in diameter) within the spore wall (Plate 3, Fig. 22). This combination of structures inside the spore may represent evidence of some type of mycoparasitism. Additionally these spores are distinguishable from those described by García Massini (2007a, 2007b) due to their large size, thicker cell wall layer, absence of pore-like attachment scars, and are not found in tightly dense clusters.

3.5. Mycorrhizal associations in the fossil record

Evidence for mycorrhizal associations has been documented several times in the fossil record, with the oldest evidence coming from the Lower Devonian Rhynie chert (Remy et al., 1994a). Overall, it is difficult to assess ecological status in fossils, especially among plant–fungal interactions. Key factors attribute to the biotrophic or mycorrhizal status of a fossil host and symbiont, which may include: presence of chlamydospores, arbuscules, zonation or spatial restriction of mycorrhizae in roots, lack of host responses, preservation of material, etc. (Taylor and Krings, 2005). Although it is impossible to definitively demonstrate physiological interactions between fossil mycorrhizal fungi and plants, based on morphological evidence and other specific characters, it is clear that this type of symbiosis is a highly conserved relationship among the land plants.

Permineralized peats of younger age from Antarctica have yielded exceptionally well preserved arbuscules. The Middle Triassic cycad Antarcticycas hosts multiple types of endomycorrhizal fungi including *Gigasporites myriamyces* and *Glomites cycestris* (Stubblefield et al., 1987a, 1987b; Phipps and Taylor, 1996). *Voltzialean* conifer roots from the same Triassic silicified peat, including mycorrhizal nodules in the form of small spherical structures on delicate lateral roots, provide additional evidence of endomycorrhizal associations (Schwendemann et al., 2011), as well as endomycorrhizal fungi in non-nodular forming roots of *Notophytum* (Harper et al., 2015; Chapter 4 of this dissertation).

3.6. Endomycorrhizal associations in the Permian ecosystem of Antarctica

The Glossopteridales are known to have occurred in a variety of environments, ranging from peat-forming swamps to seasonally dry, sandy floodplains (Cúneo et al., 1993; Cúneo, 1996; Isbell and Cúneo, 1996). The *Glossopteris* floras of Gondwana are traditionally considered to dominate coal-forming environments (e.g., McLoughlin, 1993), although in Antarctica, this floral association appears to be more wide-spread in other depositional environments (Cúneo et al., 1993). Many authors have suggested that the unusual anatomy of *Vertebraria*, which incorporates air spaces into the wood, may signal an adaptation for wetland or peat-forming environments (McLoughlin, 1993). Today, mycorrhizal associations are recorded from a diverse suite of ecosystems ranging from polar regions to swamp environments in the tropics (Tawaraya et al., 2003; Newsham et al., 2009).

Although it is more likely that Permian peat-forming environments were similar to extant swamps or marshes, it has also been hypothesized that the air spaces in *Vertebraria* roots may have served the same function as lacunae of extant mangrove plants (McLoughlin, 1993; Neish et al., 1993). This may suggest that at least some glossopterids have grown in saline coastal habitats. Further supporting this hypothesis is the fact that arbuscular mycorrhizae do occur with mangrove plants in high-salt and other abiotically stressed environments (Sengupta and Chaudhuri, 2002). It is important to note that even in extant plant mycorrhizal systems it is not possible to conclusively demonstrate a physiological role of these mycorrhizal fungi. Nevertheless, structural and morphological evidence justifies interpreting these fungi-root cell interactions as a mycorrhizal association.

The ontogeny and development of *Vertebraria* roots and rootlets was no doubt reflective of the environment in which they grew (Decombeix et al., 2009). This structure–function relationship correlates well with the ephemeral nature and evidence of mycorrhizal associations in *Vertebraria*, in that young rootlets contain an intact cortex and mycorrhizal zone until

secondary growth occurs. The relationship is further underscored by the fact that arbuscules and vesicles have only been found within young rootlets with a well-defined cortex. This suggests that mycorrhizal associations are present in the young, developing rootlets that contain cortex and that the presence of such an association may have been critical in the promotion and early establishment of these plants in the peat-forming environment. It is impossible to know precisely the frequency of colonization of certain glossopterids with mycorrhizal associations, and whether such interactions occur only in particular environments. In extant plants, for example, fungi can shift from a mutualistic to parasitic relationship relative to a changing environment (Orcutt and Nilsen, 2000).

The high-latitude light regime of Antarctica during the Late Permian may have also influenced glossopterid mycorrhizal associations. Tree ring analysis shows that the *Glossopteris* plants of Antarctica are highly adapted to their environment (Taylor and Ryberg, 2007; Gulbranson et al., 2012). Under certain abiotic stresses, e.g., low light intensities, mycorrhizal associations can be too carbon costly and detrimental to plant growth and development (Bereau et al., 2000). Due to the high carbon cost of mycorrhizal fungi for the plant, at times of low light or absence of light periods, the plants may have freely disassociated from the fungus (Hoeksema and Kummel, 2003). In addition to the ephemeral nature of arbuscules, this may help explain the absence of mycorrhizal fungi in some *Vertebraria* rootlets. In contrast, it has also been suggested that only plants that are well adapted to extreme light regimes can provide carbon for the fungus (Koltai and Kapulnik, 2010). Nevertheless, in such an environment these mycorrhizal associations may have been the critical tipping point in allowing the glossopterids to out-compete other plants in these harsh environments.

4. Conclusions

Although fossil plants have been reported throughout large segments of geologic time, in recent years there has been increased attention on interpreting their role in the ecosystems in which they lived. Less well understood are the relationships between these plants and the microbial component of the ecosystem, especially the fungi. It has been demonstrated that among all extant plants there are three genes that are essential to the establishment of mycorrhizal symbioses (Wang et al., 2010). This implies that all extinct plant groups had the potential for forming various types of mycorrhizal associations. Thus, the paucity of mycorrhizal associations known thus far in the fossil record for certain groups (e.g., sphenophytes, progymnosperms, gnetophytes, gingkophytes) is likely due to the fact that these associations have not been identified, perhaps due to poor preservation of anatomical details in fossils of some of these groups. In this context it is important to document the occurrences of plant–fungal interactions when found because they provide insight into the evolutionary history of these associations and may provide a calibration point for the establishment of symbioses in particular plant lineages. The discovery of mycorrhizal associations in *Vertebraria* contributes to a more complete understanding of the biology of at least some members of the Glossopteridales, and represents the first documented occurrence of a mycorrhizal association with a seed fern.

Chapter 4

Arbuscular mycorrhizal fungi in a voltzialean conifer from the Triassic of Antarctica

1. Introduction

Belowground ecosystems incorporate highly integrated components that form complex and dynamic communities. For example, in forest ecosystems there are just as many abiotic and biotic interactions within the rhizosphere as there are above ground (Fitter et al., 2005; Wang and Qiu, 2006). Among these diverse rhizosphere interactions are mycorrhizal symbioses, the mutualistic relationship between a fungus and plant in which both partners benefit from the exchange of nutrients (Simard and Durall, 2004). This ancient intimate relationship has been suggested as a necessary preadaptation that made it possible for plants to colonize the terrestrial realm (Pirozynski and Malloch, 1975; Simon et al., 1993; Fitter et al., 2005; Bonfante and Selosse, 2010). Today, mycorrhizal associations are common among a large majority (i.e., an estimated >80%) of extant plant families, and include most bryophytes, lycophytes, pteridophytes, gymnosperms, and angiosperms (Simard and Durall, 2004; Wang and Qiu, 2006). Plant–fungal relationships closely resembling extant mycorrhizas with regard to structure and morphology have also been reported in several extinct lineages and species of plants, e.g., early land plants (rhyniophytes), arborescent lycopsids, seed ferns, cordaitaleans, (e.g., Remy et al., 1994a; Krings et al., 2007; Strullu-Derrien et al., 2009; Krings et al., 2011; Harper et al., 2013), and fossil representatives of living plant groups, including conifers and flowering plants (e.g., Lepage et al., 1997; Stockey et al., 2001; Beimforde et al., 2011).

Triassic permineralized peats from the central Transantarctic Mountains of Antarctica have preserved an exceptionally diverse assemblage of fossil fungi, including a putative

trichomycete (White and Taylor, 1989a), a basidiomycete (Osborn and Taylor, 1989), several examples of zygomycetous fungi (White and Taylor, 1989b; Krings et al., 2012), fungal "sporocarps" (White and Taylor, 1989c), and possible saprotrophic fungi in reproductive structures (Bergene et al., 2013). Moreover, glomeromycotan fungi involved in endomycorrhizal associations were reported in the cycad *Antarcticycas schopfii* (Stubblefield et al., 1987a, 1987b; Phipps and Taylor, 1996), and mycorrhizal root nodules in narrow rootlets of the voltzialean conifer *Notophytum krauselii* (Schwendemann et al., 2011). The latter taxon is among the most completely known anatomically preserved plants of the Triassic paleoecosystems in Antarctica (Bomfleur et al., 2013). It can be viewed as a model system for studies of paleoecology in Triassic Gondwanan ecosystems due to its abundance, distribution throughout Gondwana, and known descriptions of the morphology and anatomy of roots, stems, branches, trunks (i.e., *Notophytum krauselii*; Meyer-Berthaud and Taylor, 1991; 1992), leaves (i.e., compressions: *Heidiphyllum elongatum*, permineralizations: *Notophytum* leaves; Anderson, 1978; Axsmith et al., 1998), reproductive structures, i.e., seed cones (*Telemachus* sp. and *Parasciadopitys aequata*; Yao et al., 1993; Escapa et al., 2010), pollen cones (*Switzianthus* sp.; Anderson and Anderson, 2003; Bomfleur et al., 2011), and bisaccate pollen of the *Alisporites* type (e.g., Yao et al., 1993), as well as microbial associations (e.g., Bomfleur et al., 2013).

In this study we report a vesicular-arbuscular endomycorrhiza (VAM or AM) that occurs in non-nodular roots of *N. krauselii*. The fungal partner spreads through the intercellular system of the outer and middle root cortex and consists of aseptate hyphae, thin-walled vesicles, and intracellular arbuscules within a discrete zone of the host cortex. The discovery of an AM in addition to the mycorrhizal root nodules in *N. krauselii* is important because it provides evidence that different types of endomycorrhizal associations occurred within Antarctic voltzialean conifers. The mycorrhizal systems (simultaneously or alternately) may have contributed to the

system of adaptations that enabled these plants to survive in a high-latitude peat-forming environment as has been suggested of this part of the Antarctic continent during the Triassic.

2. Results: Fungi in *Notophytum krauselii*

The peat blocks used in this study contain abundant components attributable to the voltzialean conifers, including axes of *Notophytum krauselii* (Plate 4, Fig. 24) characterized by eustelic woody stems, roots of *N. krauselii* characterized by a distinctive *phi* layer suggesting the plants may have grown in a fluctuating water table environment (Millay et al., 1987; Taylor and Ryberg, 2007), permineralized *N. krauselii* leaves (Plate 4, Fig. 25), numerous *Alisporites* pollen grains (Plate 4, Fig. 26), and ovules of *Parasciadopitys* (Plate 4, Fig. 27).

Fossil roots in general are difficult to identify at any systematic level because the characters used to define them are relatively uniform. However, *Notophytum krauselii* roots and aerial axes/stems do share several anatomical features that make it possible to assign the roots with confidence to the stems, which in turn are correlated with other vegetative and reproductive organs (e.g., Meyer-Berthaud and Taylor, 1991; Escapa et al., 2011).

The thin sections prepared for this study are composed almost entirely of roots in various planes of section, which provide the opportunity to examine slightly different stages of development and to compare the anatomical features with those roots described previously and assigned to *Notophytum krauselii* (Meyer-Berthaud and Taylor, 1991; 1992; Bomfleur et al., 2013). This also makes it possible to trace the distribution of the fungus within the roots and to analyze where it occurs within the tissue systems. Mature roots contain a distinct zone of primary xylem, well-defined endodermis, secondary xylem, cortical tissues, and a poorly preserved and locally difficult to discern epidermis (Plate 4, Fig. 28). Mature roots, however, are rarely encountered in the peat blocks relative to the smaller, immature rootlets lacking secondary

xylem. The smaller rootlets occur singly or in distinct clusters (Plate 4, Fig. 29), vary from 0.5 to 5 mm in diameter with most between 1 and 2.2 mm; some are sectioned in a way to show well-defined apices. Generally, the stele of these rootlets is poorly preserved, but the endodermis is present; the cortex of smaller rootlets is approximately 4–6 cell layers thick, and appears similar to that in mature roots; the epidermis is difficult to discern.

More than 50 young *Notophytum krauselii* rootlets have been discovered that are characterized by a distinct, continuous zone of apparently more opaque cells positioned in the cortex approximately 3–4 cell layers below the epidermis. This zone is 2–5 cells thick and can readily be recognized in both transverse (Plate 4, Fig. 30) and longitudinal sections (Plate 4, Fig. 31) because of the concentration of fungi.

This zone within the root cortex appears more opaque because it is densely packed with multi-branched intracellular arbuscules attached to trunk hyphae, and sparsely dispersed intracellular vesicles positioned terminally on parental (branch) hyphae (Plate 5, 39). Prominent hyphae (~7 μm in diameter) are perpendicular, septate, and ramify throughout the zone (Plate 5, 32). It is interesting to note that evidence of this fungus has not been found in any cells of the stele, the cortical tissues outside of the distinct zone, epidermis, or in the surrounding matrix. However, a few rootlets host other hyphae that are generally larger (~15 μm diameter) (Plate 5, 33). These hyphae have not been found attached to vesicles or arbuscules, and likely represent another fungus present in the rootlet or represent trunk hyphae from which smaller lateral hyphae branch to produce arbuscules. At this time we can only speculate on the ecological affinity of the larger hyphal type. It is possible that this may represent a saprotrophic or parasitic fungus; however, we have no direct evidence to support this, i.e., degradation of the cell walls or host responses. There are amorphous structures within cells (see Plate 5, 45) that we have interpreted

as preservational artifacts or biomimetic structures, but may also represent remnants of fungal decomposition. The smaller hyphae are more common and produce right angle branches (Plate 5, Fig. 34), possible T- or cruciform branching (Plate 5, Fig. 35), Y-branching (Plate 5, Fig. 36), and anastomoses to H-junctions (Plate 5, Fig. 38); hyphae lack a septum at each division, but can produce septa after division or branching. In rare examples, the hyphae produce a swelling or an enlarged region with some of these structures separated by a septum (Plate 5, Fig. 37).

The individual branched units that make up the arbuscule are difficult to distinguish because of their small size and three-dimensional organization; the structure of the arbuscule ranges from bulbous to narrowly tapering points of the branching hyphae. Although the composition and structure of the individual arbuscules is consistent, the point of attachment of the arbuscules is variable, with the majority occurring at the ends of hyphae (Plate 5, Fig. 40). Other attachment points result from a right angle branch of vegetative hyphae (Plate II, 10) or, less commonly, arbuscules develop directly from an individual hypha (Plate 5, Fig. 42).

Vesicles are attached to the same type of vegetative hypha that produces the arbuscules. Two distinct types of vesicles are present in the rootlets: (1) globose or spheroidal (Plate 5, Fig. 43) and (2) oblong to elliptical (Plate 5, 44–45). Vesicle development is initiated soon after arbuscules are formed and have been hypothesized to function as storage units that typically contain lipids and cytoplasm in mycorrhizal associations (Cooper and Lösel, 1978). In rare instances, however, vesicles develop thicken cell walls and may function as propagules in older, mature roots (Biermann and Linderman, 1983). Globose, spheroidal vesicles are 25–30 µm in diameter with an average diameter of 28 µm. The oblong to elliptical vesicles are 65–78 µm in length with an average of 75 µm. At the narrowest portion of the vesicle, the width can range from 10 to 15 µm in diameter with an average width of 13 µm. The widest portion of the vesicle is 35–40 µm in diameter with an average diameter of 36 µm. Both globose and oblong vesicles

are smooth walled, opaque, and with a uniform wall approximately 0.5 μm thick. A single perpendicular septum occurs at the base of each vesicle. A right-angle branch from a vegetative hypha produces the globose or spheroidal vesicles. In contrast, oblong or elliptical vesicles are produced at the terminal end of an individual hypha. Vesicles lack contents and occur inside the lumen of individual cortical cells. Only mature, fully developed vesicles have been observed in the rootlets; immature or developing vesicles have not been identified. It is possible that the bulging or swollen areas in individual hyphae (e.g., Plate 5, Fig. 37) represent a developmental stage in vesicle production.

3. Discussion

Voltzialean conifers are a group of transitional gymnosperms that is generally considered to be sister to the Cordaitales, primarily based on a shared suite of characters in the reproductive structures (Florin, 1951; Hernandez-Castillo et al., 2001; Rothwell et al., 2005; Taylor et al., 2009). The first report of a mycorrhiza in voltzialean conifers was in the form of spheroidal mycorrhizal root nodules in *Notophytum krauselii* from the Triassic of Antarctica (Schwendemann et al., 2011). These root nodules are specialized outgrowths that develop on young roots and function as the site of endomycorrhizal fungal development. In extant conifers producing mycorrhizal nodules, these structures typically form in rootlets that are close to the soil surface (Russell et al., 2002).

The fungi reported in this study occur in small secondary, young rootlets of *N. krauselii* that differ from nodule-producing roots; the anatomical features of the fungus are also different from those in the nodules. The mycorrhizal fungus reported here is characterized by distinctive vesicles and arbuscules that occur exclusively within a well-defined zone of the ontogenetically immature host rootlet cortical tissue. In contrast to the fungi described by Schwendemann

(2011), the fungus in this study differs by producing globose and oblong vesicles; fungi within the *N. krauselii* root nodules do not contain multiple types of vesicles (only spherical types were described). The fungus in this study also differs by having multiple types of arbuscule-to-hyphal attachment types and does not have associated extrarhizal spores. This complement of features corresponds with morphologies seen in many extant and several other fossil arbuscular mycorrhizal (AM-)fungi (e.g., Bonfante-Fasolo, 1984; Peterson and Farquhar, 1994; Brundrett, 2004; Dickson, 2004). The oldest fossil record of AM fungi comes from the Lower Devonian (~408 Ma) Rhynie chert, where the fungus occurs in a well-defined zone of the cortex of the prostrate and upright axes of the early land plant *Aglaophyton major* (Remy et al., 1994a). A similar mycorrhizal association has recently also been suggested for the Rhynie chert land plant *Horneophyton lignieri* (Strullu-Derrien et al., 2014). Fossil AM fungi that produce arbuscules exclusively within a specialized zone of the host cortex have also been reported to occur in *Radiculites*-type cordaitalean rootlets from the Carboniferous of France (Strullu-Derrien et al., 2009), stigmarian appendages from the Carboniferous of Great Britain (Krings et al., 2011), and the Triassic cycad *Antarcticycas schopfii* from Antarctica (Stubblefield et al., 1987a,b; Phipps and Taylor, 1996). Based on the structural correspondences of the fossils described in this study to extant and other fossil AM associations, we interpret the fossil fungi in *N. krauselii* as representing the fungal partner in a vesicular-arbuscular mycorrhiza.

Arbuscule morphology in extant plants includes two principle morphological types, i.e., the *Paris*-type, characterized by coiled hyphae, arbuscules, and predominantly intracellular development, and the *Arum*-type, characterized by highly dichotomized arbuscules and predominantly intercellular development (Dickson, 2004). The combination of characters herein, such as the highly dichotomizing hyphae and various attachment points to vegetative hyphae, suggest that the arbuscules in *Notophytum krauselii* are most like those of the *Arum*-type. The

presence of an *Arum*-type endomycorrhizal morphology in *N. krauselii* is interesting because the vast majority of arbuscular mycorrhizas in modern gymnosperms, with the possible exception of *Gingko biloba*, is of the *Paris*-type (Breuninger et al., 2000).

Today, Glomeromycotan systematics and taxonomy are based primarily on molecular-phylogenetic evidence, and morphological characters when congruent with gene phylogenies. The exclusive use of morphological data for Glomeromycota taxonomy can be used in exceptional cases, such as fossil taxa, when supporting molecular data are unambiguous or unavailable. Based on the consensus classification incorporating molecular-phylogenetic and morphological data, there are ten families of the Glomeromycota that have been identified: Acaulosporaceae, Ambisporaceae, Archaeosporaceae, Paraglomeraceae, Claroideoglomeraceae, Diversisporaceae, Geosiphonaceae, Gigasporaceae, Pacisporaceae, and Glomeraceae (Schüssler and Walker, 2010; Redecker et al., 2013). Each of these families has distinct morphological characters and in some cases, unique ecological niches that can be used to determine the closest systematic affinity of fossil endomycorrhizae. The endomycorrhiza that occurs in the young rootlets of *Notophytum krauselii* is characterized by hyphae that are straight or occasionally sinuous, and seldom produce septa. The vegetative hyphae branch dichotomously and produce Y–branches and H–junctions, with some larger hyphae that contain occasional swellings. The arbuscules produce small trunks of various attachment types, i.e., right angle or no trunk from a parental hypha, or produced on a terminal end of parental hypha, with bulbous secondary branching; vesicles are ellipsoidal to globose, which can be lateral and terminal, and a septum is present at the base. Additionally, no asexual or extraradical spores, saccules, or auxiliary spores have been found associated with this fungus.

Many of the families of the Glomeromycota do not contain these characters and can be eliminated as to their affinity with the *N. krauselii* mycorrhiza in this study: (1) the

Acaulosporaceae produces endomycorrhizae with ellipsoidal to irregular or knobby vesicles (Morton and Benny, 1990), (2) Members of the Ambisporaceae are characterized by the production and developmental processes of asexual spores (e.g., glomoid and/or acaulosporid) and spore wall structure and saccules, (3,4) All members of the Archaeosporaceae and Paraglomeraceae produce mycorrhizae that lack vesicles (Morton and Redecker, 2001), (5) the Claroideoglomeraceae is also know as the phylogenetic *Glomus* Group B, and is typified by glomoid spores that form in substrate or rarely in decaying roots, and the development of an inner wall that is produced separately or an apparent 'endospore' (Schüssler and Walker, 2010), (6) the Diversisporaceae produces arbuscular mycorrhizas with or without vesicles, with or without auxiliary cells, formation of complex spores within glomoid spores (Walker and Schüssler, 2004), (7) members of the Geosiphonaceae are characterized by specific asexual spore wall characters and are unique because one species produces endocytosymbioses with cyanobacteria (Schüssler, 2002), (8) the Gigasporaceae is primarily characterized by spore cell wall morphology, germination shield patterns and development, and auxiliary cell morphology. Additionally, *Gigaspora* spp. form endomycorrhizas with arbuscules, coiling hyphae, and do not produce vesicles (Walker and Sanders, 1986), (9) the Pacisporaceae are primarily characterized by spore surface structure, spore wall ornamentation, spore color and size, and germination shield development (Oehl and Sieverding, 2004).

The Glomeraceae contains the most number of species, i.e., *Glomus* spp., of the Glomeromycota. Morphological characters of the endomycorrhizae of Glomeraceae include the production of finely branched arbuscules with narrow trunks (<4 μm in diameter), intercellular, typically straight hyphae (1.5–5 μm in diameter) that can also produce diagnostic H–branching, intracellular hyphae (2–4 μm wide) rarely coil, and vesicles are generally elliptical to spheroidal (Pirozynski and Dalpé, 1989). The fungus in this study shares the most characters, i.e., finely

branched arbuscules, H–branching, and elliptical and spheroidal vesicles, with the Glomeraceae, specifically with the genus, *Glomus*.

The presence of AM in *Notophytum krauselii* indicates that mycorrhizal associations in this Triassic conifer did not exclusively occur in the form of root nodules, but that some also entered into a different type of mycorrhizal association (i.e., AM) within non-nodule-forming rootlets. It remains unresolved, however, as to whether these two different mycorrhizal associations occurred simultaneously in this plant, perhaps located in different parts of the root system (see below), or the plant was able to shift between different mycorrhizal associations. For example, it is possible that germlings and juvenile plants relied on AM, whereas the larger plants with more extensive root systems developed root nodules. Because nodules and AM have not been discovered together in the same roots or in different roots in organic connection, it is also possible that perhaps the two types of mycorrhizal association did not occur in the same individuals, but rather that there were some trees with root nodules and others that had AM.

Modern AM fungi differ from root nodule fungi not only with regard to structure and morphology, but also with regard to the part of the root system that they colonize, and the relative position they occupy in the soil column. For example, in podocarps (Podocarpaceae) the mycorrhizal root nodules occur in subsurface roots (Dickie and Holdaway, 2011), whereas AM fungi are typically found in young, developing roots, which can spread both laterally and vertically throughout the entire soil column (Vogt et al., 1981). The latter mycorrhizal association in the young rootlets is likely important in the initial establishment of the plants in nutrient-poor soils (Rillig and Mummey, 2006). It has also been suggested that root nodules increase the extent of mycorrhizal colonization, while minimizing the cost that would be associated with developing an extensive root system (McGee et al., 1999; Dickie and Holdaway, 2011). Nevertheless, the exact functions of mycorrhizal root nodules remain elusive. One

important difference between the host cells containing AM fungi in the form of arbuscules and those cells containing them in nodules is that the cells of the latter atrophy after the arbuscules have ceased to function and the nodules are eventually abscised, whereas cortical cells invaded by typical AM fungi remain alive after arbuscules have collapsed, and these cells can subsequently host new arbuscules.

Notophytum krauselii not only demonstrates the occurrence of different types of mycorrhizal associations, perhaps within a single fossil plant, but also provides some indirect evidence of the morphology, spatial distribution, and functioning of the root system in this Triassic voltzialean conifer with the surrounding environment. The specimens of *N. krauselii* were collected from the Fremouw Peak locality, which has been described as a warm, temperate high-latitude peat forming environment. (Bomfleur et al., 2014). Modern peat forming ecosystems are highly acidic, nutrient poor environments. Plants utilize multiple strategies to adapt to these nutrient deficient, typically anoxic, low pH environments such as increasing root surface area via mycorrhizal fungi (Marschner, 1991; Clark et al., 1999). Moreover, mycorrhizas do occur in anoxic to low oxygen environments and are beneficial in maintaining species richness and uptake of phosphorous in wetland and peat ecosystems (Cornwell et al., 2001). Fungal activity is crucial in nutrient poor peatland environments (Myers et al., 2012), therefore it is plausible that the AM fungus in the rootlets of *Notophytum* were equally important for voltzialean conifers to survive within Triassic peat ecosystems.

Additionally, the discovery suggests that in this plant, mutualistic relationships perhaps occurred at multiple soil horizons. This might have been important with regard to survival of *N. krauselii* in the Antarctic high-latitude paleoecosystems. It has been suggested that the Middle Triassic climate of Antarctica was a warm temperate to temperate environment (Cúneo et al., 2003; Cantrill and Poole, 2012) with a high degree of seasonality as indicated by fossil tree-ring

studies (Taylor and Ryberg, 2007; Gulbranson and Ryberg, 2013). Additionally, all of the necessary factors required for arborescent growth in high-latitude ecosystems (e.g., photoperiodic ecotypes, high rates of cambial activity during the growing season, appropriate crown architecture) are within the scope of adaptations to trees in polar forests (Creber, 1990; Osborne et al., 2004). One of the most significant abiotic stresses of these very high-latitude forests was the extreme light regime, i.e., four months of 24-hour darkness, four months of 24-hour daylight, and four months of transition (Taylor and Ryberg, 2007; Gulbranson et al., 2012). Additionally, extant studies and experiments on conifers show that arborescent organisms under extreme photoperiod regimes can retain the capacity to regenerate their photosynthetic pigments after time intervals of complete darkness, i.e., for up to 140 days (Larson, 1964; Kostopoulou et al., 2011). Furthermore, it is a well-understood phenomenon that under extremely stressful situations, extant trees increase carbon allocation to roots and mycorrhiza (McDowell et al., 2008; Evelin et al., 2009; Miransari, 2010; Swidrak et al., 2013). Perhaps the mycorrhizal fungi reported here were crucial to *N. krauselii* during periods of extreme light regimes. We cannot be sure if the plant was able to shift readily between different mycorrhizal associations during times of extreme biotic or abiotic stresses, the mycorrhizal types co-occurred with the same parent plant, or if each association occurred at different ontogenetic stages of *N. krauselii* during root development.

In extant gymnosperms, there can be multiple types of mycorrhizal interactions co-occurring within the same plant (Berliner and Torrey, 1989; Peterson et al., 2004). Most extant gymnosperms are characterized by having AM associations, e.g., cycads, *Ginkgo,* Araucariaceae, Podocarpaceae, Cupressaceae, Sciadopityaceae (Fontana, 1985; Halling, 2001; Fisher and Vovides, 2004; Peterson et al., 2004; Wagg et al., 2008, Brundrett, 2009). The fungal partners in these symbioses are typically of the *Glomus* type, or less commonly of the *Gigaspora* or

Scutellospora types, and form vesicles and arbuscules (Baylis et al., 1963; Bonfante-Fasolo and Fontana, 1985; Russell et al., 2002; Wubet et al., 2003b). On the other hand, mycorrhizal associations between gymnosperms and members of the Endogonales (Mucoromycotina, zygomycetous fungi) are generally considered ectomycorrhizal (Walker, 1985; Warcup, 1990) but gymnosperms can also have AM fungi that co-occur with ectomycorrhizal associations (Harley and Harley, 1987; Brundrett et al., 1990; Cázares and Trappe, 1993; Onguene and Kuyper, 2001; Wagg et al., 2008). Overall, the mycorrhizal ecology of gymnosperms is complex and occurrence of multiple types of mycorrhizal associations, and other endophytes, within the same plant in a common phenomenon in extant ecosystems (Molina et al., 1992; Vogt et al., 1983; Cázares et al., 2005; Menkis et al., 2005; Öpik et al., 2008). Therefore, it is surprising that there is a paucity of information about multiple mycorrhizas within the same plant in the fossil record.

With the current report, there are now two fossil examples of different mycorrhizal associations occurring within the same plant from the Mesozoic. The other example is the Triassic cycad *Antarcticycas schopfii*, also from the Middle Triassic peat from Antarctica, which contains two types of glomeromycotan fungi (*Glomites* and *Gigasporites*), each forming a morphologically distinctive endomycorrhizal association within the same roots (Stubblefield et al., 1987a;b; Phipps and Taylor, 1996). *Gigasporites myriamyces* is characterized by wide intercellular and intracellular hyphae that form intracellular loops and coils in the cells, whereas hyphae of *Glomites cycestris* are slightly narrower and produce thin-walled, elongate vesicles (Phipps and Taylor, 1996). Although there are two types of glomeromycotan fungi present within the *A. schopfii* roots, this does not necessarily imply that each fungus was constantly in a mycorrhizal association. In extant plants that contain multiple mycorrhizal associations, these fungi may not necessarily form mycorrhizal symbioses at the same time (Helgason et al., 2002).

The example in *N. krauselii*, however, demonstrates the presence of two endomycorrhizal associations; it remains to be demonstrated whether these interactions existed independently or functioned concurrently in the roots of this Triassic transitional conifer.

4. Conclusions

The presence of a vesicular arbuscular mycorrhiza in a Triassic voltzialean conifer, a member of a lineage considered intermediate between the Cordaitales and modern conifers, provides some interesting new insights into conifer evolution and paleobiology. We hypothesize that the progenitors of the conifers may have been predominately endomycorrhizal. Some support for this hypothesis comes from Carboniferous *Radiculites*-type cordaitalean rootlets showing evidence of AM colonization (Strullu-Derrien et al., 2009). However, more fossil evidence is needed to further resolve this hypothesis and the full extent of mycorrhizal evolution among conifers. We anticipate that future investigations of permineralized Triassic, Jurassic, and Cretaceous plants, spanning an important interval in the evolution of gymnosperm-mycorrhizal relationships, will provide opportunities to not only find earlier representatives of AM fossils, but perhaps also examples of the intermediate forms between endo- and ectomycorrhizal associations, and perhaps the earliest representatives of ectomycorrhizal interactions with ancient gymnosperms.

Chapter 5

An initial survey of microorganisms of the osmundaceous fern root ball, *Ashicaulis wolfeii* I: Implications for microecosystem dynamics and root endophytes

1. Introduction

1.1 Ecology of ferns in modern and ancient ecosystems

Ecological studies in modern ecosystems are difficult to access based on the presence (or absence) of many biotic and abiotic factors, e.g., nutrient cycling, community composition (e.g., Wardle et al., 2004). These studies are even more difficult to interpret in the fossil record because paleoecological studies are limited to the evidence present. After becoming nearly extinct in the Permian, ferns began to make a slow come back during the Triassic (Taylor et al., 2009). Ferns are excellent ecological indicators; often among the first plant groups to become established after stochastic events (George and Bazzaz, 1999). Due to the extensive fossil record of ferns, one could argue that these organisms have had more time to develop intimate relationships, either positive or negative, with other organisms such as fungi and arthropods. It is still debated whether ferns have fewer interactions with other organisms (e.g., fungi, fungal-like organisms, insects, and other arthropods) because the lack of complex reproductive structures such as flowers, fruits, seeds, and a less diverse biochemical array of secondary metabolites in comparisons with seed plants, or if ferns and seed plants have developed the same number of interactions. Such counts may be biased because ferns are of less economic importance and have received less attention from field biologists than other plants (e.g., Balick et al., 1978; Hendrix, 1980; Cooper-Driver, 1985a). On the contrary, ferns are ecologically dynamic organisms in

modern ecosystems, a field that is still poorly explored, and likely just as active with other organisms in the fossil record.

1.2 Fern and microorganism interactions

Ferns have developed a wide spectrum of antagonistic and mutualistic relationships with fungi and fungal-like organisms. It has often been assumed that ferns would have developed few interactions with fungi or that they would interact primarily with older fungal lineages (e.g., Chytridiomycota, Blastocladiomycota, zygomycetes) (Boullard, 1957; Gerson, 1979; Auerbach and Hendrix, 1980), however, the opposite is likely true such that ferns have established ancient relationships with fungi due to their longevity in the fossil record. For example, more than 80% of fern sporophytes possess endomycorrhizal associations, whereas reports about ferns with ericoid and ectendomycorrhizae are rare (Schmid et al., 1995; Siddiqui and Pichtel, 2008). Outside of studies of mutualistic fern root-fungal relationships, there are few studies on antagonistic root endophyte interactions. Interactions with parasitic, symbiotic, and neutral endophytic fungi that infect the aerial parts of the ferns seem to be as common as in seed plants (Begon et al., 2006). Saprophytic fungi are widely distributed and derive their nutrition from dead or decaying organic matter. Because these fungi cause little or no visible damage during the lifetime of the fern, this group of saprobic fungi has received less attention than more conspicuous parasitic fungi of living ferns or mycorrhizal associations (Medel and Lorea-Hernandez, 2008). Since there are few studies of saprophytic fungi, new discoveries are common, for example, Medel and Lorea-Hernandez (2008) reported five species of ascomycetes on decaying tree fern leaves, and Samuels and Rogerson (1990) described three new species of ascomycetes from fern hosts that also show the transition between parasitic and saprotrophic fungi. There are even fewer concerted studies of fungi and osmundaceous ferns, for example,

rusts (Basidiomycota) on fern leaves, i.e., *Mixia osmundae* on *Osmunda* sp. (Sjamsuridzal et al., 1999).

1.3 Fern and arthropod interactions

Most studies of fern interactions with animals document direct effects because these are easier to observe and to correlate than indirect effects. Fossil evidence for fern-feeding arthropods exists from the Carboniferous (Smart and Hughes, 1973) and the Triassic (Ash, 1997; 1999; 2000). Feeding traces on pinnules of fossil evidence for fern-feeding arthropods exists from the Carboniferous (Smart and Hughes, 1973) and the Triassic (Ash, 1997; 1999; 2000). Feeding traces on pinnules of *Cynepteris lasiophora* (Ash, 1997), leaf excisions on *Sphenopteris arizonica* (Ash, 1999), and borings containing coprolites of a mite in the stem of the filicalean tree fern *Itopsidema vancleaveii* (Ash, 2000) are evidence of fossil fern-herbivore interactions. In modern ecosystems, the proportion of interactions with insects seems to be 3-7 times lower than in seed plants (Mehltreter, 2010). This estimation is based largely on the interactions of insects and fern foliage, whereas similar to root-fungi interactions, insect and arthropod-fern root interaction studies are limited. However, a study of the moth *Papaipema speciosissima* (Noctuidae) larvae feed on the rhizomes of *Osmunda* (Bird, 1938). In general, fern herbivores of multiple plant organs are most often members of the insect orders Coleoptera, Hemiptera, and Lepidoptera and can either be generalists or insect species that have specialized on ferns (Mehltreter, 2010).

1.4 Ashicaulis *spp. fossil record*

The Osmundales have traditionally been considered as a primitive group intermediate between eusporangiate and leptosporangiate ferns and were once considered a separate

subphylum, the Protoleptosporangiatae (Grimm et al., 2015). Two families are currently recognized, Guaireaceae and Osmundaceae, and the order (Osmundales) has a long evolutionary history. Stem morphotaxa that are assigned to the Osmundaceae are much more widespread in the Mesozoic (Taylor et al., 2009). Many fossil representatives cannot be placed in modern genera and thus have been classed in a number of morphogenera. Miller (1971) reviewed these forms and placed them in a new genus, *Osmundacaulis*, which is separated into three groups. Species in the *O. herbstii* group were split into two genera, *Millerocaulis* (Tidwell, 1986) and *Ashicaulis* (Tidwell, 1994). Both *Millerocaulis* and *Ashicaulis* include rhizomatous to slightly upright forms with small stems that are known from the Triassic through the Lower Cretaceous. Each of these taxa are characterized by a wide, sclerotic outer cortex, and leaf traces exhibit only one protoxylem strand at the joint of departure from the stele. In *Millerocaulis*, leaf gaps are either lacking or occur sporadically but are usually rare, whereas *Ashicaulis* stems show numerous, well defined leaf gaps and exhibits an ectophloic dictyostele (Tidwell and Ash, 1994). To date, there are approximately 24 species of *Ashicaulis* (Matsumoto et al., 2006; Tian et al., 2013) are known primarily from the Southern Hemisphere, including multiple species from Antarctica.

Ashicaulis beardmorensis (originally described as *Osmundacaulis*) is known from Middle Triassic rocks of the central Transantarctic Mountains (Schopf, 1978). The xylem cylinder is 1.7 mm in diameter and surrounds a pith containing isolated tracheids, parenchyma, and secretory cells. Near the periphery of the cortex, leaf traces are “W”-shaped in cross section and contain up to nine endarch protoxylem points. Permineralized specimens from the Middle Triassic of Antarctica are assigned to *Ashicaulis wolfeii* (Rothwell et al., 2002). Stems are 2.5 cm in diameter and fronds are pinnate with alternate–subopposite, pinnatifid pinnae. The stele consists of a ring of eight to nine xylem segments and diverging leaf traces. Another Antarctic

example includes, the Late Cretaceous specimens of *A. livingstonensis*, and was interpreted as an erect, mound-forming ferns (Cantrill, 1997). A specimen of Aptian age, also from Livingston Island, is assigned to *A. australis* (Vera, 2007).

1.5 The microorganism and animal diversity of Ashicaulis wolfeii

Initial surveys of the root ball material have shown a rich diversity of fungal remains and provide the basis for detailed documentation of plant-fungal and plant-arthropod, and possibly fungal-arthropod interactions in a well-preserved osmundaceous fern "root ball" of *Ashicaulis wolfeii*. These include suggested affinities with putative Chytridiomycota, Peronosporomycetes, septate fungi (either Ascomycotina or Basidiomycota), and numerous fungal and fungal-like components of unknown affinity. Additionally, there is evidence of saprotrophic, and possible parasitism associations within this single specimen. Lastly, the matrix of the root mass contains numerous coprolites of varying diameters and morphologies. There have been limited studies on plant-arthropod interactions focusing on coprolites (Habgood et al., 2004; Slater et al., 2012) and none to date on the fungal component of these interactions. Overall, with the combination of information regarding fungal interactions with arthropod remnants, it will be possible to further elucidate "micro-environmental" interactions on a ecological level similar to studies made on Carboniferous material (e.g., Rössler, 2000).

2. Results

2.1 Fossil affinities

This study is concentrated on a single, large permineralized osmundaceous fern root ball approximately 40 cm in diameter (Plate 6, Figs. 49-50), which shares anatomical features and characters with *Ashicaulis wolfeii* Rothwell et al. (2002). Morphospecies of permineralized

osmundaceous plants include stems 5–7.5 mm wide with a heterogeneous pith with sclerenchyma and interspersed parenchymatous cells (Plate 6, Fig. 51). The xylem cylinder, when preserved is on average, 1.3mm wide, 0.2–0.3 mm thick with 8–9 xylem segments separated by distinct leaf gaps. The inner cortex is parenchymatous and is 0.5–0.6 mm thick, while the outer cortex is about 0.8 mm thick and composed of homogeneous sclerenchyma fibers. The frond trace is C-shaped with one endarch protoxylem strand proximally which divides in two in outer cortex, developing enrolled margins distally (Plate 6, Fig. 52). Based on multiple sections and peels, 25 frond traces have been found. Additionally, annuli attached to sporangia devoid of contents are common (Plate 6, Fig. 54). Other degraded tissues are found throughout the matrix and a single seed (Plate 6, Fig. 53) has been observed.

The fern root ball is composed primarily of small rootlets typically 1-3 mm in diameter interspersed with numerous arthropod coprolites. Most roots are characterized by diarch primary xylem surrounded by an empty space and several layers of relatively sclerenchymatous cortical cells with moderately thickened walls. In the best-preserved roots the zone between the xylem and sclerotic cortex is filled with thin-walled cells that represent phloem and a thin zone of parenchymatous cortex. Rootlets have been arbitrarily assigned as “brown” and “black” rootlets based on the color, i.e., preservation, of the roots, but more so on the cell wall thickness. Thin cell wall layers characterize brown rootlets (root type 1; Plate 6, Fig. 55), while black rootlets are characterized by thicker cell walls (root type 2; Plate 6, Fig. 55). Each of these root types contains a different mycoflora, which is discussed below. Increased detail on root anatomy is possible with the *A. wolfeii* root ball, including well-preserved root hairs (Plate 6, Fig. 57). These are directly comparable with root hairs of modern *Osmunda* sp. and are present on both root types (Plate 6, Fig. 58). The root hairs, when preserved, have a bulbous base up to 30 μm in diameter and up to 150 μm in length (Plate 6, Fig. 56).

2.2 Fungi associated with root type 1

Longitudinal sections of root type 1 contain well preserved cortical regions that are densely colonized with hyphal mycelia, spores, and isolated cells that possibly represent a host response (Plate 7, Fig. 59). The fungal root endophytes are restricted to the cortical region of the roots, and are not found in the vascular tissue, epidermal cells, or root hairs(Plate 7, Fig. 60). The hyphae are 2-4 μm in diameter, septate, branch profusely, i.e., highly dichotomized, curved branching, septa can be present at dichotomies (Plate 7, Fig. 61), and traverse longitudinally and radially within cortical cells, penetrating directly through cell walls intracellularly. Additionally, a wide array of vesicle morphologies occurs within root type 1 cortical tissue. Vesicles can range from 8-30 μm diameter and can be ellipsoidal to globose (Plate 7, Fig. 62); certain vesicles are tapered in the center, i.e., hourglass shaped (Plate 7, Fig. 67), as well as some vesicles taper at one end, i.e., pyriform (plate 7, Fig. 64, 66). Attachment points are common between parental cortical hyphae and the vesicles, septa are present at the base of vesicle (Plate 7, Fig. 63-65; 67). Vesicles can occur singly or in clusters (2-3) (Plate 7, Fig. 62, 66), however, when vesicles are found in clusters, attachment points to parental hyphae are indistinguishable (Plate 7, Fig. 66). Many of the root cell type 1 exhibit single, isolated cortical cells with thicker cell walls relative to the rest of the rootlet. Within these isolated cells are small spheroidal chained structures, about 1-2 μm in diameter, usually 2-3 cortical cell layers below the rootlet epidermis. These structures can fully occlude these isolated thick cell wall cortical cells (Plate 7, Figs. 68-69).

Other root type 1 fungi include less densely infected mycelia within cortical cells but the fungi share similar features of the abovementioned densely colonizing fungi, i.e., septate hyphae that are highly branched (Plate 7, Fig. 70). Differences include vesicles with only globose morphology, and the terminal ends of some hyphae can result in highly dichotomized,

amorphous structures within cortical cells (Plate 7, Fig. 71). Additionally, other hyphal types include smaller diameter, septate mycelia (1.5-2 μm in diameter) that can terminally end in small bulbous structures that extend through cortical cells intracellularly (Plate 7, Fig. 72). An isolated curved hypha has been observed penetrating cortical cell walls with thicker regions of the cell (possible host response) where the fungus penetrates the cell wall (Plate 7, Fig. 73). Another single example of root type 1 exhibits densely colonized mycelia (Plate 7, Figs. 74-75) with double walled vesicles ~20 μm in diameter and attached to parental hyphae (Plate 7, Fig. 76).

2.3 Fungi associated with root type 2 and matrix microorganisms

Root type 2 is characterized with thick cell walls, and can have root hairs present when preserved. There is a distinctly different fungal community associated with root type 2, most noticeably a consistent association with chytrids in different developmental stages (Plate 8, Fig. 86). In addition to chytrids, large spores (up to 60 μm) with an internal single thin cell layer can be found within poorly preserved regions of the rootlets, typically in areas where the cells are separated. Chytrids, however, are abundant within the cell lumina of root type 2. The chytrids can be found in all tissues of root type 2 including the cortical and vascular tissues (Plate 8, Fig. 85). Larger chytrids can be 8-12 μm in diameter and be single wall (Plate 8, Fig. 78), double walled (second cell wall 1.5 μm thick; Plate 8, Fig. 79), found as isolated structures, or in clusters (Plate 8, Fig. 80), as well as the second cell wall layer up to 5 μm thick (Plate 8, Fig. 81). Smaller chytrids, i.e., maximum diameter 5 μm, can contain rhizomycelia (Plate 8, Fig. 82) or well-preserved with operculum (Plate 8, Fig. 83), as well as with possible papilla (Plate 8, Fig. 84).

Additional fungi and fungal features of root type 2 include highly degraded cell walls, likely as a result of fungal degradation (Plate 8, Fig. 87). As well as septate hyphae 1-4 μm thick

within root type cell wall lumina, and can penetrate directly through cell walls (Plate 8, Fig. 88-89). Rarely, in longitudinal section of root type 2, individual spores (possibly vesicles?) occlude the cells (Plate 8, Fig. 90). Highly degraded chain like cells that fill the cell lumina of degraded root type 2 occur throughout the specimen (Plate 8, Fig. 91-93). These cells share similarities to the occurrence of the yeast-like, chains of monilioid cells that fully occlude cells of root type 1 (Plate 8, Fig. 94-95). Key differences between these two chain like cells are: root type 2 yeast-like cells can occur in the matrix and are not confided to cells (Plate 8, Fig. 91), whereas monilioid cells in root type 1 do not colonize or extend beyond the lumina of cortical cells (Plate 8, Fig. 94-95). Additionally, these yeast-like cells are better well preserved relative to root type 2 cells. Other microorganisms include the presence of a possible Peronosporomycetes 25 µm in diameter that lacks the typical antler-like projections (Plate 8, Fig. 96). A single specimen approximately 125 µm in diameter also occurs within the matrix. It has external ornamentation in the form of ovoid cells and a possible opening on the surface of the structure (Plate 8, Fig. 97).

2.4 Arthropod remains

In 100% of thin sections and peels of the *Ashicaulis* root ball contains numerous coprolites (Plate 9, Fig. 98). Coprolites can be dense to composed of fragmentary substances (Plate 9, Fig. 104). There is a large, structure 5 mm in length with 3 distinct cell wall layers (total diameter of all 3 layers: 60 µm) that may represent an arthropod cuticle (Plate 9, Fig. 100). Cell wall layer 1 (~50 µm thick): striated and individual columns can be discerned, which is directly adjacent to cell wall layer 2 (2-3 µm thick): thin, more opaque than cell wall layer 1 and lack striation, and cell wall layer 3 (5 µm thick): there is a solid, layer that lack striations, thicker than cell wall layer 2 (Plate 9, Fig. 100). Coprolites have also been associated with matrix hyphae (2-3 µm in diameter), typically septate, occasionally with swellings, and can branch dichotomizing

(Plate 9, Figs. 101-103). Coprolites are principally circular (25-65 μm) to ovoid (50-100 μm) (Plate 9, Figs. 105-108).

3. Discussion

3.1 Saprotrophic microorganism dynamics – once mycorrhizal?

Numerous examples of root endophytes can be found with the *A. wolfeii* root ball but like many fossil fungi, it is difficult to access the ecological affinity for each type of root endophyte due to the morphological diversity in many of the samples. The consistency of the branching hyphae and vesicles present within a limited region of the cortex may resemble mycorrhizal fungi, however, the hyphae are septate which is not a typical character for the Glomeromycota (Oehl, 2011). It has been reported, however, that under stressful certain conditions (e.g., damage, age, pre-penetration stages of colonization) both the intra- and extra-radical hyphae can become septate, (e.g., Gerdemann, 1955). Additionally, the hyphae vary in morphology including branching patterns and diameter, whereas many glomeromycete hyphae are relatively consistent in diameter. Last, and most importantly, definitive, diagnostic arbuscules have not been found or determined. Arbuscules are highly ephemeral, lasting for a maximum time of 3 weeks (Toljander, 2006), which may also explain the absence of arbuscules if root endophytes are mycorrhizal. Moreover, arbuscules do not all develop at the same time and constantly stagger arbuscule production within cortical tissue. Therefore, if arbuscules were present, then there would be a higher likelihood of finding them because of this interval production. It is possible that some of these root endophytes (especially in root type 1) may have been mycorrhizal at one point during the life of the rootlet, but was later secondarily colonized by a saprotrophic fungus as a result of fungal turnover (Eissenstat et al., 2000).

3.2 Host responses

The isolated cells with thickened cell walls within the cortical tissue of root type 1 represents a host response exhibited by the root as a result of to the small, monilioid cells (possibly yeast-like ascomycetous fungi) within the cell lumen. This thickened cell wall of an isolated cell has also been interrupted in Devonian fossils of *Nothia* from the Rhynie Chert (Krings et al., 2007). Interestingly, the root is exhibiting a host response to the isolated cell of yeast-like cells and not to the mycelial aggregation within the cortex, which may provide indirect evidence that the mycelium in the cortex is not that of a parasite, however, not all mycoparasites elicit a host response (e.g., Taylor et al., 1992; Hass et al., 1994; Krings et al., 2009b; 2010c).

3.3 Root hair-fungal relationships

The presence of root hairs and abundance of fungi within fossil specimens provides an ideal experimental setting to test hypotheses with correlations of fungi and root hair lengths. Many ferns in modern ecosystems are mycorrhizal (e.g., Siddiqui and Pichtel, 2008) and root hair length can be correlated to mycorrhizal association, i.e., non-mycorrhizal plants generally have longer root hairs, whereas mycorrhizal plants have short root hairs (Jones and Dolan, 2012). Therefore, in addition to further investigation for potential mycorrhizal associations in *Ashicaulis* root ball, correlation between root hair length and fungal components may provide additional data to support this mutualistic association with specimens that might be highly degraded.

3.4 The potential for chytrid life cycles

Another interesting feature of the microbial community of *Ashicaulis* includes the abundance of chytrids in what is interpreted as different stages of development. Further investigation of the association of root type 2 may provide the framework for assembling chytrid

life cycles. Other chytrid life cycles have been elucidated from the fossil record, i.e., Devonian chytrids (Taylor et al., 1992), Permian *Synchytrium* sp. (García Massini 2007a). In modern ecosystems, chytrids such as *Synchytrium athyrii* have been found associated with *Athyrium filixfemina* (Müller and Schneller, 1977). It is highly likely that the chytrids associated with root type 2 are saprotrophic organisms, similar to fungal communities described in the fossil record, e.g., chytrid fungal community in *Lepidodendron* (Krings et al., 2010e).

3.5 Various morphologies in fungi

The monilioid and yeast-like cells restricted within the cortex of some root type 1 cells superficially share resemblance with dark-septate endophytes (DSE). To date, and in modern ecosystems, DSE have not been found in ferns. However, the fungal interactions and associations are so poorly resolved in modern fern studies, and almost absent in ancient ecosystems. DSE are common in roots of plants under high stress conditions and can co-occur with multiple assemblages of fungi within roots (e.g., Jumpponen et al., 2001; Scervino et al., 2009; Knapp et al., 2012). In turn, these structures could represent the yeast-like form exhibited by other fungal non-DSE types under stressed conditions. Many fungi can exhibit multiple forms and morphological features, i.e., dimorphism, of hyphae dependent on environmental conditions (Nadal et al., 2008), this provides a fundamental problem in paleomycology as it is discipline dependent on morphology of fungi. Therefore the fungal diversity in *Ashicaulis* may not all represent different species or types of fungi, but the same fungi in dimorphic states.

3.6 Arthropod-fungal-plant interactions

The abundance of arthropod remains suggests an avenue for examining several questions for arthropod-fungal-plant, specifically fern, interactions. Studies categorizing the different class

types/sizes of coprolites from the Devonian Rhynie Chert provided insight into the food web dynamics of an ancient, i.e., Lower Devonian, ecosystem (Habgood et al., 2004). Additionally, Slater et al. (2012) conducted an extensive study on the coprolites associated with *Glossopteris* that provided information on the arthropod-fungal-plant interactions from the Permian of Antarctica. Preliminary results indicate that there are at least four distinct categories of coprolites, which can be attributed to at least two different types of arthropods. Moreover, based on feeding patterns represented by coprolite galleries, and absence of root hairs adjacent to these galleries, it is possible that the arthropods were consuming the root hairs. In extant ecosystems, there is almost nothing known about the root-arthropod interactions, especially associated arthropods, feeding patterns, feeding preferences, etc., therefore, the *Ashicaulis* fern root ball can provide into a dynamic food web and ecosystem from the Mesozoic.

4. Conclusions

Based on the small portion of the *Ashicaulis* root ball thin sections studied, i.e., less than 10% of the total specimen, only a limited interpretation can be applied to the fossil microorganisms described. However, since there is a high great diversity within a small data set the root ball ecosystem provides the foundation for an exciting opportunity to further study and develop new hypotheses that can be applied to the *Ashicaulis* root ball. Additional investigations will undoubtedly yield more insight into root endophytes and other microorganism dynamics of the root ball. Additionally, as a result of the large number of coprolites within the root ball this unique fossil offers an excellent case study and experimental setting for fern-arthropod interactions in the Mesozoic of Antarctica. As a result of this synthesis, it will be possible to integrate the data within an ecological framework that includes interactions among microorganisms, fungi, and arthropod remains in a single fern specimen. This dataset within the

tissue systems of the root ball offers a means of documenting a microecological assemblage of a Triassic fern.

Chapter 6

Wood-fungal interactions in glossopteridalean roots (*Vertebraria*) and stems (*Australoxylon)* from Antarctica: An anatomical, morphological, and geochemical approach

1. Introduction

1.1 Wood decay in modern ecosystems

Today, forests cover approximately one-third of the land surface of the earth (Bowen, 2008). Humans have used wood products in both large- and small-scale construction and have recognized forests for aesthetic, ecological, economic, and social values since antiquity (Sabine et al., 2004), and throughout this time have suffered from the fact that wood is biodegradable. Woody plant parts represent a microenvironment for a wide variety of microorganisms ranging from saprotrophs to pathogens. Some of the pathogens may trigger more or less specific host-responses in the form of morphological alterations and/or biochemical compound defenses. It is remarkable therefore, that our knowledge of the role of wood-fungal relationships in modern ecosystems is so limited, and is almost absent from the fossil record.

Wood structure is a crucial attribute in order to understand wood-fungal relationship. Coniferous wood structure is relatively homogenous, as compared to angiosperms where there is evidence for functional division in the different cell types, e.g., vessels (water conduction), fibers (support), parenchyma (nutrient storage and transport) (Schwarze et al., 2000). The cell wall components of wood cells are an important consideration while studying wood decaying fungi because many rot types are delineated by the specific component of the cell wall that the fungus enzymatically degrades. There are five distinct cell layers in an individual wood cell. From the

outmost into the lumen: (1) middle lamella composed primarily of pectin and lignin, (2) primary wall composed of cellulose and often difficult to distinguish from the middle lamella, (3) secondary cell wall further subdivided into S_1 (cellulose), S_2 (cellulose), and S_3 (cellulose, hemicellulose, and lignin) layers; with the S_1 directly adjacent to the primary wall and the S_3 the innermost layer adjoining lumen.

In modern ecosystems, wood rotting fungi are of three principal types, i.e., brown, soft, and white rot (Rayner and Boddy, 1988). Brown rot is caused exclusively by members of the basidiomycetes (e.g., Polyporaceae) and is overwhelmingly associated with conifers. These brown rot fungi preferentially degrade cellulose and hemicellulose, while modifying lignin constituents–this modification also gives the decayed wood its characteristic "brown" color; the resulting wood is brittle and has an almost crumbly, powder-like consistency (Green and Highley, 1997). Soft rot wood decay is characterized by the growth of the hyphae in relationship to the secondary wall, i.e., typically longitudinal to cell axis (Savory, 1954). The rot only occurs within the immediate vicinity of the hyphae, and the term "soft" rot is a result of decay by many Ascomycete or Deuteromycete fungi. Soft rot can be further sub-divided into (1) type 1 – fungal hyphae form a series of successive cavities with conically formed ends which follow the direction of the microfibrils with the S_2 layer and (2) type 2 – superficially resembles a simultaneous rot, but V-shaped notches are produced by the hyphae in the S_2 layer. White rot decay fungi are predominately members of the Basidiomycota and to a lesser extent, ascomycetes (i.e., Xylariaceae) (Sutherland and Crawford, 1981; Tang et al., 2009). The term "white rot" has been traditionally applied to woods that have a bleached appearance in which the lignin (and cellulose, hemicellulose) is broken down. White rot fungi is of two principal types: (1) selective delignification and (2) simultaneous rot; each of which is based on the relative rates of degradation of lignin and other cell wall components by the particular species of fungus and

conditions within the wood (Blanchette, 1984a; 1984b; Adaskaveg and Gilbertson, 1986; Rayner and Boddy, 1988). In white rot with selective delignification, initially the lignin is broken down preferentially before either the cellulose or hemicellulose, via oxidative processes by means of the phenoloxidases formed and released by the hyphae (e.g., laccase, tyrosinase, and peroxidase). There are multiple examples and species of white rots with selective delignification, including white pocket rot forming fungi (e.g., *Phellinus pini, Grifola frondosa)* in which the fungus enzymatically degrades circular to ovoid areas in the wood creating a spotted pattern on the wood of white delignified areas. Conversely, white rot fungi that exhibit simultaneous rot enzymatically degrade lignin, cellulose, and hemicellulose at relatively equal rates. The hyphae within the lumen grow on the S_3 layer, and the cell wall is broken down in the immediate vicinity of the hyphae that form erosion troughs. Fungi that cause simultaneous rot are found overwhelmingly in association with broad-leaf angiosperm trees (Eriksson et al., 1990). Recently, this three-part categorical system has been challenged by Riley et al. (2014) based on robust study of basidiomycete genome analyses, concentrating on the enzymes produced by major white and brown rot producing fungi. Many white rot species possess multiple lignin-degrading (ligninolytic class II) peroxidases (PODs) and enzymes that attack crystalline networks of cellulose. However, the authors discovered that some white rot fungi lack PODs, thus making them more similar to brown rot fungi, but still utilize crystalline cellulose enzymes. Therefore, the authors challenge this strict delineation between white rot and brown rot fungi, and suggested a new classification system to include white rot-like fungi that do not contain PODs, i.e., an intermediate form between white and brown rot fungi based the enzymes employed.

1.2 Wood fungi in the fossil record

Our current knowledge of wood fungi and decay fungi in trees is limited to fungal interactions in modern lignin producing phyla, i.e., gymnospermous and angiospermous plants. Other fossil groups, however, also produced lignified tissues, e.g., progymnosperms, certain seed ferns, etc., and studies of these early woody plants provide insight into the co-evolution between wood and fungi. The earliest appearance of wood in the fossil record is from two small axes from the Early Devonian (~407 Ma) of France and New Brunswick, Canada (~397 Ma); both taxa contain secondary xylem and are similar to the basal euphyllophyte, *Psilophyton* in anatomy (Gerrienne et al., 2011). The fossil record of wood-fungal interactions is extremely sparse and limited to only a few reports; few studies focus on wood-fungal interactions and fungi are typically only included in the description of the specimen but not discussed. The oldest evidence of a wood fungus with possible affinities with white rot occurs in a progymnosperm (*Callixylon newberryi)* from the Upper Devonian (~372 Ma) in the form of cell wall alterations (Stubblefield et al., 1985). It is important to note that in the case of the *C. newberryi* fungus, it is the disease symptoms that were used assess the systematic affinities of the fungus, and not the actual fungal characters.

Examples of Late Permian wood-fungal interactions are reported in *Dadoxylon*-type wood from the Iberian Ranges of Spain. The authors describe several specimens with rot-like symptoms, i.e., selective delignification and cell wall separation, it is important to note that no fungal remains were found within the wood (Dieguez and Lopez-Gomez, 2005). Other examples of woods ranging from Permian to the Pliocene in age from Hungary exhibit symptoms of wood decay that were originally interpreted as taxonomic characters, i.e., spirals in the wood that were not thickenings but unusually regular furrows due to wood decay (Greguss, 1967; Phillippe et al., 1999). The symptoms of wood-rotting fungi have also been described from a number of trunks in Late Triassic trees from the Petrified Forest of Arizona, but it was not possible to determine

whether the fossil infections were parasitic or saprobic (Creber and Ash, 1990) because no *bona fide* fungal remains were described or found within the Triassic woods.

A host response to a possible fungal attack by trees, indicating a parasitic fungus, has been reported from the Jurassic of Antarctica (Harper et al., 2012; Chapter 7 of this dissertation). Another example of Jurassic wood-fungal interactions includes the complex multi-level interactions of fungal-arthropod-plant interactions described in woods from the petrified forest (Monumento Natural Bosques Petrificados) of Patagonia, Argentina, in which several examples of silicified araucarian logs are decayed and contain fungal remains (hyphae) as well as galleries filled with coprolites of similar to wood-boring beetles (García Massini et al., 2012). Pieces of dicot (Ebenaceae?) wood embedded within chert from the Upper Cretaceous–Paleocene Deccan Intertrappean beds of India, contains an ascomycetous fungus that is morphologically similar to extant *Phoma* (Chitaley and Patil, 1972). Other examples from Intertrappean beds of India, include a fossil *Sonneratia*-like wood specimen with decay patterns, hyphae, and suggested fungal spores within the cell lumina (Srivastava, 2008). Geologically younger woods from the Eocene of southern Patagonia, Argentina also exhibit signs of wood decay with delignified cell walls, appositions, and cells with partially or fully detached middle lamella; the authors note that the absence of fungi could be an argument for brown rot affinities, however based on the selective delignification exhibited in the cell walls, the authors favor white rot for the most plausible causative agent (Pujana et al., 2009). There are likely numerous reports of wood descriptions that briefly mention fragments of fungal remains that have been overlooked and not included in this section or conversely, taxonomists that have described fossil woods did not include the presence of fungi within the wood. This is due to the fact that thin sections of anatomically preserved wood typically include some fungal structure, i.e., hyphal fragment. Although this is such a common occurrence, the anatomical and descriptive studies are the focus

of these reports and few studies focus exclusively on fungal wood decay components or biology.

1.3 Wood decay in fossil record - Antarctica

Similar to the many of the studies of that describe wood-fungal interactions, wood specimens from the Permian of Antarctica include evidence of decay patterns without fungal remains, thus an indirect form of fungal activity. This includes a report on *Australoxylon bainii* and *A. mondii* from the Upper Permian Bainmedart Coal Measures, northern Prince Charles Mountains, East Antarctica (Weaver et al., 1997). Specimens include decay pockets, specific patterns of the infection, and host responses (appositions). The most well-known and first concerted study of wood-fungal interactions and infection also occurs in specimens of wood form the Permian and Triassic of Antarctica. This investigation focused on the decayed specimens of glossopteridalean roots, *Vertebraria* (Permian) and stem-type, *Araucarioxylon* (Triassic) that had visible signs of decay pockets that were attributed to selective delignification white rot, specifically white pocket rot, and each of these specimens had fungal remains (Stubblefield and Taylor, 1985; 1986). Similar to the *Australoxylon* spp. from the Prince Charles Mountains, the *Vertebraria* and *Araucarioxylon* fossils had decay pockets, occurrence and symptoms of infection patterns, appositions, as well as fungal remains including, hyphae, clamp connections. It is important to note that the majority of data (fungal and decay signs) were concentrated on the Triassic *Araucarioxylon* specimens.

1.4 Analytical techniques in modern and fossil wood studies

The vast majority of wood-fungal studies in modern ecosystems are on the chemical alterations that occur in the wood after it has been enzymatically modified by the fungus. In addition to molecular analyses, modern studies of wood fungal enzymes utilizes spectral

analyses, such as Fourier transform infrared spectroscopy (FTIR), a technique that obtains infrared (IR) spectra of organic compounds or the by products of enzymatically altered woods (Fackler and Schwanninger, 2012). Which for example, can be used to examine the qualitative and quantitative changes in lignin and carbohydrate components relative to one another in order to determine the type of wood rot that occurred. Additional analytical spectral analyses include the use of near-infrared Fourier transform Raman (NIR-FTR). In one study, the determination of carbonyl content in lignin before and after extant wood decay was compared (Kihara et al., 2002). To date, there have been no studies on intact, i.e., not pyrolyized or thermally altered, permineralized wood using FTIR or Raman spectroscopy.

The integration of analytical techniques and fossil woods associated with fungi is even scarcer than focused anatomical and morphological descriptive studies on the subject. Evaluation of the roles of wood-inhabiting microorganisms in past environments requires detailed studies of fossil woods, which include the spatial and temporal resolution of all components, i.e., the biochemical and morphological responses of the host-pathogen interaction. Evidence of fungi (e.g., hyphae, spores, decay patterns) is present in the vast majority of fossil woods, but typically there are not enough morphological characters to resolve the systematic affinities of these remains or complete disease pathology descriptions (Mägdefrau, 1966).

Biomarkers are complex molecular fossils derived from biochemicals, such as lipids, in once-living organisms (Peters et al., 2007). The biomarker, Perylene, has been suggested to be an indicator of conifer fossil wood degradation by wood-decay fungi in Jurassic stem samples and Miocene wood remnants from Poland (Grice et al., 2009; Marynowski et al., 2011; 2013). Fungi are biochemical agents with numerous enzymes capable of degrading wood cell wall components, i.e., cellulose, hemicellulose, lignin, and secondary substrates (Hatakka, 2001). Each rot, decay, or parasitic fungus produces a unique set of enzymes and alter the host in a

specific manner by breaking down each of these components, such as lignin derivatives, each of which can be used for taxonomic affinity (Pandey and Pitman 2003; 2004). Examples of using lignin derivatives for taxonomic affinity has been utilized in the fossil record, for instance, key differences between gymnosperm and angiosperm fossil woods can be distinguished via biochemical systematics (Logan and Thomas, 1987). To date, however, there have been no concerted studies on determining the affinities or taxonomy of fossil fungi via direct or indirect means using biochemical or analytical techniques.

1.5 Focus of the present study and supporting hypotheses

This chapter focuses on expanding the knowledge base of fungal morphological characters and to investigate the co-evolution between wood and fungi from the Permian, using glossopterid root and stem wood as a case study. The Permian is an important time frame for ecological studies of wood and arborescent plants; due to the transition from the Carboniferous, i.e., the vast coal swamps dominated by arborescent plants, into the cooler Permian, followed by the Permian-Triassic mass extinction event, which led to a greenhouse conditions. Therefore the Permian is not only important due to the dramatic climatic changes, but also represents the last period of the Paleozoic in which to study these extinct floras. Last, the Permian of Antarctica provides an interesting experimental setting because it represents an icehouse condition, due to its position of a high paleolatitude, i.e., the southern polar latitude, plants in Antarctica also experienced extreme light regimes of 24 hours of darkness for four months, 24 hours of light for four months, and a transitionary period for 4 months, each of these parameters comprises an ecosystem with no modern analog today. Also important is the integration of analytical and geochemical techniques to further elucidate new information on wood-fungal interactions. Based on initial preliminary results, this integration provides the foundation for a new avenue into

paleomycology discipline as well as the potential for high throughput evaluation of geologic specimens based on these results.

2a. Results – Thin sections: Anatomical and morphological

2a.1 Wood affinities and taxonomy

Specimens used in this study can either be assigned to the glossopteridalean stem wood, *Australoxylon* (Marguerier, 1973) (Plate 10, Fig. 109) or lignified root wood, *Vertebraria* (Schopf, 1982) (Plate 10, Fig. 110), both characterized by pycnoxylic wood. All specimens lack preserved primary vascular anatomy, and therefore affinities are based on wood morphogenera characters. Stem characters share closest affinities with *Australoxylon* spp., which are morphologically similar to *Araucarioxylon* (Philippe, 2011). *Australoxylon* spp. have generally been regarded as a morphogenera for Permian Gondwanan woods (Marguerier, 1973; Prasad, 1982; Pant and Singh, 1987; Weaver et al., 1997) and are closely associated with *Glossopteris* flora (e.g., Merlotti and Kurzawe, 2006; Philippe, 2011). Further support for *Glossopteris* affinity includes the anatomical attachment of *Glossopteris skaarensis* leaves to wood (Pigg and Taylor, 1993). Characters of *Australoxylon* include: individual and distinct wood rings, square to rectangular tracheids in transverse section, multiple types of radial pitting (e.g., abietinean, araucariod, conspicuous arrangements of independent and spaced radial files or circular pitting), and groups of 2–3 or 4–5 pits (typically small, <15 μm in diameter) that are distinct from each other in clusters. One of the key distinguishing characteristics of *Australoxylon* wood that all specimens in this study share are mixed-type pitting on the tracheid radials (Plate 10, Fig. 111).

Specimens of *Vertebraria* were identified by the presence of the characteristic radiating wedges of secondary wood separated by lacunae rather than a solid axis. Certain specimens that

lack the characteristic wedges were not included in this study as specimens of *Vertebraria,* although portions of wood axes may also represent portions of *Vertebraria*. It is also important to note that there are rare types of *Vertebraria* spp., i.e., the "solid cylinder" type (Neish et al., 1993) that lack lacunae and were also not included in this study. *Vertebraria* axes from the Bowen Basin, Australia, Permian of Brazil, Skaar Ridge of Antarctica (this study), and the Prince Charles Mountains, East Antarctica have been reported with *Australoxylon* type wood (Mussa, 1978; Neish et al., 1993; Weaver et al., 1997; Decombeix et al., 2009) due to the characteristic opposite or mixed pitting in these *Vertebraria* specimens (Pant and Singh, 1968; Beeston, 1972; Gould, 1975).

2a.2 Fungi in wood

There are no discernable differences between fungi that occur in stem or root wood, therefore the following description of fungi applies to fungal remains that occur in both stem and root wood. Fungi are often present in both the tracheids and rays of the secondary xylem of infected specimens, as well as in the periderm when preserved. Septate hyphae range from 2 μm to up to 6.5 μm in diameter (Plate 10, Fig. 112) and are found in multiple cell types, such as tracheids and ray parenchyma. Individual hyphae are septate at regular and irregular intervals and can branch dichotomously or in cruciform patterns, both at right angles (Plate 10, Fig. 113-114). Additionally, hyphae are typically straight and rarely curve (Plate 10, Fig. 115). They exhibit simple (Plate 10, Fig. 116), medallion clamp (Plate 10, Fig. 118), and intermediate simple-medallion clamp connections (Plate 10, Fig. 117), in rare cases whorled clamp connections (Plate 10, Fig. 119-120). The presence of these multiple types of clamp connections suggests that there are several types or species of basidiomycete fungi that occur (and co-occur) within specimens, however, diagnostic characters such as polypores (fruiting bodies), sexual or

asexual structures need to resolve affinities have not been found. Vegetative hyphae traverse through specimens longitudinally and radially (Plate 10, Fig. 121, and can lie directly adjacent to cell walls or occur in central lumen of individual wood cells (Plate 10, Figs. 123-124). Hyphae can extend through radial and tangential walls and in some instances can pass from cell to cell through pits (Plate 10, 122, 125-128). Contrary to other studies of Permian wood with fungi (e.g., Weaver et al., 1997) there was an absence of bore holes in tracheid cell walls. Additional features characteristic of fungal attack, such as erosion troughs or microscopic pockets in the secondary walls are not observed, however, degraded pits are common.

2a.3 Decay patterns

The macroscopic appearance of the decayed woods is similar in both genera of stems and roots. Infected, i.e., specimens that exhibit pockets, and uninfected specimens of each *Australoxylon* stems and *Vertebraria*, were available for study, and 100% of the specimens had some evidence of fungal remains, e.g., including isolated fragments of hyphae within cells. The distribution of decayed areas and pockets varies in stems and roots. In some specimens they are distributed randomly throughout the specimen, while in others the pockets of decay are restricted to a portion of the host. Rarely, individual pockets may fall entirely within a growth ring or may span and extend through boundaries in between individual tree rings. When preserved, in the center of some stems, the decayed regions can appear to be organized in concentric rings lying along the boundary between adjacent growth layers. However, this pattern does not occur in all specimens, and areas of decay are not preferentially located across growth rings, there is not a single decay pattern that is the most common. In a survey of 400 pockets in stems and wood specimens, ~42% of the pockets were narrower than adjacent growth rings that contained them and completely occurred within a single growth ring. Individual pockets are circular to irregular

in cross section and range up to 4 mm in diameter (Plate 11, Fig. 129). In longitudinal section, pockets are typically fusiform to spindle-shaped (Plate 11, Fig. 130). The longest pockets observed were 1.5 cm but were only in incomplete specimens. Decayed axes of *Vertebraria* differ from those of *Australoxylon* stem wood only in minor respects. Pockets are more irregularly shaped in cross section, often tangentially elongated, and reach 13 mm in maximum diameter. In longitudinal section they are tapered. Decayed regions are scattered, and the impression of concentric rings of decay is less pronounced than in some specimens of *Australoxylon*. Pockets of decay are commonly entirely free of cellular debris. However, portions of partially decayed cells along the margins of pockets may persist. Additionally, specimens with irregular edge cell margins are sometimes filled with arthropod ovoid to circular coprolites ranging from 15 μm to 90 μm in diameter.

Many of the cells near pockets are in varying stages of decay and therefore represent the opportunity to study the degradation series and process of wood decay in Permian woods (Plate 11, Figs. 131-134; 135-136). Partially degraded cells in the intermediate stages of decay can occur adjacent to pockets. The radial and tangential cell walls of these tracheids are thin, although tangential walls may persist longer relative to the radial walls. The corner area between four adjacent cells, i.e., the middle lamella, is the thickest layer in these cells. Secondary tracheids can have up to four distinct cell wall layers (middle lamella, S_1-S_3 layers). Other than scanning electron microscopy (SEM), it is difficult to interpret these wall layers. Similar to extant woods, the thickest secondary wall layer occupies the position of the S_2 layer. Bounding it are layers corresponding in position to the S_1 and S_3 layers. The compound middle lamella (i.e., middle lamella and primary wall) is evident in the corners between cells but is difficult to distinguish from the supposed S_1 layer along the radial and tangential walls.

An additional variation in wood structure involves differences in the densities of cell walls and is a result of delignification of the cell wall. They are found deep within a stem as well as near its periphery and may be deep within the specimen as well. Cellular outlines are clear in this region (Plate 11, Figs. 137-142), but the thickness of the walls and the amount of the remaining organic matter are markedly reduced. The middle lamella is typically absent, and adjacent cells are generally separated. In most specimens a single layer of the cell wall persists. Sometimes an additional layer, apparently corresponding to the S_3 layer in other cells, is also present.

2a.4 Wood host responses

Certain cells exhibit evenly swollen cell layers and are separated from the other layers of the wall (Plate 12, Fig. 143). In other cells this wall layer is markedly and unevenly enlarged almost occluding the tracheid lumen (Plate 12, Figs. 144-153). The wall in these tracheids intergrades in appearance with the evenly swollen walls of other cells. The distribution of cells with pronounced uneven thickenings is not consistent. While they sometimes occur in a several-layered band among the smaller cells of the latewood, they may also be distributed throughout an individual growth ring. Although they are not restricted to one area of an axis, neither do they form a continuous ring within the specimen. Adjacent to the thickened layer in the direction of the cell lumen is a much thinner, dark layer that is sometimes separated from the thickened layer. Although this is apparently the innermost layer of the cell wall, it is not visible in all cells. Certain cells have contents that completely occlude the lumen; these structures may represent appositions or callosities, which are examples of wood host responses (Plate 12, Figs. 150, 154) (Aist, 1976; Pearce, 1989). Concentric patterns within the cavities reflect mineralization (Plate

12, Fig. 155) (Schopf, 1971). An overall comparison of wood decay characters of Permian and Triassic Antarctic wood studies can be found in Table 2.

2b. Results – Proof of concepts: Preliminary results using analytical techniques

2b.1 FTIR on permineralized specimens

Infrared (IR) spectroscopy is a vibrational spectroscopic technique that probes the vibrational behavior of organic molecules and inorganic crystal lattices. This technique affords information on the functional group content, chemical structure, molecular environment, bond angle, length, geometry, and conformation on organic and inorganic materials. The sample is irradiated typically with polychromatic mid-IR light (4000–400 cm^{-1}) and photons are absorbed, transmitted, reflected, or scattered. A change in dipole moment during a molecular vibration results in absorption of IR light. The frequency of absorbed light during the molecular vibration is characteristic for the masses of the bonded atoms involved in the vibration (atomic identity, e.g., P-O versus C-H), for bond strengths (i.e., force constants), and for the bond lengths and angles (geometry), which are parameters that constitute the structure of a molecule or crystal (Lin-Vien et al., 1991). Hence, these vibrational frequencies can be diagnostic for the identification and structural elucidation of the chemical composition of an unknown sample (Marshall et al., 2005).

Previous investigators have used petrographic thin sections of fossiliferous cherts with FTIR. However, these studies did not focus on the primary use of these thin sections for study with FTIR, rather they were standard thin sections, i.e., transmitted light microscope glass slides, epoxy to permanently attach and adhere chert wafer, standard thickness of petrographic thin section (25–100 μm) (Igisu et al., 2006; Preston et al., 2010). The resulting spectra were difficult

to interrupt based on the thickness of the specimen; therefore, band assignment and contextual evidence could not be inferred.

Our results indicate that FTIR studies on permineralized specimens is possible based on proper specimen preparation, i.e., samples are less than 5 μm in thickness, no epoxy, and specimens are placed on IR specific microscope slides. Data have not been interpreted but merely as a proof of concept for use of permineralized material analyzed via FTIR (Figure 8; Table 3).

2b.2. Raman spectroscopy results

Raman spectroscopy is a non-destructive technique and type of vibrational spectroscopy, which is used to elucidate the molecular structures present in both a qualitative and quantitative manner (Marshall and Olcott Marshall, 2013). It has been shown that Raman spectroscopy provides a promising new approach in astrobiological prospecting for rapidly screening samples containing thermally immature macromolecular hydrocarbon materials in order to determine the presence sp^2-bonded carbonaceous material via Raman spectra of well-developed G and D bands amenable to potentially successful biomarker analysis by gas chromatography-mass spectrometry (GC–MS) (Marshall and Olcott Marshall, 2014). The focus here is to apply this Raman screening method for paleontological specimens, i.e., Paleozoic woods, in order to determine if biomarker analysis would be possible in Antarctic specimens.

The vibration modes in Raman spectra are assigned by using Mulliken symmetry notation, which is standard practice in molecular spectroscopy (e.g., Glauser et al., 2014). The intense broad vibration mode at ca. 1600 cm^{-1} is assigned to the "G" band, which is attributed to doubly degenerate in-plane stretching of C\C bonds corresponding to the E_{2g2} (Mulliken symmetry notation) mode of graphite. The weak broad vibration mode at ca. 1355 cm^{-1} is

assigned to the "D" band which is due to a totally symmetric stretching mode corresponding to the $A1_g$ mode of carbon doubly bonded and singularly bonded carbon atoms in six-fold aromatic rings that becomes an allowed Raman active mode due to disorder (i.e., lattice discontinuities or structural defects) or decreasing crystallite size. The line-shape, bandwidth, and band intensity of the carbon first- order region reflect molecular structure. The spectra shown here are indicative of a macromolecular structure of disordered carbonaceous materials. Structurally, these carbonaceous materials consist of polyaromatic clusters that are graphite-like domains typically consisting of 3–4 randomly stacked graphene layers. Raman spectra also indicate a sharp peak at 464 cm^{-1}, which is the characteristic peak of SiO_2 or quartz (Hemley, 1987), attesting to the silicified, permineralized preservation of the Permian woods from Skaar Ridge (Schopf, 1971).

In summary, Raman spectra indicated that *Australoxylon* and *Vertebraria* woods from Skaar Ridge are amenable for biomarker analysis based on the presence of well-developed G and D bands. Additionally, these G and D-bands have the most pronounced peaks in areas well tracheid cells are well preserved. However, the G and D bands become less pronounced approaching the pocket where there are no cells (or lignin) preserved. Within individual pockets there is a prominent peak of quartz and absence of G and D bands. We found that G and D bands and presence of quartz are inversely correlated, i.e., in well preserved wood cell areas G and D bands are prominent and quartz is low to absent, but in pockets lacking wood cells, G and D bands are poorly pronounced and quartz peaks are prominent. Overall, the use of Raman spectroscopy provides a qualitative approach to determining that lignin is absent in pockets as a result of fungal degradation (Figure 9).

2b.3 Biomarker results

Gas chromatography–mass spectrometry (GC–MS) is an analytical technique used for

identifying biomarker compounds in thermally immature rocks. These compounds are derived exclusively from formerly living organisms. Biomarkers are complex compounds that are composed of carbon, hydrogen, and heteroatoms. Structurally, they show little or no change from their parent organic molecules in living organisms (e.g., Peters, et al., 2007). Biomarkers originate from many biological sources that are discernible from their diagnostic structural characteristics. Marshall and Olcott Marshall (2014) note "Contributions from bacteria, algae, vascular plants and animals have been recognized among the complex assemblage of molecular species present in sediments and sedimentary rocks." Most noticeably missing from this list are fungi. Based on initial screening results with Raman spectroscopy, promising Antarctic Paleozoic woods were analyzed via GC-MS to see if they would yield fungal or fungi-related biomarkers.

Preliminary results from fossil woods indicate that wood with visible signs and symptoms of fungal interactions produces several lignin-related biomarkers in response to the fungi, e.g., large polycyclic aromatic hydrocarbons (PAH) or complex ring structures (i.e., fluoranthene, phenanthrene, pyrene (Figures 10-11), *n*-alkanes (Figure 11) or chains of hydrocarbons that may represent plant lipids. Many examples of wood degrading white rot fungi can enzymatically breakdown PAHs via extracellular peroxidases, e.g., *Bjerkandera adusta, Coriolus hirsutus, Nematoloma frowardii*, *Pleurotus ostreatus* (Sack and Günther, 1993; Eggen and Majcherczyk, 1998; Bezalel et al., 1996; Günther et al., 1998; Pickard et al., 1999; Schützendübel et al., 1999; Cho et al., 2002). Each of these fungi can break down lignin derivatives such as fluorine, anthracene, phenanthrene, fluoranthene, and pyrene; each of these can also be considered by-products of white rot fungal degradation and also yields the potential as biomarkers in infected fossil woods (Marynowski et al., 2013). Additionally, the presence of *n*-alkanes indicates the possibility for taxonomic specific plant lipids in Permian root and stem woods. Studies of *n*-

alkanes as biomarkers have been used for identifying the taxonomic affinities of plants as well as which plant organ is producing the *n*-alkanes, i.e., leaf cuticle waxes, stem lipids, etc. (Poynter et al., 1989; Otto et al., 2005).

The biomarker, perylene, has been suggested as a fungal biomarker and an indicator of conifer fossil wood degradation by wood-decay fungi in Jurassic stem samples and Miocene wood remnants from Poland (Grice et al., 2009; Marynowski et al., 2011; 2013). Interestingly, our results did not yield evidence of perylene in fungal infected root or stem wood (Figure 13). Fungi were verified in specimens used by signs and symptoms of decay (pockets) as well as fungal remains in thin sections (hyphae in tracheids). Some authors have suggested that the production of perylene quinones produced by extant ascomycetous fungi is similar and the possible origin of perylene as fungal biomarkers (Grice et al., 2009). Jiang et al. (2000) further supports this ascomycete origin by stating evidence of "ascomycetous" fungi such as *Endochaetophora* in Triassic peat deposits from Antarctic (White and Taylor, 1988; Jiang et al., 2000). They suggest it is reasonable that fungi may have been the major precursor carriers for perylene in ancient sediments. We disagree with perylene as a definitive fungal biomarker for the following reasons: (1) although modern ascomycetous fungi such as *Daldinia concentrica*, a wood degrading fungus tightly associated with angiospermous trees (*Fraxinus* spp.) produce perylene quinones (Boddy et al., 1985), woods from the Paleozoic are not angiospermous, fungal remnants have clamp connections (a basidiomycete feature) within all specimens of infected woods, (2) the production of perylene quinones is also not a conserved feature throughout the phylum of the Ascomycotina, and therefore investigators should use caution implicating that perylene is a ascomycete specific biomarker, many other organisms produce perylene in marine and freshwater settings (Silliman et al., 1998), (3) justification for evidence of ascomycete fungi in the Triassic is based on an old interpretation of *Endochaetophora* fungi, which has now been

interpreted as a zygomycetous fungus and likely leaf litter degrading fungus (see Taylor et al., 2015; Chapter 9 of this dissertation for discussion). Overall, based on our preliminary results further studies on a larger data set spanning multiple points of geologic time and specimens verified with fungal remains via morphological evidence in thin sections are needed to resolve the potential of perylene as a fungal biomarker; however, based on preliminary our results, we do not think that perylene is a reliable fungal biomarker.

Overall the integration of geochemical and analytical techniques will greatly enhance the knowledge base in paleomycology while using wood decay as a platform for this new investigative avenue. We further hypothesize that fossil wood specimens showing no morphological signs or symptoms of microbial damage will yield a wide array of antimicrobial compounds (phytoanticipins) and polyphenolic deposits (Pearce, 1996) that could be elucidated via biomarkers. Generally the lignin content of gymnospermous wood is higher than that of angiospermous wood and is a quantifiable measure of taxonomic affinity, and may also be useful in taxonomic and wood-decay studies (Schwarze et al., 2000). We predict that integration of FTIR can help quantify the amount of lignin remaining in fossil wood via bulk lignin extraction of samples in order to determine lignin content post wood degradation.

3. Discussion

3.1 Differences between other Antarctic wood-decay studies and the present study

Key differences between this study and initial Antarctic wood decay studies include the first detailed description of fungal remains in *Australoxylon* and expand the data set for fungi in *Vertebraria*, decay patterns and host responses in Permian stem and root wood, as well as first application of geochemical techniques to paleomycological studies.

Evidence of wood decay in specimens of *Australoxylon bainii* with absence of fungal remains reported from the Upper Permian Bainmedart Coal Measures, northern Prince Charles Mountains, East Antarctica (Weaver et al., 1997) exhibited damage consisting of small irregular cavities with gradational decay pattern extending into the surrounding xylem tissues. Many of cell walls in degraded areas were thin and typically separated into two or more individual layers. Additionally, appositions were present in specimens of *A. bainii* providing evidence of a host response by an antagonistic causative agent. Other species from this study, *A. mondii* have decay pockets that are superficially similar to the cavities of *A. bainii*. However, these pockets occur within growth ring boundaries, scattered across tree rings, and can range from isolated areas of pockets to scattered randomly throughout the specimen. Many of the cavities were described as spindle shaped and generally lacked organic contents with the exception of cell fragments. Woods of *A. mondii* also exhibited a host response in the form of appositions. Each of which are features found in *Australoxylon* and *Vertebraria* from Skaar Ridge specimens in this study, however the most striking difference is the presence of fungal remains in *Australoxylon* and further information on fungi in *Vertebraria.* Whereas initial reports of pocket rot in *Vertebraria*, fungal remains are limited to poorly preserved hyphae that show little detail, and irregularly shaped pockets (Stubblefield and Taylor, 1985; 1986). In contrast, in longitudinal section of the tracheids of degraded areas of the Prince Charles material had small holes in the cell walls, which were more numerous and increased in frequency when closer to the edge of the cavity were completely absent in the Skaar Ridge stem and root wood material.

Stubblefield and Taylor (1985; 1986) conducted the first concerted and focused study of wood decay, and wood-fungal interactions in the fossil record. In this report, the vast majority of decay signs and symptoms occur in Triassic *Araucarioxylon* wood and are identical to the results from this study of Permian root and stem woods including as pocket distribution ranging from

isolated areas on specimens (within ring boundaries, segment of specimen) to crossing ring boundaries, circular to irregularly shaped pocket in transverse section and spindle shape in longitudinal planes. Fungal remains associated with the decay include hyphae within the pockets, tracheids, and ray parenchyma. Morphological aspects of the hyphae consist of septate, branching, and clamp-connections. The Stubblefield and Taylor (1985; 1986) study described simple and medallion clamp connections, whereas this study provides evidence of simple, medallion, simple-medallion intermediate forms, and whorled clamp connections. Each of these characters provides evidence for basidiomycete affinity, which are the most common white rotting and pocket rot fungal degraders. The initial and current study of wood rot include detailed analysis of the cell wall layer degradation indicates that the corner areas between four adjacent cells contain the thickest portion of the middle lamella and distinct separation patterns within the cell walls. Appositions or callosities are present in each case of the Triassic woods as well as Permian stem and root wood, possibly corresponding to the S_3 cell wall layer. Additionally, information on the progression of decay, interpreted as a degradational series, increased knowledge on host responses and possibility of a "Compartmentalization Of Decay In Trees" (CODIT) model (see Shigo, 1984; see Section 3.3 *Host defense mechanisms in wood*) exhibited in Permian woods, and evidence of arthropod interactions are new findings presented here. Overall, the high frequency and proliferation of pocket rot in Triassic woods (and to a lesser extent Permian woods) suggest that wood-decaying fungi played a major role as decomposers in Permian and Triassic peat forming environments.

3.2 Wood rot affinities and degradational series in decay

Of the three principal decay types, the decay pattern, symptoms, and signs are most consistent with selective delignification white rot, and more specifically white pocket rot (e.g.,

Montgomary, 1982; Blanchette, 1984b). Studies of Antarctic permineralized wood also came to the same conclusion of white rot and white pocket rot affinities (Schopf, 1970; Stubblefield and Taylor, 1985; 1986; Weaver et al., 1997). Features shared in each of these studies and with extant white rot, pocket rot fungi include: differential rates of degradation of lignin and cellulose and other cell wall constituents (i.e., lignin is broken down prior to hemicellulose of cellulose; Schwarze et al, 2000), preferential lignin degradation that results in light patches or pockets that causes lighter zones with pure cellulose remaining similar to extant species of pocket rot producing fungi, e.g., *Phellinus pini* or *Gridfola frondosa* (Hartig, 1878; Liese and Schmidt, 1966; Blanchette, 1980), and presence of spindle-shaped pockets extending throughout the specimens. Extant species of white rot fungi and pocket rot producing fungi are predominately members of the Basidiomycota, which are typified by the presence of clamp connections (Webster and Weber, 2007). Clamp connections are hyphal structures formed by basidiomycetous fungi in order to preserve the dikaryotic state and range in morphology that include simple, curved, coupled, medallion, whorled, etc. (Buchalo et al., 1983). Although taxonomic affinity of basidiomycetes cannot be assessed on the morphology of clamps alone, the presence of multiple types of clamps found within the woods in this study may indicate that there are multiple types of fungal species occurring or co-occurring within the Permian stem and root woods. However, based on the decay patterns and specific delignification of cell walls, in addition to presence of multiple types of clamp connections, we are confident that at least one of these fungal morphotypes represents a white rot, pocket rot forming fungus.

Morphological aspects of white rot and pocket rot are also well characterized in SEM studies (e.g., Blanchette, 1980). For example, white rot proceeds from the S_3, which is adjacent to the cell lumen, outward into the middle lamella via hyphae eroding each cell wall layer in between. As a result, many of these features can be studied SEM; including erosion troughs,

micro cavities in the layers via selective delignification of fungal enzymes. Many of these features were not confidentially ascribed in this study, however, preliminary SEM results indicate some features of the Permian wood that are superficially similar to extant submicroscopic features of decay (Plate 13, Figs. 160-162). In congruence with thin sections, more studies with SEM on wood decay in the fossil record will also add to the increasing data set needed for wood-fungal studies.

3.3 Host defense mechanisms in wood

Secondary xylem cells have a diverse suite of anatomical defense mechanisms to microbes via dynamic sequences of events which facilitate tree defense against antagonists (Blanchette, 1992). Among these defenses includes cell wall alterations with the production of appositions (sometimes termed papillae or callosities) at sites of infection or attempted penetration by fungi (Pearce, 1996). These appositions are composed of material and components that do not typically occur in unmodified cell walls, such as lignin, phenolic compounds, callose, silicon, plus normal cell wall components that can partially to fully occlude cell lumina to block or prevent infection (Aist, 1976; 1983). These structures are present in extant lignified plants, i.e., gymnosperms (Bonello et al., 1991) and angiosperms (Edwards and Ayres, 1981), as well as in fossil plants, e.g., Devonian progymnosperms (Stubblefield et al., 1985), Carboniferous fossil gymnosperm reproductive structures (Stubblefield et al., 1984), Triassic woods from Antarctica (Stubblefield and Taylor, 1985; 1986). All of the processes that occur in xylem at the time of wounding function to form barriers that resist adverse effects and protect the living tree (Hartig 1878). The anatomical processes that occur to form these barriers are collectively called the CODIT model (Shigo, 1970; 1976; 1984) and has two principal parts. CODIT model part 1: the events that take place within the xylem at the time of wounding and the

other to the cells formed after wounding, i.e., the reaction zone to fungi. Part 2: production of a forth secondary cell wall (normally there are only S_1-S_3) which functions as a boundary formed after injury and typically separates the new tissues from those existing at the time of injury. It has been suggested that few pathogens or parasitic microorganisms can penetrate this barrier (Shigo, 1984).

Compartmentalization processes in trees produce barriers that resist colonization by decay fungi. Many of the cells that have exhibited evenly swollen and separated cell walls are interpreted as host responses by stem and root wood cells. This can be interpreted as part 1 of the CODIT model, reaction to the fungi. We interpret this host response only as part 1 because in certain areas, hyphae can penetrate directly through the reaction zones, and is likely prior to when a barrier zone formed (part 2). In rare instances, reactions zones are directly adjacent to highly delignified tracheid cells, which again can likely be interrupted as part 1 and prior formation to part 2 barrier zones in order to prevent delignification of cells. Other specimens exhibit structures, i.e., appositions, which likely originated from cell wall contents that fully occlude the cell lumen with opaque contents and are interrupted as part 2 of the CODIT model, barrier formation. Hyphae have not been observed penetrating through cells with appositions, but do ramify through cells surrounding the appositions. There are also cells that contain structures that completely occlude the lumen but show no direct attachment to the S_3 layer in transverse view. Similar structures previously interpreted as fragments of indeterminate tissues and abundant larger spherical to oblong organics masses were also described in *Australoxylon* from the Prince Charles Mountains, see Figs. 10A, B in Weaver et al. (1997). These are rare occurrences may represent tyloses, suberized structures developed from xylem parenchyma cells and project through pits to occlude cell lumina, which is another example of wood defense mechanisms (Pearce, 1989). These proposed tyloses are not a defined as structures in other fossil

wood studies, e.g., Permian stem wood, Weaver et al. (1997) and Jurassic stem wood, Harper et al. (2012). Few examples of host responses that are illustrated in extant plants have yet to be demonstrated in infected fossil plants. Evidence from this study provides further insight into the evolution of defense mechanisms and compartmentalization in Paleozoic plants.

3.4 Arthropod interactions with wood decay

Certain cavities or pockets in the stem and root wood contain arthropod coprolites (Plate 12, Fig. 156), some are even associated with spores (Plate 12, Figs. 157-159). Occurrences of coprolites within wood cavities have been interpreted as the result of arthropod woodborers leaving behind frass (e.g., Scott and Taylor, 1983; Scott et al., 1985; Chaloner et al., 1991; Scott, 1992; Zavada and Mentis, 1992; Ash, 2000; Labandeira, 2007). Evidence of arthropod coprolites in Permian woods is a common occurrence (Weaver et al., 1997; Kellogg and Taylor, 2004) and for a detailed review on glossopterid wood and arthropod interactions, the reader is referred to Slater et al. (2012). In modern ecosystems, there are approximately 20 families and 8 orders of arthropods that have the capacity to digest wood (Martin, 1991). Extant invertebrates such as beetles and mites are the most common woodborers, and produce the most similar excavations and coprolites to those in the Antarctic woods (e.g., Weaver et al., 1997; Kellogg and Taylor, 2004). Key differences between this study and other studies focused on fossil wood decay from Antarctica, include that the initial study of wood decay by Stubblefield and Taylor (1985; 1986) described clean-cut walls characteristic of arthropod attack, but they lack coprolites and have been attributed to fungal saprophytism based on the presence of fungal remains. In contrast, Weaver et al. (1997) described numerous irregular edge pockets and galleries filled with coprolites, but wood specimens lacked fungal fossils.

The current study provides the opportunity to study insights into fungal-arthropod-wood interactions in certain specimens and likely share affinities to orbital mites, similar to coprolites to previous Permian Antarctic wood studies. Significantly, some modern wood boring beetles and fungi show mutualistic relationships, with the beetles actively or passively dispersing fungi between plants, and the insect larvae feeding (in part) on the fungi invading the plant tissues around the larval excavations galleries or chambers (Francke-Grosman, 1963; Matthews, 1976; Weaver et al., 1997).

3.5 Missing components from the fossil record regarding the wood decay life cycle – Paleozoic

Many morphological features be can recognized in the life cycle of extant wood decay basidiomycete fungi. A general, simplified life cycle begins with the large basidiocarps (e.g., polypores, shelf fungi, bracket fungi) that develop on the surface of infected trees. On the abaxial side of these polypores, spores develop on the tips of sterigmata via basidia within the gills of polypores. Once matured, spores are released and carried by wind and can enter host trees via wounds, lenticels, etc. The spores germinate and begin to infect and colonize the host tree rapidly with vegetative mycelium. The hyphae extrude and produce various degradational enzymes, which can characterize the type of rot, as well as specific decay patterns, symptoms, and signs. Typically, the host will produce defense mechanisms in response to the invading fungus, e.g., appositions, tyloses, exhibit the CODIT model. However, if the decay is severe enough, it will progress to the point in which the tree dies and at any point when the vegetative mycelium has colonized enough of the tree, complex polypores will form on the outside of the tree and the cycle will begin again (Schmidt, 2006).

Many of these components can be found in the fossil record, several of them are explicitly found in the current study with the exception of: polypore or basidiocarps that contain

sterigmata with spores. Although these structures have not been found in the Paleozoic or Mesozoic, examples have been described in geologically younger material. One of the best preserved examples are from the Lower Miocene of Libya, which includes a permineralized basidiocarp, *Ganodermites libycus*, with well preserved pilocystidia, sterigmata, and attached spores (Fleischmann et al., 2007). Therefore it is possible to have such delicate structures preserved, however, due to their soft tissue systems and their location on the outside of trees (even the outer bark portions of trees are seldom preserved; Decombeix et al., 2010), the preservation potential is low. However, the possibility of *in situ* fossil forests may provide the best opportunity to find such structures in Mesozoic and Paleozoic ecosystems, even polypore attachment points or scars on tree surfaces will greatly enhance the knowledge base of wood decay in ancient ecosystems. More data is needed to further expand the Paleozoic (and Mesozoic) wood decay life cycles, especially larger, more complete specimens of trunks with fungal infection symptoms and signs.

3.6 Molecular clock data about wood rot enzymes

Floudas et al. (2012) suggested that lignin degrading enzymes in certain groups of fungi first appeared during the Early Permian (~295 Ma) based on relaxed molecular clock analyses of multiple species of lignin-degrading fungi, together with fossil-based calibrations. The authors also discuss that this Early Permian origin of lignin decaying enzymes has implications on the decline of organic carbon, i.e., coal composed primarily of lignin, at the end of the Permo-Carboniferous, such that the decline of coal in the fossil record may in part be due to the evolution of lignin degrading fungi in the Early Permian. This broad speculation overlooks that lignin-producing organisms have been present since at least the Early Devonian (~407 Ma, see Gerrienne et al., 2011) and specific disease symptoms similar to those as a result of fungi have

also been described from the Late Devonian (~372 Ma, see Stubblefield et al., 1985). Additionally, the number of lignin producing taxa from the Devonian and Carboniferous (e.g., progymnosperms, Cordaitales, certain Paleozoic seed ferns, conifers, etc.; Taylor et al., 2009) undoubtedly served as hosts to a wide range of microorganisms, including wood degrading fungi. The study of wood-fungal interactions from this time period in particular, due to the transition from the Devonian to the Carboniferous, i.e., greater biodiversity and morphological variability (see Kerp, 2000; Krings et al., 2012), is vital because it represents an important point in geologic time in floral and ecosystem turnover, i.e., Devonian: earliest appearance of wood to the Carboniferous: dominance of arborescent plants to the Permian: well established lignified forest stands. With the inclusion of this chapter and previous work by Stubblefield and Taylor (1985; 1986), there is definitive evidence for lignin degrading fungi in the Late Permian, but these fungi likely evolved much early in geologic time due to the presence of lignified plants ~140 Ma prior to the specimens used in this study. Without question, more work is needed to resolve wood-fungal relationships in the Paleozoic.

4. Conclusions

4.1 Addressing the absence of certain wood rot types in the fossil record

The paucity of other rot types in the fossil record, i.e., brown and soft, is likely due to the very nature of the decay and resulting wood texture, and not because they were absent in ancient ecosystems. Interestingly, in white rot with selective delignification the cellulose is broken down more slowly than in simultaneous white rot, brown rot, and soft rot, so the structural integrity of the wood and the reduction in wood strength properties are less drastic (Manion, 1991). Additionally, the S_2 layer persists much longer during this type of white rot selective decay, once again contributing to the overall strength quality of the cell (Schwarze and Engels, 1998). Each

of these aspects specific to selective delignification of white rot fungi attests to its presence in the fossil record, i.e., the structural integrity of wood is more persistent relative to other rot types, thus increasing chances for fossilization relative to softer structures. This is in contrast to simultaneous white rot, brown rot, or soft rotted woods, such as brittle fracturing of the wood due to progressive degradation of the cellulose-rich secondary wall. As well as an extremely brittle or crumbly texture from brown rot that does not lend itself well for ideal preservation conditions. And to a lesser extent soft rot, in which the rot is based on hyphal morphological characters and relationship to the cell walls, which could certainly be studied via SEM if those characters were present in fossil woods. Evidence of brown and soft rots using analytical, geochemical techniques has been demonstrated in non-permineralized or mummified woods from archeological sites, e.g., 700 BC wooden coffin (soft rot) and ancient Egyptian objects (brown rot) (Blanchette et al., 1992; Blanchette, 2000). The study of each of these wood decay types could greatly benefit through further integration of geochemical analysis, especially the latter, i.e., simultaneous white rot, brown and soft rots, because these types may not be recognizable through morphological studies due to a reduction in strength properties in host woods, in turn greatly reducing the preservation potential, and could be further elucidated or verified using geochemical techniques.

4.2 The potential of analytical techniques in paleomycology

The abundance of anatomically preserved wood in the fossil record provides an almost unlimited source of material that can be used to search for the presence of fungi and potential host responses. The application of geochemical techniques in paleomycology, such as developing taxonomic- and disease-specific fungal biomarkers, provides the foundation of a new avenue for understanding fungal diversity and plant-fungal evolution geologic time. When

permineralized woods are examined the primary focus is usually the taxonomy of wood, and little attention is given to fungal host responses or the presence of fungi. Many of the key diagnostic features of the wood that would be useful in their illustration or description are decomposed, altered, and/or destroyed by the fungus rendering a specimen useless for detailed wood anatomy (Taylor et al., 2015). As a result, I believe that the abundance of well-curated collections of fossil woods, such as the University of Kansas (KU) Antarctic paleobotanical collection, and in congruence with applied analytical techniques, represents a potential source of new information about wood-fungal in the fossil record, including information about their plant hosts.

Chapter 7

Tylosis formation and fungal interactions in an Early Jurassic conifer from northern Victoria Land, Antarctica

1. Introduction

Fungi are an integral part of virtually all-modern ecosystems. One of the most recognized and important ecological roles fungi perform includes decomposition and nutrient cycling. In extant forest ecosystems, fungi are the primary organisms responsible for the delignification and degradation of wood (Dighton et al., 2005). Wood-decay fungi are of three principal types, i.e., brown, white, and soft rot. The delineation among the three types is based on the presence/absence of delignification by specific enzymes, patterns of host cell-wall degradation, affinities of the fungi involved, and type of wood most commonly used as a nutrient source (Schwarze et al., 2000). Some wood-decay fungi may also be effective as parasites and causal agents of mild to severe diseases. Tracheary elements in the wood of living plants (i.e., tracheids and/or vessels) are hollow and dead at maturity, and thus do not provide any physiological barrier against the spread of pathogenic fungi. In order to deter or prevent the infestation of wood by pathogenic microorganisms, plants exhibit various types of structural defense strategies. One defense strategy is the formation of tyloses (e.g., Barry et al., 2001). Tyloses are suberized structures that develop from ray parenchyma cells and project through pits to occlude the lumina of tracheids and vessels (Pearce, 1996). Tylosis formation is one of the main processes in the compartmentalization of decay in trees (CODIT model, e.g., Shigo, 1984) and serves to slow down or prevent the spread of pathogens. In addition, tyloses can form around wounds to prevent water loss, even in the absence of decay, in the nonfunctional xylem. Morphologically and

functionally comparable structures in the sieve cells of phloem are termed tylosoids (Evert, 2006).

An extensive fossil record of tylosis formation demonstrates that these protrusions have been a common process in woody plants since at least the late Paleozoic. The earliest reports of tyloses in fossil plants come from the Carboniferous, and include a progymnosperm (Scheckler and Galtier, 2003) and several ferns (Williamson, 1876; Weiss, 1906; Phillips and Galtier, 2005). Tyloses or tylosis-like structures have also been described in Triassic gymnosperm wood, *Araucarioxylon mineense* (Ogura, 1960; Nishida et al., 1977), as well as the Jurassic wood *Metacedroxylon scoticum* (Holden, 1915) and *Xenoxylon morrisonense* (Medlyn and Tidwell, 1975). Cretaceous and Cenozoic permineralized woods have yielded abundant reports on the presence of tyloses in fossil angiosperm wood (Jeffrey, 1904; Bancroft, 1935; Spackman, 1948; Brett, 1960; Manchester, 1983; Nishida et al., 1990; Privé-Gill et al., 1999; Castañeda-Posadas et al., 2009); however, information on whether tyloses in fossil gymnosperms formed specifically in response to infestation with fungi or other pathogens has so far been lacking and thus the evolutionary history of tylosis formation as a particular defense strategy against pathogens remains unresolved.

In this contribution, we present a permineralized conifer axis from the Lower Jurassic of Antarctica that contains numerous tyloses in both the wood and bark in association with a wood-rotting fungus. What is most significant about this fossil is that the tyloses co-occur with fungal hyphae in the tracheids in a pattern suggestive of tylosis formation in direct response to fungal colonization.

2. Description

2.1 Wood and Secondary Phloem

Specimens represent multiple segments of a conifer axis with secondary xylem and phloem, ~10 cm long and 5 cm wide (Plate 14, Fig. 163). Although growth ring boundaries are difficult to discern, it is estimated that the original diameter of the axis at this level was approximately 15 cm. Most of the axis consists of secondary xylem with numerous intercalated rays. Tracheids are polygonal in transverse section and about 20-30 μm in diameter (Plate 14, Fig. 164). The wood has abundant, evenly distributed uniseriate rays that are 5-8 cells (Plate 14, Fig. 165). Extraxylary tissue is preserved along the outer portion of the axis. Secondary phloem cells are of two principal types: a larger and more prevalent type with diameters up to 75 μm and a smaller, less common type with diameters between 18-35 μm (Plate 14, Fig. 166). The larger cells show distinct concentric layers within the cell wall. The radial walls of the tracheids are further characterized by uniseriate circular-bordered pits with wide borders and narrow apertures (Plate 14, Fig. 167).

Many of the conifer axes from the Suture Bench locality are *in situ* trunks with well-preserved secondary phloem layers; however, the preservation of the wood is overall very poor. In many sections of the specimen described here, the thick S_2 layer of the tracheid walls appears diffusely degraded and somewhat translucent. The cell walls may further show a separation and detachment of intact S_3 layers, which occur isolated and twisted within the cell lumens (Plate 14, Fig. 168). In other cases, the boundaries of individual cells are represented by translucent outlines in which it is difficult to determine tracheid wall thickness. Discrete damage structures, such as erosion channels, lysis zones, bore holes, or cavities have not been observed. The ray parenchyma is decomposed to varying degrees; in some areas, the original distribution of rays is recognizable only by opposite pairs of tyloses.

2.2 Tyloses

Abundant tyloses are found along rays in the specimen and are not concentrated in any specific area, e.g., close to ring boundaries. They originate from ray parenchyma cells and each ray cell may produce more than one tylosis; most commonly, tyloses occur in the form of one or more opposite pairs per ray cell (Plate 14, Fig. 169-170). One ray parenchyma cell will balloon out through cross-field pits into the adjacent tracheids (Plate 14, Fig. 171). Tyloses occur in different size ranges (8-25 μm in diameter), and have different morphologies that occlude the tracheid lumen entirely. During development, tyloses are initially small, bulbous protrusions with an undistinguishable base (Plate 14, Fig. 172). Intermediate stages are morphologically similar to these small protrusions but larger in size and with a more recognizable base (Plate 14, Fig. 174). Fully developed and mature tyloses are large, globose structures characterized by a narrow base, which is often the same diameter as the cross-field pit (Plate 14, Fig. 175). The main body of the tylosis may contain dark amorphous or granular material (Plate 14, Fig. 175); they are occasionally empty and more or less translucent. There is no evidence of tyloses co-occurring with extractives plugging adjacent cells as well as no discoloration of the wood.

2.3 Fungus

Remains of a fungal mycelium occur throughout the specimen. The hyphae are septate and relatively uniform in size, ranging from 1.5-3.0 μm in diameter (Plate 14, Fig. 176). Hyphal septations are irregularly spaced, at right angles to the hyphal wall, and commonly associated with a slight constriction of the hypha. Hyphae in tracheids may be irregularly swollen, with bare knob-like protuberances and short, irregularly forking branches. The mycelium extends horizontally in the wood via the rays and vertically via the tracheids. Hyphal propagation from cell to cell is essentially through pit apertures. In some sections, individual hyphae can be traced over a vertical distance of about 1 cm as they extend through the wood. Hyphae usually occur in

a relatively straight or slightly curving course (Plate 14, Fig. 177). Within the tyloses, hyphae may form dense loops, whereas knots or twisted configurations occur inside tracheid cells in close proximity to tyloses (Plate 14, Fig. 178; Plate 15, Fig. 179). In addition to being found within the tylosis, there is evidence that hyphae can penetrate the tylotic wall and either exit or enter the tylosis (Plate 15, Fig. 180). In places where hyphae change direction, they may branch to form Y-or T-shaped dichotomies (Plate 15, Fig. 181). In a ray cell, for instance, branching of a horizontal hypha commonly results in two hyphal branches that leave the ray in opposite directions through the cross-field pits. Similarly, a hypha within the main body of a tylosis may dichotomize and send off two hyphal branches that penetrate into the surrounding tracheid in opposite directions through the wall of the tylosis. Hyphae that depart a ray through a tylosis generally extend only a short vertical distance through the tracheid before re-entering into an adjacent ray parenchyma cell through the aperture of a cross-field pit. There is no evidence for penetration hyphae, boring, or any other form of hyphae penetrating the actual tracheid cell walls.

Fungal remains also occur in the secondary phloem cells, where they are particularly common in the small cell type. Hyphae are generally found along the surface of the cell wall in the lumen of the cells (Plate 15, Fig. 182). Hyphae in the phloem are usually associated with the above-mentioned concentric layering. In contrast to those in the xylem, hyphae in the phloem are found penetrating the actual cell walls horizontally. Linearly aligned, spherical structures approximately 5 μm in diameter occur in close association with these hyphae. It remains unclear whether these structures are fungal in origin.

3. Discussion

Even though there has been increased scientific attention to the fossil record of plant-fungal interactions in recent years (Taylor and Krings, 2010), reports of Jurassic fungi are still sparse. This is likely the result of a major taphonomic bias, because most of our knowledge of Jurassic floras is based on impression/compression remains that usually yield very limited information on fungal and other microbial associations. Reports of Jurassic fungi include fungal trace fossils (Martill, 1989) and lichen-forming fungi (Preat et al., 2000), as well as more readily identifiable fungal remains such as spores and hyphae (Stockey, 1980; Traverse and Ash, 1994; Ibanez and Zamuner, 1996). Our observations lead us to suggest that tylosis formation in the wood may have occurred as a non-specific host response to fungal infestation. Few reports, however, provide a detailed description of the fungi. In addition, Jurassic fossil wood has been described with particular decay patterns that have been interpreted as the result of fungal activity (e.g., Müller-Stoll, 1936; Süss and Philippe, 1993; Falaschi et al., 2011). Moreover, the new material described here therefore offers a rare opportunity to provide additional evidence for Mesozoic plant-fungal interactions and the possible affinities of a Jurassic fungus from southern Gondwana.

3.1 Tylosis formation as a host response to fungal attack?

A conspicuous feature of the Antarctic conifer wood is the high number of tyloses. In contrast to the regular formation of tyloses in the (non-functioning) heartwood of angiosperms, tylosis formation in conifer tracheids generally occurs as a response to physical damage or pathogenic stimulants, i.e., traumatic tyloses. The apparent exception is the genus *Pinus*, where they have been reported in unwounded tissue (Chrysler, 1908). They also form in resin canals in some conifers, although these are generally called tylosoids as they do not extend through pits (Chrysler, 1908; Evert, 2006). Tyloses serve to seal off damaged or infected wood areas, and to

limit or retard further spreading of pathogenic agents, including wood-rotting fungi (Chrysler, 1908; Yamada, 2001). It has been shown that once a fungal pathogen has invaded the wood, tyloses can be produced in areas of wood not yet infected (Talboys, 1964). In *Lithocarpus densiflorus* (tanoak) wood, an increase in tylosis formation has been shown to correlate directly with an increase in fungi (Collins and Parke, 2008). It therefore appears possible that the prominent tylosis formation in this Antarctic fossil was a response to the infection of a wood-rot fungus and served to build up mechanical barriers against the advancing hyphae. The commonly occurring small, knob- to club-shaped tyloses may be interpreted as not fully developed. It has been shown in extant wood that fully developed tyloses are globose and contain dark lumens (Chrysler, 1908). Hence, there may be some evidence that tylosis formation and fungal infection occurred at least in parts synchronously in the fossil. This is further supported by the common occurrence of fungal hyphae that appear to have grown around smaller tyloses.

At the same time, tylosis formation apparently occurred as a non-specific host response, because its effectiveness against this particular fungus was only limited. Throughout the wood there is abundant evidence of fungal hyphae penetrating into the tyloses, where the hyphae usually coil and branch before extending into the adjacent tracheid or ray cell. Certain fungi are known to produce enzymes that break down plant suberin (Fernando et al., 1984; Ofong and Pearce, 1994). In this respect, the presence of knob-like swellings and short irregular branches on hyphae that occur inside or in close proximity to a tylosis is of particular importance; it may indicate that this fungus was capable of producing such degradational enzymes in order to break down the wall of the tyloses and thus surmount the defense mechanism of the plant. We hypothesize that hyphal swelling and branching would have facilitated the decay of suberic substances by providing an increased surface area and thus increased enzyme concentrations at

the contact site. This relationship between tyloses and fungi are summarized and represented in Figure 14.

In extant trees, the living portion of sapwood shows a dynamic response to pathogens, including discolored wood containing various extractives (e.g., tannins, dyestuffs, oils, gums, resins, salts of organic acids) which form around an infected area (Pallardy, 2008). When these extractives are overcome by the pathogen, additional defense measures include the production of tyloses to compartmentalize the invading microbe. Diagnostic characters of wood-pathogenic interactions such as extractives occluding cells adjacent to tylosis or discoloration of the wood is not likely to be preserved in fossils. Fungal hyphae are not extensive and the colonization of the host is limited. Therefore it is reasonable to suggest that the interaction between the tree and fungus is at the initial stage of fungal colonization. Based on the evidence at hand, it is likely that this conifer represents a living tree interacting with a fungus.

3.2 Fungi and phloem relationships

In this report we provide evidence for fungi in the cells of the secondary phloem. Descriptions of fungal hyphae in fossil phloem are exceptionally rare (Stevens, 1912). The production of tylosoids in the phloem could also serve as a defense mechanism against external agents (Yamada, 2001). Tylosoids have been shown to develop in the roots of conifers (Wingfield and Marasas, 1980). In the phloem, tylosoids form similarly to tyloses in the xylem, i.e., parenchyma cells extend into the lumen of non-functioning sieve cells (e.g., Esau, 1977; Evert, 2006). The function of tylosoids is also hypothesized to be similar to that of tyloses in xylem, i.e., they serve to seal off non-functioning sieve elements (e.g., Ervin and Evert, 1967). They occur following a drop in pressure and cell death and are seasonal (Lawton and Lawton, 1971). Since tylosoids in the phloem can become lignified (e.g., Lawton and Lawton, 1971), the

thicker, concentric structures present in the fossil phloem cell lumens may represent tylosoids formed in response to fungi. Whether these cell contents represent a preservational artifact or the actual deposition of some type of secondary metabolite in the phloem remains unknown.

3.3 Possible affinities of the fungus and wood decay features

Speculation on the affinities of the fungus is limited to morphological evidence and consequently cannot be discerned with confidence without further examination of several samples from this locality. The fungus is remarkably similar in both morphology and colonization pattern to *Verticicladiella wageneri* Kendrick (teleomorph: *Ceratocystis wageneri* Goheen et Cobb) wilt pathogenic fungi. This fungus is unique because of the tracheid-limited pattern of colonization (Wagener and Mielke, 1961). Key characters of this fungus include longitudinal colonization of the host, serpentine and helical growth patterns, not penetrating through the cell wall, traveling through the bordered pits, and branching near bordered pits. It has also been noted in *Pseudotsuga menziesii* (Mirb.) Franco (Douglas-fir) that tyloses frequently occluded cells adjacent to tracheids invaded by hyphae; however, these structures seldom coalesced to block hyphal passage though lumens (Hessburg and Hansen, 1987). Additionally, the fungus in this study share resemblance with fungal blue-stain fungi (e.g., *Ceratocystis* sp., *Ophiostoma polonicum*) in colonization patterns that spread radially via the bordered pits of the xylem rays to enter the tracheid lumen (Ballard et. al, 1982; Christiansen and Solheim, 1990). It is important to note that both *Verticicladiella wageneri* and *Ceratocystis* sp. are spread through beetle vectors (Witcosky and Hansen, 1985; Goheen and Hansen, 1993; Solheim, 1994; Solheim, 1995). There is no evidence of arthropod coprolites or feeding galleries in the specimens studied. However, it is interesting to note that Bomfleur et al. 2011 reported a beetle elytron and a piece of silicified wood from the same locality (Suture Bench) as this study with characteristic holes

and tunnels less than 1 cm in diameter that were suggested to represent arthropod borings (Bomfleur et al., 2011). At the present there is not sufficient evidence to link these occurrences, but further material and study is needed to fully elucidate beetle-fungal pathogen relationships with conifer forests from the Jurassic of Antarctica.

The wood in all specimens is poorly persevered and therefore cannot provide all of the anatomical characters to a specific wood rot category. Although it is not known how brown rot fungi interacted with trees during the Jurassic, current information from extant fungi does not provide evidence nor suggest that certain types of rot, i.e., brown rot, are aggressive tree pathogens. However, the decay pattern and fungal characters in the Antarctic fossil wood indicate plausible affinities to brown rot fungi, including (1) advanced decomposition of ray parenchyma, (2) diffuse degradation (increasing translucence) of the massive S_2 layers of the tracheid cell walls, (3) the separation of intact S_3 layers due to a lack of delignification processes, (4) the absence of discrete decay structures, such as bore holes, lysis zones, erosion channels, or distinctive cavities, and (5) colonization via the rays and tracheids, with cell-to-cell migration through pit apertures (e.g., Anagnost, 1998;). This interpretation may be further supported by the observation that brown rot is the dominant form of fungal decay in conifer wood today (e.g., Schmidt, 2006; Schwarze, 2007). Again, it is difficult to assign wood rot affinities with certain confidence, but it is important to document these observations as a platform for further research of brown-rot fungi in fossil woods.

The vast majority of brown-rot fungi are polyporalean basidiomycetes (e.g., Schmidt, 2006). Clamp connections, a synapomorphy of the Basidiomycota, have not been observed in these Antarctic fossils, but certain groups of modern polyporalean brown-rot fungi lack clamp connections (e.g., Stalpers, 1978; Larsen, 1983; Zmitrovich et al., 2006). A further characteristic of Polyporales is the presence of large, shelf- or bracket-shaped fruiting bodies (basidiocarps)

that develop on the trunk surface. Fossil basidiocarps are overall very rare (e.g., Andrews and Lenz, 1947; Poinar and Singer, 1990; Fleischmann et al., 2007). Although there is no such structure preserved on the present specimen, the exclusively vegetative state of the fungus inside the wood provides some support to the hypothesis that the reproductive features of this possible wood-rot fungus were confined to separate structures outside the trunk.

3.4 Antarctic Jurassic wood and tyloses

Although there is relatively little information available about continental Antarctic floras during the Jurassic, some areas were apparently dominated by conifers (Townrow, 1967; Jefferson et al., 1983; del Valle et al., 1997; Garland et al., 2007). The presence of fungi in these Jurassic conifers underscores the plasticity of these ancient organisms and their interactions. As in modern temperate forests, these trees must have encountered a diverse suite of microorganisms and developed several mechanisms for defense, including the production of tyloses to deter the spread of pathogenic fungi. Documentation of tylosis formation in fossil woods from Antarctica to date has been restricted to Cretaceous angiosperm wood (Poole and Francis, 1999; Poole and Cantrill, 2001). This report provides the first evidence of Jurassic conifer wood from Antarctica with well-preserved fungi and the formation of tyloses, as well as the first reports of fungi in fossil phloem from Antarctica and possible production of tylosoids in response to these fungi. Furthermore, the presence of the fungus in this study as well as the documented evidence of beetle remains and possible bore holes in specimens from at Suture Bench (Bomfleur et al., 2011), may provide the foundation to linking these components in a future study. In addition to climate change, beetle-fungal pathogens may have added to the disappearance of conifers on mainland Antarctica. Our results build upon our current

understanding of the relationships in paleoecosystems and the co-evolutionary processes that have developed between trees and external biotic agents through geologic time.

Chapter 8

An initial survey of the fungi and fungal-like organism associations with *Glossopteris* leaves and leaf mats

1. Introduction

1.1 The modern phyllosphere

The phyllosphere includes the ecological interactions of the interior tissues and surface environment together as a whole (Carroll et al., 1977), which provides habitats for a variety of microorganisms, which include fungi as endophytes (colonize the interior of leaves) and epiphytes (colonize surface of leaves) (Petrini, 1991). Leaves constitute a harsh environment for fungi due to a variety of abiotic and biotic factors, e.g., temporary nutrient availability, extreme fluctuations in humidity, temperature, gas exchange gradients, and ultraviolet radiation (Krings et al., 2012a). Modern studies and understanding of microbial composition within the phyllosphere focus heavily on bacterial-leaf associations via high throughput DNA sequencing and to a lesser extent, fungi (Jumpponen and Jones, 2009). In contrast to the rhizosphere, which is a constant system of the roots and surrounding soil matrix, the phyllosphere, depending on the leaf longevity of the plant (e.g., deciduous vs. evergreen), can be considered an ephemeral system (Kikuzawa and Lechowicz, 2011). Leaves also possess a suite of anatomical and morphological features that function to prevent external antagonists from infection or colonization, e.g., a hydrophobic waxy cuticle that covers the epidermal cells to reduce the evaporation of water, but at the same time reduces leaching of plant metabolites resulting in a low nutrient environment for microbial communities (Vorholt, 2012). Despite these factors, leaf endophytes and epiphytes represent a major component of extant fungal diversity.

1.2 Leaf fungi in the fossil record

The difficulty in studying epiphyllous fungi in the fossil record is that the fine microdetail of the fungus, i.e., sexual, asexual, and vegetative remains needed for taxonomic assignment, are often not preserved or lost through preparation techniques, especially in permineralized material. Hyphae are sometimes the only record of epiphyllous fungi on the surface of fossil leaves (Taylor et al., 2015). The fossil record of leaf-associated fungi is predominately based on Cenozoic cuticular epiphyllous fungi, which also include several examples of reproductive structures (e.g., Dilcher, 1963; 1965; Selkirk, 1972; Lange, 1978; Phipps, 2001; 2007; Phipps and Rember, 2004). To date there is little evidence of permineralized pre-Cretaceous fungal endophytes and epiphytes on or within leaves with the exception of well-preserved leaf endophytes from the Carboniferous. Examples of permineralized endophytes found in Carboniferous foliage types within coal swamp environments include: fern pinnules with hyphae of unknown affinity within hypodermal cells; the fungus was described as a septate, branching endophyte with elongated hyphal swellings (Krings et al., 2009a), fungal spores and hyphae within vascular and parenchymatous tissues (Barthel, 1961; Krings, 2001), and possible fungal microsclerotia, resting spores, and hyphae within fern pinnule hypodermal cells (Krings et al., 2010a). There is also a single report of permineralized Permian leaf fungi from Antarctica (Holdgate et al., 2005). There is evidence for filamentous hyphae ramifying through the mesophyll tissues of *Noeggerathiopsis* leaves. There was no discussion of the potential ecological affinity of the fungus, but it may represent a saprotrophic fungus within the peat.

1.3 Permineralized Glossopteris *spp. from Antarctica*

The Glossopteridales are an extinct group of seed plants that dominated the vegetation of the southern supercontinent Gondwana during the Permian (~300–250 mya; Taylor et al., 2009). The most commonly found remains of glossopterids are leaves of the morphogenus *Glossopteris*, which is historically important as its presence on several of the southern continents represented some of the early evidence for the existence of continental drift (Wegener, 1924). *Glossopteris* specimens are characterized by a lanceolate to tongue-shaped, entire leaf, which is constructed of a midrib made up of multiple veins and reticulate second order venation *Glossopteris* leaves, and most are commonly found as impression/compression fossils. Since the original description of *Glossopteris* by Brongniart (1828), several species from Gondwana have been described.

Permineralized, i.e., anatomically preserved, specimens have greatly enhanced our understanding of the glossopterids in silicified peat deposits from the Bowen Basin of Queensland, Australia, and the central Transantarctic Mountains of Antarctica (Schopf, 1970; Gould and Delevoryas, 1977; Taylor et al., 1989a, Taylor and Taylor, 1990). Two distinct species of leaves have been described from Antarctica (*G. schopfii* and *G. skaarensis*), and these also appear to be present in Australia, in addition to a third species that has only been found in Australia (*G. homevalensis*) (Pigg, 1990; Pigg and Taylor, 1990).

As common as *Glossopteris* floras are in Permian, to date, there is no information available regarding the microbial component or interactions with this important leaf type regardless of the preservation mode. *Glossopteris* spp. permineralized leaf mats are known from Antarctica, e.g., from Skaar Ridge (e.g., Schwendemann, 2012) and Collinson Ridge (McManus et al., 2002), but no foliar fungi have been identified. This study focuses on surveying these Permian permineralized deposits for any fungal remnant associated with the leaves, e.g., potential fungal endophytes, epiphytes, saprotrophs, parasites, etc. as well as microorganisms within the surrounding peat matrix in these leaf mats. This component of the study focuses on

bridging the gap between documented Carboniferous leaf fungi and Triassic leaf related fungi (e.g., *Endochaetophora* in Antarctic leaf litter deposits, see Chapter 9 of this dissertation) in order to broaden our ever-increasing knowledge base of Paleozoic fungi, especially the meager record of foliar fossil fungi.

2. Results

2.1 Leaf associated fungi

Glossopteris leaf mats are comprised of highly degraded, poorly preserved leaves. Many of the leaves are lacking diagnostic characters that render it impossible to assign species. Paradermal sections of *Glossopteris* leaves are characterized by large meshes and a more prominent midrib. In transverse sections, the bundle sheath, when preserved, is composed of thin-walled cells that sometimes include dark contents. Stomata are rarely preserved, but are sunken. Typically the only remaining component of the leaf that is consistent are the parallel, thick walled vascular bundles (Plate 16, Fig. 183).

There are examples of ramifying, septate hyphae from 2–4 μm in diameter that penetrate the cell walls of the xylem (Plate 16, Fig. 184). Additional remains within xylem include spherical structures that fully occlude xylem cells with attachment points at the base (Plate 16, Fig. 185). In transverse sections of leaves in the highly degraded portions of the mesophyll cells there are small circular to pyriform structures that range from 8–10 μm in diameter, and that may represent chytrids (Plate 16, Figs. 186-188). Only one of these examples of chytrids (Plate 16, Fig. 187) possess a rhizomycelia attachment <1μm in diameter. Additional specimens in transverse section yield examples of hyphae in cross section on the surface of poorly degraded leaves (Plate 16, Fig. 189). Many of the leaves in transverse section contain minute, ramifying mycelia hyphae 1-3 μm in diameter (Plate 16, Fig. 190) that branch at right angles and are

septate (Plate 16, Fig. 191). When mesophyll tissue is preserved, the septate hyphae can directly penetrate through the cell wall (Plate 16, Fig. 192). Interestingly, in a two specimens of transverse *Glossopteris* leaves are examples of clustered spores surrounded by a hyphal mantle or mycelium (Plate 16, Figs. 193-195). In one example, the spores are up to 37 μm in diameter are clustered in 3, and the hyphal mycelia surrounding the spores are 2 μm in diameter and interwoven (Plate 16, Fig. 194). The other example is a pair of clustered spores with similar interwoven hyphae and internal contents (Plate 16, Fig. 195). There is one single example of a large aggregation of mycelia within the leaf mat material composed of highly interlaced mycelia with septate hyphae (Plate 16, Figs. 196-198).

2.2 Glossopteris *leaf mat fungi and fungal-like organisms*

There are several examples of asexual spores and Peronosporomycetes in the matrix of *Glossopteris* leaf mats. These spores are designated by spore and peronosporomycete types. Spore types that have hyphal attachment are all terminal and there is no evidence of where they originate. Spore type 1 is 40 μm in diameter and shows no discernable spore wall features, but contains 3 partially preserved internal each spores approximately 10 μm in diameter (Plate 17, Fig. 199). Spore type 2 is 50 μm in diameter with a spore wall of 3 μm in diameter with hyphal attachment that is 5 μm in diameter with internal spores that are 6 to 10 μm in diameter (Plate 17, Fig. 200). Spore type 3 is similar to spore type 2 but lacks internal contents, is 45 μm in diameter with a 2 μm diameter spore wall and hyphal attachment of 5 μm in diameter, but this spore type is found within the root tissue of *Vertebraria* (Plate 17, Fig. 201). Spore type 4 is slightly pyriform and is approximately 35 μm at the widest point with a 4-5 μm thickness to the cell wall, at the narrow end of the spore may represent a hyphal attachment (Plate 17, Fig. 202). Spore type 5 approximately 80 μm in diameter has a wall a 6-8 μm thick with small spherical

structures in the lumen that may represent a form of mycoparasitism (Plate 17, Fig. 203). There are also numerous example of spore type 6 throughout the peat that range from 15-25 μm in diameter and can occur within tissues or in the matrix, and at varying focal planes some surface ornamentation can be distinguished (Plate 17, Fig. 204). Spore type 7 is a double walled spore approximately 40 μm in diameter with a 5-7 μm cell wall (Plate 17, Fig. 205). Spore type 8 is a double walled spore with a blunt attachment point approximately 50 μm in diameter and a cell wall of 8 μm thick (Plate 17, Fig. 206). Peronosporomycete type 1 is pyriform to subglobose oogonia with spiny or occasionally truncated papillations arranged regularly across the surface approximately 50 μm in diameter; papillations bear 2–3 antler-like extensions which dichotomize once or more near their tips (Plate 17, Fig. 207). Remaining peronosporomycete types 2-4 are ellipsoidal to pyriform (40-60 μm in diameter) with blunt papillations with a consistent surface ornament pattern and antlers are poorly preserved or absent (Plate 17, Figs. 208-210).

3. Discussion

3.1 Anatomical features that affect leaf fungi

The cuticle on the leaves serve two principal functions: (1) a hydrophobic barrier that prevents desiccation in terrestrial plants and (2) external barrier and structural defense against several abiotic and biotic factors that leaves encounter (Martin, 1964; Kerstiens, 1996; Nawarth, 2006). Permineralized specimens of *Glossopteris* from Skaar Ridge and Collinson Ridge did not have any cuticle preserved within the leaf mats in the peat. *Glossopteris* cuticle, however, has been described by several authors, e.g., Zeiller 1896; Sahni, 1923; Pant and Singh, 1974; Maheshwari and Tewari, 1992, and has been problematic when discussing *Glossopteris*

taxonomy (Pigg and Nishida, 2006); the cuticle may provide important insight into *Glossopteris*-fungal relationships. In extant ecosystems, leaf cuticles exhibit a wide array of defense compounds, e.g., phenolics (flavonoids), secondary metabolites, essential oils, some of which serve as anti-fungal defense compounds (Canhoto and Graça, 1999; Domínguez et al., 2011). This would provide an opportunity to apply geochemical techniques to analyze the chemical content, possibly biomarkers, in order to elucidate the hypothesis: do *Glossopteris* leaf cuticles have a higher abundance of anti-fungal compounds? Similar studies have been applied to geologically younger material (Late Cretaceous) in which investigators analyzed the lipid contents in fungal infected conifers and uninfected conifer cuticle (Tu, et al. 2000). The results of this study indicated that fungi in the infected conifer specimens produced certain degradational compounds, but did not yield or focus on anti-fungal compounds produced by the conifers. This study, however, confers that biogeochemical data regarding fungal interactions can be extracted from fossil plant cuticle and therefore may be important in assessing in *Glossopteris* specimens.

3.2 Abiotic factors that affect foliar fungi

One of the many abiotic factors that make Permian forest ecosystems of Antarctica a unique experimental laboratory with no modern analog is that these forests experienced extreme light regimes, i.e., 4 months of 24-hours light exposure, 4 months of 24-hours of darkness, and 4 months of transitionary light regime (e.g., Taylor and Ryberg, 2007). One of the many research foci using this experimental setting include leaf longevity of *Glossopteris* plants, i.e., deciduous versus an evergreen leaf habit (Gulbranson et al., 2014). The presence of leaf mats suggested that many of these high-paleolatitude forests exhibited deciduous leaf habits (e.g., Axelrod, 1984). However, recent studies indicate that Permian *Glossopteris* forests contained mixed populations of evergreen and deciduous trees (Gulbranson et al., 2012; 2014). The physiology of these

Permian plants is also unique, Schwendemann (2012) suggested that *Glossopteris* plants exhibited a mixed C_3-C_4 intermediate physiology which may have played a vital role in adaptation to extreme light regimes and possibly to low CO_2 conditions; although leaves in the Late Permian (Skaar Ridge and Collinson Ridge specimens) would have experienced higher levels of CO_2 relative to the Early and Middle Permian (Schwendemann, 2012).

The combination of these abiotic factors would have greatly influenced the microbial community, including fungal endophytes. Factors such as seasonality and leaf age greatly influence epiphytic and endophytic fungi, for example, a study by Osono (2008) indicated that seasonal variation influence foliar fungi more so than leaf age, but state that patterns of fungal colonization of evergreen leaves due to seasonal and leaf age variation are difficult to predict. Light availability during season change is likely one of the many factors that affect fungal colonization of leaves in modern ecosystems, as it probably did in the ancient ecosystems. Perhaps this provides an additional explanation as to the absence of leaf endophytes in *Glossopteris* leaves. Twenty-four hours of exposure of light is likely detrimental to epiphyllous fungi, while 24 hour of darkness is detrimental to epiphyllous and endophytic fungi due to reduction in photosynthetic conduction and production rates. It is probable, that if these microbial communities were present then likely peaked during the transitionary periods of light regimes. Additionally, currently it is impossible to determine leaf longevity based solely on permineralized leaf specimens. Therefore, when these leaf specimens are found within peat matrices they may represent either deciduous or evergreen, which are important factors in determining the roles of *Glossopteris*-fungal partners. Additional studies are needed to further elucidate the leaf habit and physiology within leaf mats, which in turn, will aide in understanding the microbial communities.

3.3 Ecological niche: epiphytes, endophytes, or leaf litter saprotrophs

It is difficult to assess the taxonomic affinity of many leaf litter fungi due to the lack of diagnostic characters, let alone the ecological niche of these organisms. Leaf litter communities are comprised of multiple phyla of fungi, which are involved in many integral niches, e.g., mutualists, saprotrophs, parasites, and necrotrophs (Voříšková, and Baldrian, 2013). It is most likely that the majority, if not all fungi found associated with the *Glossopteris* leaves in this study are saprotrophic entities. Examples of putative zygomycetous fungi and chytrids found within highly degraded leaf tissues are likely functioning as decomposers, similar to their role in modern ecosystems (Marano et al., 2011). There is also discussion in Chapter 9 of this dissertation that zygomycetous fungi served as one of the principal degradational fungi within Mesozoic ecosystems, and possibly in Paleozoic leaf litter ecosystems. Additionally, since several examples of hyphae are found in all tissue systems, versus specific tissues like specialized endophytes or epiphytes, these hyphae probably belong to generalist saprotrophic fungi. Although there are hyphal cross sections on the epidermis of degraded leaves or hyphae within mesophyll cells, this does not qualify these fungi as epiphytes or endophytes, respectively, due to the lack of consistency, diagnostic characters, and single occurrence. The greatest likelihood to find epiphyllous fungi is probably within *Glossopteris* cuticular remains, whereas endophytes could be elucidated within permineralized specimens but need to follow specific criteria for fossil fungi ecological affinities (see Chapter 1 – section 12. Considerations when studying fossil fungi).

3.4 Matrix fungi and fungal-organism diversity

Many of the spore structures from this study have been interpreted as resting structures within the Permian matrix. Some of the spores have internal contents (spore types 1, 2, 5, 8) that

may represent that the larger parental spores serve as propagules (Taylor, et al., 2015) or these internal structures might represent mycoparasites (Hass et al., 1994). A few of these spores are attached to parental hyphae (1?, 2, 3, 4?, 8) that lack septa at the base, similar to many Glomeromycota spp., (Stürmer, 2012). It is important to note that spore types that have hyphal attachment points are in close proximity to *Vertebraria* rootlets within the peat matrix. *Vertebraria* rootlets have been shown to have mycorrhizal fungi (Harper et al., 2013; Chapter 3 of this dissertation) and these spores could be the Glomeromycotan asexual spores associated with this mycorrhizae.

There are also examples of Peronosporomycetes within the Skaar Ridge and Collinson Ridge peats. Other examples of Peronosporomycetes have been described from the Permian of Antarctica. Two distinct species of *Combresomyces* spp. have been described by Slater et al. (2013) from the Middle to Late Permian of the Prince Charles Mountains. Each species has prominent ornamentation and occur within the matrix. *C. caespitosus* is characterized by long, hollow, slender, conical papillae with at least two orders of strongly divergent, sharply pointed, apical branches. It was noted that *C. caespitosus* was found in association in matrices near *Vertebraria* roots and leaves of *Glossopteris* and *Noeggerathiopsis*. In contrast, *C. rarus* is a spherical oogonia bearing long, hollow, broad, conical papillae that terminate in at least one bifurcation producing a pair of, generally acutely divergent, sharply pointed branches. *C. rarus* is less abundant, i.e., present in 25% of peat samples studied, than *C. caespitosus,* i.e., present in 50% of total peat sample examined. Both species were noted to have a short truncate extension, likely where the parent hyphal attachment occurred. Slater et al. (2014) suggested that the *Combresomyces* spp. likely played a significant role in degradation of organic matter or perhaps existed as a parasite of plants and/or animals. Peronosporomycetes types 2–4, including the Collinson Ridge specimen, are more similar to *C. caespitosus*, but differ in length (specimens in

this study are smaller, blunt ornamentation, and more pyriform in shape, and thus may not be additional examples of *C. caespitosus*.

It is important to note that the peronosporomycete specimen from Collinson Ridge represent the only microorganism described from this locality to date. The preservation of the material makes it difficult to analyze the specimens at higher magnification in order to accurately survey for fungi.

Combresomyces spp. is an oogonium possessing complex, compound surface ornaments (sometimes termed "antler-like" extensions) of hollow papillations of the oogonial wall (Dotzler et al., 2008; Taylor et al., 2015). A report of *Combresomyces cornifer* has been described in the matrix and near a well-preserved seed with embryo from the Triassic of Antarctic, and may represent a possible parasite (Schwendemann et al., 2009; 2010b). These specimens are morphologically similar to the type specimen from the Carboniferous, but are much larger in diameter. Peronosporomycete type 1 from this study is morphologically equivalent to *C. cornifer* and is the first example of this species described from the Permian. The persistence of *Combresomyces* spp. in the Permian and Triassic Antarctic suggest that these organisms are quiet resilient during times of global climate change and floral turnover, as well as their possible role as generalists in high latitude peat forming environments.

4. Conclusions

Expansive surveys and a larger dataset will undoubtedly yield more examples of Permian leaf fungi. It is now established that there are fungi associated with *Glossopteris* leaves but are probably represent generalist saprotrophs rather than host-specific epiphytic or endophytic fungi. At this time, it is difficult to resolve the taxonomic affinity for these fungi other than phylum level general characters, i.e., septate hyphae suggest either a Basidiomycete or Ascomycete.

Other examples superficially appear to be certain types of fungi, the possible zygomycetous forms, but lack definitive characters such as oogonia or gametangia that support confident taxonomic affiliation. Relative to the data set of *Glossopteris* leaves examined for this study, there was a limited number of fungal remains discovered. This paucity of remains could be explained by several hypotheses, such as the leaf longevity and physiology of the *Glossopteris* plant may not support a constant microbial community, i.e., leaf epiphytes or endophytes. Also, *Glossopteris* leaves may have exhibited an array of biochemical compounds that acted as anti-fungal defense mechanisms, which prevented fungal colonization. As well as the ability to simply recognize endophytic fungi associated with leaves in the fossil record. Similar to all fossil studies, an expanded data set and newly collected material will undoubtedly increase our knowledge set for the relationship of leaf and microbial communities from the Paleozoic of Antarctica.

Chapter 9

Life history and developmental biology of *Endochaetophora antarctica*: A leaf litter fungus from the Triassic of Antarctica

1. Introduction

1.1 Descriptive studies of isolated fossil fungi

Throughout the fossil record, many fungal structures are found as isolated units either within the matrix or in close association with plants, with no obvious morphological clues or evidence as to the affinities or ecological significance of such structures (e.g., Meschinelli, 1898). Until a large source of structural and morphological data is assembled on the importance of these isolated structures remain in the descriptive stage. With an increased dataset, additional features of the fungus, and sometimes details about the life history biology can be interpreted (Remy et al., 1994b). There are several examples of fossil fungi that occur relatively commonly in Paleozoic and Mesozoic ecosystems, yet their precise affinities and aspects of their biology continue to be elusive. One of the most common of these are the so-called "sporocarps" (e.g., Carruthers, 1873; Spencer, 1893; Scott, 1911; McLean, 1922; Hutchinson, 1955; Baxter, 1960; Davis and Leisman, 1962; Stubblefield and Taylor, 1983; Stubblefield et al., 1983; White and Taylor, 1991; Krings et al., 2010d; Krings et al., 2011a,b; Krings and Taylor, 2012c; Krings et al., 2014).

1.2 "Sporocarps"

The Carboniferous coal balls and chert from Europe and North America and to a lesser extent (e.g., Williamson 1873; 1882; Stopes and Watson, 1909; Andrews, 1951), the Triassic

peat ecosystems of Antarctica (White and Taylor, 1991), are characterized by an abundance of 100–500 μm, typified by the morphology of surface ornamentation, can occur singularly or in clusters, and include a central cavity (with or without contents) surrounded by an investment or mantle with particular hyphal arrangement (Taylor et al., 2015). Some of these are variously ornamented with spines and other structures (e.g., Stubblefield and Taylor, 1983). Recently it has been suggested that the collective use of the term sporocarp for these fossils may be inaccurate, and thus, if used, the name should be put in quotation marks (Krings and Taylor, 2010). "Sporocarps" typically occur as individual units, but there are some specimens in which several individuals are clustered together (e.g. Williamson, 1880, McLean, 1922; Hutchinson, 1955; Stubblefield et al., 1983). The central cavity is surrounded by an investment or mantle of loosely arranged interlacing and/or tightly compacted hyphae, which may be septate or aseptate. In all types, there is evidence to suggest that the investment is bounded on the inside by a narrow non-hyphal layer. Additionally, "sporocarps" infers that the parental status or reproductive biology is unknown, and that the function is perhaps some type of resting structure (Taylor et al., 2014).

1.3 "Sporocarps" from new Triassic Antarctica material

Various types of "sporocarps" have been described and studied from Antarctica, e.g., *Mycocarpon, Endochaetophora* (White and Taylor, 1991). In *Endochaetophora antarctica*, a spherical fossil from the Middle Triassic of Antarctica that is somewhat similar morphologically to the "sporocarps" described in the foregoing sections, the investment is tripartite, with the middle layer believed to have formed secondarily between the two pre-existing layers (White and Taylor, 1988, 1989). Extending from the surface are numerous radially oriented and aseptate appendages (up to 125 μm long) that appear to arise from the inner layer of the wall.

Newly collected leaf litter material collected during the 2010-2011 austral summer Antarctic field season from the Triassic Fremouw Peak locality has yielded an abundance of *Endochaetophora* specimens that demonstrate interactions with leaf and plant axes. These new discoveries suggest that *Endochaetophora* had a significant role in the decomposition of leaf mats and in the formation of litter communities. As a result of this material we also suggest a hypothesized life cycle that includes both a sexual and asexual stage. Previous reports on *Endochaetophora* likely only represent the asexual resting stage of the life cycle. Moreover, this contribution provides insight in the complexity of Mesozoic communities but also on the parental and life history biology of structures that have been contemplated by even some of the earliest paleobotanists, e.g., (Williamson, 1873). These fossils provide additional evidence on "sporocarps", which based on our findings, are extremely dynamic under the correct circumstances and provide crucial roles and niches in ancient ecosystems.

2. Description

2.1 New specimens of Endochaetophora antarctica

"Sporocarps" of *Endochaetophora antarctica* White and Taylor (1988) occur in several different interpreted ontogenetic stages and are associated with various plant organs in leaf litter material of Fremouw Peak. These fungal "sporocarps" and initial reports of *Endochaetophora* share the same features of thick wall, appendages, woven mantle of hyphae surrounding the "sporocarp", and presence of a distinct ostiole. The *Endochaetophora "*sporocarps" (n=382) in this study had diameters that ranged from 82 μm to 988 μm, with an average diameter of 304 μm. "Sporocarps" can occur singularly, i.e., 17 occurred singularly, or in clusters, i.e., 39 groups of clusters were examined.

2.1 Isolated and cluster specimens of Endochaetophora

Single "sporocarps" can occur adjacent to poorly preserved leaves and axes, some "sporocarps" with clearly visible appendages (Plate 18, Fig. 211). More commonly, isolated thin-walled "sporocarps" appear to have translucent matrix surrounding them (Plate 18, Fig. 212-213). The translucent matrix composed of a meshwork of tightly interlaced hyphae. "Sporocarps" within the translucent matrix completely surround the degraded leaves and axes. Within the matrix, some "sporocarps" lack appendages (Plate 18, Fig. 212) or the appendages are difficult to define because of their delicate wall (Plate 18, Fig. 213). Small, isolated spherical structures with rarely occur associated with plant remains within the matrix and may represent ontogenetically younger or immature *Endochaetophora* "sporocarps" (Plate 18, Fig. 213). Where *Endochaetophora* "sporocarps" come in contact with leaves there is no clearly defined evidence of hyphae penetrating the leaf or axis surface. Additionally, there are no hyphae within the plant tissues that are associated with the clusters of *Endochaetophora* "sporocarps" (Plate 18, Fig. 213). Clusters of *Endochaetophora* range from 2 (Plate 18, Fig. 214) to more than 66 in a single plane (Plate 18, Fig. 223) with the individual "sporocarps" enclosed within the interwoven mycelium. Of the 382 individual sporocarps examined, there were 39 groups of clusters, i.e., more than one *Endochaetophora* in a group, and 35 of the 39 clustered groups had interlaced hyphal networks present.

2.3 Meshwork of tightly interlaced hyphae-"sporocarp" associations

The translucent matrix is constructed of numerous, interwoven individual hyphae (Plate 18, Fig. 215). Hyphae are of similar size, i.e., the diameter, and shape to the hyphal appendages surrounding the outer wall of *Endochaetophora*. All mycelia hyphae are aseptate. Of the 35 groups of clustered *Endochaetophora* "sporocarps" with this mycelia network present, only 21

had clearly visible hyphal mycelia within the meshwork of hyphae (Plate 18, Fig. 216-218). A slightly smaller number that lack distinctive hyphae have remnants of organic matter scattered throughout the surrounding mycelia (Plate I, Figures 2-4, 9-13). The absence of clearly visible hyphae within a mycelia network may be the result of poor preservation since there is a wide variation of preservation and completeness, i.e., an individual "sporocarp" is intact with complete cell walls, and developmental stage of "sporocarps" within the network of interlaced hyphae. Additionally, there is considerable variation of the "sporocarp" cell wall, e.g., if hyphal appendages are present or not, as well as the type of plant organ associated with the mycelial network. "Sporocarps" of *Endochaetophora* within the hyphal network can partially (Plate 18, Fig. 216, 218, 220) to completely (Plate 18, Fig. 221-223) surround plant organs, or occur rarely within the matrix adjacent to plant remnants (Plate 18, Fig. 212, 217). Typically, "sporocarps" within the opaque network of hyphae have thin walls, i.e., a single cell layer, and the appendages are clearly visible (Plate 18, Fig. 217) or difficult to discern (Plate 18, Fig. 218). The preservation of individual "sporocarps" is highly variable, ranging from examples that are (1) well preserved (Plate 18, Fig. 216), (2) intermixed of "sporocarps" of well preserved and degraded individuals, both encased within the same hyphal network (Plate 18, Fig. 217), and (3) the majority of *Endochaetophora "*sporocarps" are degraded and cell walls are broken up (Plate 18, Fig. 218). Several examples specimens with interwoven network of hyphae have been found fully encasing and covering plant organs such as leaves (Plate 18, Fig. 219) or axes (Plate 18, Fig. 221-213). Interlaced mycelial networks thickness, i.e., the measurement of the maximum diameter of a translucent matrix containing *Endochaetophora "*sporocarps", ranges from 232 μm to 14.02 mm, with an average of 3.06 mm.

2.4 Endochaetophora-*plant associations*

The vast majority of plant-associated hyphal networks are with leaves (n=34), followed by axes (n=8), and least common, interwoven mycelia with no plant organ associated and isolated in the matrix (n=6). Meshwork networks of hyphae containing *Endochaetophora* are associated with plant organs in multiple orientations and at different ranks, such as interwoven networks of mycelia can fully surround abaxial and adaxial sides of fronds with midviens (Plate 18, Fig. 219), or on a single side of a leaf (Plate 18, Fig. 220). Additionally, *Endochaetophora* hyphal networks can surround or partially encase a single axis (Plate 18, Fig. 216-217) to multiple axes within the same interwoven network of hyphae such as two small axes (Plate 18, Fig. 221) or three axes (Plate 18, Fig. 222). Typically *Endochaetophora "*sporocarps" are arranged in a single row, e.g., Plate 18, Fig. 216, 218, 222), but in a few specimens multiple rows of *Endochaetophora* "sporocarps" occur surrounding an axis (Plate 18, Fig. 223).

In contrast to the single cell wall layered sporocarps, which are often found within mycelial networks, isolated *Endochaetophora* sporocarps with thick outer wall composed of three distinct cell walls, which sometimes lacks appendages occur in the matrix (Plate 19, Fig. 224). Of the 382 "sporocarps" studied, 69 *Endochaetophora* had a thick outer wall that ranged from 13 µm to 125 µm in thickness, with an average of 46 µm. Some of the "sporocarps" contain contents in the central lumen (Plate 19, Fig. 225), which may be amorphous material to defined spores. *Endochaetophora* is characterized by the presence of an ostiole (Plate 19, Fig. 226). Trilayered, thick-walled sporocarps that bare ostioles lack appendages (Plate 19, Fig. 226) or contain appendages (Plate 19, Fig. 227). Additionally, thick-walled spores and thin walled, i.e., single cell layer thick "sporocarps", could be found within the same meshwork of tightly interlaced hyphae (Plate 19, Fig. 228-233).

3. Discussion

3.1 Comparison to other Triassic sporocarps

Initial descriptions of *Endochaetophora* are based on a suite of morphological characters that are found associated with the leaves described here. These include sporocarp wall composed of three distinctive cell walls, hyphal appendages, uneven development of the middle wall, ostiole, and spherical spores within the central lumen of the sporocarp (White and Taylor, 1988). Additional studies by White and Taylor (1989 a, b) of the structural details of the sporocarp walls of *Endochaetophora* further subdivided the sporocarp into three categories: tripartite cell wall with distinctive cellular structure on all three layers (referred to as specimen 1 in the study), thin wall with single cell layer, with hyphal appendages (referred to as specimen 2), and specimens with three cell wall layers but with a middle layer composed of acellular material (referred to as specimen 3) (White and Taylor, 1989). Based on this suite of characters described by White and Taylor (1988; 1989) and the consistency with the specimens described in this study, provides greater confidence that the structures as the focus of this investigation are example of *E. antarctica* (Plate 19, Figs. 234-238; Plate 20, Figs. 239-242).

3.2 Life history biology

Extant fungi and fungal-like organism life cycles are both difficult to study and interpret. Most microbes have complex and intricate life histories, e.g., sexual and asexual forms, host specificity that is necessary to complete their life cycle, the requirement of an intermediate host, various temperate or environmental requirements, etc. (Webster and Weber, 2007). Deciphering life history biology in the fossil record is often further compounded by a lack of specimens that reflect varying stages. As a consequence life cycles of fossil fungi from the Paleozoic and Mesozoic are extremely sparse. There is a high occurrence morphological plasticity of fungi throughout the fossil record, which increases the likelihood that fungi also share a similar

plasticity in their life history. Many of the life cycle stages might not be preserved or recognized as part of the same organism due to the morphological differences within the life cycle, as well as structures may be morphologically equivalent but differ genetically. Much of our understanding of paleomycological life history biology is based on comparisons with extant fungi (e.g., Remy et al., 1994b; García Massini, 2007a), therefore, portions that not preserved or explicitly found are hypothesized and further interpreted from extant fungi that share characters with the fossil specimen. There are problems that can arise from comparing with extant fungi because the fossil forms may represent forms that are extinct and share no modern analog, within their life cycle.

The large number of specimens in this study that appear to be at different ontogenetic stages make it possible to reconstruct a series of developmental stages that possibly represent stages in the life history biology of *Endochaetophora*. This is an important contribution because one of the criteria for "sporocarps" is the lack of knowledge regarding the parental or developmental status of the organism. The following sections discuss a hypothesized life cycle for *Endochaetophora* based on the specimens at hand, in congruent with current knowledge of lower fungi, i.e., zygomycetous, life cycles. Zygomycetous fungi, like the majority of fungi, can undergo sexual and asexual reproduction under specific environmental conditions and cues (Webster and Weber, 2007), therefore it is likely that fossil representatives that share closest affinities with zygomycetous fungi can also exhibit a sexual and asexual stage. When appropriate, it is noted which areas of the proposed life cycle has a representative specimen for that stage and areas that lack fossil evidence and are hypothesized.

3.2.1 Sexual stage of hypothesized life cycle

Early stages in the life history of *Endochaetophora* may be represented by isolated spores in close proximity to plant material and debris. Such spores give rise to hyphae, degradational enzymes, and material necessary to produce a meshwork of tightly interlaced hyphae which may be interpreted as a gleba, or the fleshy, amorphous-gelatinous spore-bearing matrix of some fungi, principally zygomycetes (Ulloa and Hanlin, 2012). Other occurrences of gleba in the fossil record include zygomycetous structures such as *Jimwhitea circumtecta* (Krings et al., 2012b) that have been suggested to be associated with "sporocarps" but no direct attachment was detected. If this interpretation is correct, it gives greater confidence in the affinities of *Endochaetophora* and other fossil "sporocarps" as closest affinities with modern zygomycetous fungi (Gibson et al., 1986).

3.2.1.1 Interactions and development within the mycelial network or gleba (?)

In extant fungi, the gleba is an amorphous, gelatinous material comprised of degradational enzymes, hyphae, and the various other proteins, amino acids, and building blocks for further development of subsequent stages of the life cycle (Krings et al., 2013). In members of the lower fungi such as the zygomycetes (Kirk et al., 2008), there are plus and minus strand types, which are genetically different (Takó and Csernetics, 2005). Obviously this stage in the life history cannot be demonstrated in the fossil record. It is, however, likely that during development of the interwoven hyphae or gleba, exchange of genetic material was common and because we cannot discern between hyphal types, and there is no evidence of structural differentiation between hyphae, plus and minus hyphae may represent the early stage of *Endochaetophora*. Since small "sporocarps", i.e., less than the average 304 μm in diameter, are most prevalent embedded within mycelial network matrices, they are possibly borne on or within an interwoven meshwork of hyphae. This is similar to the description by White and Taylor

(1988) of mycelial aggregations, which form a hollow chamber devoid of contents. This may represent an early stage of the structural development of immature, or ontogenetically younger "sporocarps" borne within mycelia aggregations.

3.2.1.2 Cell wall development

Among the specimens of *Endochaetophora* are "sporocarps" demonstrating multiple stages in cell wall development. Based on the multiple specimens of "sporocarps" within interwoven networks of hyphae studied, it is most likely that the "sporocarp" wall develops the most inner wall, termed: cell wall 1 (closest to the central lumen) first, them the outer wall, termed: cell wall 2, and the middle layer, termed: cell wall 3, in between the two cell walls last. White and Taylor (1989) also noted that some "sporocarps" contained an acellular middle wall layer (cell wall 3), while others had a fully developed tripartite cell wall. This indicated that the middle cell wall layer (cell wall 3) developed last, i.e., acellular to definitive cellular definition within the middle layer. Additionally, White and Taylor 1989 described an "assemblage" of "sporocarps" that shared similar characteristics, i.e., non-prominent or lacking appendages, thin or absent middle layer. Based on the current study, this "assemblage" is now interpreted as a interwoven network of hyphae, or presumed gleba containing "sporocarps". The development, presence or absence of specific features of the "sporocarp" cell wall can help distinguish stages of both the sexual and asexual stages of the life history. We hypothesize that the majority of the sexual stage of the life cycle occurs within the gleba; which may be characterized by "sporocarps" that possess a thinner cell layer 3 and often lacks or has inconspicuous hyphal appendages.

3.2.1.3 "Sporocarps" as propagules in sexual stage and spore production

"Sporocarps" devoid of any contents in the lumen together with this set cell wall characters within the mycelial network may be interpreted as propagules prior to spore production. Some of the sporocarps within the hyphal meshwork that have multiple cell walls contain contents. These may be: (1) amorphous, undifferentiated material, (2) isodiametric spores that have a pattered or textured appearance, similar to the parental sporocarp, or (3) in rare instances, a combination of the amorphous material and spores. We hypothesize that this amorphous, undifferentiated material is initially produced within the sporocarp lumen, and then consolidates and eventually develops into the spores. The spores range in diameter from 10–25 μm in diameter and can be found in clusters of 2 to 30 within a single "sporocarp" lumen. The spores are found within the central lumen of the "sporocarps" also contain hyphal attachment, which may represent the parental hyphae; these hyphae are 2–4 μm in diameter and lack septa. We are unsure of or where the attached hyphae terminate and/or are initially attached to within the lumen, or produced by and/or attached to the "sporocarp" wall. It is most likely that hyphae are attached to central point within the lumen, i.e., similar to *Sclerocystis* spp. (a glomeromycete) that also has centrally attached hyphae that produce spores (Stubblefield et al., 1987). After the spores are mature and prior to dispersal, we suggest that at this stage the ostiole is formed (Plate 20, Figs. 243-251).

3.2.1.4 Ostiole formation

The cell wall where the ostiole is produced is reduced to single layer with no evidence of a middle layer. The ostiole consists of a raised rim that surrounds a conical to funnel-shaped opening. Once fully mature the spores are released from enclosed "sporocarp" into the leaf litter and can reinitiate the sexual cycle, or undergo asexual reproduction. *Endochaetophora* "sporocarps" that have an ostiole, but that lack internal spores are interpreted as "sporocarps"

that have released their spores. “Sporocarps” within presumed gleba or hyphal networks can occur in multiple stages of development. In examples of interwoven networks of hyphae that fully surround plant axes or leaves, it is common for thin walled, or single layer cell walled “sporocarps” (with and without appendages) are usually closer in proximity to the surrounded plant organ, while thicker wall, i.e., more than two cell wall layered “sporocarps” (with and without contents, e.g., spores or undifferentiated material) are more prevalent on the outer periphery of the hyphal mycelia aggregation. This suggests that those “sporocarps” closer to the plant material may be in the earliest stages of the sexual cycle, and as these structures mature, they are pushed further to the outer periphery of the gleba. As a result new space for additional closer to the original plant organ is created. In some cases, thick walled, tripartite walled sporocarps are exclusively found on the outer periphery of interlaced hyphal network. These may have completed their lifecycle, or may be released as some type of resting structure that may at some point undergo asexual reproduction (Plate 20, Figs. 252-254) (see discussion below).

3.2.2 Asexual stage of hypothesized life cycle

In contrast to the sexual cycle of *Endochaetophora*, which begins with production of an extensive mycelial network or gleba where the vast majority of the sexual stage of the life cycle is hypothesized to occur, the asexual stage is hypothesized to take place within the matrix of leaf litter communities. And suggest that perhaps spores released from parental “sporocarps” that do not find favorable conditions reside as resting structures within the leaf litter. The spores encyst and produce the thick walled, tripartite “sporocarp” wall, similarly to the “sporocarps” within the sexual stage of the cycle, i.e., cell wall layers 1 and 2 are produced with the skeletal framework of the hyphal appendages with cell wall layer 3 (middle layer) formed last. One of the key differences between the sexual and asexual stages in cell wall development is that the middle

layer is prominent and cells are distinguishable (versus the acellular layer cell wall layer 3 in the sexual stage). In rare cases during the interpreted asexual stage, three layers of the "sporocarp" wall are present, but appendages are lacking or less prominent. After the cell walls are fully developed and appendages are produced, the amorphous central material begins to differentiate into the spores. An ostiole is formed in the outer cell wall, and the spores are released to repeat the cycle or begin the sexual stage. Based on this hypothesized life cycle, the initial description of *Endochaetophora* by White and Taylor (1988) represents a single component of the asexual stage of the life cycle. Specifically, the final stages of the asexual stage, i.e., full development of the three cell wall layers, prominent hyphal appendages, production of an ostiole, and mature spores within the lumen.

3.3 Cues for sexual vs. asexual stage initiation

We are unsure as to what is necessary for the initiation of either the sexual or asexual stage of the life cycle. The surrounding matrix material of sexual and asexual structures may provide insight into favorable conditions for the start of either cycle. It is common to find tight aggregations of mycelia in matrices with partially degraded to poorly preserved leaves and plant axes. While, asexual structures are commonly found within matrices that are composed of highly degraded and indiscernible plant material. Additionally, all sporocarp structures studied by White and Taylor (1988) occurred exclusively within matrices composed of rootlets. Perhaps the sexual stages of *Endochaetophora* occurred only in the leaf litter matrix with the asexual stages confined to other matrices (Figure 15).

3.4 Hypothesized components of the Life History Biology in Endochaetophora

The hypothesized portions of the life cycle of *Endochaetophora* is based on a large number of specimens that we interpret s as representing different stages of development and in turn comparing these to morphological and structural stages found among modern fungi. Fossil examples of the *Endochaetophora* life cycle for which we have no evidence includes: (1) spores attached to the surface of a leaf or axis, (2) differential hyphal mating types immature "sporocarps" arising from hyphal fusion, and (3) formation of a spherical chamber within the hyphal mycelia.

3.5 Roles in environment

In modern ecosystems, especially in leaf litter systems, ascomycetes occupy many of the fundamental niches between fungi-rhizosphere and plant-fungal interactions (Muehlbauer et al., 2009). These associations are thought to have greatly expanded when the diversification of the ascomycetes was perhaps most rapid (Cai et al., 2006; Schoch et al., 2009). Prior to the Tertiary, leaf litter communities were completely different in floral composition, therefore, it is highly likely the microbial component was equally different. Based on this study, we believe that *Endochaetophora* is a highly prevalent leaf litter fungus within the Triassic leaf litter peats of Antarctica, and suggest that this zygomycete occupies a similar niche to that of ascomycetes in modern ecosystems, i.e., principal saprotrophs (Voříšková and Baldrian, 2013). Today, zygomycetes may be considered transient within leaf litter communities and contribute minimally to decomposition (Marano et al., 2010). Perhaps zygomycetes had a much larger role in ancient ecosystems as the leading drivers of saprotrophic processes in leaf litter communities based on their high abundant and plant-fungal interactions in Mesozoic leaf litters.

3.6 Affinities with no modern fungal analogs

Initially, *Endochaetophora* was thought to be included with members of the Ascomycotina, specifically spore producing structures such as perithecia and pycnidia, based on shared morphological features (White and Taylor 1988). However, members of the Ascomycota have septate hyphae and do not have internal tissue between wall layers of the "sporocarp" (Gäumann, 1928; Webster and Weber, 2007). It has also been suggested that *Endochaetophora* may represent a member of the Endogonaceae, based on the presences of a cellular wall layer (Taylor and White, 1989), some type of Glomeromycete (based on the presence of an acellular inner wall, similar to *Glomus;* Schwarzott et al., 2001). More recently it has been suggested that "sporocarps" that have highly ornamented surfaces and mantle sheaths are most closely related to some type of zygomycete (Krings et al., 2014; Taylor et al., 2015). Based on this assessment, as well as the production of the gleba, or the meshwork of tightly interlaced hyphae (in extant fungi is produced at the proximal end of the macrosuspensor that gives rise to the gametangia in modern zygomycetes), we concur that *Endochaetophora* has its closest affinities with the zygomycetous fungi. The reproductive biology, i.e., life cycle, of most modern zygomycetous fungi is not well known, therefore, to date we are limited in the known and detailed zygomycetous reproductive biology.

Another possibility is that *Endochaetophora,* among other fossil "sporocarps" represent fungi or fungal-like organisms with no modern analog. The hypothesized *Endochaetophora* reproductive biology certainly has no modern analog as far as the production of a "sporocarp", asexual, sexual, and internal spore-producing stage. These "sporocarp" structures are somewhat common in the Paleozoic and Mesozoic (Taylor et al., 2015), but their fossil record ceases after the Triassic. Perhaps "sporocarps" and organisms similar to that provide a clear example for the necessity to erect a new fungal phylum of an extinct group with no modern analog, which would be the first for the fungal Kingdom. This is contrast to other Kingdoms in biology, i.e., animals

with the extinct group of dinosaurs, plants with extinct groups of seed ferns, progymnosperms, etc. One of the main difficulties in paleomycology is the inclination to forcibly constrain fossil fungi into modern fungal phyla, and as new specimens of fungi are discovered eventually there will be a need to expand the systematics and taxonomy of fungi and extend it into the fossil record. As our knowledge base increases on fossil fungi and the respective modern fungal analogs, we can be begin to build a complete picture of fungal evolution.

4. Conclusions

4.1 Importance for continued data collecting in paleomycology

The constant accumulation of paleomycological data, i.e., fossil representatives of fungi and fungal-like organisms, is crucial to understanding fungal evolution and biology. *Endochaetophora* is an interesting example of a fossil that has been reported multiple times with new data and interpretations each time new specimens are collected. The initial description of *Endochaetophora* was based on five "sporocarps", although it was noted in the description that "sporocarps" occur singly or in groups of 2–5. Additional specimens were found that elucidated the structural and cell wall details of the "sporocarps". New material collected from Fremouw Peak has provided new information about the developmental and life history biology of *Endochaetophora.* Additional material will likely provide new information about the life history biology of *Endochaetophora*, including filling in some of the gaps of the life cycle, fossil evidence for some of the missing components, or new areas. With this new material, additional data including information on development and life history biology can be incorporated so as to more completely circumscribe the biology of *Endochaetophora.*

Paleomycology is at an interesting point in which the diversity in some forms of fossils may represent different stages in the life history. This underscores how integral continued

collection and accumulation of fossil material is to the field of paleobiology. As we continue to collect, study, and interpret new specimens, we can build microbial community ecosystem interaction schemes and webs. Thus, taking the typical paradigm of paleobiology from a purely descriptive science to one that considers ecological and other biological interactions.

Chapter 10

Conclusions and future directions

Paleomycology is an emerging field that is at a critical moment as a discipline, since investigators are now beginning to recognize the importance of microorganisms in past ecosystems. Fungi and fungal-like organisms are components of ecosystems that are often unnoticed but that have a profound impact on the environment as a whole, and it is without question that they impacted ancient ecosystems in an equally significant manner. This study of fossil fungi and fungal interactions spanning the Permian, Triassic, and Jurassic of Antarctica fundamentally increases our knowledge set of Paleozoic and Mesozoic plant-fungal relationships. It is unsurprising that as major floral turnover events occurred, spanning the Paleozoic into the Mesozoic, that the fungi (for the most part) remain stable in times of great climate changes. Mycorrhizal associations still persist with different hosts, wood rotting fungi degrade different groups of trees, parasites and other antagonistic forms develop new strategies to combat defense mechanisms, and saprotrophic organisms continue to degrade any component of organic matter within leaf litter systems or within the rhizosphere.

This back drop provides the foundation for the opportunity to develop new hypotheses and questions derived from these systems, especially from Antarctica, because as intensely studied as the floral components are, the microbial associations with many of these plants are still relatively unknown. This chapter is organized by outlining concluding and salient points from each chapter within this dissertation, as well as areas of potential future research in paleomycology. Relative to the large data set of our current understanding of Antarctic paleobiology, this dissertation represents only a small sampling of the microbial diversity that has yet to be discovered.

Chapter 1

- Antarctica, overall provides an interesting experimental setting for the study of fossil fungi as it serves as an ecosystem with no modern analog, contains permineralized material spanning multiple points of geologic time, and many of the floras are well known and the plants described in detail.
- Permineralized material provides the best opportunity to study fungal fossils due to the anatomical preservation, as well as the best opportunity to study plant-fungal interactions and relationships.
- In order to study interactions and ecological niche associations of fungi, it is necessary to know the plant organ (and taxon, if possible), i.e., root, stem, leaf, reproductive structure, that the fungus occurs within or with in order to confidently determine the association type. This is in comparison to strict descriptive studies of fossil fungi.
- Multiple fungal phyla appear to lack fossil representatives from Antarctica. Many of the fungi described also lack definitive characters for confident taxonomic assignment. To date, there are no representatives of the Blastocladiomycota, Ascomycota, lichens, mycetozoan fossils, or bacteria.

Chapter 2

- Overall, thin sections are a better preparation technique relative to acetate peels due to minimal specimen loss and three-dimensionality of the fossil specimens.
- Focal stacking techniques of serial thin section images provides a much more comprehensive view of specimens in order to study the detailed area that may be overlooked or unavailable when studying specimens in a single z-plane.

Chapter 3

- First report of mycorrhizal fungi present in seed ferns, i.e., the young rootlets of *Vertebraria* of the *Glossopteris* plants.
- It is highly likely that other plants from the Paleozoic, as well as other from multiple time periods, also have mycorrhizal associations. Sphenophytes, progymnosperms, gnetophytes, gingkophytes have not been described with mycorrhiza in the fossil record.

Chapter 4

- Voltzialean conifers have types of endomycorrhizal associations, including mycorrhizae in non-nodular forming roots. Multiple mycorrhizas are a common occurrence in extant ecosystems, and this is the second documented occurrence of multiple mycorrhizas in the fossil record.
- Voltzialean conifers, are considered to be the intermediate between the Cordaitales and modern conifers, therefore I hypothesize that the progenitors of the conifers may have been predominately endomycorrhizal.
- Future investigations of permineralized Triassic, Jurassic, and Cretaceous plants, spanning an important interval in the evolution of gymnosperm-mycorrhizal relationships, will provide opportunities to not only find earlier representatives of arbuscular mycorrhizal fossils, but perhaps also examples of the intermediate forms between endo- and ectomycorrhizal associations, and possibly the earliest representatives of ectomycorrhizal interactions with ancient gymnosperms.
- The Triassic of Antarctica is rich in plant diversity, therefore I hypothesize that many plant groups also contain mycorrhizal associations. There are numerous groups from Triassic Antarctic floras that have not been investigated, e.g., ferns, lycophytes, etc.

Studies that can identify taxon specific root associations are critical in order to identify and access new mycorrhizal associations with these plants.

Chapter 5

- The *Ashicaulis* root ball "confined" system has a high diversity of plant-fungal-arthropod interactions, including multiple examples of root endophytes, host-responses, saprotrophic fungi, and arthropod remains.
- This dynamic ecosystem provides an important case study since not all root fungi are mycorrhizal associations, and may represent root endophytes.
- There should be a strict character system in fossil fungal studies when interpreting a root fungus as being mycorrhizal, and the comparison between *Ashicaulis* and previous chapters provide a distinct difference between root endophytes and mycorrhizal fungi.
- The high abundance of chytrids present within the specimen represents a potential to interpret life cycles.
- Certain cells exhibit a host response to fungal structures within the same root that has other fungi that do not elicit a host response. This provides context on defense mechanisms utilized by plants and possibly insight in fungal parasite-plant interactions.

Chapter 6

- The abundance of anatomically preserved wood in the fossil record provides an almost unlimited source of material that can be used to search for the presence of fungi and potential host responses.
- Infected Permian wood specimens contain numerous fungal remains, decay patterns, host responses, similar to woods from the Triassic of Antarctica.

- It is highly probable that there are multiple types and species of fungi present in the woods from the Permian of Antarctica, and should not all be categorized into a single species.
- The absence of other wood rot types (soft, brown, simultaneous white rot) in the fossil record is likely a result of the structural integrity of the wood after degradation by the rot fungi, rather than an absence of these rot types in the past.
- Certain characters and stages of the wood decay life cycle are present, including fossil evidence of Paleozoic and Mesozoic polypores. The possibility of *in situ* fossil forests may provide the best opportunity to find such structures in Mesozoic and Paleozoic ecosystems, even polypore attachment points or scars on tree surfaces will greatly enhance the knowledge base of wood decay in ancient ecosystems.
- The application of geochemical techniques in paleomycology, such as developing taxonomic- and disease-specific fungal biomarkers, provides the foundation of a new avenue for understanding fungal diversity and plant-fungal evolution in geologic time.

Chapter 7

- Not all fungi found within woods represent wood degrading fungi. The fungus associated with the tylosis formation is likely a parasitic wood fungus.
- This study represents one of the few reports on fungi from the Jurassic of Antarctica.
- Provides the first evidence of Jurassic conifer wood from Antarctica with well-preserved fungi and the formation of tyloses, as well as the first report of fungi in fossil phloem from Antarctica and the possible production of tylosoids in response to these fungi.
- Overall, this study provides insights into parasitic fungi and host responses exhibited by ancient plants, and one of the rare opportunities to indicate that the tree was living during the preservation process.

Chapter 8

- Paleozoic leaves and leaf mat communities include fungi and fungal like organisms.
- The terms “epiphyte” and “endophyte” when applied to fossil leaf fungi should be treated with caution, because the presence of hyphae on the surface or epidermis of a leaf does not necessarily mean the fungus is an epiphyte. Endophytes, on the other hand, can be applied to any fungus that colonizes the interior of a plant organ, but caution should be noted when interrupting the leaf endophytes as specialists.
- The scarcity of leaf fungi associated with *Glossopteris* may be due to a number of reasons including the leaf longevity, physiology, and the possibility that *Glossopteris* leaves produced specific anti-fungal biochemicals.
- Overall, the fungi found associated with *Glossopteris* leaves are all likely saprotrophs, and not host specific fungal epiphytes or endophytes.

Chapter 9

- The constant accumulation of paleomycological data, i.e., fossil representatives of fungi and fungal-like organisms, is crucial to understanding fungal evolution and biology.
- With the addition of newly collected material, more information on *Endochaetophora* has been elucidated and a hypothesized life cycle proposed.
- Additional material will likely provide even more new information about the life history biology of *Endochaetophora*, including filling in some of the gaps of the life cycle, fossil evidence for some of the missing components, or new areas.
- Perhaps “sporocarps”, and organisms of a similar organization suggest of an example for a new fungal phylum of an extinct group with no modern analog, which would be the first for the fungal Kingdom.

- One of the main difficulties in paleomycology is the inclination to place the fossil into modern fungal phyla. In this context it may be necessary to expand the systematic and taxonomic ecosystem of fungi with fossil representative for which there appear to be no modern analogs.

References

Numbers in brackets at the end of each citation refer to the chapter(s) containing the citation.

Abràmoff, M. D., Magelhães, P. J., Ram, S. J., 2004. Image Processing with ImageJ. Biophotonics International 11, 36–42. [2]

Adaskaveg, J. E., Gilbertson, R. L., 1986. In vitro decay studies of selective delignification and simultaneous decay by the white rot fungi *Ganoderma lucidum* and *G. tsugae*. Canadian Journal of Botany 64, 1611–1619. [6]

Adl, S. M., Simpson, A. G., Farmer M. A., Andersen, R. A., Anderson, O. R., Barta, J. R., Bowser, S. S., Brugerolle, G., Fensome, R. A., Fredericq, S., James, T. Y., Karpov, S., Kugrens, P., Krug, J., Lane, C. E., Lewis, L. A, Lodge, J., Lynn, D. H., Mann, D. G., McCourt, R. M., Mendoza, L., Moestrup, O., Mozley-Standridge, S. E., Nerad, T. A., Shearer, C. A., Smirnov, A. V., Spiegel, F. W., Taylor, M. F., 2005. The new higher level classification of eukaryotes with emphasis on the taxonomy of protists. Journal of Eukaryotic Microbiology 5, 399–451. [1]

Aggarwal, N., Krings, M., Jha, N., Taylor, T. N., 2015. Unusual spheroidal inclusions in Late Permian gymnosperm pollen grains from southern India revisited: Evidence of a fungal nature. Grana 1–10. [1]

Ahlgren, C. E., Hansen, H. L., 1957. Some effects of temporary flooding on coniferous forests. Journal of Forestry 55, 647–650. [6]

Aist, J., 1976. Papillae and related wound plugs of plant cells. Annual Review of Phytopathology 14, 145–163. [6]

Aist, J. R., 1983. Structural responses as resistance mechanisms. In: Bailey, J. A., Deverall, B. J. (Eds.), The Dynamics of Host Defence. Academic Press, New York, NY, 33–70. [6]

Anagnost, S. E., 1998. Light microscopic diagnosis of wood decay. IAWA Journal 19, 141–167. [7]

Anderson, H. M., 1978. *Podozamites* and associated cones and scales from the Upper Triassic Molteno Formation, Karoo Basin, South Africa. Palaeontologia Africana 21, 57–77. [4]

Anderson, J. M., Anderson, H. M., 2003. Heyday of the Gymnosperms: Systematics and Biodiversity of the Late Triassic Molteno Fructifications. National Botanical Institute, Pretoria, South Africa, 398 pp. [4]

Andrews, H. N. 1951. American coal-ball floras. The Botanical Review 17, 431–469. [1, 9]

Andrews, H. N., Lenz, L., 1947. Fossil polypores from Idaho. Annals of the Missouri Botanical Garden 34, 113–114. [7]

Ash, S. R., 1997. Evidence of arthropod-plant interactions in the Upper Triassic of the southwestern United States. Lethaia 29, 237–248. [5]

Ash, S. R., 1999. An upper Triassic *Sphenopteris* showing evidence of insect predation from Petrified Forest National Park, Arizona. International Journal of Plant Science 160, 208–215. [5]

Ash, S., 2000. Evidence of oribatid mite herbivory in the stem of a Late Triassic tree fern from Arizona. Journal of Paleontology 74, 1065–1071. [5, 6]

Atkinson, B. A., Rothwell, G. W., Stockey, R. A., 2014a. *Hubbardiastrobus cuninghamioides* gen. et sp. nov., Evidence for a Lower Cretaceous diversification of Cunninghamioid Cupressaceae. International Journal of Plant Sciences 175, 256–269. [1]

Atkinson, B. A., Rothwell, G. W., Stockey, R. A., 2014b. *Hughmillerites vancouverensis* sp. nov. and the Cretaceous diversification of Cupressaceae. American Journal of Botany

101, 1–12. [1]

Auerbach, M., Hendrix, S. D., 1980. Insect–fern interactions: Macrolepidoteran utilization and species–area association. Ecological Entomology 5, 99–104. [5]

Axelrod, D. I., 1984. An interpretation of Cretaceous and Tertiary biota in polar regions. Palaeogeography, Palaeoclimatology, Palaeoecology 45, 105–147. [8]

Axsmith, B. J., Taylor, T. N., Taylor, E. L., 1998. Anatomically preserved leaves of the conifer *Notophytum krauselii* (Podocarpaceae) from the Triassic of Antarctica. American Journal of Botany 85, 704–713. [2, 4, 9]

Baldrian, P., Větrovský, T., Cajthaml, T., Dobiášová, P., Petránková, M., Šnajdr, J., Eichlerová, I., 2013. Estimation of fungal biomass in forest litter and soil. Fungal Ecology 6, 1–11. [1]

Balick, M. J., Furth, D. G., Cooper-Driver, G., 1978. Biochemical and evolutionary aspects of arthropod predation on ferns. Oecologia 35, 55–89. [5]

Ballard, R. G. Walsh, M. A., Cole, W. E. 1982. Blue-stain fungi in xylem of lodgepole pine: A light-microscope study on extent of hyphal distribution. Canadian Journal of Botany 60, 2334–2341. [7]

Bancroft, H., 1935. Some fossil dicotyledonous woods from Mount Elgon, East Africa. I. American Journal of Botany 22, 164–183. [7]

Barry, K. M., Pearce, R. B., Evans, S. D., Hall, L. D., Mohammed, C. M., 2001. Initial defence responses in sapwood of *Eucalyptus nitens* (Maiden) following wounding and fungal inoculation. Physiological and Molecular Plant Pathology 58, 63–72. [7]

Barthel, M., 1961. Ein Pilzrest aus dem Saarkarbon. Geologie 10, 856–857. [1]

Baxter, R. W. 1960. *Sporocarpon* and allied genera from the American Pennsylvanian. Phytomorphology 10, 19–25. [9]

Baylis, G. T. S., McNabb, R. F. R., Morrison, T. M., 1963. The mycorrhizal nodules of podocarps. Transactions of the British Mycological Society 46, 378–384. [4]

Beeston, J. W., 1972. A specimen of *Araucarioxylon arberi* (Seward) Beeston comb. Nov. from Queensland. Geological Survey of Queensland Publication 352, 17–20. [6]

Bedini, S., Maremmani, A., Giovannetti, M., 2000. *Paris*-type mycorrhizas in *Smilax aspera* L. growing in a Mediterranean scherophyllous wood. Mycorrhiza 10, 9–13. [3]

Begon, M., Harper, J. L., Townsend, C. R., 2006. Ecology. Fourth Edition. Blackwell Publishers, Malden, MA, USA. [5]

Beimforde, C., Schäfer, N., Dörfelt, H., Nascimbene, P. C., Singh, H., Heinrichs, J., Reitner, J., Rana, R. S., Schmidt, A. R., 2011. Ectomycorrhizas from a Lower Eocene angiosperm forest. New Phytologist 192, 988–996. [4]

Benton, M. J., Newell, A. J., 2014. Impacts of global warming on Permo-Triassic terrestrial ecosystems. Gondwana Research 25, 1308–1337. [1]

Berbee, M., Taylor, J., 2007. Rhynie chert: A window into a lost world of complex plant-fungus interactions. New Phytologist. 174, 475–479. [1]

Bercovici, A., Hadley, A., Villanueva-Amadoz, U., 2009. Improving depth of field resolution for palynological photomicrography. Palaeontologia Electronica. 12(2), 12 p. <http://palaeo-electronica.org/2009_2/170/170.pdf> (accessed May 17, 2011). [1, 2, 3, 4, 6, 7]

Bergene, J. A., Taylor, E. L., Taylor, T. N., 2013. *Dordrechtites arcanus* sp. nov., an Anatomically Preserved Gymnospermous Reproductive Structure from the Middle Triassic of Antarctica. International Journal of Plant Sciences 174, 250–265. [1, 4]

Berliner, R., Torrey, J. G., 1989. Studies on mycorrhizal associations in Harvard Forest, Massachusetts. Canadian Journal of Botany 67, 2245–2251. [4]

Bezalel, L., Hadar, Y., Cerniglia, C. E., 1996. Mineralization of Polycyclic Aromatic

Hydrocarbons by the White Rot Fungus *Pleurotus ostreatus*. Applied Environmental Microbiology 62, 292–295. [6]

Biermann, B., Linderman, R. G., 1983. Use of vesicular-arbuscular mycorrhizal roots, intraradical vesicles and extraradical vesicles as inoculum. New Phytologist 95, 97–105. [4]

Bird, H., 1938. The longevity of *Osmunda cinnamomea* with notes on some fern-feeding larvae. American Fern Journal 28, 151–157. [5]

Blanchette, R. A., 1980. Wood decomposition by *Phellinus* (Fomes) *pini*: A scanning electron microscope study. Canadian Journal of Botany 58, 1496–1503. [6]

Blanchette, R. A., 1984a. Selective delignification of eastern hemlock by *Ganoderma tsugae*. Phytopathology 74, 153–160. [6]

Blanchette, R. A., 1984b. Screening wood decayed by white rot fungi for preferential lignin degradation. Applied Environmental Microbiology 48, 647–653. [6]

Blanchette, R. A., 1991. Delignification by wood-decay fungi. Annual Review of Phytopathology 29, 381–398. [6]

Blanchette, R. A., 1992. Anatomical responses of xylem to injury and invasion by fungi. In: Blanchette, R. A., Biggs, A. R. (Eds.), Defense Mechanisms of Woody Plants Against Fungi. Springer-Verlag, Berlin Heidelberg New York, NY, pp. 76–95. [6]

Blanchette, R. A., 2000. A review of microbial deterioration found in archaeological wood from different environments. International Biodeterioration and Biodegradation 46, 189–204. [6]

Blanchette, R. A., Simpson, E., 1992. Soft rot and wood pseudomorphs in an ancient coffin (700 BC) from Tumulus MM at Gordion, Turkey. IAWA Journal 13, 201–213. [6]

Böcher, T. W., 1964. Morphology of the vegetative body of *Metasequoia glyptostroboides*.

Dansk Botanisk Arkiv 24, 1–70. [3]

Bomfleur, B., Kerp, H., 2010a. *Dicroidium* diversity in the Upper Triassic of north Victorian Land, East Antarctica. Review of Palaeobotany and Palynology 160, 67–101. [1]

Bomfleur, B., Kerp, H., 2010b. The first record of the dipterid fern leaf *Clathropteris* Brongniart from Antarctica and is relations to *Polyphacelus stormensis* Yao, Taylor and Taylor. Review of Palaeobotany and Palynology 160, 143–153. [1]

Bomfleur, B., Schneider, J., Schöner, R., Viereck-Götte, L., Kerp, H., 2007. Exceptionally well-preserved Triassic and Early Jurassic floras from north Victoria Land, Antarctica. In: Cooper, A. K., Raymond, C. R., 10th ISAES Editorial Team (Eds.), Antarctica: A Keystone in a Changing World – Online Proceedings of the 10th ISAES, USGS Open-File Report 2007–1047, Extended Abstract 034, 4 p. [1]

Bomfleur, B., Pott, C., Kerp, H., 2011a. Plant assemblages from the Shafer Peak Formation (Lower Jurassic), north Victoria Land, Transantarctic Mountains. Antarctic Science 23, 188–208. [1]

Bomfleur, B., Schneider, J., Schöner, R., Viereck-Götte, L., Kerp, H., 2011b. Fossil sites in the continental Victoria and Ferrar groups (Triassic-Jurassic) of north Victoria Land, Antarctica. Polarforschung 80, 88–99. [1, 7]

Bomfleur, B., Taylor, E. L., Taylor, T. N., Serbet, R., Krings, M., Kerp, H., 2011c. Systematics and paleoecology of a new peltaspermalean seed fern from the Triassic polar vegetation of Gondwana. International Journal of Plant Sciences 172, 807–835. [1]

Bomfleur, B., Serbet, R., Taylor, E. L., Taylor, T. N., 2011d. The possible pollen cone of the Late Triassic conifer *Heidiphyllum/Telemachus* (Voltziales) from Antarctica. Antarctic Science 23, 379–385. [4]

Bomfleur, B., Decombeix, A. -L., Escapa, I. H., Schwendemann, A. B., Axsmith, B., 2013.

Whole-plant concept and environment reconstruction of a *Telemachus* conifer (Voltziales) from the Triassic of Antarctica. International Journal of Plant Sciences 174, 425–444. [1, 4]

Bomfleur, B., Decombeix, A. -L., Schwendemann, A. B., Escapa, I. H., Taylor, E. L., Taylor, T. N., McLoughlin, S., 2014a. Habit and ecology of the Petriellales, an unusual group of seed plants form the Triassic of Gondwana. International Journal of Plant Sciences 175, 1062–1075. [1, 4, 6]

Bomfleur, B., Klymiuk, A. A., Taylor, E. L., Taylor, T. N., Gulbranson, E. L., Isbell, J. L., 2014b. Diverse bryophyte mesofossils from the Triassic of Antarctica. Lethaia 47, 120–132. [1]

Bomfleur, B., Schöner, R., Schneider, J. W., Viereck, L., Kerp, H., McKellar, J. L., 2014c. Transantarctic Basin to the Ferrar Large Igneous Province—New palynostratigraphic age constraints for Triassic–Jurassic sedimentation and magmatism in East Antarctica. Review of Palaeobotany and Palynology 207, 18–37. [1, 2, 6]

Bomfleur, B., McLoughlin, S., Vajda, V., 2014d. Fossilized nuclei and chromosomes reveal 180 million years of genomic stasis in royal ferns. Science 343, 1376–1377. [2]

Bonan, G. B., 2008. Forests and climate change: Forcings, feedbacks, and the climate benefits of forests. Science 320, 1444–1449. [6]

Bonello, P., Pearce, R. B., Watt, F., Grime, G. W., 1991. An induced papilla response in primary root of Scots pine challenged *in vitro* with *Cylindrocarpon destructans*. Physiological and Molecular Plant Pathology 39, 231–228. [6]

Bonfante, P., Perotto, S., 1995. Strategies of arbuscular mycorrhizal fungi when infecting host plants. New Phytologist 130, 3–21. [3]

Bonfante, P., Selosse, M. A., 2010. A glimpse into the past of land plants and of their mycorrhizal affairs: From fossils to evo-devo. New Phytologist 186, 267–270. [4]

Bonfante, P., Balestrini, R., Genre, A., Lanfranco, L., 2009. Establishment and functioning of arbuscular mycorrhizas. In: Deising, H. B. (Ed.), The Mycota V: Plant Relationships, Part B, Springer Verlag, Berlin, Germany, pp. 259–274. [2]

Bonfante-Fasolo, P., 1984. Anatomy and morphology of VA mycorrhizae. In: Conay, L., Powell, C., Bagyara, D. J. (Eds.), VA Mycorrhiza. CRC Press, Boca Raton, FL, pp. 5–33. [3, 4]

Bonfante-Fasolo, P., Fontana, A., 1985. VAM fungi in *Gingko biloba* roots: Their interactions at cellular level. Symbiosis 1, 53–67. [4]

Boullard, B., 1957. La mycotrophie chez les pteridophytes. Sa fréquence, ses caractères, sa signification. Botaniste 41, 1–185. [in French] [5]

Boullard, B., 1971. The endophytic fungi of *Rhynia gwynne-vaughanii* morphological study and deductions as to their biology. Le Botaniste 54, 49–89. [3]

Boucher, L. D., Taylor, E. L., Taylor, T. N., 1995. *Dicroidium* compression floras from southern Victoria Land. Antarctic Journal of the United States 30, 40–41. [1]

Boyce, C. K., Cody, G. D., Fesser, M., Knoll, A. H., Wirich, S., 2002. Organic chemical differentiation within fossil plant cell walls detected with X-ray spectromicroscopy. Geology 30, 1039–1042. [1]

Brassell, S. C., 1992. Biomarkers. In: Pratt, L. M., Comer, J. B., Brassell, S. C. (Eds.), Geochemistry of Organic Matter in Sediments and Sedimentary Rocks, Text for short course No. 27, Tulsa, OK: SEMP. 100 pp. [6]

Brett, D. W., 1960. Fossil oak wood from the British Eocene. Palaeontology 3, 86–92. [7]

Breuninger, M., Einig, W., Magel, E., Cardoso, E., Hampp, R., 2000. Mycorrhiza of Brazil Pine (*Araucaria angustifolia* [Bert. O. Ktze.]). Plant Biology 2, 4–10. [4]

Bromfield, K., Burrett, C. F., Leslie, R. A., Meffre, S., 2007. Jurassic volcaniclastic–basaltic andesite–dolerite sequence in Tasmania – new age constraints for fossil plants from Luna River. Australian Journal of Earth Sciences 54, 965–974. [1]

Brongniart, A. T., 1828. Prodrome d'une histoire des végétaux fossiles Strasbourg, F. G. Levrault, Paris, France. 198 pp. [in French] [8]

Bronson, A. W., Klymiuk, A. A., Stockey, R. A., Tomescu, A. M. F., 2013. A Perithecial Sordariomycete (Ascomycota, Diaporthales) from the Lower Cretaceous of Vancouver Island, British Columbia, Canada. International Journal of Plant Sciences 174, 278–292. [1]

Brundrett, M., 2004. Diversity and classification of mycorrhizal associations. Biological Reviews 79, 473–495. [4]

Brundrett, M. C., 2009. Mycorrhizal associations and other means of nutrition of vascular plants: Understanding the global diversity of host plants by resolving conflicting information and developing reliable means of diagnosis. Plant and Soil 320, 37–77. [4]

Brundrett, M. C., Kendrick, B., 1988. The mycorrhizal status, root anatomy, and phenology of plants in a sugar maple forest. Canadian Journal of Botany 66, 1153–1173. [3]

Brundrett, M., Kendrick, B., 1990. The roots and mycorrhizas of herbaceous woodland plants. I. Quantitative aspects of morphology. New Phytologist 114, 457–468. [3]

Brundrett, M. C., Murase, G., Kendrick, B., 1990. Comparative anatomy of roots and mycorrhizae of common Ontario trees. Canadian Journal of Botany 68, 551–578. [4]

Buchalo, A. S., Zakordonec, O. A., Šašek, V., 1983. Scanning Electron Microscopic Study of Clamp Connections in Higher Basidiomycetes. Folia Microbiologica 28, 420–423. [6]

Cai, J. J., Woo, P. C. Y., Lau, S. K. P., Smith, D. K., Yuen, K.-Y., 2006. Accelerated Evolutionary Rate May Be Responsible for the Emergence of Lineage-Specific Genes in

Ascomycota. Journal of Molecular Evolution 63, 1–11. [9]

Canhoto, C., Graça, M. A. S., 1999. Leaf barriers to fungal colonization and shredders (*Tipula lateralis*) consumption of decomposing *Eucalyptus globulus*. Microbial Ecology 37, 163–172. [8]

Cantrill, D. J., Drinnan, A. N., 1994. Late Triassic megaspores from the Amery Group, Prince Charles Mountains, East Antarctica. Alcheringa 18, 71–78. [1]

Cantrill, D. J., 1997. The pteridophyte *Ashicaulis livingstonensis* (Osmundaceae) from the Upper Cretaceous of Williams Point, Livingston Island, Antarctica. New Zealand Journal of Geology and Geophysics 40, 315–323. [5]

Cantrill, D. J., Hunter, M. A., 2005. Macrofossil floras of the Latady Basin, Antarctic Peninsula. New Zealand Journal of Geology and Geophysics 48, 537–553. [1]

Cantrill, D. J., Poole, I., 2013. The Vegetation of Antarctica Through Geological Time. Cambridge University Press, Cambridge, UK. 490 pp. [1, 2, 4]

Cantrill, D. J., Drinnan, A. N., Webb, J. A., 1995. Late Triassic plant fossils from the Prince Charles Mountains, East Antarctica. Antarctic Science 7, 51–62. [1]

Carroll, G. C., Muller, E. M., Sutton, B. C., 1977. Preliminary studies on the incidence of needle endophytes in some European conifers. Sydowia 29, 87–103. [8]

Carruthers, W., 1873. On *Traquairia*, a Radiolarian Rhizopod from the Coal-Measures. Report of the 42nd Annual Meeting of the British Association for the Advancement of Science (Brighton, August 1872). John Murray, London, UK, pp. 126. [9]

Castañeda-Posadas, C., Calvillo-Canadell, L., Cevallos-Ferriz, S. R. S., 2009. Woods from Miocene sediments in Panotla, Tlaxcala, Mexico. Review of Palaeobotany and Palynology 156, 494–506. [7]

Cázares, E., Trappe, J. M., 1993. Vesicular endophytes in roots of the Pinaceae. Mycorrhiza 2, 153–156. [4]

Cázares, E., Trappe, J. M., Jumpponen, A., 2005. Mycorrhiza-plant colonization patterns on a subalpine glacier forefront as a model system of primary succession. Mycorrhiza 15, 405–406. [4]

Cevallos-Ferriz, S. R. S., Stockey, R. A., Pigg, K. B., 1991. The Princeton chert: Evidence for in situ aquatic plants. Review of Palaeobotany and Palynology 70, 173–185. [1]

Chaloner, W. G., Scott, A. C., Stephenson, J., 1991. Fossil evidence for plant-arthropod interactions in the Palaeozoic and Mesozoic. Philosophical Transactions of the Royal Society of London, Series B 333, 123–177. [6]

Char, M. B. S., Bhat, S. S., 1975. Antifungal activity of pollen. Naturwissenschaften 62, 536. [1]

Chitaley, S. D., Patil, G. V., 1972. An ebenaceous fossil wood infected with deuteromyceteous fungus from the Deccan Intertrappean beds of India. Botanique 3, 99–105. [6]

Cho, S. J., Park, S. J., Lim, J. S., Rhee, Y. H., Shin, K. S., 2002. Oxidation of polycyclic aromatic hydrocarbons by laccase of *Coriolus hirsutus*. Biotechnology Letters 24, 1337–1340. [6]

Christiansen, E., Solhiem, H., 1990. The bark beetle-associated blue-stain fungus *Ophiostoma polonicum* can kill various spruces and Douglas fir. European Journal of Forest Pathology 20, 436–446. [7]

Chrysler, M. A., 1908. Tyloses in tracheids of conifers. New Phytologist 7, 198–204. [7]

Clark, R. B., Zeto, S. K., Zobel, R. W., 1999. Arbuscular mycorrhizal fungal isolate effectiveness on growth and root colonization of Panicum viratum in acidic soil. Soil Biology and Biochemistry 31, 1757–1763. [4]

Collins, B., Parke, J., 2008. Spatial and temporal aspects of tylosis formation in tanoak inoculated with *Phytophthora ramorum*. In: Frankel, S. J., Kliejunas, J. T., Palmieri, K. M. (Eds.), Proceedings of the Sudden Oak Death Third Science Symposium, U.S. Department of Agriculture General Technology Report PSW-GTR-214, p. 335. [7]

Collinson, J. W., Isbell, J. L., Elliot, D. H., Miller, M. F., Miller, J. M. G., Veevers, J. J., 1994. Permian-Triassic Transantarctic basin. Geological Society of America Memoir 184, 173–222. [1]

Collinson, J. W., Hammer, W. R., 1996. New observations on the Triassic stratigraphy of the Shackleton Glacier region. Antarctic Journal of the United States 31, 9–12. [2]

Cooper-Driver, G. A., 1985. The distribution of insects on ferns. American Journal of Botany 72, 921. [5]

Cooper, K. M., Lösel, D. M., 1978. Lipid physiology of vesicular-arbuscular mycorrhiza. I. Composition of lipids in roots on onion, clover and ryegrass infected with *Glomus mosseae*. New Phytologist 80, 143–151. [4]

Cornwell, W. K., Bedford, B. L., Chapin, C. T., 2001. Occurrence of arbuscular mycorrhizal fungi in a phosphorus-poor wetland and mycorrhizal response to phosphorus fertilization. American Journal of Botany 88, 1824–1829. [4]

Creber, G. T., 1990. The south polar forest ecosystem. In: Taylor, T. N., Taylor, E. L. (Eds.), Antarctic Paleobiology: Its Role in the Reconstruction of Gondwana. Springer-Verlag, New York, NY, pp. 37–41. [4]

Cridland, A. A., 1963. *Glossopteris* flora from the Ohio Range, Antarctica. American Journal of Botany 50, 186–195. [1]

Cúneo, N. R., 1996. Permian phytogeography in Gondwana. Palaeogeography, Palaeoclimatology, Palaeoecology 125, 75–104. [3]

Cúneo, N. R., Isbell, J. L., Taylor, E. L., Taylor, T. N., 1993. The Glossopteris flora from Antarctica: Taphonomy and paleoecology. Competes Rendus Palevol 2, 13–40. [1, 2, 3]

Cúneo, N. R., Taylor, E. L., Taylor, T. N., Krings, M., 2003. *In situ* fossil forest from the upper Fremouw Formation (Triassic) of Antarctica, paleoenvironmental setting and paleoclimate analysis. Palaeogeography, Palaeoclimatology, Paleoecology 197, 239–261. [1, 2, 4, 6]

Currah, R., Stockey, R., Lepage, B., 1998. An Eocene tar spot on a fossil palm and its fungal hyperparasite. Mycologia 90, 667–673. [1]

Davis, B., Leisman, G. A., 1962. Further observations on *Sporocarpon* and allied genera. Bulletin of the Torrey Botanical Club 89, 97–109. [9]

Decombeix, A. -L., Taylor, E. L., Taylor, T. N., 2009. Secondary Growth in *Vertebraria* Roots from the Late Permian of Antarctica: A Change in Developmental Timing. International Journal of Plant Sciences 170, 644–656. [1, 3, 6]

Decombeix, A. -L., Taylor, E. L., Taylor, T. N., 2010a. Epicormic shoots in a Permian gymnosperm from Antarctica. International Journal of Plant Sciences 171, 772–782. [3]

Decombeix, A. -L., Taylor, E. L., Taylor, T. N., 2010b. Anatomy and affinities of permineralized gymnospermous trunks with preserved bark from the Middle Triassic of Antarctica. Review of Palaeobotany and Palynology 163, 26–34. [6]

Decombeix, A. -L., Taylor, E. L., Taylor, T. N., 2011. Root suckering in a Triassic conifer from Antarctica: Paleoecological and evolutionary implications. American Journal of Botany 98, 1222–1225. [6]

Decombeix, A. -L., Bomfleur, B., Taylor, E. L., Taylor, T. N., 2014. New insights into the anatomy, development, and affinities of corystosperm trees from the Triassic of Antarctica. Review of Palaeobotany and Palynology 203, 22–34. [1, 4, 6]

Delevoryas, T., Taylor, T. N., Taylor, E. L., 1992. A marattialean fern from the Triassic of Antarctica. Review of Palaeobotany and Palynology 74, 101–107. [1]

del Valle, R. A., Lirio, J. M., Lusky, J. C., Morelli, J. R., Nuñez, H. J., 1997. Jurassic trees at Jason Peninsula, Antarctica. Antarctic Science 9, 443–444. [7]

Dick, M. W., 2001. Straminipilous fungi: Systematics of the Peronosporomycetes, Including Accounts of the Marine Straminipilous Protists, the Plasmodiophorids, and Similar Organisms. Kluwer Academic Publishers, Dordrecht, The Netherlands, 670 pp. [1]

Dickie, I. A., Holdaway, R. J., 2011. Podocarp roots, mycorrhizas, and nodules. In: Turner, B. L., Cernusak, L. A. (Eds.), Ecology of the Podocarpaceae in Tropical Forests, Smithsonian Contributions to Botany 95, 175–187. [1, 4]

Dickson, S., 2004. The *Arum-Paris* continuum of mycorrhizal symbioses. New Phytologist 163, 187–200. [3, 4]

Dieguez, C., Lopez-Gomez, J., 2005. Fungus–plant interaction in a Thuringian (Late Permian) *Dadoxylon* sp. in the SE Iberian Ranges, eastern Spain. Palaeogeography Palaeoclimatology Palaeoecology 229, 69–82. [6]

Dietrich, D., Witke, K., Rössler, R., Marx, G., 2001. Raman spectroscopy on *Psaronius* sp.: A contribution to the understanding of the permineralization process. Applied Surface Science 179, 230–233. [2]

Dighton, J., White, J. F., Peter, O., 2005. The Fungal Community: Its Organization and Role in the Ecosystem, Third Edition. CRC Press, Boca Raton, FL, 960 pp. [3, 7]

Dilcher, D. L., 1965. Epiphyllous fungi from Eocene deposits in western Tennessee, U.S.A. Palaeontographica 116B, 1–54. [8]

Dilcher, D. L., 1963. Eocene epiphyllous fungi. Science 142, 667–669. [8]

Dolinar, N. A., Gaberščik, A., 2010. Mycorrhizal colonization and growth of *Phragmites*

australis in an intermittent wetland. Aquatic Botany 93, 93–98. [3]

Domínguez, E., Cuartero, J., Heredia, A., 2011. An overview on plant cuticle biomechanics. Plant Science 181, 77–84. [8]

Dotzler, N., Krings, M., Agerer, R., Galtier, J., Taylor, T. N., 2008. *Combresomyces cornifer* gen. sp. nov., an endophytic peronosporomycete in *Lepidodendron* from the Carboniferous of central France. Mycological Research 112, 1107–1114. [1]

Edwards, D. E., 1986. *Aglaophyton major*, a non-vascular land-plant from the Devonian Rhynie Chert. Botanical Journal of the Linnaean Society 93, 173–204. [3]

Edwards, M. C., Ayres, P. G., 1981. Cell death and cell wall papillae in the resistance of oak species to powdery mildew disease. New Phytologist 89, 411–418. [6]

Eggen, T., Majcherczyk, A., 1998. Removal of polycyclic aromatic hydrocarbons (PAH) in contaminated soil by white rot fungus *Pleurotus ostreatus*. International Biodeterioration and Biodegradation 41, 111–117. [6]

Eissenstat, D. M., Wells, C. E., Yanai, R. D., Whitbeck, J. L., 2000. Building roots in a changing environment: Implications for root longevity. New Phytologist 147, 33–42. [5]

Elliot, D. H., Fleming, T. H., 2008. Physical volcanology and geological relationships of the Jurassic Ferrar Large Igneous Province, Antarctica. Journal of Volcanology and Geothermal Research 172, 20–37. [1]

Elsik, W. C., 1966. Biologic degradation of fossil pollen grains and spores. Micropaleontology 12, 515–518. [1]

Eriksson, K. E. L., Blanchette, R. A., Ander, P., 1990. Microbial and enzymatic degradation of wood and wood components. Springer-Verlag, Berlin Heidelberg, New York, NY, 407 pp. [6]

Ervin, E. L., Evert, R. F., 1967. Aspects of sieve element ontogeny and structure in *Smilax*

rotundifolia. Botanical Gazette 128, 138–144. [7]

Esau, K., 1977. Anatomy of Seed Plants, Second Edition. John Wiley & Sons, Inc., New York, NY, 767 pp. [7]

Escapa, I. H., Decombeix, A. L., Taylor, T. N., Taylor, E. L., 2010. Evolution and relationships of the conifer *Telemachus*: Evidence from the Triassic of Antarctica. International Journal of Plant Sciences 171, 560–573. [4]

Escapa, I. H., Cúneo, N. R., Rothwell, G., Stockey, R., 2013. *Pararaucaria delfueyoi* sp. nov. from the Late Jurassic Cañadón Calcáreo Formation, Chubut, Argentina: Insights into the evolution of the Cheirolepidiaceae. International Journal of Plant Sciences 174, 458–470. [1]

Escapa, I. H., Taylor, E. L., Cúneo, R., Bomfleur, B., Bergene, J., Serbet, R., Taylor, T. N., 2011. Triassic floras of Antarctica: Plant diversity and distribution in high paleolatitude communities. PALAIOS 26, 522–544. [1, 4]

Evelin, H., Kapoor, R., Giri, B., 2009. Arbuscular mycorrhizal fungi in alleviation of salt stress: A review. Annals of Botany 104, 1263–1280. [4]

Evert, R. F., 2006. Esau's Plant Anatomy: Meristems, Cells, and Tissues of the Plant Body–Their Structure, Function, and Development. Wiley-Interscience, Hoboken, NJ, 601 pp. [7]

Fackler, K., Schwanninger, M., 2012. How spectroscopy and microspectroscopy of degraded wood contribute to understand fungal wood decay. Applied Microbiology and Biotechnology 96, 587–599. [6]

Falaschi, P., Grosfeld, J., Zamuner, A. B., Foix, N., Rivera, S. M., 2011. Growth architecture and silhouette of Jurassic conifers from La Matilde Formation, Patagonia, Argentina. Palaeogeography, Palaeoclimatology, Palaeoecology 302, 122–141. [7]

Farabee, M. J., Taylor, E. L., Taylor, T. N., 1990. Correlation of Permian and Triassic palynomorphs from the central Transantarctic Mountains, Antarctica. Review of Palaeobotany and Palynology 65, 257–265. [2, 4]

Faure, G., Mensing, T. M., 2010. The Transantarctic Mountains: Rocks, Ice, Meteorites and Water. Springer, New York, NY, 804 pp. [2, 4]

Fernando, G., Zimmermann, W., Kolattukudy, P. E., 1984. Suberin-grown *Fusarium solani* f. sp. *pini* generates a cutinase-like esterase which depolymerizes the aliphatic components of suberin. Physiological Plant Pathology 24, 143–155. [7]

Fisher, J. B., Vovides, A. P., 2004. Mycorrhizae are present in cycad roots. The Botanical Review 70, 16–23. [4]

Fitter, A. H., Gilligan, C. A., Hollingsworth, K., Kleczkowski, A., Twyman, R. M., Pitchford, J. W., 2005. Biodiversity and ecosystem function in soil. Functional Ecology 19, 369–377. [4]

Fleischmann, A., Krings, M., Mayr, H., Agerer, R., 2007. Structurally preserved polypores from the Neogene of North Africa: *Ganodermites libycus* gen. et sp. nov. (Polyporales, Ganodermataceae). Review of Palaeobotany and Palynology 145, 159–172. [6, 7]

Florin, R., 1951. Evolution in cordaites and conifers. Acta Horti Bergiani 15, 285–388. [4]

Floudas, D., Binder, M., Riley, R., Barry, K., Blanchette, R. A., Henrissat, B., Martinez, A. T., Otillar, R., Spatafora, J. W., Yadav, J. S., Aerts, A., Benoit, I., Boyd, A., Carlson, A., Copeland, A., Coutinho, P. M., de Vries, R. P., Ferreira, P., Findley, K., Foster, B., Gaskell, J., Glotzer, D., Gorecki, P., Heitman, J., Hesse, C., Hori, C., Igarashi, K., Jurgens, J. A., Kallen, N., Kersten, P., Kohler, A., Kues, U., Kumar, T. K. A., Kuo, A., LaButti, K., Larrondo, L. F., Lindquist, E., Ling, A., Lombard, V., Lucas, S., Lundell, T., Martin, R., McLaughlin, D. J., Morgenstern, I., Morin, E., Murat, C., Nagy, L. G., Nolan,

M., Ohm, R. A., Patyshakuliyeva, A., Rokas, A., Ruiz-Duenas, F. J., Sabat, G., Salamov, A., Samejima, M., Schmutz, J., Slot, J. C., St John, F., Stenlid, J., Sun, H., Sun, S., Syed, K., Tsang, A., Wiebenga, A., Young, D., Pisabarro, A., Eastwood, D. C., Martin, F., Cullen, D., Grigoriev, I. V., Hibbett, D. S., 2012. The Paleozoic Origin of Enzymatic Lignin Decomposition Reconstructed from 31 Fungal Genomes. Science 336, 1715–1719. [6]

Fontana, A., 1985. Vesicular-arbuscular mycorrhizas of *Ginkgo biloba* L. in natural and controlled conditions. New Phytologist 99, 441–447. [4]

Francke-Grosman, H., 1963. Some new aspects in forest entomology. Annual Review of Entomology 8, 415–438. [6]

Freeman, B. C. Beattie, G. A., 2008. An Overview of Plant Defenses against Pathogens and Herbivores. The Plant Health Instructor. DOI: 10.1094/PHI-I-2008-0226-01 [1]

Galtier, J. 1997. Coal-ball floras of the Namurian-Westphalian of Europe. Review of Palaeobotany and Palynology 95, 51–72. [1]

Galtier, J., Taylor, T. N., 1994. The first record of ferns from the Permian of Antarctica. Review of Palaeobotany and Palynology 83, 227–239. [1]

Galtier, J., Phillips, T. L., 1999. The acetate peel technique. In: Jones, T. P., Rowe, N. P. (Eds.), Fossil Plants and Spores: Modern Techniques. The Geological Society, London, UK, pp. 67–70. [1, 2, 3, 4, 7]

García Massini, J., 2007a. A possible endoparasitic chytridiomycete fungus from the Permian of Antarctica. Palaeontologia Electronica 10. doi:16a [1, 3, 5]

García Massini, J., 2007b. A glomalean fungus from the Permian of Antarctica. International Journal of Plant Sciences 168, 673–678. [1, 3]

García Massini, J. L., Falaschi, P., Zamuner, A. B., 2012. Fungal–arthropod–plant interactions from the Jurassic petrified forest Monumento Natural Bosques Petrificados, Patagonia, Argentina. Palaeogeography Palaeoclimatology Palaeoecology 329/330, 37–46. [6]

Garland, M. J., Bannister, J. M., Lee, D. E., White, J. D. L., 2007. A coniferous tree stump of late Early Jurassic age from the Ferrar Basalt, Coombs Hills, southern Victoria Land, Antarctica. New Zealand Journal of Geology and Geophysics 50, 263–269. [1, 7]

Gäumann, E. A., 1928. Comparative Morphology of Fungi. McGraw-Hill Book Company, Inc., New York, NY, 701 pp. [9]

Gerdemann, J. W., 1955. Wound-healing of hyphae in a phycomycetous mycorrhiza fungus. Mycologia 47, 916–918. [3, 5]

Gerdemann, J. W., 1965. Vesicular-arbuscular mycorrhizae formed on maize and tuliptree by *Endogone fasciculata*. Mycologia 57, 562–575. [3]

George, L. O., Bazzaz, F. A., 1999. The fern understory as an ecological filter: Emergence and establishment of canopy-tree seedlings. Ecology 80, 833–845. [5]

Gerrienne, P., Gensel, P. G., Strullu-Derrien, C., Lardeux, H., Steemans, P., Prestianni, C., 2011. A simple type of wood in two Early Devonian plants. Science 333, 837–837. [6]

Gerson, U., 1979. The association between pteridophytes and arthropods. Fern Gazette 12, 29–45. [5]

Gibson J. L., Kimbrough J. W., Benny G. L., 1986. Ultrastructural observations on Endogonaceae (Zygomycetes): *Endogone pisiformis*. Mycologia 78, 543–553. [9]

Giovannetti, M., Sbrana, C., Avio, L., Citernesi, A. S., Logi, C., 1993. Differential hyphal morphogenesis in arbuscular mycorrhizal fungi during pre-infection stages. New Phytologist 125, 587–593. [3]

Glauser, A. L., Harper, C. J., Taylor, T. N., Taylor, E. L., Marshall, C. P., Olcott Marshall, A., 2014. Reexamination of cell contents in Pennsylvanian spores and pollen grains using Raman spectroscopy. Review of Palaeobotany and Palynology 210, 62–68. [6]

Goheen, D. and Hansen, E., 1993. Effects of pathogens and bark beetles on forests. In: Schowalter, T. D., Filip, G. M. (Eds.), Beetle-Pathogen Interactions in Conifer Forests. Academic Press, London, UK, pp. 175–196. [7]

Goldstein, S., 1960. Degradation of pollen by phycomycetes. Ecology 41, 543–545. [1]

Gould, R. E., 1975. A preliminary report on petrified axes of *Vertebraria* from the Permian of eastern Australia. In: Campbell, K. S. W. (Eds.), Gondwana Geology. Australian National University Press, Canberra, Australia 09–115. [6]

Gould, R. E., Delevoryas, T., 1977. The biology of *Glossopteris*: Evidence from petrified seed-bearing and pollen-bearing organs. Alcheringa 1, 387–399. [8]

Greguss, P., 1967. Fossil gymnosperm woods in Hungary from the Permian to the Pliocene. Akadémiai Kiadó, Budapest, Hungary, 222 pp. [in Hungarian] [6]

Grice, K., H. Lu, Atahan, P., Asif, M., Hallmann, C., Greenwood, P., Maslen, E., Tulipani, S., Williford, K., Dodson, J., 2009. New insights into the origin of Perylene in geological samples. Geochimica et Cosmochimica Acta 73, 6531–6543. [6]

Grimm, G. W., Kapli, P., Bomfleur, B., McLoughlin, S., Renner, S. R., 2015. Using more than the oldest fossils: Dating Osmundaceae with three Bayesian Clock approaches. Systematic Biology. In press: doi:10.1093/sysbio/syu108 [5]

Gulbranson, E. L., Isbell, J. L., Taylor, E. L., Ryberg, P. E., Taylor, T. N., Flaig, P. P., 2012. Permian polar forests: Deciduousness and environmental variation. Geobiology 10, 479–495. [4, 6, 8]

Gulbranson, E. L., Ryberg, P. E., 2013. Paleobotanical and geochemical approaches to studying fossil tree rings: Quantitative interpretations of paleoenvironment and ecophysiology. PALAIOS 28, 137–140. [4]

Gulbranson, E. L., Ryberg, P. E., Decombeix, A.-L., Taylor, E. L., Taylor, T. N., Isbell, J. L., 2014. Leaf habit of Late Permian Glossopteris trees from high-palaeolatitude forests. Journal of the Geological Society 171, 493–507. [8]

Günther, T., Sack, U., Hofrichter, M., Lätz, M., 1998. Oxidation of PAH and PAH-derivatives by fungal and plant oxidoreductases. Journal of Basic Microbiology 38, 113–122. [6]

Habgood, K. S., Hass, H., Kerp, H., 2004. Evidence for an early terrestrial food web: Coprolites from the Early Devonian Rhynie chert. Transactions of the Royal Society of Edinburgh Earth Science 94, 371–389. [1, 5]

Halling, R. E., 2001. Ectomycorrhizae: Co-evolution, significance, and biogeography. Annals of the Missouri Botanical Garden. 88, 5–13. [4]

Hammer, W. R., 1990. Triassic terrestrial vertebrate faunas of Antarctica. In: Taylor, T. N., Taylor, E. L. (Eds.), Antarctic Paleobiology: Its Role in the Reconstruction of Gondwana. Springer-Verlag, New York, NY, pp. 42–50. [2, 4]

Harley, J. L., Harley, E. L., 1987. A check-list of mycorrhiza in the British flora. New Phytologist, 105, Suppl. s1, 1–102. [4]

Harper, C. J., Bomfleur, B., Decombeix, A. -L., Taylor, E. L., Taylor, T. N., Krings, M., 2012. Tylosis formation and fungal interactions in an Early Jurassic conifer from northern Victoria Land, Antarctica. Review of Palaeobotany and Palynology 175, 25–31. [1]

Harper, C. J., Taylor, T. N., Krings, M., Taylor, E. L., 2013. Mycorrhizal symbiosis in the Paleozoic seed fern *Glossopteris* from Antarctica. Review of Palaeobotany and Palynology 192, 22–31. [1, 4, 8]

Harper, C. J., Taylor, T. N., Krings, M., Taylor, E. L., 2015. Arbuscular mycorrhizal fungi in a voltzialean conifer from the Triassic of Antarctic. Review of Palaeobotany and Palynology 215, 76–84. [1]

Hartig, R., 1878. Die Zersetzungserscheinungen des Holzes der Nadelholzbäume und der Eiche in forstlicher, botanischer und chemischer Richtung. Springer-Verlag, Berlin Heidelberg, New York, NY, 218 pp. [in German] [6]

Hass, H., Taylor, T. N., Remy, W., 1994. Fungi from the Lower Devonian Rhynie chert: Mycoparasitism. American Journal of Botany 81, 29–37. [1, 5, 8]

Hass, H., Rowe, N. P., 1999. Thin sections and wafering. In: Jones, T. P., Rowe, N. P. (Eds.), Fossil Plants and Spores: Modern Techniques. The Geological Society, London, UK, pp. 76–81. [1, 3, 4, 7]

Hatakka, A., 2001. Biodegradation of lignin. In: Hofrichter, M., Steinbüchel, A. (Eds.), Biopolymers: Volume 1: Lignin, Humic Substances, and Coal. Weinheim, Germany. Wiley-VCH, 129–180. [6]

Helgason, T., Merryweather, J. W., Denison, J., Wilson, P., Young, J., Fitter, A. H., 2002. Selectivity and functional diversity in arbuscular mycorrhizas of co-occurring fungi and plants from a temperate deciduous woodland. Journal of Ecology 90, 371–384. [4]

Hellawell, J., Ballhaus, C., Gee, C. T., Mustoe, G. E., Nagel, T. J., Wirth, R., Rethemeyer, J., Tomaschek, F., Geisler, T., Greef, K., Mansfeldt, T., 2015. Incipient silicification of recent conifer wood at a Yellowstone hot spring. Geochimica et Cosmochimica 149, 79–87. [2]

Hemley, R. J., 1987. Pressure dependence of Raman spectra of SiO_2 polymorphs: Alpha-quartz, coesite and stishovite. In: Manghnani, M. H., Syono, Y. (Eds.), High-pressure Research

in Mineral Physics. Terra Scientific Publishing Company and AGU, Washington, DC, pp. 347–360. [6]

Hendrix, S. D., 1980. An evolutionary and ecological perspective of the insect fauna of ferns. American Naturalist 115, 171–196. [5]

Hergt, J. M., Brauns, C. M., 2001. On the origin of the Tasmanian dolerite. Australian Journal of Earth Sciences 48, 543–549. [1]

Hernandez-Castillo, G. R., Rothwell, G. W., Mapes, G., 2001. Compound pollen cone in a Paleozoic conifer. American Journal of Botany 88, 1139–1142. [4]

Hessburg, P. F., Hansen, E. M. 1987. Pathological anatomy of black stain root disease of Douglas-fir. Canadian Journal of Botany 65, 962–971. [7]

Hick, T., Cash, W., 1884. Contributions to the Fossil Flora of Halifax. Part IV. Proceedings of the Yorkshire Geological Society 8, 370–377. [2]

Hieger, T. J., Serbet, R., Harper, C. J., Taylor, T. N., Taylor, E. L., Gulbranson, E. L., 2015. Cheirolepidiaceous diversity: An anatomically preserved pollen cone from the Lower Jurassic of southern Victoria Land, Antarctica. Review of Palaeobotany and Palynology. *accepted.* [1]

Hilton, J., Wang, S. -J., Galtier, J., Li, C. -S., 2001. An Early Permian plant assemblage from the Taiyuan Formation of northern China with compression/impression and permineralized preservation. Review of Palaeobotany and Palynology 114, 175–189. [1]

Hilton, J., Wang, S. -J., Galtier, J., Glasspool, I., Stevens, L., 2004. An upper Permian permineralized plant assemblage in volcaniclastic tuff from the Xuanwei Formation, Huizhou Province, southern China, and its palaeofloristic significance. Geological Magazine 141, 661–674. [1]

Holden, R., 1915., A Jurassic wood from Scotland. The New Phytologist 14, 205–209. [7]

Holdgate, G. R., McLoughlin, S., Drinnan, A. N., Finkelman, R. B., Willett, J. C., Chiehowsky, L. A., 2005. Inorganic chemistry, petrography and palaeobotany of Permian coals in the Prince Charles Mountains, East Antarctica. International Journal of Coal Geology 63, 156–177. [1, 3]

Holt, K., Allen, G., Hodgson, R., Marsland, S., Flenley, J., 2011. Progress towards an automated trainable pollen location and classifier system for use in the palynology laboratory. Review of Palaeobotany and Palynology 167, 175–183. [2]

Hu, H. H., Cheng, W. C., 1948. On the new family Metasequoiaceae and on *Metasequoia glyptostroboides*, a living species of the genus *Metasequoia* found in Szechuan and Hupeh. Bulletin of the Fan Memorial Institute of Biology 1, 153–161. [3]

Huber, B. T., MacLeod, K. G., Wing, S. L., (Eds.), 2000. Warm Climates in Earth History. Cambridge University Press, Cambridge, UK, 462 pp. [1]

Hunter, M. A., Cantrill, D. J., Flowerdew, M. J., Millar, I. L., 2005. Mid-Jurassic age for the Botany Bay Group: implications for Weddell Sea Basin creation and southern hemisphere biostratigraphy. Journal of the Geological Society 162, 745–748. [1]

Hunter, M. A., Cantrill, D. J., Flowerdew, M., 2006. Latest Jurassic–earliest Cretaceous age for a fossil flora from the Latady Basin, Antarctic Peninsula. Antarctic Science 18, 261–264. [1]

Hutchinson, S. A., 1955. A review of the genus *Sporocarpon* Williamson. Annals of Botany 19, 425–435. [9]

Ibáñez, C. G., Zamuner, A. B., 1996. Hyphomycetes (Deuteromycetes) in cones of *Araucaria mirabilis* (Spegazzini) Windhausen, Middle Jurassic of Patagonia, Argentina. Mycotaxon 59, 137–143. [7]

Igisu, M., Nakashima, S., Ueno, Y., Awramik, S. M., 2006. *In situ* infrared microspectroscopy of ~850 million-year-old prokaryotic fossils. Applied Spectroscopy 60, 1111–1120. [6]

Iglesias, A., Artabe, A. E., Morel, E. M., 2011. The evolution of Patagonian climate and vegetation from the Mesozoic to the present. Biological Journal of the Linnaean Society 103, 409–422. [1]

Isbell, J. L., Cúneo, N. R., 1996. Depositional framework of Permian coal-bearing strata southern Victoria Land Antarctica. Palaeogeography, Palaeoclimatology, Palaeoecology 125, 217–238. [3]

Isbell, J. L., Leneaker, P. A., Askin, R. A., Miller M. F., Babcock, L. E., 2003. Reevaluation of the timing and extent of the late Paleozoic glaciation in Gondwana: Role of the Transantarctic Mountains. Geology 31, 977–980. [1]

Jabloniski, D., 2004. Extinction: Past and present. Nature 427, 589. [1]

Jefferson, T. H., Siders, M. A., Havan, M. A., 1983. Jurassic trees engulfed by lavas of the Kirkpatrick Basalt Group, northern Victoria Land. Antarctic Journal of the United States 18, 14–16. [1, 7]

Jeffrey, E. C., 1904. A fossil *Sequoia* from the Sierra Nevada. Botanical Gazette 38, 321–332. [7]

Jiang, C., Alexander, R., Kagi, R. I., Murray, A. P., 2000. Origin of perylene in ancient sediments and its geological significance. Organic Geochemistry 31, 1545–1559. [6]

Jones, V. A. S., Dolan, L., 2012. The evolution of root hairs and rhizoids. Annals of Botany 110, 205–212. [5]

Joy, K. W., Willis, A. J., Lacey, W. S., 1956. A rapid cellulose peel technique in palaeobotany. Annals of Botany 20, 635–637. [1, 2, 3, 4, 6]

Jumpponen, A., 2001. Dark septate endophytes - are they mycorrhizal? Mycorrhiza 11, 207–211.

[3, 5]

Jumpponen, A., Trappe, J. M., 1998. Dark septate endophytes: A review of facultative biotrophic root-colonizing fungi. New Phytologist 140, 295–310. [3]

Jumpponen, A., Jones, K. L., 2009. Massively parallel 454 sequencing indicates hyper diverse fungal communities in temperate *Quercus macrocarpa* phyllosphere. New Phytologist 184, 438–448. [8]

Karatygin I. V., Snigirevskaya N. S., Demchenko K. N., 2006. Species of the genus *Glomites* as plant mycobionts in Early Devonian ecosystems. Paleontological Journal 40, 572–579. [3]

Kellogg, D. W., Taylor, E. L., 2004. Evidence of oribatid mite detritivory in Antarctica during the late Paleozoic and Mesozoic. Journal of Paleontology 78, 1146–1153. [6]

Kerstiens, G., 1996. Signaling across the divide: a wider perspective of cuticular structure—function relationships. Trends in Plant Science 1, 125–129. [8]

Kidder, D. L., Worsley, T. R., 2004. Causes and consequences of extreme Permo-Triassic warming to global equable climate and relation to the Permo-Triassic extinction and recovery. Palaeogeography, Palaeoclimatology, Palaeoecology 203, 207–237. [1]

Kidder, D. L., Worsley, T. R., 2010. Phanerozoic Large Igneous Provinces (LIPs), HEATT (Haline Euxinic Acidic Thermal Transgression) episodes, and mass extinctions. Palaeogeography, Palaeoclimatology, Palaeoecology 295, 162–191. [1]

Kihara, M., Takayama, M., Wariishi, H., Tanaka, H., 2002. Determination of the carbonyl groups in native lignin utilizing Fourier transform Raman spectroscopy. Spectrochimica Acta, Part A 58 2213–2221. [6]

Kikuzawa, K., Lechowicz, M. J., 2011. Ecology of leaf longevity. Ecological Research Monographs, Springer Tokyo, Japan. 147 pp. [8]

Kinden, D. A., Brown, M. F., 1976. Electron microscopy of vesicular–arbuscular mycorrhizae of yellow poplar. IV. Host-endophyte interactions during arbuscular deterioration. Canadian Journal of Microbiology 22, 64–75. [3]

Kirk, P. M., Cannon, P. F., Minter, D. W., Stalpers, J. A., 2008. Ainsworth & Bisby's dictionary of the fungi. CABI Publishing, Wallingford, UK, 771 pp. [3, 9]

Klavins, S. D., Taylor, T. N., Taylor, E. L., 2004. Matoniaceous ferns (Gleicheniales) from the Middle Triassic of Antarctica. Journal of Paleontology 78, 211–217. [1]

Klymiuk, A. A., Taylor, T. N., Taylor, E. L., Krings, M., 2013a. Paleomycology of the Princeton Chert II. Dark-septate fungi in the aquatic angiosperm *Eorhiza arnoldii* indicate a diverse assemblage of root-colonizing fungi during the Eocene. Mycologia 105, 1100–1109. [1]

Klymiuk, A. A., Taylor, T. N., Taylor, E. L., Krings, M., 2013b. Paleomycology of the Princeton Chert I. Fossil hyphomycetes associated with the early Eocene aquatic angiosperm, *Eorhiza arnoldii*. Mycologia 105, 521–529. [1]

Knapp, D. G., Pintye, A., Kovács, G. M., 2012. The dark side is not fastidious – dark septate endophytic fungi of native and invasive plants of semiarid sandy areas. PLoS ONE 7, e32570–8. [5]

Konoe, R., 1957, Über das Vorkommen der Vurzelpilze bie Metasequoia und den Nächst verwandten Pflanzen. Journal of the Institute of the Polytechnic, Osaka City University, Series B, Biology 8, 179–184. [3]

Kostopoulou, P., Radoglou, K., Dini-Papanastasi, O., 2011. Performance and quality of *Cupressus sempervirens* L. mini-plug seedlings under reduced photoperiod. European Journal of Forest Research 130, 579–588. [4]

Krings, M., 2001. Pilzreste auf und in den Fiedern zweier Pteridospermen aus dem Stefan von Blanzy-Montceau (Zentralfrankreich). Geologica Saxonica–Abhandlungen des

Staatlichen Museums für Mineralogie und Geologie Dresden 46/47, 189–196. [1]

Krings, M., Taylor, T. N., 2012c. Fungal reproductive units enveloped in a hyphal mantle from the Lower Pennsylvanian of Great Britain, and their relevance to our understanding of Carboniferous fungal "sporocarps." Review of Palaeobotany and Palynology 175, 1–9. [1, 9]

Krings, M., Taylor, T. N., Hass, H., Kerp, H., Dotzler, N., Hermsen, E. J., 2007. Fungal endophytes in a 400-million-yr-old land plant: Infection pathways, spatial distribution, and host responses. New Phytologist 174, 648–657. [4, 5]

Krings, M., Dotzler, N., Taylor, T. N., 2009a. *Globicultrix nugax* nov. gen. et nov. spec. (Chytridiomycota), an intrusive microfungus in fungal spores from the Rhynie chert. Zitteliana A 48/49, 165–170. [1, 5]

Krings M., Dotzler N., Taylor T. N., Galtier, J., 2009b. A Late Pennsylvanian fungal leaf endophyte from Grand-Croix, France. Review of Palaeobotany and Palynology 156, 449–453. [1]

Krings, M., Dotzler, N., Galtier, J., Taylor, T. N., 2010a. Oldest fossil basidiomycete clamp connections. Mycoscience 52, 18–23. [1]

Krings M., Taylor T. N., Galtier J., Dotzler, N., 2010b. Microproblematic endophytes and epiphytes of fern pinnules from the Upper Pennsylvanian of France. Geobios 43, 503–510. [1]

Krings, M., Dotzler, N., Longcore, J. E., Taylor, T. N., 2010c. An unusual microfungus in a fungal spore from the Lower Devonian Rhynie chert. Palaeontology 53, 753–759. [1]

Krings, M., Dotzler, N., Taylor, T. N., Galtier, J., 2010d. A fungal community in plant tissue from the Lower Coal Measures (Langsettian, Lower Pennsylvanian) of Great Britain. Bulletin of Geoscience 85, 679–690. [5]

Krings , M., Dotzler, N., Taylor, T. N., Galtier, J., 2010e. Microfungi from the Upper Visean (Mississippian) of central France: Structure and development of the sporocarp *Mycocarpon cinctum* nov. sp . Zitteliana A 50, 127–135. [5, 9]

Krings, M., Taylor, T. N., Taylor, E. L., Dotzler, N., Walker, C., 2011a. Arbuscular mycorrhizal-like fungi in Carboniferous arborescent lycopsids. New Phytologist 191, 311–314. [1, 3, 4]

Krings, M., Dotzler, N., Taylor, T. N., 2011b. Mycoparasitism in *Dubiocarpon*, a fungal sporocarp from the Carboniferous. Neues Jahrbuch für Geologie und Palaontologie, Abhandlungen 262, 24 –245. [9]

Krings, M., Taylor, T. N., White, J. F., 2011c. Fungal sporocarps from the Carboniferous: An unusual specimen of *Traquairia*. Review of Palaeobotany and Palynology 168, 1–6. [9]

Krings, M., Taylor, T. N., Dotzler, N., 2012a. Fungal endophytes as a driving force in land plant evolution: Evidence from the fossil record. In: Southworth, D. (Ed.), Biocomplexity of Plant-Fungal Interactions. John Wiley & Sons, Inc., New York, NY, pp. 5–27. [1, 3]

Krings, M., Taylor, T. N., Dotzler, N., Persichini, G., 2012b. Fossil fungi with suggested affinities to the Endogonaceae from the Middle Triassic of Antarctica. Mycologia 104, 835–844. [1, 4]

Krings, M., Taylor, T. N., Dotzler, N., 2013. Fossil evidence of the zygomycetous fungi. Persoonia - Molecular Phylogeny and Evolution of Fungi 30, 1–10. [9]

Krings, M., Taylor, T. N., Taylor, E. L., Kerp, H., Dotzler, N., 2014. First record of a fungal "sporocarp" from the Lower Devonian Rhynie chert. Palaeobiodiversity and Palaeoenvironments 94, 221–227. [9]

Krull, E. S., 1999. Permian palsa mires as palaeoenvironmental proxies. PALAIOS 14, 530–544. [1]

Kubota, M., McGonigle, T. P., Hyakumachi, M., 2004. Co-occurrence of *Arum*- and *Paris*-type morphologies of arbuscular mycorrhizae in cucumber and tomato. Mycorrhiza 15, 73–77. [3]

Kyle, R. A., Schopf, J. M., 1982. Permian and Triassic palynostratigraphy of the Victoria Group, Transantarctic Mountains. In: Craddock, C. (Ed.), Antarctic Geoscience. University of Wisconsin Press, Madison, WI, pp. 649–659. [1]

Labandeira, C., 2007. The origin of herbivory on land: Initial patterns of plant tissue consumption by arthropods. Insect Science 14, 259–275. [6]

Lacey, W. S., Lucas, R. C., 1981. A Lower Permian flora from the Theron Mountains, Coats Land. British Antarctic Survey Bulletin 53, 153–156. [1]

Lange, R. T., 1978. Southern Australian Tertiary epiphyllous fungi, modern equivalents in the Australasian region, and habitat indicator value. Canadian Journal of Botany 56, 532–541. [8]

Larsen, M. J., 1983. Notes on tomentelloid fungi. V. Additional new species of *Pseudotomentella*. Mycologia 75, 556–562. [7]

Larson, P. R., 1964. Contribution of different-aged needles to growth and wood formation of young red pines. Forest Science 10, 224–238. [4]

Lawton, J. R., Lawton, J. R. S., 1971. Seasonal variations in the secondary phloem of some forest trees from Nigeria. New Phytologist 71, 335–348. [7]

Lepage, B., Currah, R., Stockey, R., Rothwell, G., 1997. Fossil ectomycorrhizae from the middle Eocene. American Journal of Botany 84, 410–412. [1, 4]

Lepage, B. A., Currah, R. S., Stockey, R., 1994. The Fossil Fungi of the Princeton Chert. International Journal of Plant Sciences 155, 828–836. [1]

Liese, W., Schmidt, R., 1966. Untersuchungen über den Zellwandabbau von Nadelholz durch *Trametes pini*. Holz als Roc-Wekst 24, 454–460. [in German] [6]

Lindström, S., McLoughlin, S., 2007. Synchronous palynofloristic extinction and recovery after the end-Permian event in the Prince Charles Mountains, Antarctica: Implications for palynofloristic turnover across Gondwana. Review of Paleobotany and Palynology 145, 89–122. [1]

Lin-Vien, D., Colthup, N. B., Fateley, W. G., Grasselli, J. G., 1991. The Handbook of Infrared and Raman Characteristic Frequencies of Organic Molecules. Elsevier, New York, NY, 503 pp. [6]

Little, S.A., Stockey, R.A., 2003. Vegetative growth of *Decodon allenbyensis* (Lythraceae) from the Middle Eocene Princeton Chert with anatomical comparisons to *Decodon verticillatus*. International Journal of Plant Sciences 164, 453–469. [1]

Logan, K. J., Thomas, B. A., 1987. The distribution of lignin derivatives in fossil plants. New Phytologist 105, 157–173. [6]

Lücking, R., Huhndorf, S., Pfister, D. H., Plata, E. R., Lumbsch, H. T., 2009. Fungi evolved right on track. Mycologia 101, 810–822. [3]

Mägdefrau, K., 1966. Die Strukturerhaltung fossiler Pflanzen. Bild der Wissenschaft 12, 988–997. [in German] [6]

Maheshwari, H. K., Tewari, R., 1992. Epidermal morphology of some Indian species of the genus *Glossopteris* Brongniart. Palaeobotanist 39, 338–380. [8]

Manchester, S. R., 1983. Fossil wood of the Engelhardieae (Juglandaceae) from the Eocene of North America: *Engelhardioxylon* gen. nov. Botanical Gazette 144, 157–163. [7]

Manion, P. D., 1991. Tree disease concepts, Second Edition. Prentice-Hall, Inc., Englewood Cliffs, NJ, 399 pp. [6]

Marano, A. V., Pires-Zottarelli, C. L. A., Barrera, M. D., Steciow, M. M., Gleason, F. H., 2010. Diversity, role in decomposition, and succession of zoosporic fungi and straminipiles on submerged decaying leaves in a woodland stream. Hydrobiologia 659, 93–109. [8, 9]

Marguerier, J., 1973. Paléoxylologie du Gondwanan africain: Étude et affinities du genre *Australoxylon*. Palaeontologia Africana 16, 37–58. [in French] [6]

Marschner, H., 1991. Mechanisms of Adaptation of plants to acid soils. In: Wright, R. J., Baliger, V. C., Murrmann, R. P. (Eds.), Plant-soil Interactions at Low pH: Proceedings of the Second International Symposium on Plant-soil Interactions at Low pH, Beckley, WV. 24–29 June 1991. Kluwer Academic Publisher, Dordrecht, Netherlands pp. 683–702. [4]

Marschner, H., Dell, B., 1994. Nutrient uptake in mycorrhizal symbiosis. Plant and Soil 159, 89–102. [3]

Marshall, C., Javaux, E., Knoll, A., Walter, M., 2005. Combined micro-Fourier transform infrared (FTIR) spectroscopy and micro-Raman spectroscopy of Proterozoic acritarchs: A new approach to Palaeobiology. Precambrian Research 138, 208–224. [2, 6]

Marshall, C. P., Olcott Marshall, A., 2013. Raman Hyperspectral Imaging of Microfossils: Potential Pitfalls. Astrobiology 13, 920–931. [6]

Marshall, C. P., Olcott Marshall, A., 2014. Raman spectroscopy as a screening tool for ancient life detection on Mars. Philosophical Transactions of the Royal Society A 372, 20140195. [6]

Martill, D. M., 1989. Fungal borings in neoselachian teeth from the Lower Oxford Clay of Peterborough. Mercian Geology 12, 1–4. [7]

Martin, M. M., 1991. The evolution of cellulose digestion in insects. Philosophical Transactions of the Royal Society of London, Series B 333, 281–288. [6]

Matsumoto, M., Saiki, K., Zhang, W., Zheng, S., Wang, Y. -D., 2006. A new species of

osmundaceous fern rhizome, *Ashicaulis macromedullosus* sp. nov., from the Middle Jurassic, northern China. Paleontological Research 10, 195–205. [5]

Martin, J. T., 1964. Role of cuticle in the defense against plant disease. Annual Review of Phytopathology 2, 81–100. [8]

Marynowski, L., Szeląg E., Jędrysek M. O., Simoneit, B. R. T., 2011. Effects of weathering on organic matter: Part II: Fossil wood weathering and implications for organic geochemical and petrographic studies. Organic Geochemistry 42, 1076–1088. [6]

Marynowski, L., Smolarek, B. R. T., Bechtel, J. A., Philippe, M., Kurkiewicz, S., Simoneit, B. R. T., 2013. Perylene as an indicator of conifer fossil wood degradation by wood degrading fungi. Organic Geochemistry 59, 143–151. [6]

Masood, K. R., Taylor, T. N., Horner, T., Taylor, E. L., 1994. Palynology of the Mackellar Formation (Beacon Supergroup) of East Antarctica. Review of Palaeobotany and Palynology 83, 329–337. [1]

Matekwor Ahulu, E., Nakata, M., Nonaka, M., 2004. *Arum*- and *Paris*-type arbuscular mycorrhizas in a mixed pine forest on sand dune soil in Niigata Prefecture, central Honshu, Japan. Mycorrhiza 15, 129–136. [3]

Matsunaga, K. K. S., Stockey, R. A., Tomescu, A. M. F., 2013. *Honeggeriella complexa* gen. et sp. nov., a heteromerous lichen from the Lower Cretaceous of Vancouver Island (British Columbia, Canada). American Journal of Botany 100, 450–459. [1]

Matthews, E. G., 1976. Insect ecology. University of Queensland Press, St. Lucia, 226 pp. [6]

McLean, R. C., 1922. On the fossil genus *Sporocarpon*. Annals of Botany 36, 71–90. [9]

McDowell, N., Pockman, W. T., Allen, C. D., Breshears, D. D., Cobb, N., Kolb, T., Plaut, J., Sperry, J., West, A., Williams, D. G., Yepez, E. A., 2008. Mechanisms of plant survival

and mortality during drought: Why do some plants survive while others succumb to drought? New Phytologist 178, 719–739. [4]

McElwain, J. C., Beerling, D. J., Woodward, F. I., 1999. Fossil plants and global warming of the Triassic-Jurassic boundary. Science 285, 1386–1390. [1]

McGee, P. A., Bullock, S., Summerell, B. A., 1999. Structure of mycorrhizae of the Wollemi Pine (*Wollemia nobilis*) and related Araucariaceae. Australian Journal of Botany 47, 85–95. [4]

McLoughlin, S., 1992. Late Permian plant megafossils from the Bowen Basin, Queensland, Australia: Part 1. Palaeontographica Abteilung B 228, 105–149. [3]

McLoughlin, S., 1993. Plant fossil distributions in some Australian Permian non-marine sediments. Sedimentary Geology 85, 601–619. [3]

McLoughlin, S., Drinnan, A. N., 1996. Anatomically preserved *Noeggerathiopsis* leaves from East Antarctica. Review of Palaeobotany and Palynology 92, 207–227. [1]

McLoughlin, S., Larsson, K., Lindström, S., 2005. Permian plant macrofossils from Fossilryggen, Vestfjella, Dronning Maud Land. Antarctic Science 17, 73–86. [1]

McLoughlin, S., Carpenter, R. J., Jordan, G. J., Hill, R. S., 2008. Seed ferns survived the end-Cretaceous mass extinction in Tasmania. American Journal of Botany 95, 465–471. [3]

McLoughlin, S., Drinnan, A. N., Slater, B. J., Hilton, J., 2015. *Paurodendron stellatum*: A new Permian permineralized herbaceous lycopsid from the Prince Charles Mountains, Antarctica. Review of Palaeobotany and Palynology, *in press.* DOI: 10.1016/j.revpalbo.2015.04.004 [1]

McManus, H. A., Taylor, E. L., Taylor, T. N., Collinson, J. W., 2002. A petrified *Glossopteris* flora from Collinson Ridge, central Transantarctic Mountains: Late Permian or Early Triassic. Review of Palaeobotany and Palynology 120, 233–246. [1, 8]

McManus, H. A., Boucher, L., Taylor, E. L., Taylor, T. N., 2002. *Hapsidoxylon terpsichorum* gen. et sp. nov., a stem with unusual anatomy from the Triassic of Antarctica. American Journal of Botany 89, 1958–1966. [1]

Medel, R., Lorea-Hernández, F., 2008. Hyaloscyphaceae (Ascomycota) growing on tree ferns in Mexico. Mycotaxon 106, 209–218. [5]

Medlyn, D. A., Tidwell, W. D., 1975. Conifer wood from the Upper Jurassic of Utah. Part I: *Xenoxylon morrisonense* sp. nov. American Journal of Botany 62, 203–208. [7]

Mehltreter, K., 2010. Interactions of ferns with fungi and animals. In: Mehltreter, K., Walker, L. R., Sharper, J. M. (Eds.), Fern ecology. Cambridge University Press, Cambridge, UK, pp. 220–254. [5]

Menkis, A., Vasiliauskas, R., Taylor, A. F. S., Stenlid, J., Finlay, R., 2005. Fungal communities in mycorrhizal roots of conifer seedlings in forest nurseries under different cultivation systems, assessed by morphotyping, direct sequencing and mycelial isolation. Mycorrhiza 16, 13–41. [4]

Merlotti, S., Kurzawe, F., 2006. Estudo taxonômico do gênero *Australoxylon* Marguerier 1973 com a descricão de A. *catarinensis* sp. no. para o Permiano inferior, bacia do Paraná, Brasil. Revista Brasileira de Paleontologia 9, 73–81. [in Portuguese] [6]

Meschinelli, A., 1898. Fungorum Fossilium Omnium Hucusque Cognitorum Iconographia 31 Tabulis Exornata, Volumen Unicum. Typis Aloysii Fabris, Venice, Italy. 144 pp. [9]

Meyer-Berthaud, B., Taylor, T. N., 1991. A probable conifer with podocarpacean affinities from the Triassic of Antarctica. Review of Palaeobotany and Palynology 67, 179–198. [4]

Meyer-Berthaud, B., Taylor, T. N., 1992. Permineralized conifer axes from the Triassic of Antarctica. Courier Forschungsinstitut Senckenberg 147, 191–197. [4]

Meyer-Berthaud, B., Taylor, T. N., Taylor, E. L., 1992. Reconstructing the Gondwana seed fern

Dicroidium: Evidence from the Triassic of Antarctica. Geobios 25, 341–344. [1]

Meyer-Berthaud, B., Wendt, J., Galtier, J., 1997. First record of a large *Callixylon* trunk from the late Devonian of Gondwana. Geological Magazine 134, 847–853. [1]

Millay, M., Taylor, T. N., 1978. Chytrid-like Fossils of Pennsylvanian Age. Science 200, 1147–1149. [1]

Millay, M. A., Taylor, T. N., Taylor, E. L., 1987. Phi thickenings in fossil seed plants from Antarctica. IAWA Bulletin 8, 191–201. [4]

Millay, M. A., Taylor, T. N., Taylor, E. L., 1992. Reconstructing the Gondwana seed fern *Dicroidium*: Evidence from the Triassic of Antarctica. Geobios 25, 341–344. [1]

Miller, C. N., Jr., 1971. Evolution of the fern family Osmundaceae based on anatomical studies. Contributions from the Museum of Paleontology, University of Michigan 23, 105–169. [5]

Miller, M. F., Isbell, J. L., 2010. Reconstruction of a high-latitude, postglacial lake: Mackellar Formation (Permian), Transantarctic Mountains. Geological Society of America Special Papers 468, 193–207. [1]

Miransari, M., 2010. Contribution of arbuscular mycorrhizal symbiosis to plant growth under different types of soil stress. Plant Biology 12, 563–569. [4]

Molina, R., Massicotte, H., Trappe, J. M., 1992. Specificity phenomena in mycorrhizal symbioses: Community-ecological consequences and practical implications. In: Allen, M. (Ed.), Mycorrhizal Functioning: An Integrative Plant-Fungal Process. Routledge, Chapman, & Hall Inc., New York, NY, pp. 357–423. [4]

Montgomary, R. A. P., 1982. The role of polysaccharidease enzymes in the decay of wood by basidiomycetes. In: Frankland, J. C., Hedger, J. N., Swift, M. J. (Eds.), Decomposer Basidiomycetes. Cambridge University Press, Cambridge, UK, pp. 51–61. [6]

Morton, J. B., 1988. Taxonomy of VA mycorrhizal fungi: Classification, nomenclature and identification. Mycotaxon 32, 267–324. [3]

Morton, J. B., Benny, G. L., 1990. Revised classification of arbuscular mycorrhizal fungi (Zygomycetes): A new order, Glomales, two new suborders, Glomineae and Gigasporineae, and two new families, Acaulosporaceae and Gigasporaceae, with an emendation of Glomeraceae. Mycotaxon 37, 471–491. [4]

Morton, J. B., Redecker, D., 2001. Two new families of Glomales, Archaeosporaceae and Paraglomeraceae, with two new genera *Archaeospora* and *Paraglomus*, based on concordant molecular and morphological characters. Mycologia 93, 181–195. [4]

Muehlbauer, J., LeRoy, C., Lovett, J., Flaccus, K., Vlieg, J., Marks, J., 2009. Short-term responses of decomposers to flow restoration in Fossil Creek, Arizona, USA. Hydrobiologia 618, 35–45. [9]

Müller, E., Schneller, J. J., 1977. A new record of *Synchytrium athyrii* on *Athyrium filixfemina*. Fern Gazette 11, 313–314. [5]

Müller-Stoll, W. R., 1936. Pilzzerstörungen an einem jurassischen Koniferenholz. Paläontologische Zeitschrift 18, 202–212. [in German] [7]

Mussa, D., 1978. On the anatomy of wood showing affinities with the genus *Vertebraria* Royle from the Irati Formation, State of São Paulo, Brazil. Boletim, Instituto de Geociências, Universidade de São Paulo (IG-USP) 9, 153–201. [6]

Muthukumar, T., Senthilkumar, M., Rajangam, M., Udaiyan, K., 2006. Arbuscular mycorrhizal morphology and dark septate fungal associations in medicinal and aromatic plants of Western Ghats, Southern India. Mycorrhiza 17, 11–24. [3]

Myers, B., Webster, K. L., McLaughlin, J. W., Basiliko, N., 2012. Microbial activity across boreal peatland nutrient gradient: The role of fungi and bacteria. Wetlands Ecology and Management 20, 77–88. [4]

Nadal, M., García-Pedrajas, M. A. D., Gold, S. E., 2008. Dimorphism in fungal plant pathogens. F.E.M.S. Microbiology Letters 284, 127–134. [5]

Nasdala, L., Beyssac, O., Schopf, J. W., Bleisteiner, B., 2012. Application of Raman-based images in the Earth sciences. In: Raman Imaging Techniques and Applications. Springer Berlin Heidelberg, pp. 145–187. [2]

Nawrath, C., 2006. Unraveling the complex network of cuticular structure and function. Current Opinions in Plant Biology 9, 281–287. [8]

Neish, P. G., Drinnan, A. N., Cantrill, D. J., 1993. Structure and ontogeny of *Vertebraria* from silicified Permian sediments in East Antarctica. Review of Palaeobotany and Palynology 79, 221–224. [3]

Newsham, K. K., Upson, R., Read, D. J., 2009. Mycorrhizas and dark septate root endophytes in polar regions. Fungal Ecology 2, 10–20. [3]

Nishida, M., Adachi, M., Abe, H., 1977. A petrified wood from the so-called Paleozoic strata in northern region of Sekigahara, Gifu Prefecture. Journal of Japanese Botany 52, 33–38. [7]

Nishida, M., Ohsawa, T., Nishida, H., 1990. Anatomy and affinities of the petrified plants from the Tertiary of Chile (VI). The Botanical Magazine, Tokyo 103, 255–268. [7]

Noldt, G., Bauch, J., Koch, G., 2004. Structure of the fine roots of *Metasequoia glyptostroboides* Hu et Cheng and its adaptability to various sites. Journal of Applied Botany and Food Quality 78, 178–184. [3]

Oehl, F., Sieverding, E., 2004. *Pacispora*, a new vesicular arbuscular mycorrhizal fungal genus in the Glomeromycetes. Journal of Applied Botany 78, 72–82. [4]

Oehl, F., Silva, G. A. D., Goto, B. T., Sieverding, E., 2011. *Glomeromycota*: Three new genera and glomoid species reorganized. Mycotaxon 116, 75–120. [3, 5]

Ofong, A. U., Pearce, R. B., 1994. Suberin degradation by *Rosellinia desmazieresii*. European Journal of Forest Pathology 24, 316–322. [7]

Ogura, Y., 1960. Tyloses in tracheids in *Araucarioxylon*. Journal of the Faculty of Science University of Tokyo, Section 3, 7, 501–509. [7]

Olcott, A. N., 2005. Biomarker evidence for photosynthesis during neoproterozoic glaciation. Science 310, 471–474. [2]

Olcott Marshall, A., Marshall, C. P., 2015. Vibrational spectroscopy of fossils. Palaeontology 58, 201–211. [2]

Onguene, N. A., Kuyper, T. W., 2001. Mycorrhizal associations in the rain forest of South Cameroon. Forest Ecology and Management 140, 277–287. [4]

Öpik, M., Moora, M., Zobel, M., Saks, Ü., Wheatley, R., Wright, F., Daniell, T., 2008. High diversity of arbuscular mycorrhizal fungi in a boreal herb-rich coniferous forest. New Phytologist 179, 867–876. [4]

Orcutt, D. M., Nilsen, E. T., 2000. The Physiology of Plant Under Stress, Volume 2: Soil and Biotic Factors. John Wiley and Sons, New York, NY, 696 pp. [3]

Osborn, J. M., Taylor, T. N., 1989. *Palaeofibulus* gen. nov., a clamp-bearing fungus from the Triassic of Antarctica. Mycologia 81, 622–626. [1, 4]

Osborne, C. P., Royer, D. L., Beerling, D. J., 2004. Adaptive role of leaf habit in extinct polar forests. International Forestry Review 6, 181–186. [4]

Osono, T., 2008. Endophytic and epiphytic phyllosphere fungi of *Camellia japonica*: seasonal and leaf age-dependent variations. Mycologia 100, 387–391. [8]

Otto, A., Simoneit, B. R. T., Rember, W. C., 2005. Conifer and angiosperm biomarkers in clay sediments and fossil plants from the Miocene Clarkia Formation, Idaho, USA. Organic Geochemistry 36, 907–922. [6]

Pálfy, J., Kocsis, Á. T., 2014. Volcanism of the Central Atlantic magmatic province as the trigger of environmental and biotic changes around the Triassic-Jurassic boundary. Geological Society of America Special Papers 505, 245–261. [1]

Pallardy, S. G., 2008. Physiology of Woody Plants, Third Edition. Academic Press, Burlington, MA. 464 pp. [7]

Pandey, K. K., Pitman, A. J., 2003. FTIR studies of the changes in wood chemistry following decay by brown-rot and white-rot fungi. International Biodeterioration & Biodegradation 52, 151–160. [2, 6]

Pandey, K. K., Pitman, A. J., 2004. Examination of the lignin content in a softwood and a hardwood decayed by a brown-rot fungus with the acetyl bromide method and Fourier transform infrared spectroscopy. Journal of Polymer Science, Part A 42, 2340–2346. [6]

Pant, D. D., Singh, R. S., 1974. On the stem and attachment of *Glossopteris* and *Gangamopteris* leaves. Part II.—Structural features. Palaeontographica 147B, 42–73. [8]

Pant, D. D., Singh, V. K., 1987. Xylotomy of some woods from Raniganj Formation (Permian), Raniganj Coalfield, India. Palaeontographica B 203, 1–82. [6]

Patterson, D. J. 1999. The Diversity of Eukaryotes. American Naturalist 154, S96–S124. [1]

Pearce, R. B., 1989. Cell wall alterations and antimicrobial defense in perennial plants. In: Lewis, N.G., Paice, M.G. (Eds.), Plant Cell Wall Polymers. American Chemical Society Symposium Series No. 339, Washington, DC, pp. 346–360. [6]

Pearce, R. B., 1996. Antimicrobial defences in the wood of living trees. New Phytologist 132, 203–233. [1, 6, 7]

Peters, K. E., Walters, C. C., Moldowan, J. M., 2007. The biomarker guide. Volume 1: Biomarkers and isotopes in the environment and human history. Second Edition. Cambridge University Press, Cambridge, UK, 492 pp. [6]

Peterson, R. L., Farquhar, M. L., 1994. Mycorrhizas: Integrated development between roots and fungi. Mycologia 86, 311–326. [3, 4]

Peterson, R. L., Massicotte, H. B., Melville, L. H., 2004. Mycorrhizas: Anatomy and Cell Biology. NRC Research Press / CABI Publishing, Ottawa, Canada, 173 pp. [4]

Petrini, O., 1991. Fungal endophytes of tree leaves. In: Andrews J. H., Hirano S. S. (Eds.) Microbial ecology of leaves. Springer Verlag, New York. p 179–197. [8]

Philippe, M., 2011., How many species of *Araucarioxylon*? Competes Rendus Palevol 10, 201–208. [3, 6]

Philippe, M., Zijlstra, G., Barbacka, M., 1999. Greguss's morphogenera of homoxylous fossil woods: A taxonomic and nomenclatural review. Taxon 48, 667–676. [6]

Phillips, T. L., Galtier, J., 2005. Evolutionary and ecological perspectives of late Paleozoic ferns, Part I. Zygopteridales. Review of Palaeobotany and Palynology 135, 165–203. [7]

Phillips, T. L., Galtier, J., 2011. Evolutionary and ecological perspectives of late Paleozoic ferns, Part II. The genus *Ankyropteris* and the Tedeleaceae. Review of Palaeobotany and Palynology 164, 1–29. [7]

Phipps, C. J., Taylor, T. N., 1996. Mixed arbuscular mycorrhizae from the Triassic of Antarctica. Mycologia 88, 707–714. [1, 3, 4]

Phipps, C. J., Taylor, T. N., Taylor, E. L., Cúneo, N. R., Boucher, L. D., Yao, X., 1998. *Osmunda* (Osmundaceae) from the Triassic of Antarctica: An example of evolutionary

stasis. American Journal of Botany 85, 888–895. [1]

Phipps, C. J., Axsmith, B. J., Taylor, T. N., Taylor, E. L., 2000. *Gleichenipteris antarcticus* gen. et sp. nov. from the Triassic of Antarctica. Review of Palaeobotany and Palynology 108, 75–83. [1]

Phipps, C. J., 2001. The evolution of epiphyllous fungal communities with an emphasis on the Miocene of Idaho, Ph.D. Dissertation. University of Kansas, Lawrence, KS. 151 pp. [8]

Phipps, C. J., 2007. *Entopeltacites remberi* sp. nov. from the Miocene of Clarkia, Idaho, USA. Review of Palaeobotany and Palynology 145, 193–200. [8]

Phipps, C. J., Rember, W. C., 2004. Epiphyllous fungi from the Miocene of Clarkia, Idaho: Reproductive structures. Review of Palaeobotany and Palynology 129, 67–79. [8]

Pickard, M. A., Roman, R., Tinoco, R., Vazquez-Duhalt, R., 1999. Polycyclic Aromatic Hydrocarbon Metabolism by White Rot Fungi and Oxidation by *Coriolopsis gallica* UAMH 8260 Laccase. Applied Environmental Microbiology 65, 3805–3809. [6]

Pigg, K., 1990. Anatomically preserved *Dicroidium* foliage from the central Transantarctic Mountains. Review of Palaeobotany and Palynology 66, 129–145. [2, 9]

Pigg, K. B., 1990. Anatomically preserved *Glossopteris* foliage from the central Transantarctic Mountains. Review of Palaeobotany and Palynology 66, 105–127. [8]

Pigg, K. B., Taylor, T. N., 1990. Permineralized *Glossopteris* and *Dicroidium* from Antarctica. In: Taylor, T. N., Taylor, E. L. (Eds.), Antarctic Paleobiology: Its Role in the Reconstruction of Gondwana. Springer-Verlag, New York, NY, pp. 164–172. [1, 8]

Pigg, K. B., Taylor, T. N., 1993. Anatomically preserved *Glossopteris* stems with attached leaves from the central Transantarctic Mountains, Antarctica. American Journal of Botany 80, 500–516. [3, 6]

Pigg, K. P., Rothwell, G. W., 2000. Anatomically preserved *Woodwardia virginica*

(Blechnaceae) and a new filicalean fern from the middle Miocene Yakima Canyon flora of central Washington, USA. American Journal of Botany 88, 777–787. [1]

Pigg, K. P., DeVore, M. L., 2004. *Shirleya grahamae* gen. et sp. nov. (Lythraceae), *Lagerstroemia*-like fruits from the middle Miocene Yakima Canyon flora, central Washington State, USA. American Journal of Botany 92, 242–251. [1]

Pigg, K. B., Nishida, H., 2006. The significance of silicified plant remains to the understanding of *Glossopteris*-bearing plants: an historical review. The Journal of the Torrey Botanical Society 133, 46–61. [8]

Pirozynski, K. A., 1976. Fossil Fungi. Annual Review of Phytopathology 14, 237–246. [1, 9]

Pirozynski, K. A., Malloch, D. W., 1975. The origin of land plants: A matter of mycotrophism. Biosystems 6, 153–164. [1, 3, 4]

Pirozynski, K. A., Dalpé, Y., 1989. Geological history of the Glomaceae with particular reference to mycorrhizal symbiosis. Symbiosis 7, 1–36. [4]

Plumstead, E. P., 1962. Fossil floras from Antarctica. In: Scientific Reports (Trans-Antarctic Expedition 1955–1958) 9 (Geology). London: The Trans-Antarctic Expedition Committee, 154 pp. [1]

Plumstead, E. P., 1964. Palaeobotany of Antarctica. In: Adie, R. J. (Ed.), Antarctic Geology: Proceedings of the First International Symposium on Antarctic Geology, Cape Town, 16–21 September 1963. North-Holland Publishing Company, Amsterdam, The Netherlands, pp. 637–680. [1]

Plumstead, E. P., 1975. A new assemblage of fossil plants from the Milorgfjella, Dronning Maud Land. British Antarctic Survey Scientific Reports 83, 1–30. [1]

Poinar, G. O., Singer, R., 1990. Upper Eocene gilled mushroom from the Dominican Republic. Science 248, 1099. [7]

Poole, I., Cantrill, D., 2001. Fossil woods from Williams Point beds, Livingston Island, Antarctica: A Late Cretaceous southern high latitude flora. Palaeontology 44, 1081–1112. [7]

Poole, I., Francis, J. E., 1999. The first record of fossil atherospermataceous wood from the Upper Cretaceous of Antarctica. Review of Palaeobotany and Palynology 107, 97–107. [7]

Pott, C., 2014. The Upper Triassic flora of Svalbard. Acta Palaeontologica Polonica 59, 709–740. [1]

Poynter, J. G., Farrimond, P., Robinson, N., Eglinton, G., 1989. Aeolian-derived higher plant lipids in the marine sedimentary record: Links with palaeoclimate. In: Leinen, M., Sarnthein, M. (Eds.), Paleoclimatology and Paleometeorology: Modern and Past Patterns of Global Atmospheric Transport, NATO ASI Series Volume 282. Springer, Netherlands, Dordrecht, pp. 435–462. [6]

Prasad, M. N. V., 1982. An annotated synopsis of Indian Palaeozoic gymnospermous woods. Review of Palaeobotany and Palynology 38, 119–156. [6]

Preat, A., Mamet, B., De Ridder, C., Boulvain, F., Gillan, D., 2000. Iron bacterial and fungal mats, Bajocian stratotype (Mid-Jurassic, northern Normandy, France). Sedimentary Geology 137, 107–126. [7]

Preston, L. J., Genge, M. J., 2010. The Rhynie Chert, Scotland, and the Search for Life on Mars. Astrobiology 10, 549–560. [6]

Preto, N., Kustatscher, E., Wagnall, P. B., 2010. Triassic climates – state of the art and perspectives. Palaeogeography, Palaeoclimatology, Palaeoecology 147, 121–139. [1]

Privé-Gill, C., Thomas, H., Lebret, P., 1999. Fossil wood of *Sindora* (Leguminosae, Caesalpiniaceae) from the Oligo-Miocene of Saudi Arabia: Paleobiogeographical

considerations. Review of Palaeobotany and Palynology 107, 191–199. [7]

Pujana, R. R., García Massini, J. L., Brizuela, R. R., Burrieza, H. P., 2009. Evidence of fungal activity in silicified gymnosperm wood from the Eocene of southern Patagonia (Argentina). Geobios 42, 639–647. [6]

Oliver, R. P., Soloman, P. S., 2008. Recent fungal diseases of crop plants: Is lateral gene transfer a common theme? Molecular Plant-Microbe Interactions 21, 287–293. [1]

Osborn, J. M., Taylor, T. N., 1989. Structurally preserved sphenophytes from the Triassic of Antarctica: Vegetative remains of *Spaciinodum* gen. nov. American Journal of Botany 76, 1594–1601. [1]

Ozerskaya, S., Kochkina, G., Ivanushkina, N., Gilichinsky, D. A., 2009. Fungi in permafrost. In: Margesin, R. (Ed.), Permafrost Soils, Soil Biology 16. Springer Berlin Heidelberg, Berlin, Germany, pp. 85–95. [1]

Raven, J. A., 1977. The Evolution of Vascular Land Plants in Relation to Supracellular Transport Processes. Advances in Botanical Research 5, 153–219. [1]

Rayner, A. D. M., Boddy, L., 1988. Fungal decomposition of wood: Its biology and ecology. John Wiley & Sons, Chichester, UK, 602 pp. [6]

Redecker, D., Raab, P., 2006. Phylogeny of the Glomeromycota (arbuscular mycorrhizal fungi): Recent developments and new gene markers. Mycologia 98, 885–895. [3]

Rees, P. M., Cleal, C. J., 2004. Lower Jurassic floras from Hope Bay and Botany Bay, Antarctica. Special Papers in Palaeontology 72, 1–96. [1]

Remy, W., Taylor, T. N., Hass, H., 1994. Early Devonian fungi: A blastocladalean fungus with sexual reproduction. American Journal of Botany 81, 690–702. [9]

Remy, W., Taylor, T. N., Hass, H., Kerp, H., 1994a. Four hundred-million-year-old vesicular arbuscular mycorrhizae. Proceedings of the National Academy of Sciences of the United

States of America 91, 11841–11843. [3, 4]

Remy, W., Kerp, H., Hass, H., Taylor, T. N., 1996. The veterans of the Scottish Rhynie chert: Revelations from 400-million-year-old fungi. German Research 96, 16–17. [1]

Renault, B., 1894. Sur quelques nouveaux parasites des *Lépidodendrons*. Société d'histoire naturelle d'Autun Procès-Verbauzdes Séances 1893, 168–178. [in French] [2]

Renault, B., 1896. Recherches sur les Bactériacées fossiles. Annales des Science Naturelles, Botanique, Série 8, 275–349. [in French] [1]

Rice, C. M., Trewin, N., Anderson, L. I., 2002. Geological setting of the Early Devonian Rhynie cherts, Aberdeenshire, Scotland: An early terrestrial hot spring system. Journal of the Geological Society, London 159, 203–214. [1]

Rigby, J. F., 1969. Permian sphenopsids from Antarctica. United States Geological Survey Professional Paper 613F, 1–13. [1]

Riley, R., Salamov, A. A., Brown, D. W., Nagy, L. G., Floudas, D., Held, B. W., Levasseur, A., Lombard, V., Morin, E., Otillar, R., Linquist, E. A., Sun, H., LaButti, K. M., Schmutz, J., Jabbour, D., Luo, H., Baker, S. E., Pisabarro, A. G., Walton, J. D., Blanchette, R. A., Henrissat, B., Martin, F., Cullen, D., Hibbett, D. S., Grigoriev, I. V., 2014. Extensive sampling of basidiomycete genomes demonstrates inadequacy of the white-rot/brown-rot paradigm for wood decay fungi. Proceedings of the National Academies of the United States 111, 9923–9928. [6]

Riley, T. R., Curtis, M. L., Leat, P. T., Watkeys, M. K., Duncan, R. A., Millar, L., Owens, R. H., 2006. Overlap of Karoo and Ferrar magma types in KwaZulu-Natal, South Africa. Journal of Petrology 47, 541–566. [1]

Rillig, M. C., Mummey, D. L., 2006. Mycorrhizas and soil structure. New Phytologist 171, 41–53. [4]

Rössler, R., 2000. The late Palaeozoic tree fern *Psaronius*—an ecosystem unto itself. Review of Palaeobotany and Palynology 108, 55–74. [1, 5]

Rössler, R., 2006. Two remarkable Permian petrified forests: Correlation, comparison and significance. In: Lucas, S.G., Cassinis, G., Scheider, J.W. (Eds.), Non-Marine Permian Biostratigraphy and Biochronology. Geological Society, London, Special Publications, 265, 39–63. [1]

Rössler, R., Philippe, M., van Konijnenburg-van Cittert, J. H. A., McLoughlin, S., Sakala, J., Zijlstra, G., 2014. Which name(s) should be used for Araucaria-like fossil wood?—Results of a poll. Taxon 63, 177–184. [3]

Rothwell, G. W., Basinger, J. F., 1979. *Metasequoia milleri* n. sp., anatomically preserved pollen cones from the Middle Eocene (Allenby Formation) of British Columbia. Canadian Journal of Botany 75, 958–970. [3]

Rothwell, G. W., Taylor, E. L., Taylor, T. N., 2002. *Ashicaulis woolfei* n. sp.: Additional evidence for the antiquity of osmundaceous ferns from the Triassic of Antarctica. American Journal of Botany 89, 352–361. [1, 5]

Rothwell, G. W., Mapes, G., Hernandez-Castillo, G. R., 2005. *Hanskerpia* gen. nov. and phylogenetic relationships among the most ancient conifers (Voltziales). Taxon 54, 733–750. [4]

Ruhl, M., Kürschner, W. M., 2011. Multiple phases of carbon cycle disturbance from large igneous province formation at the Triassic-Jurassic transition. Geology 39, 431–434. [1]

Russell, A. J., Bidartondo, M. I., Butterfield, B. G., 2002. The root nodules of the Podocarpaceae harbour arbuscular mycorrhizal fungi. New Phytologist 156, 283–295. [4]

Ryberg, P. E., 2009. Reproductive diversity of Antarctic glossopterid seed-ferns. Review of Palaeobotany and Palynology 158, 167–179. [1, 3]

Ryberg, P. E., Taylor, E. L., Taylor, T. N., 2012a. The First Permineralized Microsporophyll of the Glossopteridales: *Eretmonia macloughlinii* sp. nov. International Journal of Plant Sciences 173, 812–822. [1]

Ryberg, P. E., Taylor, E. L., Taylor, T. N., 2012b. Antarctic glossopterid diversity on a local scale: The presence of multiple megasporophyll genera, Upper Permian, Mt. Achernar, Transantarctic Mountains, Antarctica. American Journal of Botany 99, 1531–1540. [3]

Sabine, C. L., Heiman, M., Artaxo, P., Bakker, D., Chen, C. -T. A., Field, C.B., Gruber, N., LeQuéré, C., Prinn, R. G., Richey, J. E., Lankao, P. R., Sathaye, J., Valentini, R., 2004. Current status and past trends of the carbon cycle. In: Field, C. B., Raupach, M. R. (Eds.), The Global Carbon Cycle: Integrating Humans, Climate, and the Natural World. Island Press, Washington, DC, pp. 17–44. [6]

Sack, U., Günther, T., 1993. Metabolism of PAH by fungi and correlation with extracellular enzymatic activities. Journal of Basic Microbiology 33, 269–277. [6]

Sahni, B., 1923. On the structure of the cuticle in *Glossopteris angustifolia* Brongn. Records of the Geological Survey of India 54, 277–280. [8]

Saupe, E. E., Selden, P. A., 2009. First fossil Mecysmaucheniidae (Arachnida, Chelicerata, Araneae), from Lower Cretaceous (uppermost Albian) amber of Charente-Maritime, France. Geodiversitas 31, 49–60. [4]

Scheckler, S. E., Galtier, J., 2003. Tyloses and ecophysiology of the Early Carboniferous progymnosperm tree *Protopitys buchiana*. Annals of Botany 91, 739–747. [7]

Scervino, J. M., Gottlieb, A., Silvani, V. A., Pérgola, M., Fernández, L., Godeas, A. M., 2009. Exudates of dark septate endophyte (DSE) modulate the development of the arbuscular mycorrhizal fungus (AMF) *Gigaspora rosea*. Soil Biology and Biochemistry 41, 1753–1756. [5]

Schmid, E., Oberwinkler, F., 1995. A light- and electron-microscopic study on vesicular-arbuscular host-fungus interaction in gametophytes and young sporophytes of the Gleicheniaceae (Filicales). New Phytologist 129, 317–324. [5]

Schmidt, O., 2006. Wood and Tree Fungi. Springer-Verlag, Berlin-Heidelberg, Germany, 346 pp. [6, 7]

Schoch, C. L., Sung, G. H., Lopez-Giraldez, F., Townsend, J. P., Miadlikowska, J., Hofstetter, V., Robbertse, B., Matheny, P. B., Kauff, F., Wang, Z., Gueidan, C., Andrie, R. M., Trippe, K., Ciufetti, L. M., Wynns, A., Fraker, E., Hodkinson, B. P., Bonito, G., Groenewald, J. Z., Arzanlou, M., Sybren de Hoog, G., Crous, P. W., Hewitt, D., Pfister, D. H., Peterson, K., Gryzenhout, M., Wingfield, M. J., Aptroot, A., Suh, S. O., Blackwell, M., Hillis, D. M., Griffith, G. W., Castlebury, L. A., Rossman, A. Y., Lumbsch, H. T., Lucking, R., Budel, B., Rauhut, A., Diederich, P., Ertz, D., Geiser, D. M., Hosaka, K., Inderbitzin, P., Kohlmeyer, J., Volkmann-Kohlmeyer, B., Mostert, L., O'Donnell, K., Sipman, H., Rogers, J. D., Shoemaker, R. A., Sugiyama, J., Summerbell, R. C., Untereiner, W., Johnston, P. R., Stenroos, S., Zuccaro, A., Dyer, P. S., Crittenden, P. D., Cole, M. S., Hansen, K., Trappe, J. M., Yahr, R., Lutzoni, F., Spatafora, J. W., 2009. The Ascomycota Tree of Life: A Phylum-wide Phylogeny Clarifies the Origin and Evolution of Fundamental Reproductive and Ecological Traits. Systematic Biology 58, 224–239. [9]

Schopf, J. M., 1970. Petrified peat from a Permian coal bed in Antarctica. Science 169, 274–277. [1, 3, 8]

Schopf, J. M., 1971. Notes on plant tissue preservation and mineralization in a Permian deposit of peat from Antarctica. American Journal of Science 271, 522–543. [2, 6]

Schopf, J. M. 1975. Modes of fossil preservation. Review of Palaeobotany and Palynology 20, 27–53. [1, 2]

Schopf, J. M., 1976. Morphological interpretation of fertile structures in glossopterid gymnosperms. Review of Palaeobotany and Palynology 21, 25–64. [1]

Schopf, J. M., 1978. An unusual osmundaceous specimen from Antarctica. Canadian Journal of Botany 56, 3038–3095. [1, 5]

Schopf, J. M., 1982. Forms and facies of *Vertebraria* in relation to Gondwana coal. American Geophysical Union, Antarctic Research Series 36, 37–62. [6]

Schüssler, A., 2002. Molecular phylogeny, taxonomy, and evolution of *Geosiphon pyriformis* and arbuscular mycorrhizal fungi. Plant and Soil 244, 75–83. [4]

Schüssler, A., Walker, C. (Eds.), 2010. The Glomeromycota. A species list with new families and new genera. The Royal Botanic Garden Edinburgh, The Royal Botanic Garden Kew, Botanische Staatssammlung Munich, and Oregon State University. Electronic edition updated 2011, retrieved from www.amf-phylogeny.com ; species list updated 2013, retrieved from http://schuessler.userweb.mwn.de/amphylo/. [4]

Schüssler, A., Walker, C., 2011., Evolution of the “Plant-symbiotic” fungal phylum, *Glomeromycota*. In: Poggeler, S., Wostemeyer, J. (Eds.), The Mycota XIV. Springer-Verlag Berlin Heidelberg, pp. 163–185. [3]

Schützendübel, A., Majcherczyk, A., Johannes, C., Hüttermann, A., 1999. Degradation of fluorene, anthracene, phenanthrene, fluoranthene, and pyrene lacks connection to the production of extracellular enzymes by *Pleurotus ostreatus* and *Bjerkandera adusta*. International Biodeterioration and Biodegradation 43, 93–100. [6]

Schwarze, F. W. M. R., 2007. Wood decay under the microscope. Fungal Biology Reviews 21, 133–170. [7]

Schwarze, F. W. M. R., Engels, J., 1998. Cavity Formation and the Exposure of Peculiar Structures in the Secondary Wall (S_2) of Tracheids and Fibres by Wood Degrading Basidiomycetes. Holzforschung 52, 117–132. [6]

Schwarze, F. W. M. R., Engels, J., Mattheck, C., Linnard, W., 2000. Fungal strategies of wood decay in trees. Springer-Verlag, Berlin, Heidelberg, New York, NY. 185 pp. [1, 6, 7]

Schwarzott, D., Walker, C., Schüssler, A., 2001. Glomus, the Largest Genus of the Arbuscular Mycorrhizal Fungi (Glomales), Is Nonmonophyletic. Molecular Phylogenetics and Evolution 21, 190–197. [3, 9]

Schwendemann, A. B., Taylor, T. N., Taylor, E. L., Serbet, R., Hermsen, E. J., 2007. Permineralized plants from the Jurassic of Antarctica (abstract). Botany and Plant Biology 2007 Joint Congress Program and Abstract Book, p. 210. [1]

Schwendemann, A. B., Taylor, T. N., Taylor, E. L., Krings, M., Dotzler, N., 2009. *Combresomyces cornifer* from the Triassic of Antarctica: Evolutionary stasis in the Peronosporomycetes. Review of Palaeobotany and Palynology 154, 1–5. [1, 8]

Schwendemann, A. B., Decombeix, A. -L., Taylor, E. L., Taylor, T. N., 2010a. *Collinsonites schopfi* gen. et sp. nov., a herbaceous lycopsid from the Upper Permian of Antarctica. Review of Paleobotany and Palynology 158, 291–297. [1]

Schwendemann, A. B., Taylor, T. N., Taylor, E. L., Krings, M., 2010b. Organization, anatomy, and fungal endophytes of a Triassic conifer embryo. American Journal of Botany 97, 1873–1883. [1, 8]

Schwendemann, A. B., Decombeix, A. -L., Taylor, T. N., Taylor, E. L., Krings, M., 2011. Morphological and functional stasis in mycorrhizal root nodules as exhibited by a Triassic conifer. Proceedings of the National Academy of Sciences of the United States of America 108, 13630–13634. [1, 3, 4]

Schwendemann, A. B., 2012. Paleophysiology of Permian and Triassic Seed Plants. Ph.D. Dissertation. University of Kansas, Lawrence, KS. 290 pp. [8]

Scott, A. C., 1992. Trace fossils of plant-arthropod interactions. In: Maples, C. G., West, R. R. (Eds.), Trace Fossils. Short Courses in Paleontology. Society, University of Tennessee, Knoxville, TN, pp. 197–222. [6]

Scott, A. C., Taylor, T. N., 1983. Plant animal interactions during the Upper Carboniferous. Botanical Review 49, 259–307. [6]

Scott, A. C., Rex, G., 1985. The formation and significance of Carboniferous Coal Balls. Philosophical Transactions of the Royal Society of London, Series B 311, 123–137. [1, 2]

Scott, A. C., Stephenson, J., Chaloner, W. G., 1985. Evidence of pteridophytes-arthropod interactions in the fossil record. Proceedings of the Royal Society of Edinburgh, Series B 86, 133–140. [6]

Scott, A. C., Mattey, D. P., Howard, R., 1996. New data on the formation of Carboniferous coal balls. Review of Palaeobotany and Palynology 93, 317–331. [2]

Scott, R., 1911. On *Traquairia*. Annals of Botany 25, 459–467. [9]

Selkirk, D. R., 1972. Fossil *Manginula*-like fungi and their classification. Proceedings of the Linnaean Society of New South Wales 97, 141–149. [8]

Selosse, M. A., Le Tacon, F., 1998. The land flora: A phototroph–fungus partnership? TRENDS in Ecology and Evolutionary Biology 13, 15–20. [1, 3]

Sengupta, A., Chaudhuri, S., 2002. Arbuscular mycorrhizal relations of mangrove plant community at the Ganges river estuary in India. Mycorrhiza 12, 169–174. [3]

Shigo, A. L., 1970. An expanded concept of decay in living trees. Laval University Bulletin 13, 7–9. [6]

Shigo, A. L., 1976. Compartmentalization of discolored and decayed wood in trees. Material und Organismen 3, 221–226. [6]

Shigo, A. L., 1984. Compartmentalization: A conceptual framework for understanding how trees grow and defend themselves. Annual Review of Phytopathology 22, 189–214. [6, 7]

Siddiqui, Z. A., Pichtel, J., 2008. Mycorrhizae: An overview. In: Siddiqui, Z. A., Akhtar, M. S., Futai, K. (Eds.), Mycorrhizae: Sustainable Agriculture and Forestry. Springer Science and Business Media B. V., pp. 1–35. [5]

Sidor, C. A., Damiani, R., Hammer, W. R., 2008. A new Triassic temnospondyl from Antarctica and a review of Fremouw Formation biostratigraphy. Journal of Vertebrate Paleontology 28, 656–663. [4]

Silliman, J. E., Meyers, P. A., Eadie, B. J., 1998. Perylene: An indicator of alteration processes or precursor materials? Organic Geochemistry 29, 1737–1744. [6]

Simard, S. W., Durall, D. M., 2004. Mycorrhizal networks: A review of their extent, function, and importance. Canadian Journal of Botany 82, 1140–1165. [4]

Simon, L., Bousquet, J., Levesque, R. C., Lalonde, M., 1993. Origin and diversification of endomycorrhizal fungi and coincidence with vascular land plants. Nature 363, 67–68. [3]

Sjamsuridzal, W., Nishida, H., Ogawa, H., Kakishima, M., Sugiyama, J., 1999. Phylogenetic positions of rust fungi parasitic on ferns: evidence from 18S rDNA sequence analysis. Mycoscience 40, 21–27. [5]

Slater, B. J., McLoughlin, S., Hilton, J., 2011. Guadalupian (Middle Permian) megaspores from a permineralised peat in the Bainmedart Coal Measures, Prince Charles Mountains, Antarctica. Review of Palaeobotany and Palynology 167, 140–150. [1]

Slater, B. J., McLoughlin, S., Hilton, J., 2012. Animal–plant interactions in a Middle Permian permineralised peat of the Bainmedart Coal Measures, Prince Charles Mountains,

Antarctica. Palaeogeography, Palaeoclimatology, Palaeoecology 363–364, 109–126. [1, 3, 5, 6]

Slater, B. J., McLoughlin, S., Hilton, J., 2013. Peronosporomycetes (Oomycota) from a Middle Permian Permineralised Peat within the Bainmedart Coal Measures, Prince Charles Mountains, Antarctica. PLoS ONE 8, e70707–9. doi:10.1371/journal.pone.0070707 [1, 8]

Slater, B. J., McLoughlin, S., Hilton, J., 2014. A high-latitude Gondwanan lagerstätte: The Permian permineralised peat biota of the Prince Charles Mountains, Antarctica. Gondwana Research 1–28. [1, 8]

Smart, J., Hughes, N., 1973. The insect and the plant: Progressive palaeoecological integration. In: Van Emden, H. (Ed.), Insect Plant Relationships, No. 6. Royal Entomological Society, London. pp. 143–155. [5]

Smith, F. A., Smith, S. E., 1997. Structural diversity in (vesicular)-arbuscular mycorrhizal symbioses. New Phytologist 137, 373–388. [3]

Smith, S. Y., Stockey, R. A., 2003. Aroid seeds from the Middle Eocene Princeton Chert (*Keratosperma allenbyense*, Araceae): Comparisons with extant Lasioideae. International Journal of Plant Sciences 164, 239–250. [1]

Smith, S., Currah, R., Stockey, R., 2004. Cretaceous and Eocene Poroid Hymenophores from Vancouver Island, British Columbia. Mycologia 96, 180–186. [1]

Smoot, E. L., Taylor, T. N., 1985. Ovules from the Permian of Antarctica. American Journal of Botany 72, 900. [1]

Smoot, E. L., Taylor, T. N., Delevoryas, T., 1985. Structurally preserved fossil plants from Antarctica I. *Antarcticycas* gen. nov., a Triassic cycad stem from the Beardmore Glacier area. American Journal of Botany 72, 1410–1423. [1]

Solheim, H., 1994. A comparison of blue-stain fungi associated with the North-American spruce

beetle *Dendroctonus rugipennis* and the Eurasian spruce bark beetle *Ips typographus*. In: Aamlid, D. (Ed.), Forest Pathology Research in the Nordic Countries 1994, Proceedings from the SNS-meeting in forest pathology at Skogbrukets Kurssenter, Biri, Norway 9.-12. August 1994. Aktuelt fra Skogforsk 4/95: 76 s. pp. 61–67. [7]

Solheim, H. 1995., Early stages of blue-stain fungus invasion of lodgepole pine sapwood following mountain pine beetle attack. Canadian Journal of Botany 73, 70–74. [7]

Song, H., Wignall, P. B., Tong, J., Yin, H., 2013. Two pulses of extinction during the Permian–Triassic crisis. Nature Geoscience 6, 52–56. [1]

Spackman, W., Jr., 1948. A dicotyledonous wood found associated with the Idaho *Tempskyas*. Annals of the Missouri Botanical Garden 35, 107–115. [7]

Spencer, J., 1893. Recreations in fossil botany. (*Sporocarpons* and *Zygosporites*). Hardwicke's Science-Gossip: An Illustrated Medium of Interchange and Gossip for Students and Lovers of Nature 19, 155–158. [9]

Srivastava, P., 2008. Fossil woods resembling *Sonneratia* with fungal infection from Deccan Intertrappean sediments of Seoni District, Madhya Pradesh. Geophytology 37, 87–92. [6]

Stalpers, J. A., 1978. Identification of wood-inhabiting Aphllophorales in pure culture. Studies in Mycology 16, 1–248. [7]

Stevens, K. J., Wellner, M. R., Acevedo, M. F., 2010. Dark septate endophyte and arbuscular mycorrhizal status of vegetation colonizing a bottomland hardwood forest after a 100 year flood. Aquatic Botany 92, 105–111. [3]

Stevens, N. E., 1912. A palm from the Upper Cretaceous of New Jersey. American Journal of Science 34, 421–436. [7]

Stockey, R. A., 1980. Anatomy and morphology of *Araucaria sphaerocarpa* Carruthers from the Jurassic Inferior Oolite of Bruton, Somerset. Botanical Gazette 141, 116–124. [7]

Stockey, R. A., 1994. Mesozoic Araucariaceae: Morphology and systematic relationships. Journal of Plant Research 107, 493–502. [1]

Stockey, R. A., Pigg, K. B., 1991. Flowers and fruits of *Princetonia allenbyensis* (Magnoliopsida; family indet.) from the Middle Eocene Princeton chert of British Columbia. Review of Palaeobotany and Palynology 70, 163–172. [1]

Stockey, R. A., Nishida, H., Rothwell, G. W., 1999. Permineralized ferns from the Middle Eocene Princeton Chert. I. *Makotopteris princetonensis* gen. et sp. nov. (Athyriaceae). International Journal of Plant Sciences 160, 1047–1055. [1]

Stockey, R. A., Rothwell, G. W., Addy, H. D., Currah, R. S., 2001. Mycorrhizal association of the extinct conifer *Metasequoia milleri*. Mycological Research 105, 202–205. [3, 4]

Stokland, J. N., Siitonen, J., Jonsson, B. G., 2012. Biodiversity in Dead Wood. Cambridge University Press, Cambridge, UK, 509 pp. [1, 6]

Stopes, M. C., Watson, D. M. S. 1909. On the present distribution and origin of the calcareous concretions in coal seams, known as "coal ball". Philosophical Transactions of the Royal Society of London, Series B 200, 167–218. [1, 9]

Strullu-Derrien, C., Rioult, J. -P., Strullu, D. -G., 2009. Mycorrhizas in Upper Carboniferous *Radiculites*-type cordaitalean rootlets. New Phytologist 182, 561–564. [1, 3, 4]

Strullu-Derrien, C., McLoughlin, S., Philippe, M., Mørk, A., Strullu, D. G., 2012. Arthropod interactions with bennettitalean roots in a Triassic permineralized peat from Hopen, Svalbard Archipelago (Arctic). Palaeogeography, Palaeoclimatology, Palaeoecology 348/9, 45–58. [1]

Strullu-Derrien, C., Kenrick, P., Pressel, S., Duckett, J. G., Rioult, J. -P., Strullu, D. -G., 2014. Fungal associations in *Horneophyton lignieri* from the Rhynie Chert (*c.* 407 million year

old) closely resemble those in extant lower land plants: Novel insights into ancestral plant–fungus symbioses. New Phytologist 203, 964–979. [4]

Stubblefield, S. P., Taylor, T. N., 1983. Studies of Paleozoic fungi I. The Structure and Organization of *Traquairia* Ascomycota. American Journal of Botany 70, 387–399. [1, 9]

Stubblefield, S. P., Taylor, T. N., 1985. Fossil Fungi in Antarctic wood. Antarctic Journal of the United States 20, 7–8. [1, 6]

Stubblefield, S. P., Taylor, T. N., 1986a. Wood decay in silicified gymnosperms from Antarctica. Botanical Gazette 147, 116–125. [2, 3, 6]

Stubblefield, S. P., Taylor, T. N., 1986b. Wood decay in silicified gymnosperms from the Permian and Triassic of Antarctica (abstract). American Journal of Botany 73, 1–3. [1, 2]

Stubblefield, S. P., Taylor, T. N., Miller, C. E., Cole, G. T., 1983b. Studies of Carboniferous fungi II The Structure and Organization of *Mycocarpon, Sporocarpon, Dubiocarpon*, and *Caleocarpon* (Ascomycotina). American Journal of Botany 70, 1482–1498. [1]

Stubblefield, S. P., Taylor, T. N., Miller, C. E., Cole, G. T., 1984. Studies of Paleozoic fungi. III. Fungal parasitism in a Pennsylvania gymnosperm. American Journal of Botany 71, 1275–1282. [6]

Stubblefield, S. P., Taylor, T. N., Beck, C. B., 1985. Studies of Paleozoic fungi. IV. Wood-decaying fungi in *Callixylon newberryi* from the Upper Devonian. American Journal of Botany 72, 1765–1774. [6, 7]

Stubblefield, S. P., Taylor, T. N., Seymour, R. L., 1987a. A possible endogonaceous fungus from the Triassic of Antarctica. Mycologia 79, 905–906. [1, 9]

Stubblefield, S. P., Taylor, T. N., Trappe, J. M., 1987b. Vesicular-Arbuscular Mycorrhizae from the Triassic of Antarctica. American Journal of Botany 74, 1904–1911. [1, 3, 4]

Stubblefield, S. P., Taylor, T. N., Trappe, J. M., 1987c. Fossil mycorrhizae: A case for

symbiosis. Science 237, 59–60. [1, 3, 4]

Stürmer, S. L., 2012. A history of the taxonomy and systematics of arbuscular mycorrhizal fungi belonging to the phylum Glomeromycota. Mycorrhiza 22, 247–258. [3, 8]

Süss, H., Philippe, M., 1993. Holzanatomische Untersuchungen an einem fossilen Holz, *Circoporoxylon grandiporosum* Müller-Stoll et Schultze-Motel, aus dem Unteren Jura von Frankreich. Feddes Repertorium 104, 451–463. [in German] [7]

Swidrak, I., Schuster, R., Oberhuber, W., 2013. Comparing growth phenology of co-occurring deciduous and evergreen conifers exposed to drought. Flora 208, 609–617. [4]

Takó, M., Csernetic, Á., 2005. Genotypic analysis of variability in zygomycetes. Acta Biologica Hungarica 56, 345–357. [9]

Talbot, J. M., Allison, S. D., Treseder, K. K., 2008. Decomposers in disguise: Mycorrhizal fungi as regulators of soil C dynamics in ecosystems under global change. Functional Ecology 22, 955–963. [1]

Talboys, P. W., 1964. A concept of the host-parasite relationship in *Verticillium* wilt diseases. Nature 361, 361–364. [7]

Tang, A. M. C., Jeewon, R., Hyde, K. D., 2009. A re-evaluation of the evolutionary relationships within the *Xylariaceae* based on ribosomal and protein-coding gene sequences. Fungal Diversity 34, 127–155. [6]

Tawaraya, K., Takaya, Y., Turjaman, M., Tuah, S. J., Limin, S. H., Tamai, Y., Cha, J. Y., Wagatsuma, T., Osaki, M., 2003. Arbuscular mycorrhizal colonization of tree species grown in peat swamp forests of Central Kalimantan, Indonesia. Forest Ecology and Management 182, 381–386. [3]

Taylor , E. L., Taylor, T. N., 1990. Structurally preserved Permian and Triassic floras from Antarctica. In: Taylor, T. N., Taylor, E. L. (Eds.), Antarctic Paleobiology: Its Role in the

Reconstruction of Gondwana. Springer-Verlag, New York, NY, pp. 149–163. [1, 2, 8]

Taylor, E. L., Taylor, T. N., 1992. Reproductive biology of the Permian Glossopteridales and their suggested relationships to flowering plants. Proceedings of the National Academy of Sciences of the United States of America 89, 11495–11497. [1]

Taylor, E. L., Ryberg, P. E., 2007. Tree growth at polar latitudes based on fossil tree ring analysis. Palaeogeography, Palaeoclimatology, Palaeoecology 225, 246–264. [3, 4, 6, 8]

Taylor, E. L., Taylor, T. N., Collinson, J. W., Elliot, D. H., 1986. Structurally preserved Permian plants from Skaar Ridge, Beardmore Glacier region. Antarctic Journal of the United States 21, 27–28. [1]

Taylor, E. L., Taylor, T. N., Collinson, J. W., 1989a. Depositional setting and paleobotany of Permian and Triassic permineralized peat from the central Transantarctic Mountains, Antarctica. International Journal of Coal Geology 12, 657–679. [1, 2, 4, 8]

Taylor, E. L., Taylor, T. N., Isbell, J. L., Cúneo, N. R., 1989b. Fossil floras of southern Victoria Land: 2. Kennar Valley. Antarctic Journal of the United States 24, 26–28. [1]

Taylor, E. L., Taylor, T. N., Cúneo, N. R., 1992. The present is not the key to the past: A polar forest from the Permian of Antarctica. Science 257, 1675–1677. [1, 5, 6]

Taylor, T. N., Taylor, E. L., 1997. The distribution and interactions of some Paleozoic fungi. Review of Palaeobotany and Palynology 95, 83–94. [3]

Taylor, T. N., White, J. F., 1989. Fossil fungi (Endogonaceae) from the Triassic of Antarctica. American Journal of Botany 76, 389–396. [1, 9]

Taylor, T. N., Krings, M., 2005. Fossil microorganisms and land plants: Associations and interactions. Symbiosis 40, 119–135. [3]

Taylor, T. N., Krings, M., 2010. Paleomycology: The rediscovery of the obvious. PALAIOS 25, 283–286. [2, 7]

Taylor, T. N., Taylor, E. L., Collinson, J. W., 1986. Paleoenvironment of Lower Triassic plants from the Fremouw Formation. Antarctic Journal of the United States 21, 26–27. [2, 4]

Taylor, T. N., Taylor, E. L., Isbell, J. L., 1989. Glossopterid reproductive organs from Mount Achernar, Antarctica. Antarctic Journal of the United States 24, 28–30. [3]

Taylor, T. N., Remy, W., Hass, H., 1992. Fungi from the Lower Devonian Rhynie Chert-Chytridiomycetes. American Journal of Botany 79, 1233–1241. [1, 5]

Taylor, T. N., Galtier, J., Axsmith, B. J., 1994. Fungi from the Lower Carboniferous of central France. Review of Palaeobotany and Palynology 83, 253–260. [1]

Taylor, T. N., Remy, W., Hass, H., Kerp, H., 1995. Fossil arbuscular mycorrhizae from the Early Devonian. Mycologia 87, 560–573. [3]

Taylor, T. N., Klavins, S. D., Krings, M., 2007. Fungi from the Rhynie chert: A view from the dark side. Transactions of the Royal Society of Edinburgh: Earth Sciences 94, 457–473. [1]

Taylor, T. N., Taylor, E. L., Krings, M., 2009. Paleobotany: The Biology and Evolution of Fossil Plants, Second Edition. Academic Press, Burlington, MA., 1230 pp. [2, 3, 4, 5]

Taylor, T. N., Krings, M., Galtier, J., Dotzler, N., 2011. Fungal endophytes in *Astromyelon*-type (Sphenophyta, Equisetales, Calamitaceae) roots from the Upper Pennsylvanian of France. Review of Palaeobotany and Palynology, 1–35. [1]

Taylor, T. N., Krings, M., Dotzler, N., Galtier, J., 2011. The advantage of thin section preparations over acetate peels in the study of late Paleozoic fungi and other microorganisms. PALAIOS 26, 239–244. [1, 2, 6]

Taylor, T. N., Krings, M., Taylor, E. L., 2015. Fossil Fungi. Academic Press, London, UK, 382 pp. [1, 6, 8, 9]

Tian, N., Wang, Y., Zhang, W., Jiang, Z., Dilcher, D. L., 2013. *Ashicaulis beipiaoensis* sp. nov.,

a New Osmundaceous Fern Species from the Middle Jurassic of Liaoning Province, Northeastern China. International Journal of Plant Sciences 174, 328–339. [5]

Tidwell , W. D., 1986. *Millerocaulis*, a new genus with species formerly in *Osmundacaulis* Miller (Fossils: Osmundaceae). SIDA 11, 401–405. [5]

Tidwell , W. D., 1994. *Ashicaulis*, a new genus for some species of *Millerocaulis* (Osmundaceae). SIDA 16, 253–261. [5]

Tidwell, W. D., Ash, S. R., 1994. A review of selected Triassic to Early Cretaceous ferns. Journal of Plant Research 107, 417–442. [5]

Toljander, J. F., Artursson, V., Paul, L. R., Jansson, J. K., Finlay, R. D., 2006. Attachment of different soil bacteria to arbuscular mycorrhizal fungal extraradical hyphae is determined by hyphal vitality and fungal species. F.E.M.S Microbiology Letters 254, 34–40. [3, 5]

Toth, R., Miller, R. M., 1984. Dynamics of arbuscule development and degeneration in a Zea mays mycorrhiza. American Journal of Botany 449–460. [2]

Townrow, J. A., 1967a. Fossil plants from Allan and Carapace Nunataks, and from the Upper Mill and Shackleton glaciers, Antarctica. New Zealand Journal of Geology and Geophysics 10, 456–473. [1]

Townrow, J. A., 1967b. On a conifer from the Jurassic of East Antarctica. Papers and Proceedings of the Royal Society of Tasmania 101, 137–148. [1, 7]

Traverse, A., Ash, S. R., 1994. Well-preserved fungal spores from Jurassic rocks of Hells Canyon on the Idaho-Oregon border. Journal of Paleontology 68, 664–668. [7]

Treseder, K. K., Mack, M. C., Cross, A., 2004. Relationships among fires, fungi, and soil dynamics in Alaskan boreal forests. Ecological Applications 14, 1826–1838. [1]

Trewin, N., Fayers, S., Kelman, R., 2003. Subaqueous silicification of the contents of small ponds in an Early Devonian hot-spring complex, Rhynie, Scotland. Canadian Journal of

Earth Sciences 40, 1697–1712. [1]

Tu, T., Derenne, S., Largeau, C., Mariotti, A., Bocherens, H., Pons, D., 2000. Effects of fungal infection on lipid extract composition of higher plant remains: comparison of shoots of a Cenomanian conifer, uninfected and infected by extinct fungi. Organic Geochemistry 31, 1743–1754. [8]

Ulloa, M., Hanlin, R. T., 2012. Illustrated Dictionary of Mycology, Second Edition. The American Phytopathological Society, St. Paul, MN, 767 pp. [9]

Vera, E. I., 2007. A new species of Ashicaulis Tidwell (Osmundaceae) from Aptian strata of Livingston Island, Antarctica. Cretaceous Research 28, 500–508. [5]

Vogt, K. A., Edmonds, R. L., Grier, C. C., 1981. Seasonal changes in biomass and vertical distribution of mycorrhizal and fibrous-textured conifer fine roots in 23- and 180-year-old subalpine *Abies amabilis* stands. Canadian Journal of Forest Research 11, 224–230. [4]

Vogt, K. A., Moore, E. E., Vogt, D. J., Redlin, M. J., Edmonds, R. L., 1983. Conifer fine root and mycorrhizal root biomass within the forest floors of Douglas-fir stands of different ages and site productivities. Canadian Journal of Forest Research 13, 429–437. [4]

Vorholt, J. A., 2012. Microbial life in the phyllosphere. Nature Reviews Microbiology 10, 828–840. [8]

Voříšková, J., Baldrian, P., 2013. Fungal community on decomposing leaf litter undergoes rapid successional changes. International Society for Microbial Ecology Journal 7, 477–486. [8, 9]

Wagener, W. W., Mielke, J. L., 1961. A staining fungus root disease of ponderosa, Jeffrey and pinyon pines. Plant Disease Reports 45, 831–835. [7]

Wagg, C., Pautler, M., Massicotte, H. B., Peterson, R. L., 2008. The co-occurrence of ectomycorrhizal, arbuscular mycorrhizal, and dark septate fungi in seedlings of four members of the Pinaceae. Mycorrhiza 18, 103–110. [4]

Wagner, C. A., Taylor, T. N., 1981. Evidence for endomycorrhizae in Pennsylvanian age plant fossils. Science 212, 562–563. [3]

Wagner, C. A., Taylor, T. N., 1982. Fungal chlamydospores from the Pennsylvanian of North America. Review of Palaeobotany and Palynology 37, 317–328. [3]

Walker, C. A., 1985. *Endogone lactiflua* forming ectomycorrhizas with *Pinus contorta*. Transactions of the British Mycological Society 84, 353–355. [4]

Walker, C. A., Sanders, F. E., 1986. Taxonomic concepts in the Endogonaceae: III. The separation of *Scutellospora* gen. nov. from *Gigaspora* Gerd. & Trappe. Mycotaxon 27, 169–182. [4]

Walker, C., Schüssler, A., 2004. Nomenclatural clarifications and new taxa in the Glomeromycota. Mycological Research 108, 979–982. [4]

Wang, B., Qiu, Y. L., 2006. Phylogenetic distribution and evolution of mycorrhizas in land plants. Mycorrhiza 16, 299–363. [3, 4]

Wang, B., Yeun, L. H., Xue, J. -Y., Liu, Y., Ané, J. -M., Qiu, Y. -L., 2010. Presence of three mycorrhizal genes in the common ancestor of land plants suggests a key role of mycorrhizas in the colonization of land by plants. New Phytologist 186, 514–525. [3]

Wang, S. -J., Hilton, J., Liang, M. -M., Stevens, L. 2006. Permineralized seed plants from the Late Permian of Southern China: A new species of *Cardiocarpus*. International Journal of Plant Sciences 167, 1247–1257. [1]

Warcup, J. H., 1990. Taxonomy, culture and mycorrhizal associations of some zygosporic Endogonaceae. Mycological Research 94, 173–176. [4]

Wardle, D. A., Lindahl, B. D., 2014. Disentangling global soil fungal diversity. Science 346, 1052–1053. [1]

Wardle, D. A., Bardgett, R. D., Klironomos, J. N., Setälä, H., van der Putten, W. H., Wall, D. H., 2004. Ecological linkages between aboveground and belowground biota. Science 304, 1629–1633. [5]

Weaver, L. S., McLoughlin, S., Drinnan, A. N., 1997. Fossil woods from the Permian Bainmedart Coal Measures, northern Prince Charles Mountains, East Antarctica. Australian Geological Survey Organisation Journal of Geology and Geophysics 16, 655–676. [1, 3, 6]

Webster, J., Weber, R., 2007. Introduction to the fungi. Third Edition. Cambridge University Press, Cambridge, UK, 855 pp. [6]

Wegener, A., 1924. The origin of continents and oceans, translated from the 3rd German edition, by J. G. A. Skerl. Methuen and Company, London. 212 pp. [8]

Weiss, F. E., 1904. A mycorrhiza from the Lower Coal-Measures. Annals of Botany 18, 255–264. [3]

Weiss, F. E., 1906. On the tyloses of *Rachiopteris corrugata*. New Phytologist 5, 1–5. [7]

White, J. F., Taylor, T. N., 1988. Triassic fungus from Antarctica with possible Ascomycetous affinities. American Journal of Botany 75, 1495–1500. [1, 9]

White, J. F., Taylor, T. N., 1989a. An evaluation of sporocarp structure in the Triassic fungus *Endochaetophora*. Review of Palaeobotany and Palynology 61, 341–345. [1, 4, 9]

White, J. F., Taylor, T. N., 1989b. Triassic fungi with suggested affinities to the Endogonales Zygomycotina. Review of Palaeobotany and Palynology 61, 53–61. [1, 4]

White, J. F., Taylor, T. N., 1989c. A trichomycete-like fossil from the Triassic of Antarctica. Mycologia 81, 643–646. [4]

White, J. F., Taylor, T. N., 1991. Fungal sporocarps from Triassic peat deposits in Antarctica. Review of Palaeobotany and Palynology 67, 229–236. [1, 9]

Williams, H., Turner, F. J., Gilbert, C. M., 1982. Petrography: An introduction to the study of rocks in thin section. W. H. Freeman and Company, San Francisco, US. 626 pp. [2]

Williamson, W. C., 1873. On the Organization of the Fossil Plants of the Coal-Measures. Part IV. *Dictyoxylon*, *Lyginodendron*, and *Heterangium*. Philosophical Transactions of the Royal Society of London, Series B 163, 377–408. [9]

Williamson, W. C., 1874. On the Organization of the Fossil Plants of the Coal-Measures. Part VI. Ferns. Philosophical Transactions of the Royal Society of London, Series B 164, 675–703. [2]

Williamson, W. C., 1876. On the organization of the fossil plants of the Coal-Measures. Part VII. *Myelopteris, Psaronius*, and *Kaloxylon*. Philosophical Transactions of the Royal Society of London, Series B 166, 1–25. [7]

Williamson, W. C., 1882. On the organisation of the fossil plants of the coal measures. Part XII. Proceedings of the Royal Society of London, Series B 34, 31–35. [1, 9]

Wilson, L. R., 1962. A Permian fungus spore type from the Flowerpot Formation of Oklahoma. Oklahoma Geology Notes 22, 91–96. [3]

Wingfield, M. J., Marasas, W. F. O., 1980. *Verticicladiella alacris* sp. nov., associated with a root disease of pines in South Africa. Transactions of the British Mycological Society 75, 21–28. [7]

Witcosky, J. J., Hansen, E. M., 1985. Root-colonizing insects recovered from Douglas-fir in various stages of decline due to black-stain root disease. Phytopathology 75, 399–402. [7]

Wu, B., Isobe, K., Ishii, R., 2004. Arbuscular mycorrhizal colonization of the dominant plant species in primary successional volcanic deserts on the Southeast slope of Mount Fuji.

Mycorrhiza 14, 391–395. [3]

Wubet, T., Kottke, I., Teketay, D., Oberwinkler, F., 2003. Mycorrhizal status of indigenous trees in dry Afromontane forests of Ethiopia. Forest Ecology and Management 179, 387–399. [3]

Wubet, T., Weiss, M., Kottke, I., Oberwinkler, F., 2003. Morphology and molecular diversity of arbuscular mycorrhizal fungi in wild and cultivated yew (*Taxus baccata*). Canadian Journal of Botany 81, 255–266. [4]

Yamada, T., 2001. Defense mechanisms in the sapwood of living trees against microbial infection. Journal of Forest Research 6, 127–137. [7]

Yao, X., Taylor, T. N., Taylor, E. L., 1991. Silicified dipterid ferns from the Jurassic of Antarctica. Review of Palaeobotany and Palynology 67, 353–362. [1]

Yao, X., Taylor, T. N., Taylor, E. L., 1993. The Triassic seed cone *Telemachus* from Antarctica. Review of Palaeobotany and Palynology 78, 269–276. [4]

Yao, X., Taylor, T. N., Taylor, E. L., 1995. The corystosperm pollen organ *Pteruchus* from the Triassic of Antarctica. American Journal of Botany 82, 535–546. [1]

Zavada, M. S., Mentis, M. T., 1992. Plant-animal interaction: The effect of Permian megaherbivores on the glossopterid flora. American Midland Naturalist 127, 1–12. [6]

Zeiller, R., 1896. Étude sur quelques plantes fossiles, en particulier *Vertebraria* et *Glossopteris* des environs de Johannesburg (Transvaal). Bulletin de la Société géologique de France 3rd Series 24, 349–377. [in French] [8]

Ziegler, A. M., Parrish, J. M., Yao, J., Gyllenhaal, E. D., Rowley, D. B., Parrish, J. T., Shangyou, N., Bekker, A., Hulver, M. L., 1993. Early Mesozoic phytogeography and climate. Philosophical Transactions of the Royal Society of London, Series B 341, 297–305. [1]

Zmitrovich, I. V., Malysheva, V. F., Spirin, W. A., 2006. A new morphological arrangement of

the Polyporales. I. Phanerochaetineae. Mycena 6, 4–56. [7]

Figures, tables, and plates

Table 1. Fungi and fungal-like organisms in permineralized material from Late Paleozoic and Mesozoic of Antarctica. This table is organized by age, then locality and stratigraphy, and by the plant organ or matrix that the specimen is associated or found in close association with (roots, stems, leaves, reproductive structures, or matrix). Solid black circles (●) indicate definitive evidence for taxonomy or affinity; Open white circles (○) indicate putative or speculative affinity.

Age	Stratigraphy	Locality	Plant organ or matrix	Species or fungal description	Major fungal phyla: Chytridiomycota	Blastocladiomycota	Zygomycetes	Glomeromycota	Ascomycota	Basidiomycota	Unknown Affinity	Lichen	Fungal Spores	Fungal Interactions	Fungal-like: Peronosporomycetes	Myxcetozoa	Bacteria	Reference(s)
Middle to Late Permian (Roadian to Wordian)	Toplofe Member, Amery Group, lower Bainmedart Coal Members	northern Prince Charles Mountains, East Antarctica	matrix	*Combresomyces caespitosus*											●			Slater et al., 2013
				Combresomyces canus											●			
				Fungal morphotype 1: non-septate/aseptate hyphae			○	○			○							Slater et al., 2014
				Fungal morphotype 2: septate hyphae					○	○	○							
				Fungal morphotype 3: hyphae with swellings				○			○							
				Fungal morphotype 5: large smooth-weakly ornamented spores	○			○			○							
				Fungal morphotype 7: fungi within pollen	○						○							
				Fungal morphotype 8: disc-like clusters of small fungal cells	○						○							
				Fungal morphotype 10: sclerotia							○							
			matrix; roots	Fungal mophotype 4: smooth-weakly ornamented spores	○						○							
				Fungal morphotype 9: complex fruiting bodies				○			○							
			matrix; stem wood	Coprolites with fungal spores							○			●				Slater et al., 2012
			stem	Hyphae cross sections in metaxylem of axes							○							McLoughlin et al., 2015
			reproductive structure (pollen)	Fungal morphotype 6: spinose oblong spores					○		○							Slater et al., 2014
Middle to Late Permian	Toplofe Member, Bainmedart Coal Members	moraines of Mount Rymill, southern Prince Charles Moutains, East Antarctica	leaves	*Noeggerathiopsis* with hyphae							○							Holdgate et al., 2005
			matrix	Fungal fruiting body with numerous spores							○							
Late Permian	Amery Group, lower Bainmedart Coal Members	Beaver Lake area, edge of Lambert Glacier, northern Prince Charles Mountains, East Antarctica	stem wood	Wood decay (no fungi) in *Australoxylon baniali* and *A. mondii*						○								Weaver et al., 1997
	Upper Buckley Formation, Victoria Group, Beacon Supergroup	Skaar Ridge, Beardmore Glacier area, Queen Alexandra Range, central Transantarctic Mountains, Antarctica	matrix	Fungal *zygosporangium* (likely peronosporomycete)							○				○			Schopf et al., 1970
				Synchytrium permicus	○													Massini, J., 2007a
			roots	*Glomerphites intercalaris* (chlamydospore)				○										Massini, J., 2007b
				Glomites vertebraviae (mycorrhiza in *Vertebraria*)				●										Harper et al., 2013
			root wood	Wood decay (no fungi) in *Vertebraria*					●									Schopf et al., 1970
			stem and root wood	pocket rot in axes of Vertebraria and *Araucarioxylon*-type wood						●								Stubblefield and Taylor, 1985; 1986
				pocket rot in axes of Vertebraria and *Araucarioxylon*-type wood						●								Stubblefield and Taylor, 1986

Table 1. Review of Paleozoic and Mesozoic Antarctic permineralized fungi.

Middle Triassic (Anisian)	Fremouw Formation, Victoria Group, Upper Beacon Supergroup	Fremouw Peak, Beardmore Glacier area, Queen Alexandra Range, central Transantarctic Mountains of Antarctica	matrix	*Sclerocystis*-like fungus				○										Stubblefield et al., 1987c
				Endochaetophora antarctica			○											White and Taylor, 1988; 1989a
				Mycocarpon asterineum			●											Taylor and White, 1989
				Fungal type No. 2 "sporocarp" with mycelial peridium with internal spores			○											White and Taylor, 1989c
				Fungal type No. 3 "sporocarp" with mycelial peridium with internal mantled spores			○											
				Fungal type No. 5 Subglobose sporangium							○							
				Fungal type No. 6 Subglobose sporangium with a radially orientated straited cell wall							○							
				Trichomycete-like fungus			○							○				White and Taylor, 1989b
				Fossil 1 "sporocarp" composed of irregularly thick interwoven hyphae			○											White and Taylor, 1991
				Fossil 2 trilayer "sporocarp"			○											
				Fossil 3 globose "sporocarp" surrounded with interwoven mycelium with internal septate hyphae			○											
				Fossil 4 ovate "sporocarp" surrounded with interwoven mycelium with internal septate hyphae			○											
				Fossil 6 "sporocarp" surrounded with interwoven mycelium			○											
				Fossil 7 Multiple cell wall "sporocarp" with inner acelluar layer with internal spores			○											
				Fossil 8 double isodiametric cell wall "sporocarp" with internal spores			○											
				Fossil 9 double cell wall "sporocarp" with membraneous contents			○											
				Fossil 10 thick wall "sporocarp" with internal spores			○											
				Combresomyces cornifer											●			Schwendemann et al., 2009
				Jimwhitea circumtecta			●											Krings et al., 2012b
			matrix; roots	Fungal type No. 1 Globose spores in clusters									○					White and Taylor, 1989c
				Fungal type No. 4 Trilayer "sporocarp" with internal globose spores with possible gametangia			○											
				Fossil 5 possible chlamydospore with mycoparasite				○						○				White and Taylor, 1991
			multiple organs	*Palaeofibulus antarctica*						●								Osborn et al., 1989
			reproductive structure (embryo)	*Mycocarpon asterineum* in *Parasciadopitys aequata*			●											Schwendemann et al., 2010b
				Fungal hyphae in *Parasciadopitys aequata*					○	○	○							
			roots	Mycorrhizae in *Antarcticycas schopfii*				●										Stubblefield et al., 1987a; 1987b
				Gigasporites myriamyces (mycorrhizae in *Antarcticycas schopfii)*				●										Phipps and Taylor, 1996
				Glomites cycestris (mycorrhizae in *Antarcticycas schopfii)*				●										
				Mycorrhizal root nodules in *Notophytum krauselii*				●										Schwendemann et al., 2011
				Mycorrhizae in *Notophytum krauselii*				●										Harper et al., 2015
			stem wood	pocket rot in *Araucarioxlyon* wood						●								Stubblefield and Taylor, 1985; 1986
		Mount Falla, Beardmore Glacier area, Queen Alexandra Range of the central Transantarctic Mountains of Antarctica	reproductive structure	Fungal hyphae in *Dordrechtites arcanus*							○							Bergene et al., 2013
Middle or early Late Triassic	uppermost part of member C of the Fremouw Formation, Victoria Group, Upper Beacon Supergroup	north side of Fremouw Peak, Beardmore Glacier area, Queen Alexandra Range of the central Transantarctic Mountains of Antarctica	stem	Fungal "sporocarps" near *Rudixylon serbetianum*			○				○							Bomfleur et al., 2013
Late Early Jurassic (early Toarcian)	Shafer Peak Formation	Mount Carson, east of the Gair Mesa range in northern Victoria Land, Transantarctic Mountains, East Antarctica	matrix	Fungal remains in microbial mats							○							Bomfleur et al., 2007
	Ferrar Group	Suture Bench, a small bench east of the Gair Mesa range in northern Victoria Land, Transantarctic Mountains, East Antarctica	stem wood	Tylosis formation and fungi in wood							○			○				Harper et al., 2012

Table 1. cont. Review of Paleozoic and Mesozoic Antarctic permineralized fungi.

Figure 1. Overview map of Antarctic localities and sites. **A.** Map of Antarctica with key areas and localities highlighted, including sites discussed in Chapter 1. Modified from Cantrill and Poole, 2012. **B.** Detailed map of inset A of the Permian and Triassic localities in central Transantarctic Mountains, indicated localities include sites where permineralized material has been described; localities in red denote used in current study. **C.** Detailed map of inset B of the Permian, Triassic, and Jurassic localities in central Transantarctic Mountains, indicated localities include sites where permineralized material has been described; localities in red denote used in current study.

Figure 1. Overview map of Antarctic localities and sites.

Figure 2. Permian and Triassic Antarctica locality map and stratigraphic column. **A.** Stratigraphic map of the Devonian to Late Triassic strata of the Central Transantarctic Mountains, Antarctica. Color bar indicates area of Triassic specimen collection; Red bar indicated area of Permian specimen collection. Modified from Collinson et al., 1994. **B.** Skaar Ridge and Fremouw Peak locality locations in Antarctica. Map from of USGS Landsat Image Mosaic of Antarctica (LIMA). **C.** Skaar Ridge (Permian) locality field image. People in field for scale (arrow). Image courtesy of A.-L. Decombeix. **D.** Fremouw Peak (Triassic) locality field image. Image courtesy of A.-L. Decombeix.

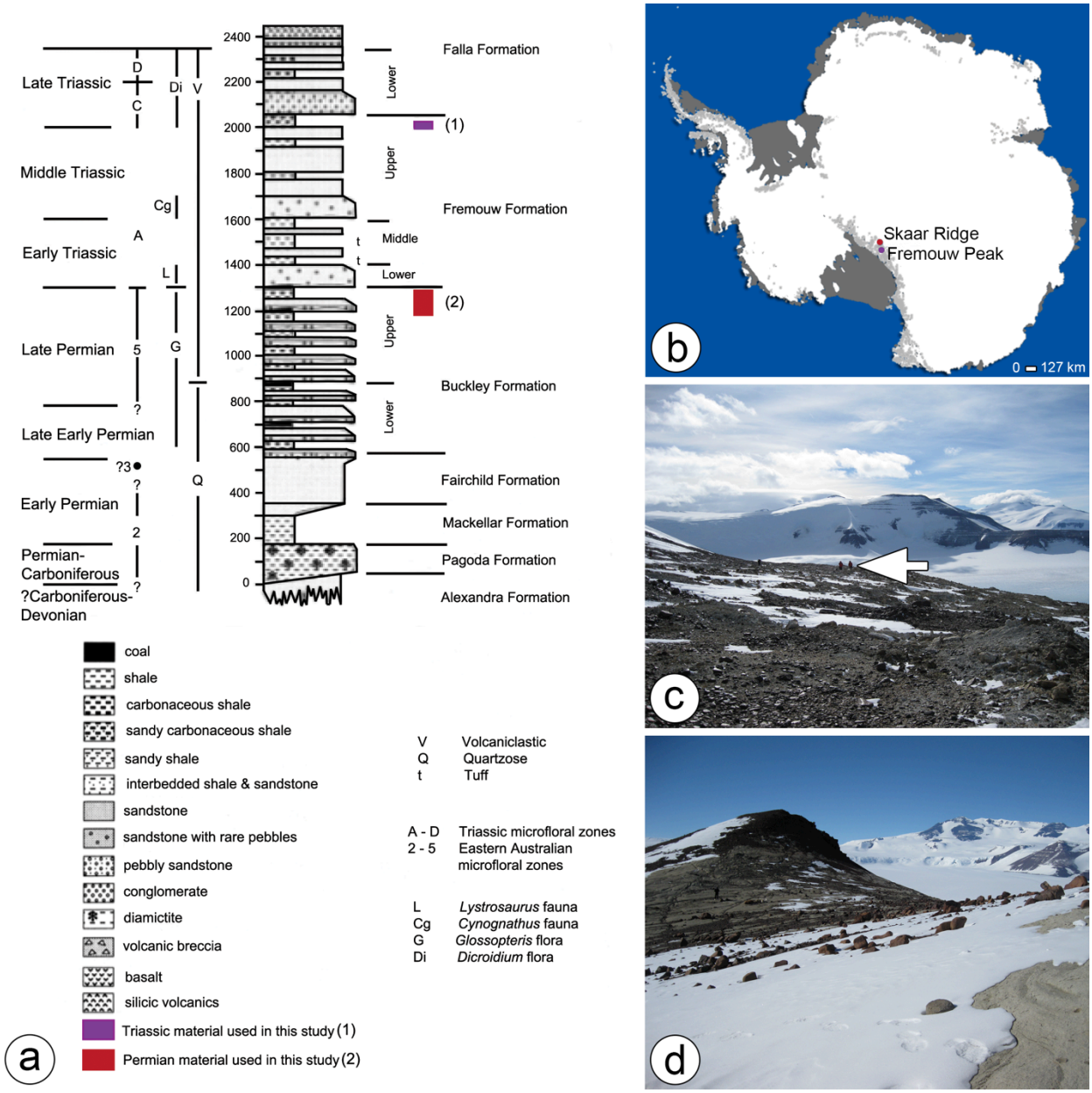

Figure 2. Permian and Triassic Antarctica locality map and stratigraphic column.

Figure 3. Locality map, field images, and stratigraphic column of the late Pliensbachian-early Toarcian (late Early Jurassic) locality at Suture Bench, Gair Mesa in northern Victoria Land, Transantarctic Mountains, East Antarctica. Modified from Bomfleur et al., 2011b; 2014c with permission from author. **A.** Map showing the study area and sections sampled during GANOVEX IX (2005/2006). **B.** Base of the Kirkpatrick Lavas at Suture Bench. **C.** Exposed parts of upright tree stems engulfed by lava flows. **D.** Simplified lithostratigraphic column of the exposed sedimentary section at Suture Bench in southern north Victoria Land, East Antarctica.

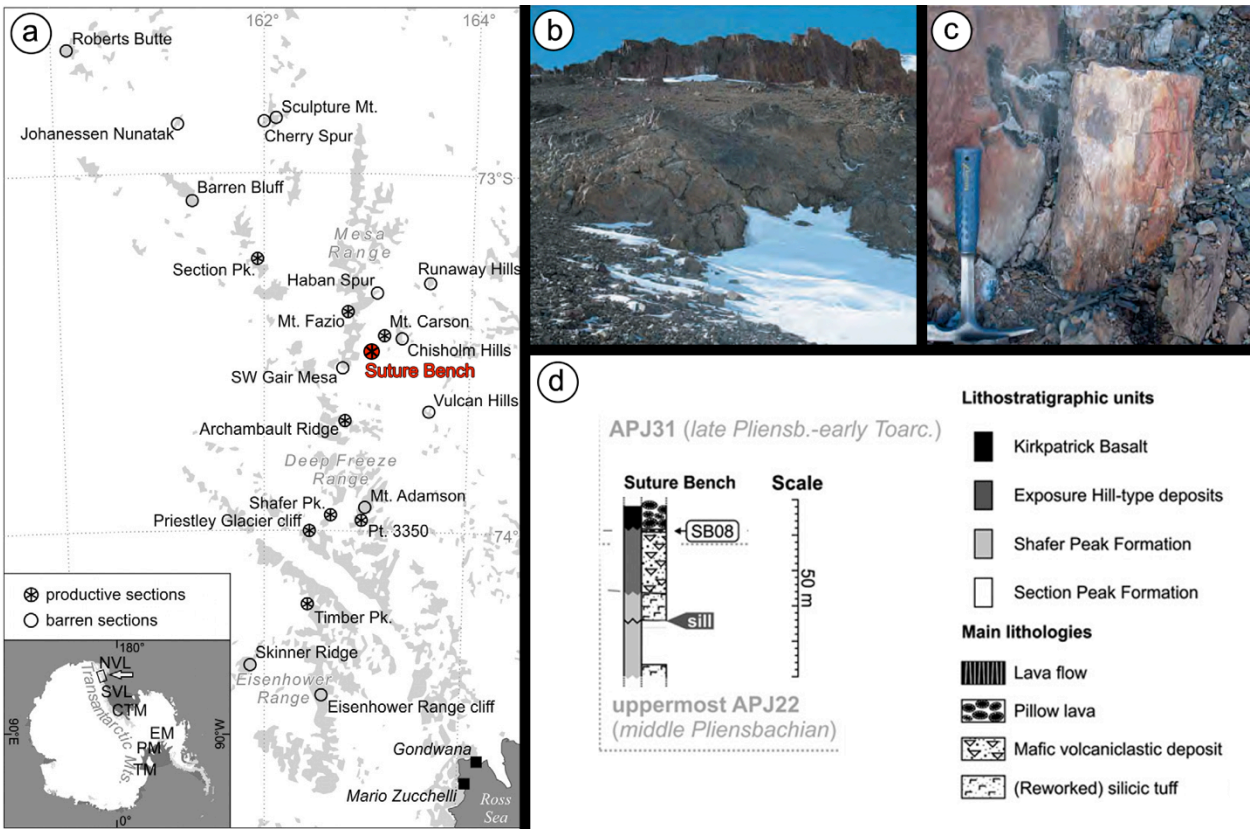

Figure 3. Locality map, field images, and stratigraphic column of the late Pliensbachian-early Toarcian (late Early Jurassic) locality at Suture Bench, Gair Mesa in northern Victoria Land, Transantarctic Mountains, East Antarctica. Modified from Bomfleur et al., 2011b; 2014c with permission from author.

Figure 4. Thin section technique. **A.** Preparation of rock specimens with specific size restrictions. Initial cut is to be completed with a table saw and the surface of interest must be smooth and even, e.g., use a silicon carbide grit. **B**. Adherence of rock sample to glass via epoxy. Note that the rock sample and epoxy are attached on the frosted portion of the microscope slide. Additional inset of planar view of microscope slide with frosted surface and corner removed for orientation purposes. **C.** Initial cut via a diamond embedded blade on thin section machine to remove majority of rock specimen. Resulting cut will yield a thin section from 200-500 μm in thickness. **D.** Secondary cut via a cup wheel on thin section machine. Each pass must decrease about 30 μm and a slow process will produce a more even thin section. **E.** Final steps in polishing and grinding down thin section by hand. Turning the slide over, so the rock specimen can come into contact with the silicon carbide and water mixture on a glass plate. Check thin section constantly and grind down to desired thickness. **F.** Example of common thin section problematic results, such as a lateral wedge or center wedge of rock sample. **G.** Method to rectify wedge problems in thin sections. Applying pressure at the thickest points on the thin section while completing the final polishing steps will typically result in an even thin section again. **H.** Studying thin sections under transmitted light microscopy. It is best to use a light filter in between the light source and thin section. Note that rock sample side is closest to the objective while studying thin sections.

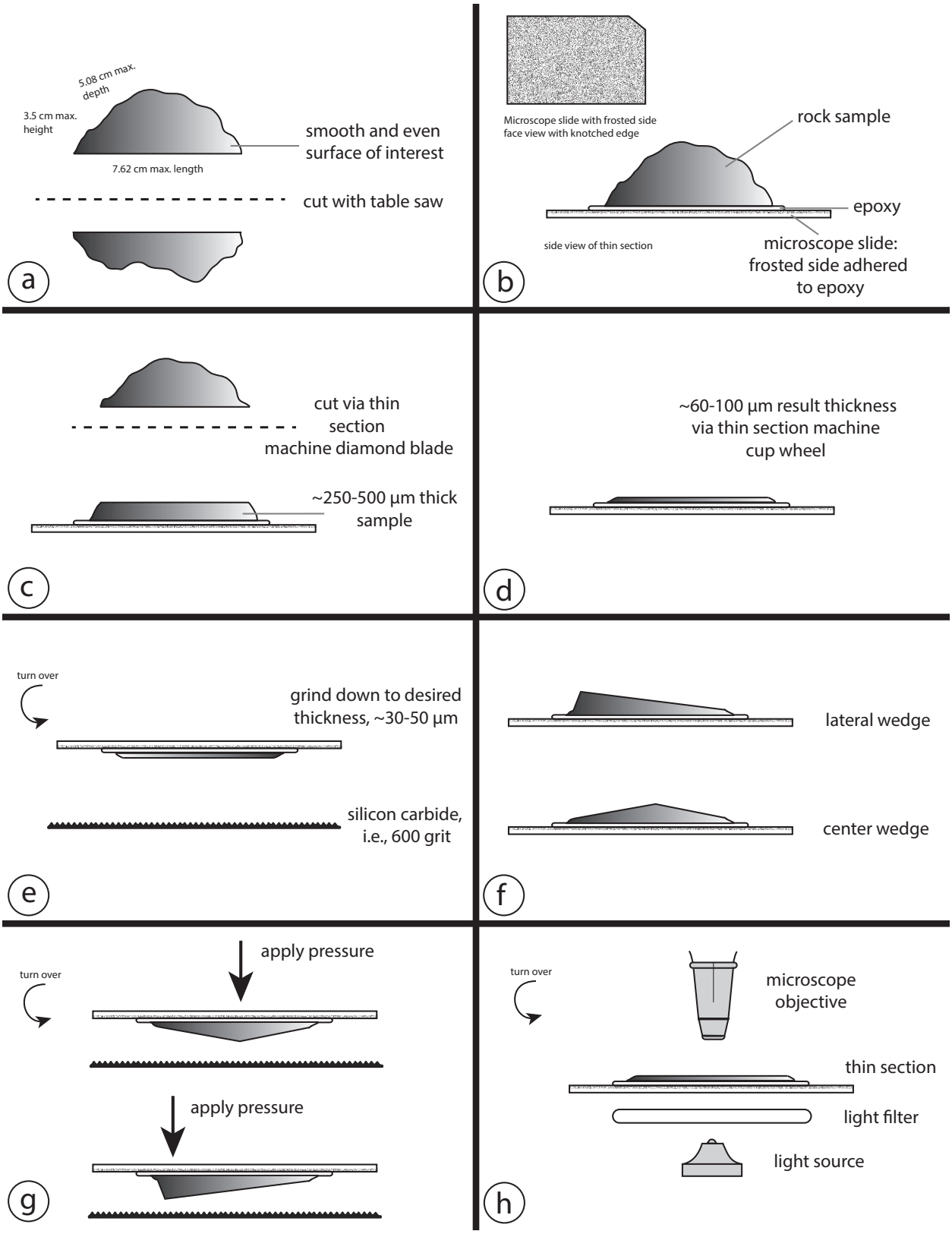

Figure 4. Thin section technique.

Figure 5. Focal stacking example 1 of 3. **A**. Basic layout in Adobe Photoshop CS6 on Mac OS. Note all six images for focal stacking (i.e., fungal hyphae within a longitudinal section of a root cell) example have been imported and are in separate layers, are in reverse sequential order, layers 2 through 6 have been hidden, and only the first layer is visible (arrow). **B**. Layers 1 and 2 are now visible, but layer 2 will be the working layer (arrow). This is the layer that will be erased (see text for eraser specifications) and worked on to reveal the features visible in layer 1 but not layer 2.

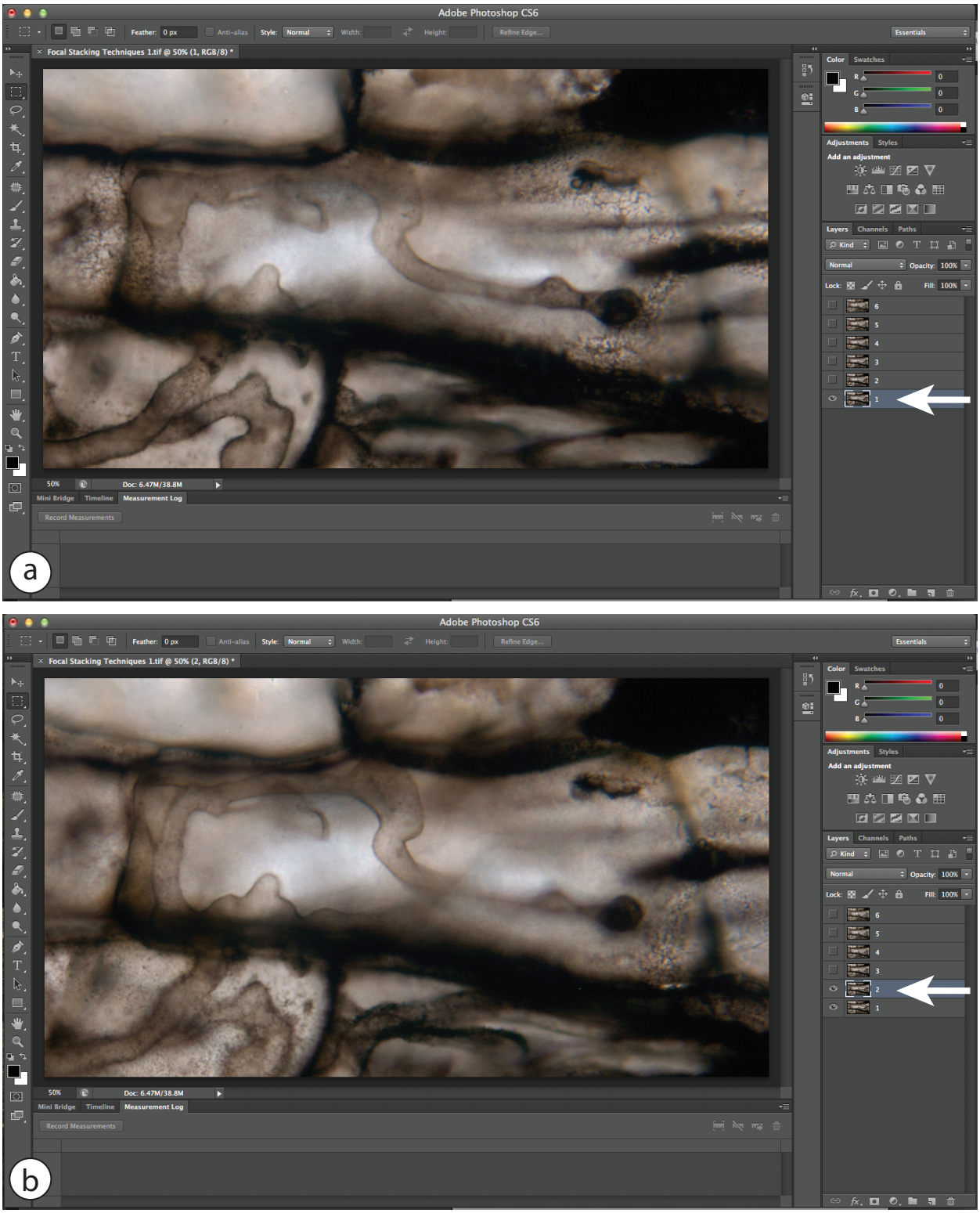

Figure 5. Focal stacking example 1 of 3.

Figure 6. Focal stacking example 2 of 3. **A**. Only layer 2 is visible (arrow) to emphasize areas that have been erased in layer 2. These areas in layer 1 show different features than layer 2. **B**. Layers 1 and 2 now visible (arrows), and focal stacked, with the features in layer 1 now visible in layer 2. Compare to Figure 3a to note the differences between figures.

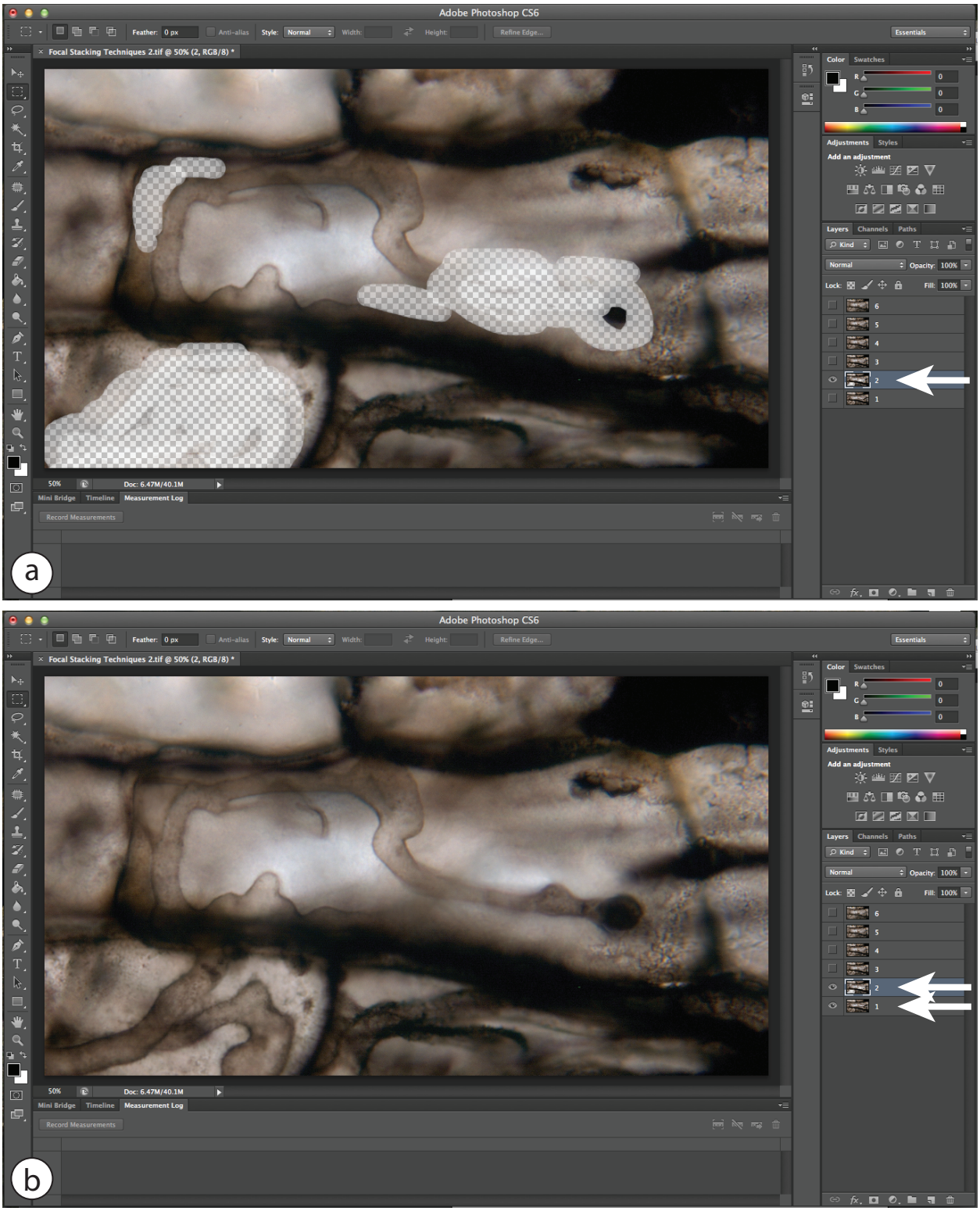

Figure 6. Focal stacking example 2 of 3.

Figure 7. Focal stacking example 3 of 3. **A**. Completely focal stacked image using layer 1 through 6 (arrow). **B**. Only layer 1 visible (arrow) while layers 2-6 are hidden. Compare to Figure 5a to note differences between a fully focal stacked composite image and an individual image.

Figure 7. Focal stacking example 3 of 3.

Chapter 3. **Plate 1**. Anatomy and fungal features of *Vertebraria*.

Plate 1, Figure 1. Transverse section of two young *Vertebraria* roots showing intact cortex (left) and central vascular bundle. Slide 26834; Scale bar=100 μm.

Plate 1, Figure 2. Transverse section of young root with mycorrhizal infection. Box is region where hyphae are common. Slide 23172; Specimen 15491 G bot; Scale bar=100 μm.

Plate 1, Figure 3. Transverse section of *Vertebraria* rootlet showing sections of intracellular hyphae within cortical cells. Slide 26835. Scale bar=25 μm.

Plate 1, Figure 4. Longitudinal section of cortex showing intracellular hyphae in multiple planes of section. Slide 23214; Specimen 15685 A. Scale bar=25 μm.

Plate 1, Figure 5. Longitudinal section of rootlet showing hyphae traversing intracellularly (arrow) and H branch (HB). Slide 26831. Scale bar=25 μm.

Plate 1, Figure 6. Hyphae with perpendicular septum (arrow). Slide 26831. Scale bar=25 μm.

Plate 1, Figure 7. Hyphae with right angle branching; note absence of septum at base (arrow). Slide 26831. Scale bar=25 μm.

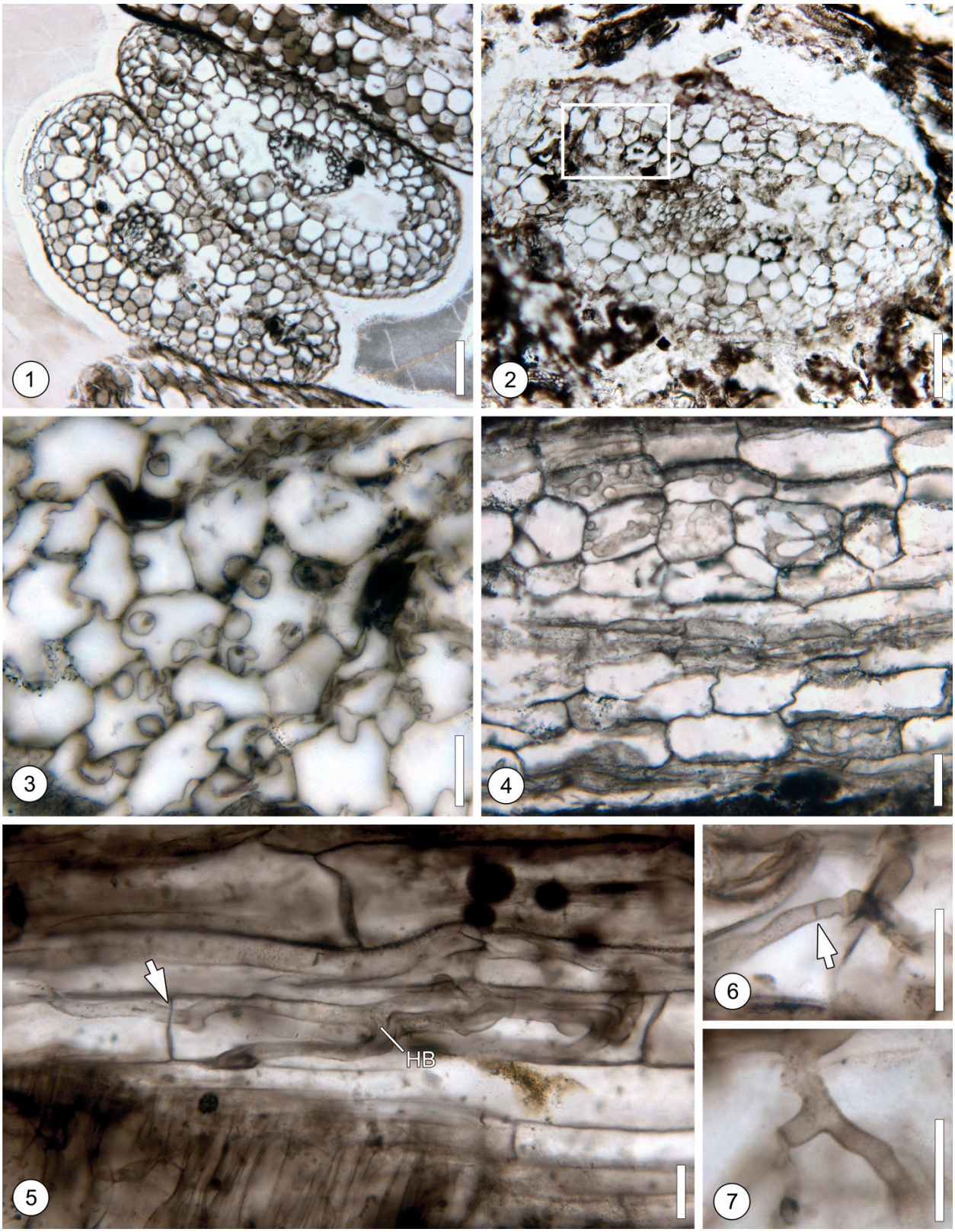

Chapter 3. **Plate 1**. Anatomy and fungal features of *Vertebraria*.

Chapter 3. **Plate 2**. Mycorrhizal association in *Vertebraria*.

Plate 2, Figure 8. Longitudinal section of root showing relationship between vascular bundle (VB) and *Paris*-type mycorrhizal zone (MZ). Boxed area enlarged in Plate 2, Figure 9. Slide 26831. Scale bar=100 μm.

Plate 2, Figure 9. Detail of Plate 2, Figure 8. Cortical cells with *Paris*-type mycorrhizal hyphae in the lumen of cells. Attached partial vesicle (V?) or artifact. Arrow indicates hyphal knob. Photomicrograph is partially focal stacked to show detail of attached vesicle and prominent loops in lumen. Slide 26831. Scale bar=25 μm.

Plate 2, Figure 10. Cortical cells showing *Paris*-type mycorrhizal hyphae. Photomicrograph is fully focal stacked to show detail and prominence of *Paris*-type mycorrhizal hyphae in mycorrhizal zone. Slide 26831. Scale bar=25 μm.

Plate 2, Figure 11. Highly coiled mycorrhizal hyphal morphology in single cortical cell; Boxed area (enlarged in Plate II, Fig. 5) highlights possible initial development stage of vesicle. Slide 26831. Scale bar=25 μm.

Plate 2, Figure 12. Enlargement of boxed area in Plate 2, Figure 11. Detail of attachment site (arrow) (septa?) of immature vesicle (V). Slide 26831. Scale bar=10 μm.

Plate 2, Figure 13. Cortical section showing position of vesicle (V) attached to branched hypha. Slide 26832. Scale bar=25 μm.

Plate 2, Figure 14. Detail of nearly complete intracellular vesicle (V). Slide 26832. Scale bar=25 μm.

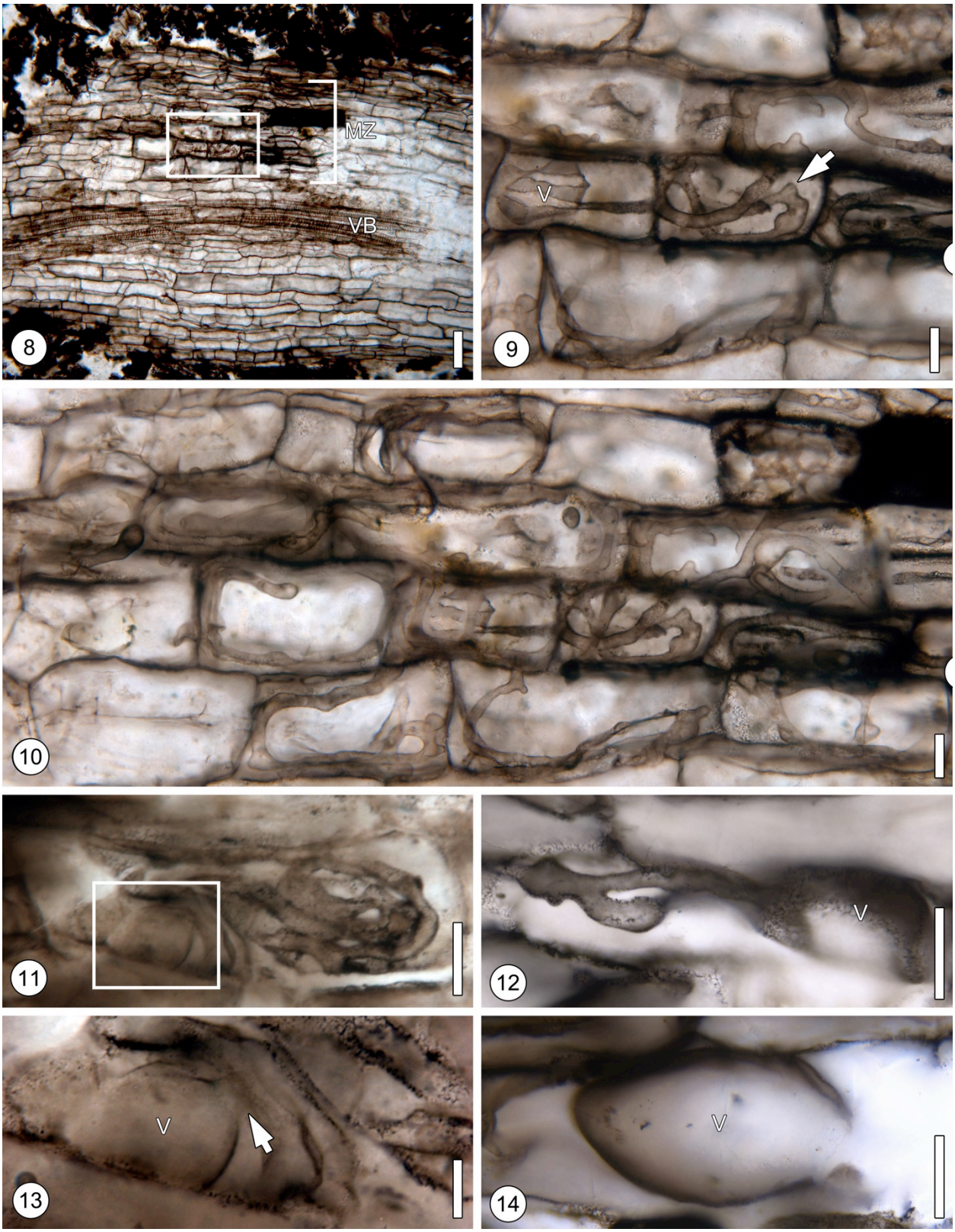

Chapter 3. **Plate 2**. Mycorrhizal association in *Vertebraria*.

Chapter 3. Plate 3. Comparison to extant mycorrhizae and other fossil fungal components.

Plate 3, Figure 15. Extant *M. glyptostroboides* mycorrhizal association; Note sparse distribution of arbuscules in root cortex. UAPC PAF Slide. Scale bar=100 μm.

Plate 3, Figure 16. Extant *M. glyptostroboides* mycorrhizal association showing *Paris*-type mycorrhizal hyphae coiled in single cell layer of cortical region; arrow indicates intracellular growth. Slide UAPC PAF Slide. Scale bar=25 μm.

Plate 3, Figure 17. Extant *M. glyptostroboides* mycorrhizal association; isolated mycorrhizal coil in cell lumen. Arrow indicates hyphal knob. UAPC PAF Slide. Scale bar=25 μm.

Plate 3, Figure 18. Extant *M. glyptostroboides* mycorrhizal association; Elongate, oblong vesicle attached to hypha in cortex of rootlet. UAPC PAF Slide. Scale bar=25 μm.

Plate 3, Figure 19. Two cortical cells of *Vertebraria* with tightly packed hyphae of varying diameters. Slide 26834. Scale bar=25 μm.

Plate 3, Figure 20. Interesting hyphal morphology confined to end of *Vertebraria* cortical cell. Similar to fan-shaped morphology of some mycorrhizal hyphae found in pteridophytes. Slide 26834. Scale bar=25 μm.

Plate 3, Figure 21. Asexual spore in the matrix containing the *Vertebraria* roots showing mycorrhizal fungus with subtending hypha (arrow). Slide 26833. Scale bar=25 μm.

Plate 3, Figure 22. Intact asexual spore from silicified peat matrix with small spherical structures in the lumen that may represent a form of mycoparasitism. Slide 26832.

Plate 3, Figure 23. Surface of cortical cell in longitudinal section of root covered in hyphal mycelia. Arrow indicated septate hypha. Slide 26834. Scale bar=25 μm.

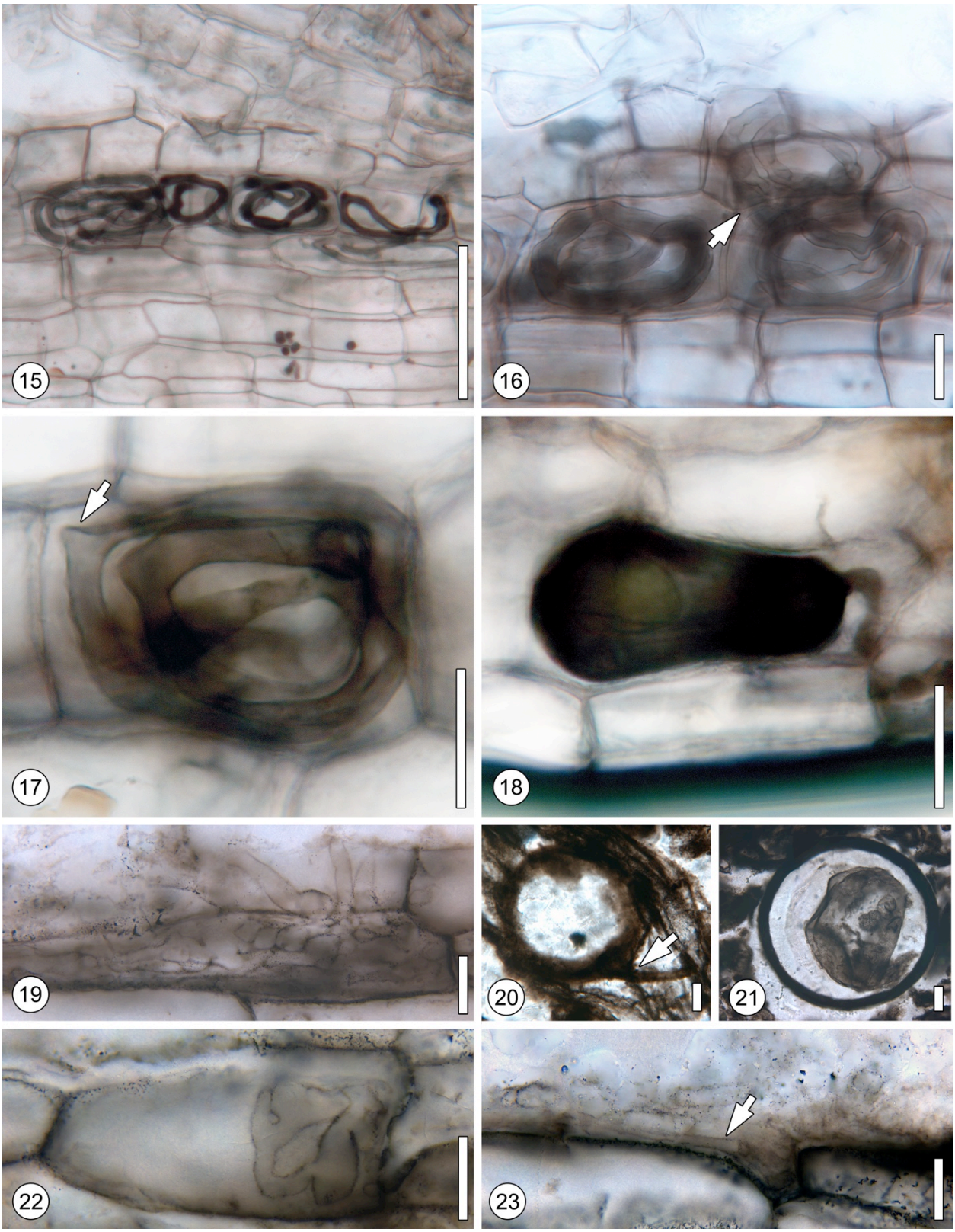

Chapter 3. Plate 3. Comparison to extant mycorrhizae and other fossil fungal components.

Chapter 4. Plate 4. Components of the *Notophytum krauselii* plant from permineralized peat, Middle Triassic of Antarctica, including arbuscular rootlets.

Plate 4, Figure 24. Oblique cross-section of woody axis with cortex (C) and secondary xylem (2ºX). Slide no. 30002; scale bar = 500 µm.

Plate 4, Figure 25. Cross-section of permineralized leaf with poorly preserved abaxial and adaxial epidermis, mesophyll, vascular bundle (VB; arrow). Slide no. 30000; scale bar = 500 µm.

Plate 4, Figure 26. *Alisporites* pollen grain Slide no. 30000; scale bar = 25 µm.

Plate 4, Figure 27. Preserved ovule of *Parasciadopitys* type. Slide no. 30003; scale bar = 500 µm.

Plate 4, Figure 28. Mature root with primary xylem (1ºX), secondary xylem (2°X), endodermis (En), cortex (C), and poorly preserved epidermis (E). Slide no. 30002; scale bar = 500 µm.

Plate 4, Figure 29. Cluster of immature rootlets (R). Slide no. 30005; scale bar = 500 µm.

Plate 4, Figure 30. Oblique cross section of rootlet with distinct mycorrhizal zone (MZ), i.e., darkened layer of cells. Arrow = vesicle. Slide no. 26590; scale bar = 500 µm.

Plate 4, Figure 31. Oblique longitudinal section of rootlet with darkened mycorrhizal zone (MZ). Brackets indicate area of mycorrhizal zone. Arrows = vesicles. Slide no. 26590; scale bar = 500 µm.

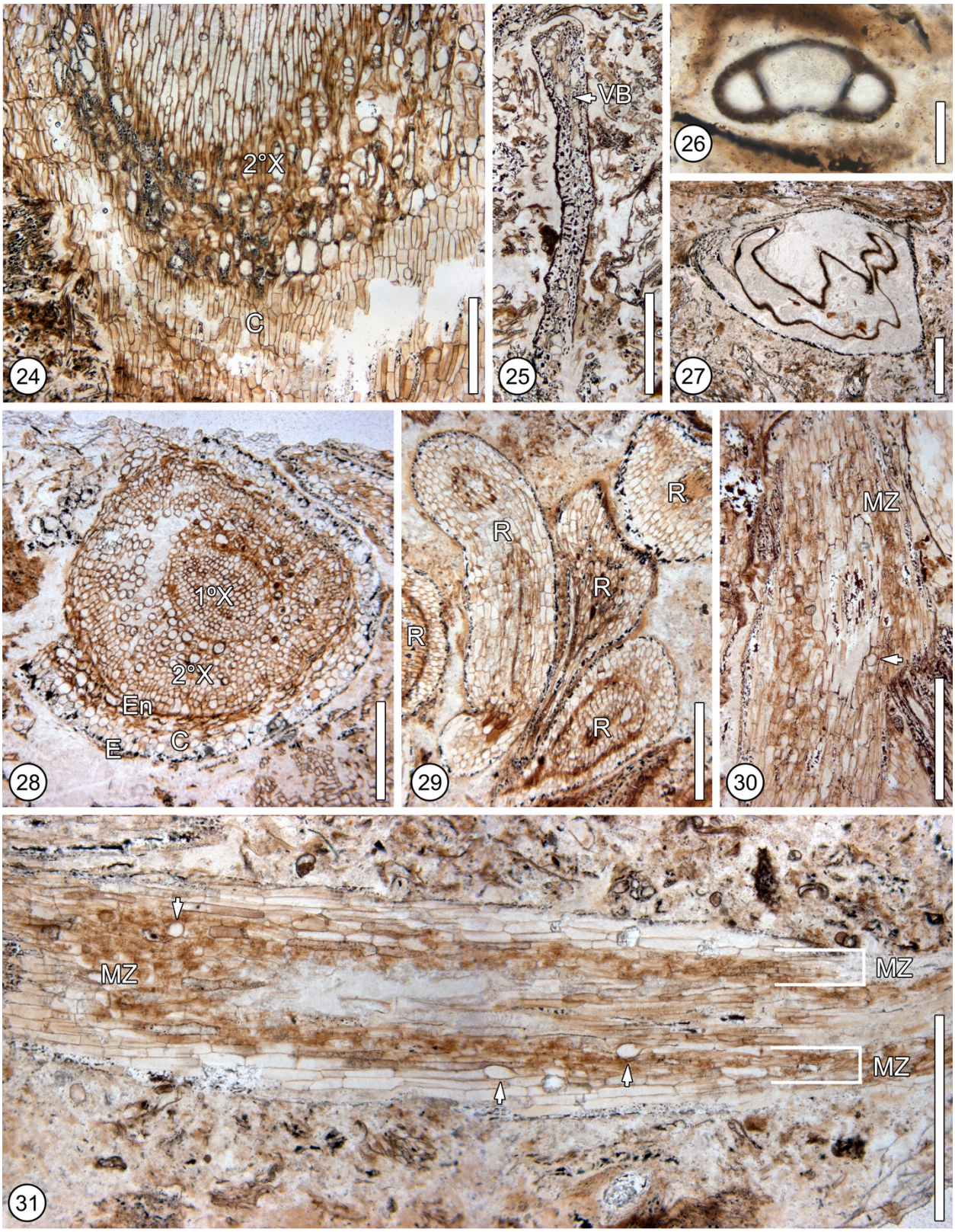

Chapter 4. Plate 4. Components of the *Notophytum krauselii* plant from permineralized peat, Middle Triassic of Antarctica, including arbuscular rootlets.

Chapter 4. Plate 5. Vesicular-arbuscular mycorrhizae in *Notophytum krauselii* rootlets.

Plate 5, Figure 32. Vegetative hypha of mycorrhizal fungus in cortical cell of rootlet. Arrow = transverse septum. Slide no. 26590; scale bar = 25 μm.

Plate 5, Figure 33. Larger, second type of hypha in cortical cell of rootlet, which may not be associated with the mycorrhizal fungus, as no direct connection has been found. Arrow = transverse septum. Slide no. 26590; scale bar = 25 μm.

Plate 5, Figure 34. Right-angle branch of vegetative mycorrhizal fungus. Arrow = point of branching. Slide no. 26590; scale bar = 25 μm.

Plate 5, Figure 35. Possible T–branch or cruciform branch pattern of hypha in rootlet cortical cell. Arrow = possible point of hyphal attachment which would represent a cruciform branching pattern. Slide no. 26590; scale bar = 25 μm.

Plate 5, Figure 36. Y–branching mycorrhizal vegetative hyphae. Slide no. 26590; scale bar = 25 μm.

Plate 5, Figure 37. Swelling or expansion of vegetative hyphae. Arrow = septum. Slide no. 26590; scale bar = 25 μm.

Plate 5, Figure 38. H–branch (HB) of vegetative mycorrhizal fungus. Slide no. 26590; scale bar = 25 μm.

Plate 5, Figure 39. Dense clustering of arbuscules in mycorrhizal zone of rootlet. Darkened area to the left of single spherical vesicle (V) represents a preservational artifact. Slide no. 26590; scale bar = 25 μm.

Plate 5, Figure 40. Single attached arbuscule in cortical cell of rootlet showing region of attachment (arrow). Slide no. 26590; scale bar = 25 μm.

Plate 5, Figure 41. Single arbuscule in cortical cell of rootlet with right-angle attachment point type. Arrow = point of attachment to vegetative hypha Slide no. 26590; scale bar = 25 µm.

Plate 5, Figure 42. Single attached arbuscule in cortical cell of rootlet with direct attachment point on side of vegetative hypha. Arrow = point of attachment. Slide no. 26590; scale bar = 25 µm.

Plate 5, Figure 43. Single attached spherical vesicle (V). Arrows = septa on vegetative hypha. Slide no. 26590; scale bar = 25 µm.

Plate 5, Figure 44. Single oblong to ellipsoidal vesicle (V). Arrow = septum on vegetative hypha. Slide no. 26590; scale bar = 25 µm.

Plate 5, Figure 45. Single oblong to ellipsoidal vesicle (V). Arrow = septum on vegetative hypha. Note poorly preserved material or preservational artifact (decayed organic matter?) in cortical cell above. Slide no. 26590; scale bar = 25 µm.

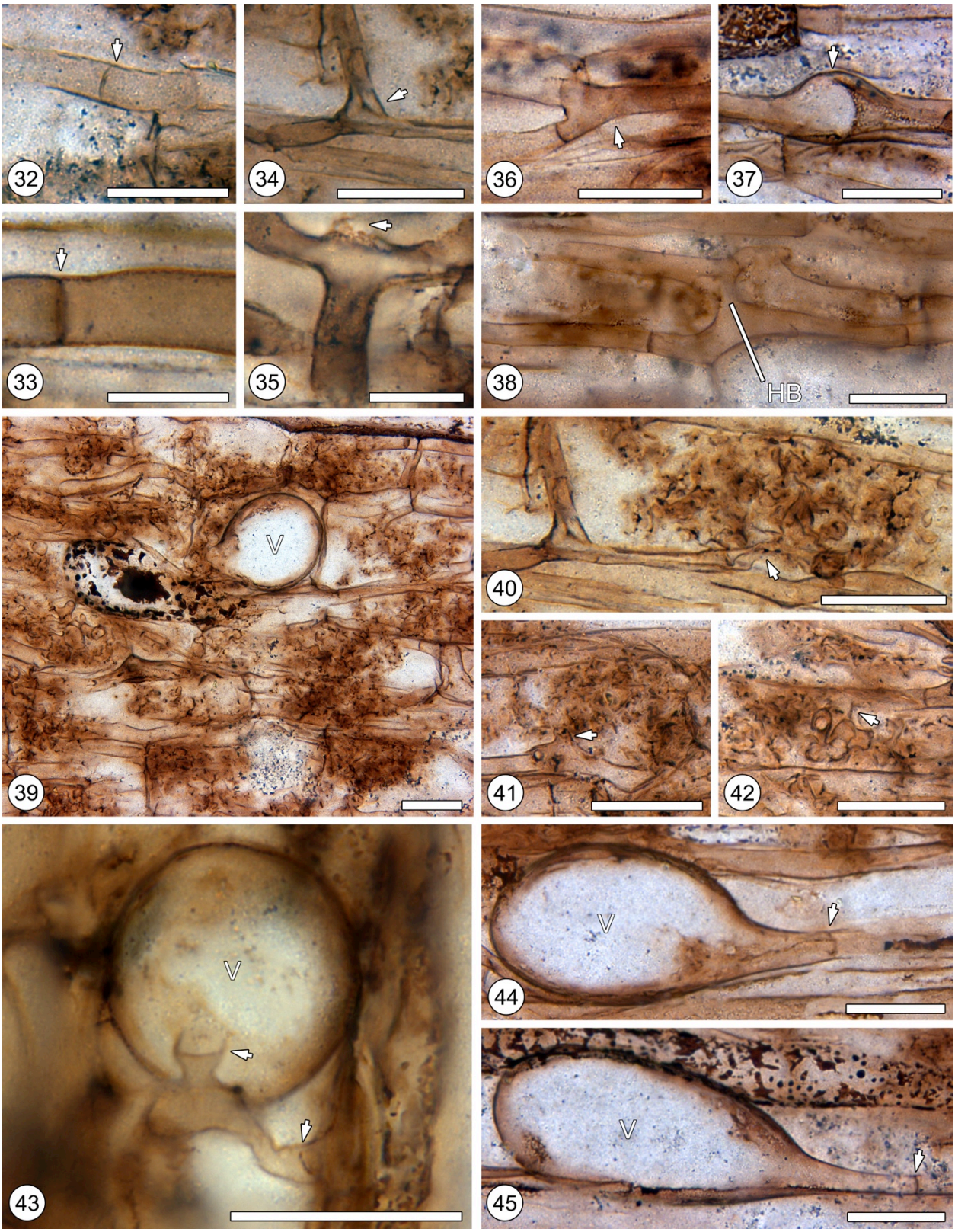

Chapter 4. Plate 5. Vesicular-arbuscular mycorrhizae in *Notophytum krauselii* rootlets.

Chapter 5. Plate 6. Locality, reconstruction, and plant components of *Ashicaulis*.

Plate 6, Figure 46. Excavation of Ashicaulis root ball at Fremouw Peak during 2010-2011 field season. Image courtesy of R. Serbet.

Plate 6, Figure 47. Surface view of root ball (arrow) at Fremouw Peak during 2010-2011 field season. Image courtesy of R. Serbet.

Plate 6, Figure 48. Exposed surface view of root ball (rock hammer for scale) at Fremouw Peak during 2010-2011 field season. Note weathered surface. Image courtesy of R. Serbet.

Plate 6, Figure 49. Overall view of *Ashicaulis* root ball system. Note light tan, weathered portion, and black portion of specimen which was buried. 17608; scale bar = 20 cm.

Plate 6, Figure 50. Reconstruction of *Ashicaulis* root ball system based on features found in acetate peels. Several petiole and stem traces were found, and possible pinnules, but with no attachment points (arrow). 17608; scale bar = 20 cm.

Plate 6, Figure 51. Stem oblique cross section with brackets surrounded by several sclerotic nests. Note middle of stem has rootlets in center. 17608; scale bar = 5 mm

Plate 6, Figure 52. Transverse section of frond trace with enrolled margins. 17608; scale bar = 1 mm.

Plate 6, Figure 53. Isolated longitudinal section of seed within matrix. 17608; scale bar = 1mm.

Plate 6, Figure 54. Partial fern annulus with prominent sporangial wall (arrows). 17608; scale bar = 1 mm.

Plate 6, Figure 55. Two morphotypes of rootlets within *Ashicaulis* matrix. Root type 1 (Br) and Root type 2 (Bl). Each root type has a distinct associated mycoflora. 17608; scale bar = 1 mm.

Plate 6, Figure 56. Individual root hair with bulbous base and elongated hair (arrow). 17608; scale bar = 25 μm.

Plate 6, Figure 57. Overview of *Ashicaulis* root type 1 with prominent root hairs (arrow). 17608; scale bar = 100 μm.

Plate 6, Figure 58. Overview of extant *Osmunda* root with prominent root hairs (arrow). Courtesy of CUPAC 620-7; scale bar = 100 μm.

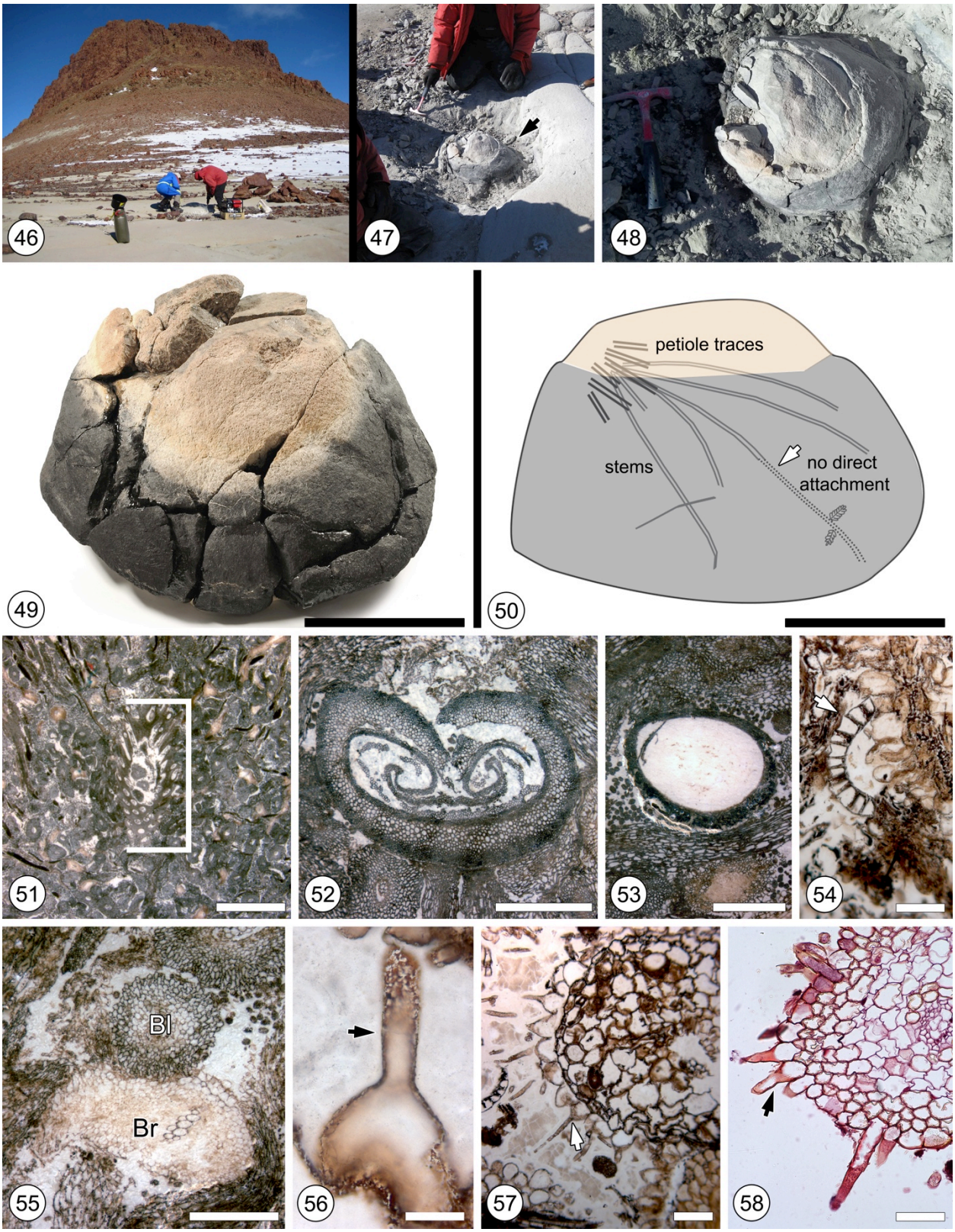

Chapter 5. Plate 6. Locality, reconstruction, and plant components of *Ashicaulis*.

Chapter 5. Plate 7. Root endophytes of *Ashicaulis*.

Plate 7, Figure 59. Longitudinal section of root type 1 with cortex infected with fungi (white arrow) and isolated host response cell (black arrow). 17608; scale bar = 100 µm.

Plate 7, Figure 60. Detail of longitudinal section of root type 1 with cortex infected with fungal hyphae (white arrow). 17608; scale bar = 25 µm.

Plate 7, Figure 61. Cruciform branching hyphae with septa at branching point (arrow). 17608; scale bar = 25 µm.

Plate 7, Figure 62. Cluster of 3 globose and elongated vesicles (V) within cortex of root type 1. 17608; scale bar = 25 µm.

Plate 7, Figure 63. Isolated vesicles (V) attached to parental hypha (arrow) within cortex of root type 1. 17608; scale bar = 25 µm.

Plate 7, Figure 64. Isolated vesicles (V) with tapered point, attached to branching parental hypha (arrow) within cortex of root type 1. 17608; scale bar = 25 µm.

Plate 7, Figure 65. Isolated globose vesicles (V), attached to parental hypha (arrow) within cortex of root type 1. 17608; scale bar = 25 µm.

Plate 7, Figure 66. Paired vesicles (V) one with tapered point (arrow) adjacent to globose vesicle within cortex of root type 1. 17608; scale bar = 25 µm.

Plate 7, Figure 67. Hourglass shaped vesicle (V) (arrow) attached to hypha within cortex of root type 1. 17608; scale bar = 10 µm.

Plate 7, Figure 68. Isolated cell from Plate 7, Figure 59 (black arrow in that figure) with thick cell walls (arrow) that may represent host response to spheroidal structures within lumen. 17608; scale bar = 25 µm.

Plate 7, Figure 69. Isolated cell with thick cell walls (arrow) that may represent host response to spheroidal structures within lumen. 17608; scale bar = 25 µm.

Plate 7, Figure 70. Longitudinal section of root type 1 fungi include less densely infected mycelia within cortical cells (arrow). 17608; scale bar = 100 µm.

Plate 7, Figure 71. Vesicles (V) with only globose morphology attached to hypha with no septa at base (white arrow), and the terminal ends of some hyphae can result in highly dichotomized, amorphous structures (black arrow) within cortical cells. 17608; scale bar = 25 µm.

Plate 7, Figure 72. Hyphal types include smaller diameter, septate mycelia (white arrow) that can terminally end in small bulbous structures (black arrow) that extend through cortical cells intracellularly. 17608; scale bar = 25 µm.

Plate 7, Figure 73. An isolated curved hypha has been observed penetrating cortical cell walls with thicker regions of the cell (possible host response, arrow) where the fungus penetrates the cell wall. 17608; scale bar = 25 µm.

Plate 7, Figure 74. Transverse section of single example of root type 1 exhibits densely colonized mycelia; colonized areas are bracketed. 17608; scale bar = 100 µm.

Plate 7, Figure 75. Detail of Plate 7, Fig. 74 Transverse of root type 1 exhibits densely colonized mycelia with vesicles (V). 17608; scale bar = 100 µm.

Plate 7, Figure 76. Detail of Plate 7, Fig. 74 Transverse of root type 1 exhibits densely colonized mycelia with septate hyphae (arrow) and double walled vesicles (V). 17608; scale bar = 100 µm.

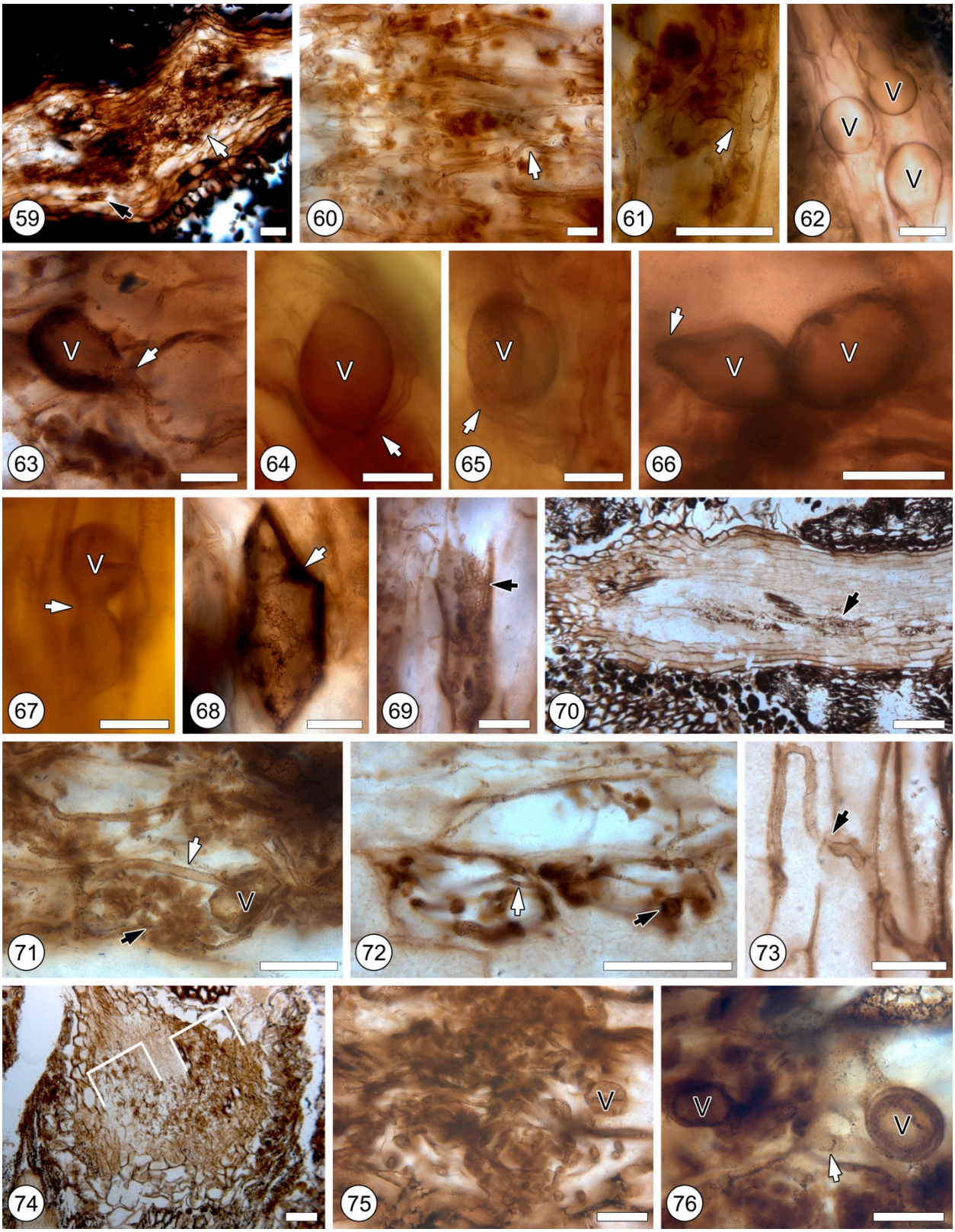

Chapter 5. Plate 7. Root endophytes of *Ashicaulis*.

Chapter 5. Plate 8. Chytrids, degradational fungi, and fungal-like organisms.

Plate 8, Figure 77. In addition to chytrids, large spores (arrow) with an internal single thin cell layer can be found within poorly preserved regions of the rootlets, typically in areas where the cells are separated. 17608; scale bar = 25 μm.

Plate 8, Figure 78. Chytrid with single cell wall layer within tracheid of root type 2. 17608; scale bar = 10 μm.

Plate 8, Figure 79. Chytrid with double cell wall layers within tracheid of root type 2. 17608; scale bar = 10 μm.

Plate 8, Figure 80. Paired chytrids with double cell wall layers within tracheid of root type 2. 17608; scale bar = 10 μm.

Plate 8, Figure 81. Chytrid with thick double cell wall layers within tracheid of root type 2. 17608; scale bar = 10 μm.

Plate 8, Figure 82. Chytrid with rhizomycelia (arrows) within tracheid of root type 2. 17608; scale bar = 10 μm.

Plate 8, Figure 83. Chytrid with operculum (arrow) within tracheid of root type 2. 17608; scale bar = 10 μm.

Plate 8, Figure 84. Chytrid with papilla (arrow) within tracheid of root type 2. 17608; scale bar = 10 μm.

Plate 8, Figure 85. Chytrid within vascular tissue (arrow) within tracheid of root type 2; cluster of chytrids bracketed. 17608; scale bar = 25 μm.

Plate 8, Figure 86. Root type 2 is with thick cell walls with partial root hairs. 17608; scale bar = 100 μm.

Plate 8, Figure 87. Root type 2 include highly degraded cell walls, likely as a result of fungal degradation. 17608; scale bar = 25 μm.

Plate 8, Figure 88. Hyphae can penetrating directly through cell walls (arrows). 17608; scale bar = 25 μm.

Plate 8, Figure 89. Septate hypha (arrow) in root type 2 tracheid. 17608; scale bar = 25 μm.

Plate 8, Figure 90. Longitudinal section of root type 2, individual spores (S) (possibly vesicles?) occlude the cells. 17608; scale bar = 25 μm.

Plate 8, Figure 91. Highly degraded chain like cells fill the cell lumina of degraded root type 2 (arrow). 17608; scale bar = 25 μm.

Plate 8, Figure 92. Detail of highly degraded chain like cells fill the cell lumina of degraded root type 2 (arrow). 17608; scale bar = 10 μm.

Plate 8, Figure 93. Isolated tracheid with highly degraded chain like cells fill the cell lumina of degraded root type 2 (arrow). 17608; scale bar = 25 μm.

Plate 8, Figure 94. Yeast-like, chains of monilioid cells that fully occlude cells of root type 1 (arrows). 17608; scale bar = 25 μm.

Plate 8, Figure 95. Detail of Yeast-like, chains of monilioid cells that fully occlude cells of root type 1 (arrow). 17608; scale bar = 25 μm.

Plate 8, Figure 96. Pair of Peronosporomycetes (P) in diameter that lacks the typical antler-like projections. 17608; scale bar = 25 μm.

Plate 8, Figure 97. Spore with external ornamentation in the form of ovoid cells and a possible opening on the surface of the structure. 17608; scale bar = 50 μm.

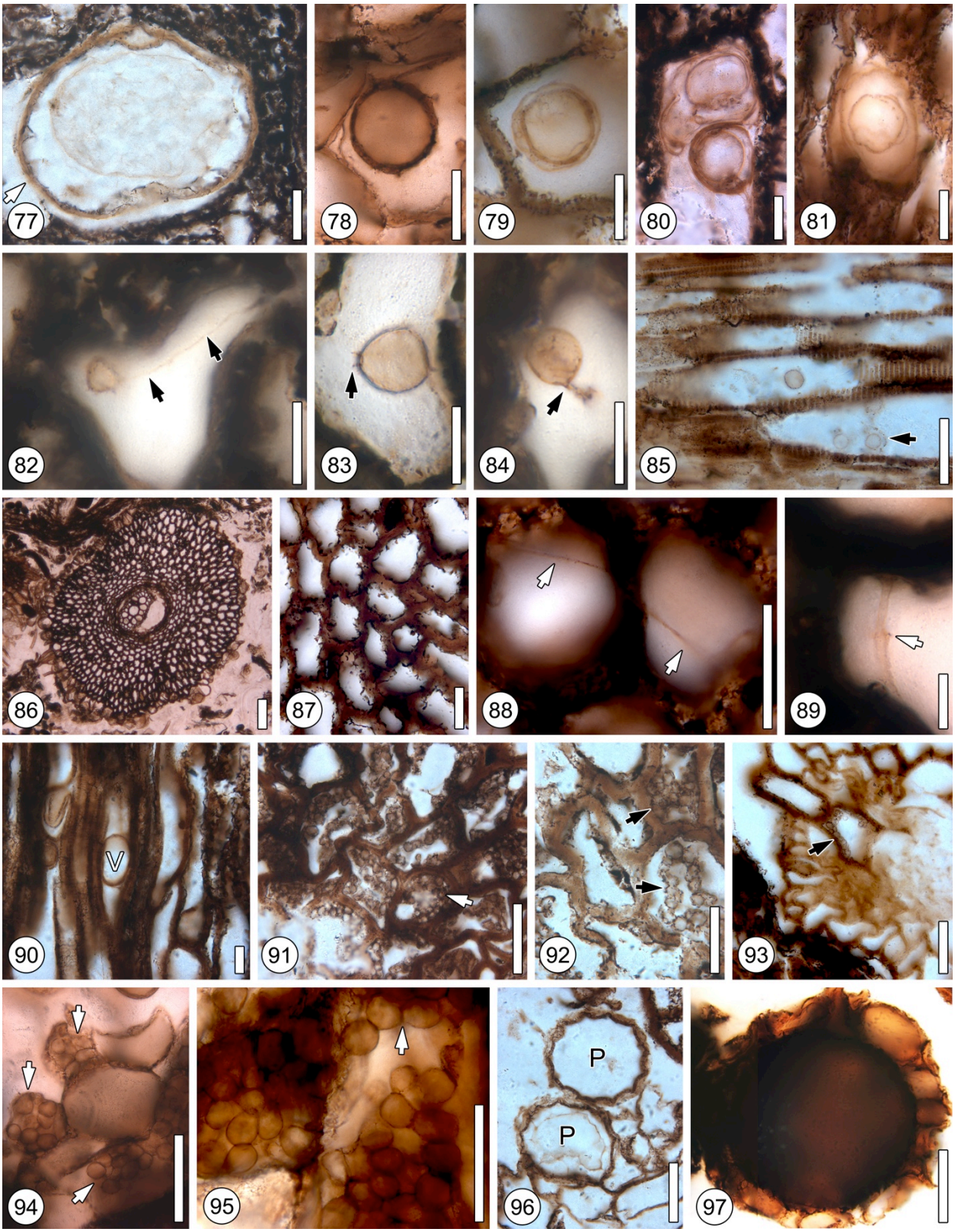

Chapter 5. Plate 8. Chytrids, degradational fungi, and fungal-like organisms.

Chapter 5. Plate 9. Arthropod evidence of *Ashicaulis*.

Plate 9, Figure 98. Thin sections and peels of the *Ashicaulis* root ball contains numerous coprolites (arrow). 17608; scale bar = 250 μm.

Plate 9, Figure 99. There is a large, structure 5 mm in length with 3 distinct cell wall layers that may represent an arthropod cuticle (C). 17608; scale bar = 100 μm.

Plate 9, Figure 100. Cell wall layer **1** (~50 μm thick): striated and individual columns can be discerned, which is directly adjacent to cell wall layer **2** (2-3 μm thick): thin, more opaque than cell wall layer 1 and lack striation, and cell wall layer **3** (5 μm thick): there is a solid, layer that lack striations, thicker than cell wall layer 2. 17608; scale bar = 25 μm.

Plate 9, Figure 101. Coprolites associated with matrix hyphae with swellings (arrows). 17608; scale bar = 25 μm.

Plate 9, Figure 102. Coprolites associated with matrix hyphae (arrows). 17608; scale bar = 25 μm.

Plate 9, Figure 103. Coprolites associated with branching matrix hyphae (arrows). 17608; scale bar = 25 μm.

Plate 9, Figure 104. Coprolites can be dense to composed of fragmentary substances. 17608; scale bar = 25 μm.

Plate 9, Figure 105. Large circular coprolite. 17608; scale bar = 25 μm.

Plate 9, Figure 106. Small circular coprolite. 17608; scale bar = 25 μm.

Plate 9, Figure 107. Large ellipsoidal coprolite. 17608; scale bar = 25 μm.

Plate 9, Figure 108. Small ellipsoidal coprolite. 17608; scale bar = 25 μm.

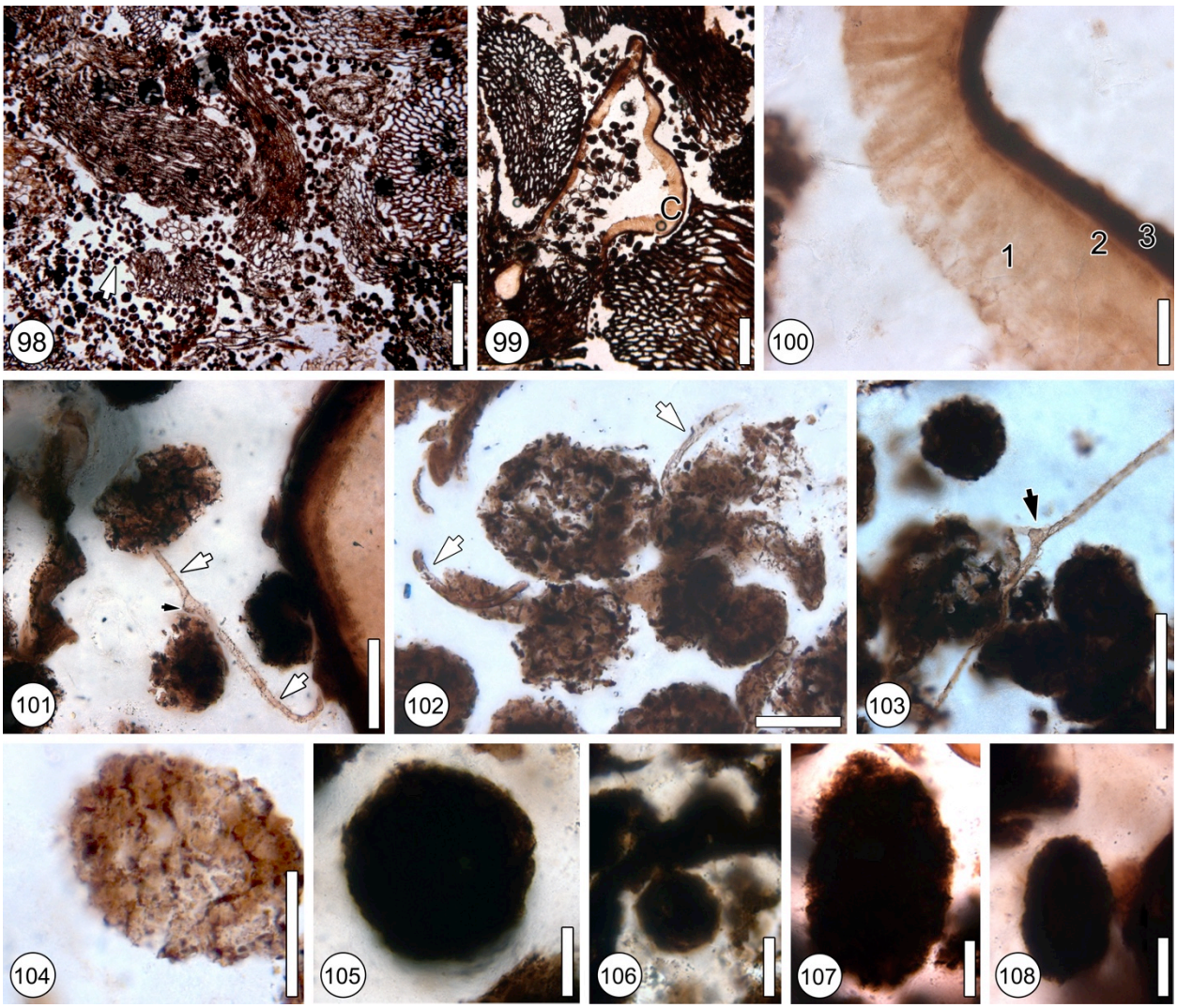

Chapter 5. Plate 9. Arthropod evidence of *Ashicaulis*.

Chapter 6. Plate 10. Overview of Permian stem and root wood, fungal remains.

Plate 10, Figure 109. Highly degraded hand specimen of *Australoxylon* stem wood with poorly preserved tree rings (white arrows) and pockets (black arrow). Scale bar = 1 cm.

Plate 10, Figure 110. Highly degraded hand specimen of *Vertebraria* root wood with distinct lacunae (white arrow) and pockets (black arrow). Scale bar = 1 cm.

Plate 10, Figure 111. Longitudinal section of stem wood. All specimens in this study share are mixed-type pitting on the tracheid radials, cluster of 5 pits bracketed (MP). Scale bar = 25 cm.

Plate 10, Figure 112. Septate hypha in transverse section tracheid cell (arrow). Scale bar = 10 μm.

Plate 10, Figure 113. Right angle branching septate hypha in longitudinal tracheid cells (arrows). Scale bar = 25 μm.

Plate 10, Figure 114. Right angle branching septate hypha in transverse section of tracheid cells (arrow). Scale bar = 10 μm.

Plate 10, Figure 115. Curved branch hyphae (white arrow) and cruciform branching septate hypha in transverse tracheid cells (black arrow). Scale bar = 10 μm.

Plate 10, Figure 116. Simple clamp connection. Scale bar = 10 μm.

Plate 10, Figure 117. Simple-intermediate medallion clamp connection. Scale bar = 10 μm.

Plate 10, Figure 118. Medallion clamp connection. Scale bar = 10 μm.

Plate 10, Figure 119. Whorled clamp connection. Scale bar = 10 μm.

Plate 10, Figure 120. Partially formed clamp connection. Scale bar = 10 μm.

Plate 10, Figure 121. Hypha penetrating directly through transverse multiple cells. (arrows). Scale bar = 25 µm.

Plate 10, Figure 122. Longitudinal section of tracheid with hypha that can travel via rays (arrows). Scale bar = 25 µm.

Plate 10, Figure 123. Transverse section of tracheids with cross sections of hyphae within cell lumina (arrow). Scale bar = 25 µm.

Plate 10, Figure 124. Transverse section of tracheids with cross sections of hyphae directly adjacent to cell lumen wall (arrow). Scale bar = 25 µm.

Plate 10, Figure 125. Transverse section of hyphae penetrating via pits (arrow). Scale bar = 25 µm.

Plate 10, Figure 126. Longitudinal section of hyphae penetrating via pits (arrow). Scale bar = 25 µm.

Plate 10, Figure 127. Transverse section of hyphae penetrating via pits (arrows); hypha can be discerned traversing via pit. Scale bar = 10 µm.

Plate 10, Figure 128. Transverse section of hyphae penetrating via pits (black arrow); area where hypha degraded cell wall (white arrow). Scale bar = 10 µm.

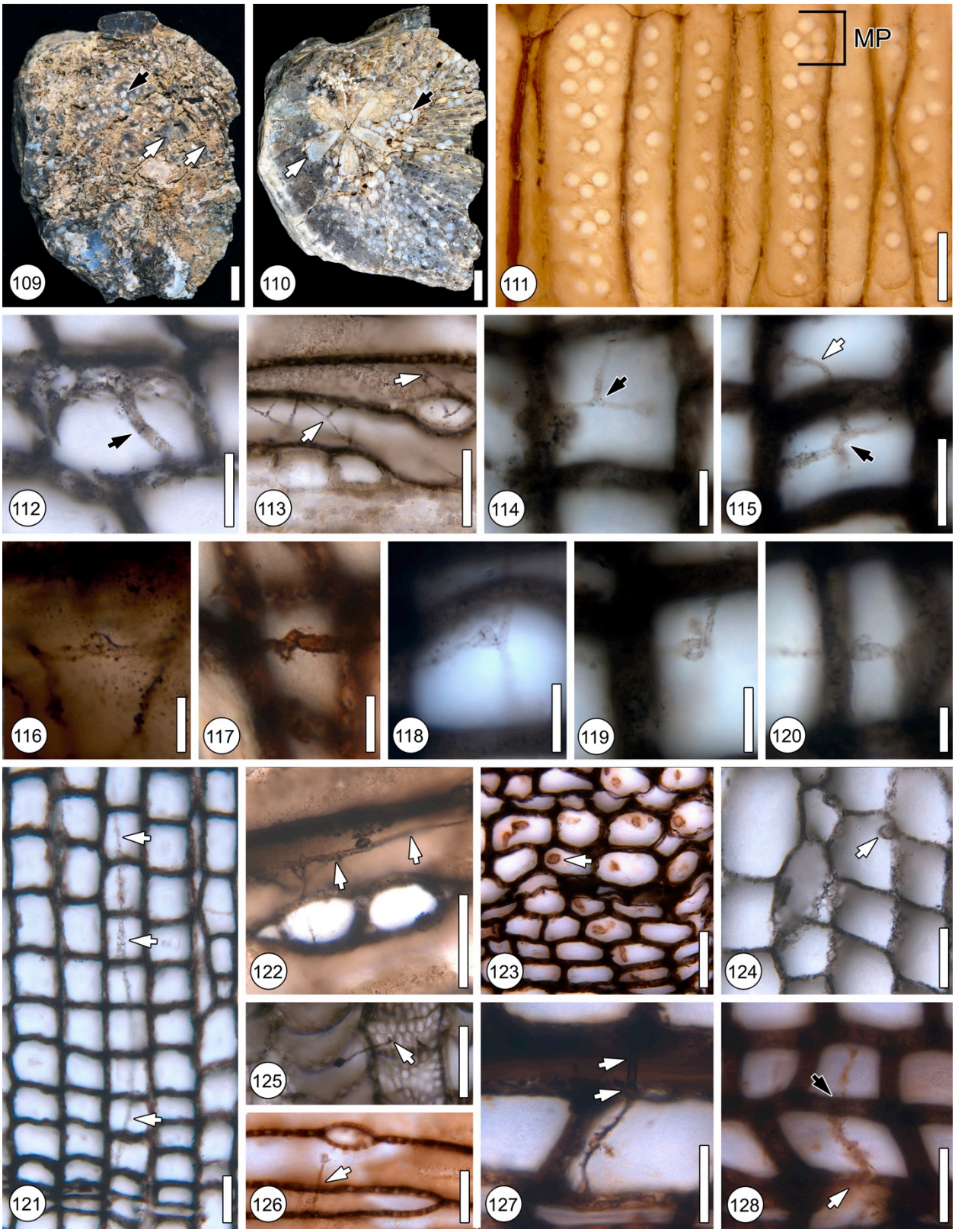

Chapter 6. Plate 10. Overview of Permian stem and root wood, fungal remains.

Chapter 6. Plate 11. Permian stem and root wood decay features.

Plate 11, Figure 129. Overview of transverse section of wood decay pockets (P). Scale bar = 500 µm.

Plate 11, Figure 130. Overview of longitudinal section of spindle shaped wood decay pockets (P). Scale bar = 500 µm.

Plate 11, Figure 131. Early stage of wood decay, lighter color delignified cells adjacent to normal cells (arrow). Scale bar = 500 µm.

Plate 11, Figure 132. Detail of early stage of wood decay, lighter color delignified cells (D) adjacent to normal cells. Scale bar = 100 µm.

Plate 11, Figure 133. Intermediate stage of wood decay, lighter color delignified cells (D) adjacent to pocket (P). Scale bar = 500 µm.

Plate 11, Figure 134. Late stage of wood decay, lighter color delignified cells (D) adjacent to large pocket. Margin of pocket is irregular (IP), i.e., portions of tracheids extending into pocket. Scale bar = 500 µm.

Plate 11, Figure 135. Transverse section of stem wood with no decay symptoms or signs. Scale bar = 25 µm.

Plate 11, Figure 136. Distal portion of same specimen as Plate 11, Fig. 135, of stem wood with decay symptoms or signs. Areas of delignified cells and complete cell wall degradation (arrows). Scale bar = 25 µm.

Plate 11, Figure 137. Complete delignification of cell walls (arrows) with outline of cell wall, adjacent to normal tracheid cells. Scale bar = 25 µm.

Plate 11, Figure 138. Intermixed delignification of cell walls (arrows) with outline of cell wall, adjacent to normal tracheid cells. Scale bar = 25 µm.

Plate 11, Figure 139. Portions of cell walls completely fractured, possibly by wood degrading fungi. Scale bar = 25 μm.

Plate 11, Figure 140. Similar fracturing of cell wall as in Plate 11, Figure 139, adjacent to delignified cells. Scale bar = 25 μm.

Plate 11, Figure 141. Later stage of fracturing of cell wall as in Plate 11, Figure 139, adjacent to progressed decay in delignified cells. Scale bar = 25 μm.

Plate 11, Figure 142. Example of powered, fragmentary appearance of wood tracheids; this is a rare occurrence in specimens. Scale bar = 25 μm

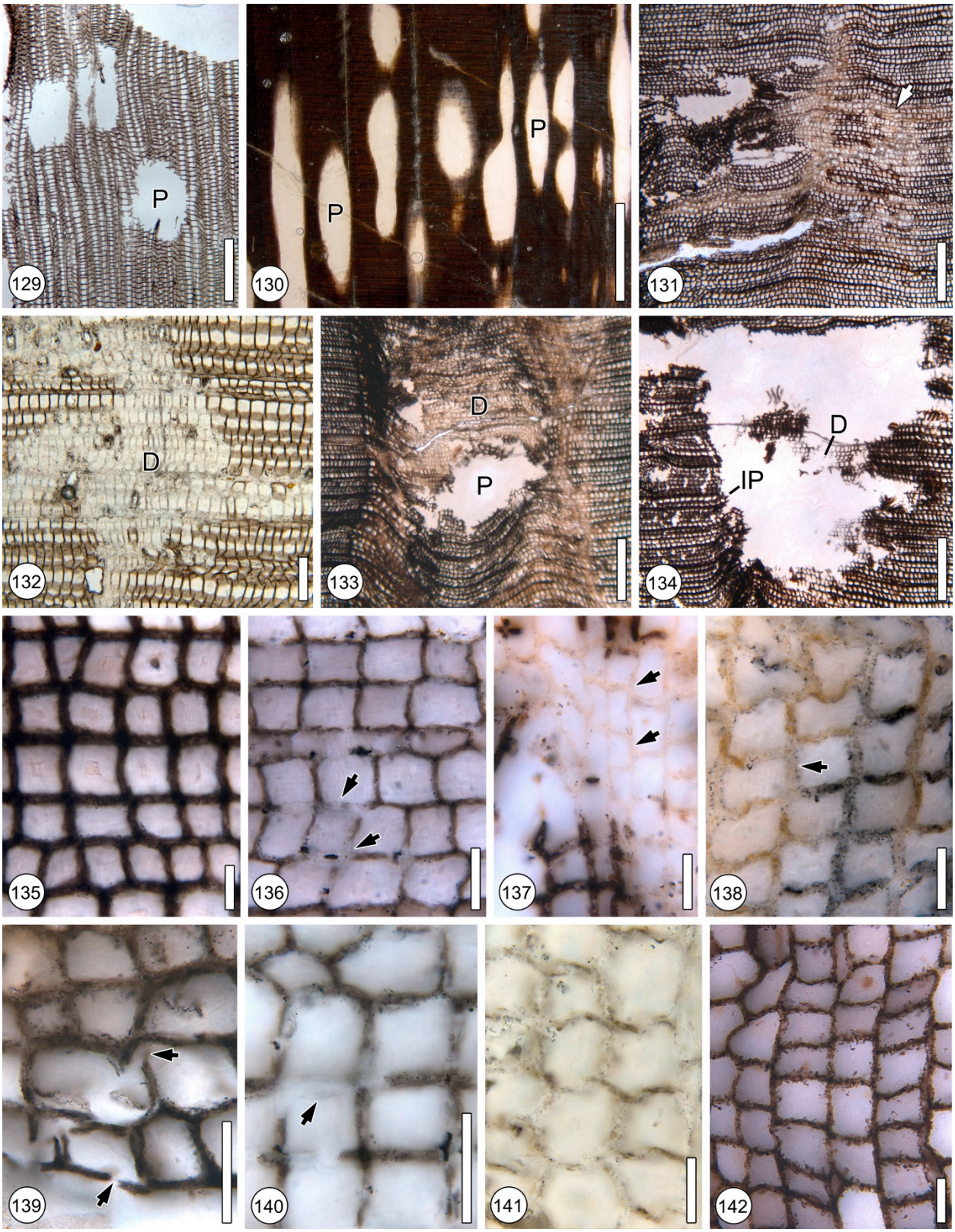

Chapter 6. Plate 11. Permian stem and root wood decay features.

Chapter 6, Plate 12. Wood host responses, arthropod interactions, spores.

Plate 12, Figure 143. Evenly swollen cell layers (arrow) separated from other cell wall layers (S). Scale bar=25 µm.

Plate 12, Figure 144. Evenly swollen cell layers that almost occlude cell lumen (arrow). Scale bar=25 µm.

Plate 12, Figure 145. Evenly swollen cell with narrow middle lamella wall (arrow). Scale bar=25 µm.

Plate 12, Figure 146. Branching fungal hypha (arrow) in lumen of cell with evenly swollen cell layers. Scale bar=10 µm.

Plate 12, Figure 147. Swollen cell wall pinching into cell lumen (arrows). Scale bar=25 µm.

Plate 12, Figure 148. Area of middle lamella unevenly degraded encased in swollen cell layers (arrow). Scale bar=25 µm.

Plate 12, Figure 149. Transverse section of cells with degraded cells (D) adjacent to areas of swollen cell wall layer cells (arrow). Scale bar=25 µm.

Plate 12, Figure 150. Complete separation of cell wall layers (arrow). Cells fully occluded with opaque contents (O) and early stage of possible apposition (A). Scale bar=25 µm.

Plate 12, Figure 151. Transverse section of cells with degraded cells (D) adjacent to areas of swollen cell wall layer cells (H). Scale bar=25 µm.

Plate 12, Figure 152. Single hypha (arrows) penetrating directly through tracheid cell walls, surrounding cells are occluded with opaque contents. Scale bar=25 µm.

Plate 12, Figure 153. Transverse section of cells with tylosis formation (T) adjacent to occluded cells with opaque contents (O). Scale bar=25 µm

Plate 12, Figure 154. Transverse section of cells with tylosis formation (T) adjacent to apposition (A). Scale bar=25 µm.

Plate 12, Figure 155. Possible apposition (arrow) with central content (mineral formation?). Scale bar=25 µm.

Plate 12, Figure 156. Overview of wood with galleries filled with coprolites (arrow). Scale bar=100 µm.

Plate 12, Figure 157. Overview of wood with irregular bordered galleries with spores in surrounding matrix (arrow). Scale bar=100 µm.

Plate 12, Figure 158. Detail of spore in matrix, note no discernable surface or cell wall features (S). Scale bar=25 µm.

Plate 12, Figure 159. Detail of spore (S) in matrix with hyphal attachment (arrow). Scale bar=25 µm.

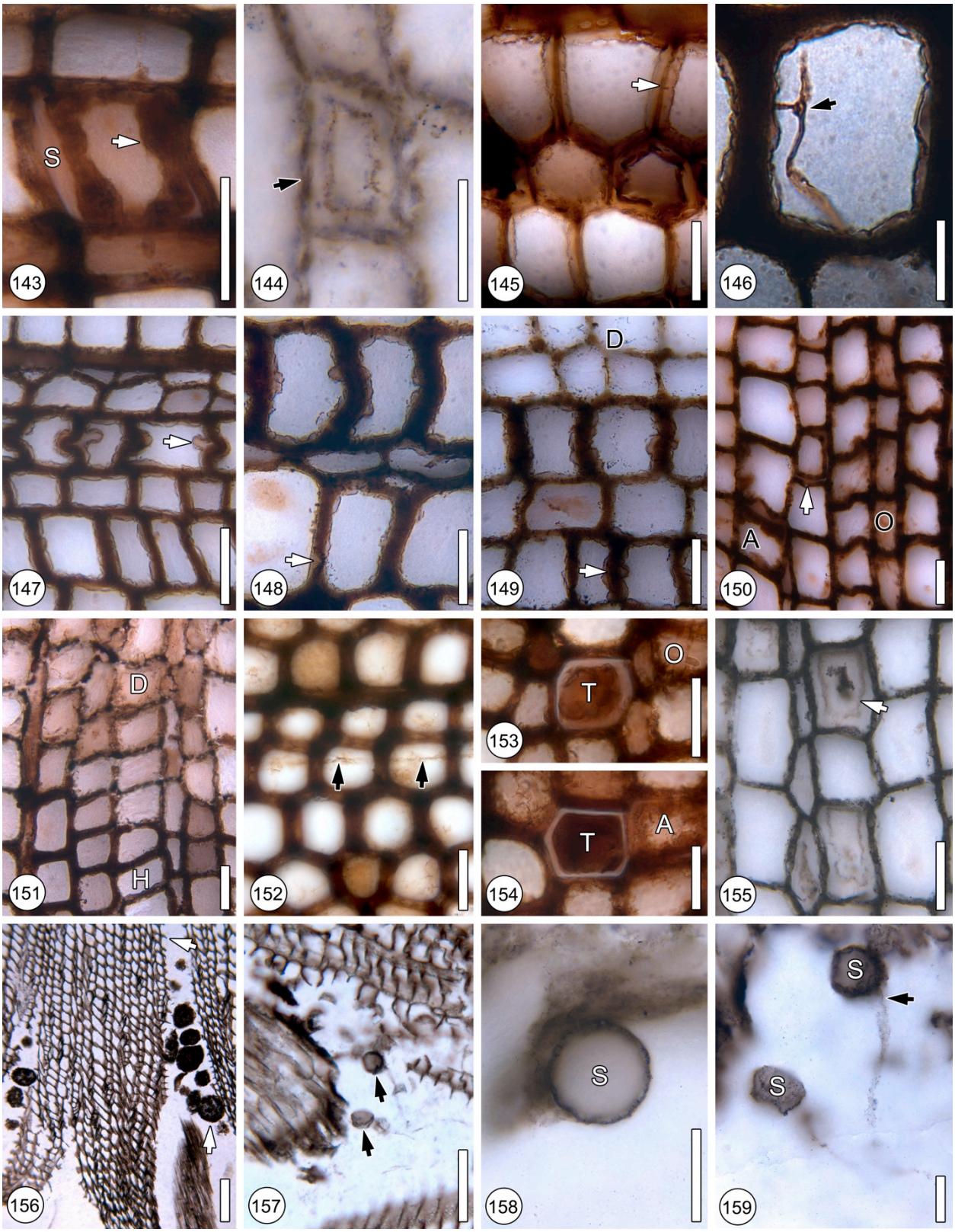

Chapter 6, Plate 12. Wood host responses, arthropod interactions, spores.

Chapter 6, Plate 13. SEM images of Permian wood fungi.

Plate 13, Figure 160. Longitudinal section of Permian stem wood with pocket rot. Single hypha (arrows) associated with tracheids. Scale bar=40 µm.

Plate 13, Figure 161. Longitudinal section of Permian stem wood with pocket rot. Single hypha (arrows) associated with tracheids. Possible microboring hole In tracheids (MB) Scale bar=40 µm.

Plate 13, Figure 162. Longitudinal section of Permian stem wood tracheids (T) with pocket rot. Well defined erosion troughs (arrow). Scale bar=100 µm.

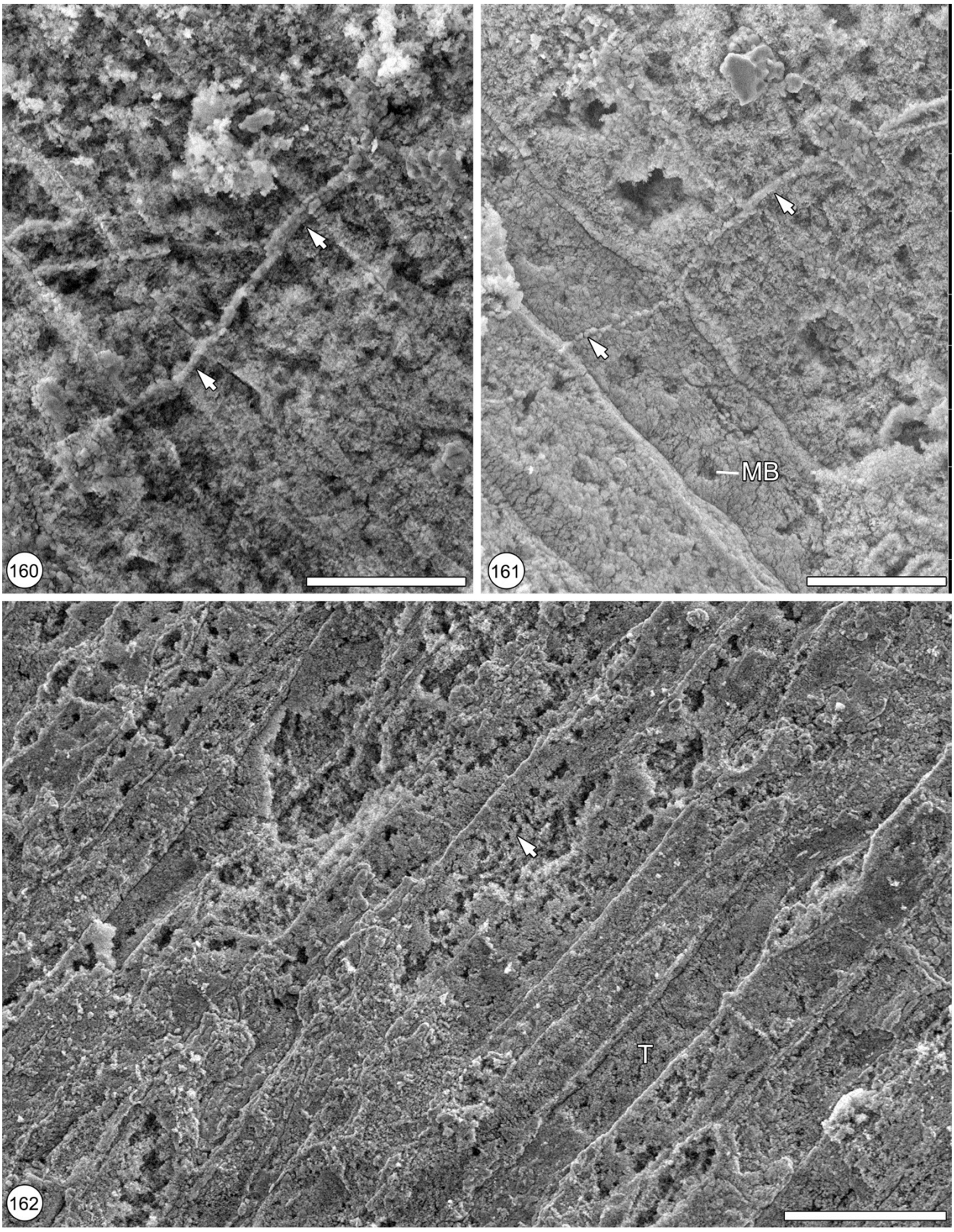

Chapter 6, Plate 13. SEM images of Permian wood fungi.

Table 2. Wood decay characters comparison of Permian and Triassic Antarctic wood studies. Summary comparison table of fungal, decay, host response, and arthropod evidence characters of current study and previous studies of Permian (and Triassic) woods from Antarctica that exhibited decay signs and symptoms.

Antarctic wood chaaracters	Results from current study *Australoxylon* and *Vertebraria*		Stubblefield and Talor, 1985; 1986 *"Araucaroxylon"* (Triassic)		*Vertebraria*		Weaver et al., 1997 *Australoxylon* spp.		Slater et al., 2012 *Australoxylon* and *Vertebraria*	
Fungal Characters										
Hyphae – branching	X		X		X					
Hyphae – clamp connections	X		X							
Hyphae – septate	X		X							
Fungi pass through cell walls	X		X		X					
Fungi pass through cells via pits	X		X							
Decay Characters										
Pockets within ring boundaries	X		X				X			
Pockets cut across ring boundaries	X		X				X			
Pockets localized on specimen	X		X				X			
Pockets throughout specimen	X		X				X			
Circular to ovoid pockets	X		X		X		X			
Irregular pockets	X		X		X		X		X	
Microborings in wood	X - SEM only						X			
Collapsed tracheids	X		X							
Pattern of degradation	X		X				X		X	
Degradational series of wood decay	X									
Host Responses										
Unevenly thickened walls (appositions?)	X		X				X			
Tylosis formation	X									
CODIT model example	X									
Arthropod Evidence										
Coprolites associated with decay	X						X		X	

Table 2. Wood decay characters comparison of Permian and Triassic Antarctic wood studies.

Figure 8. FTIR thin section results. Results from proof of concept study conducting FTIR analysis on thin section of permineralized material. **A.** Thinnest portion of thin section and corresponding spectra, which yielded best results of areas analyzed. **B.** Middle portion of thin section and corresponding section. **C.** Thickest portion of thin section and corresponding spectra, this area yielded poorest results of areas studied. **D-G.** Represents regions for interpretation of IR spectra of organics. **D.** Small mass single bonds. **E.** Triple bonds. **F.** Double bonds. **G.** Mass of attached atoms; organic finger print region.

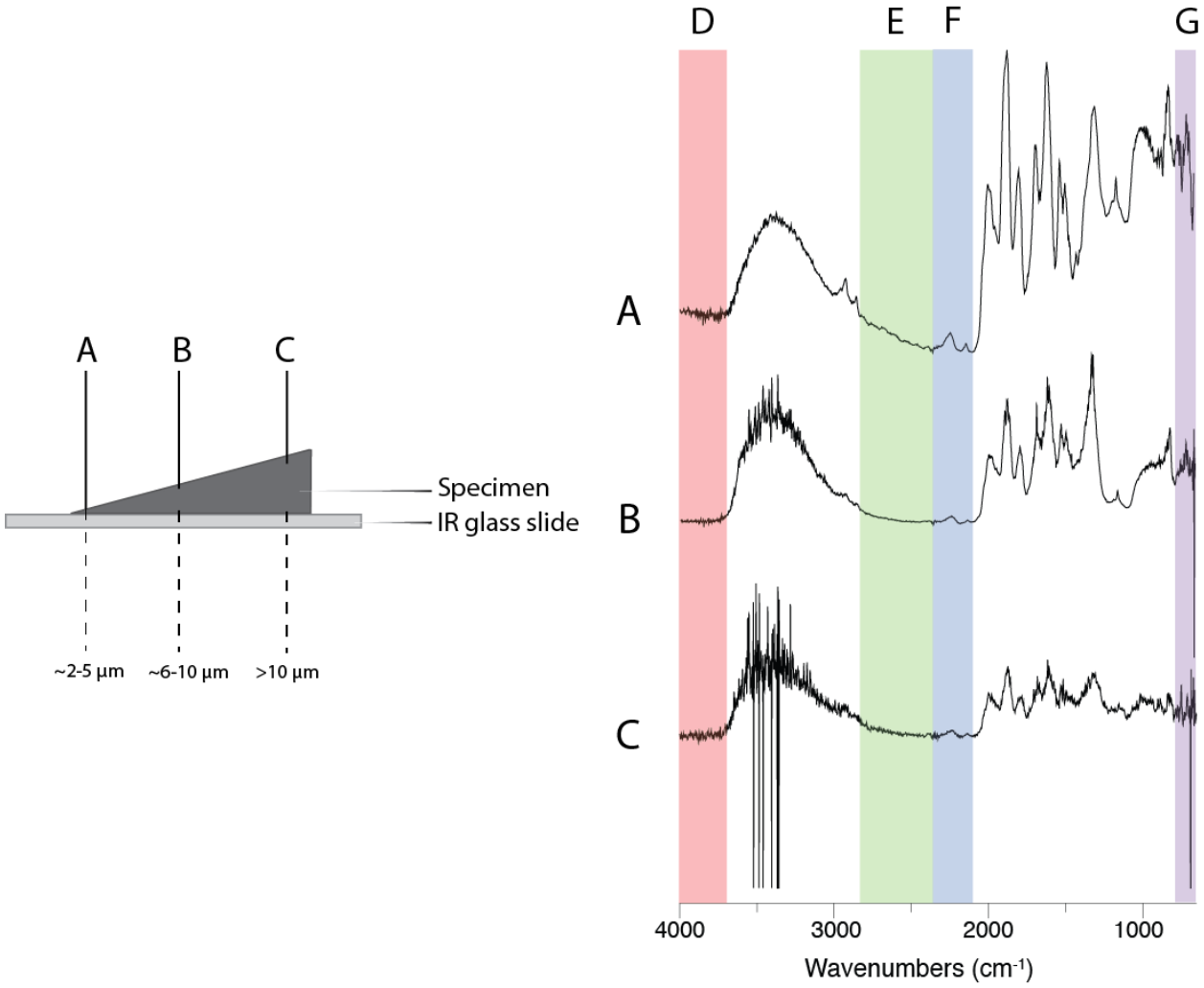

Figure 8. FTIR thin section results.

Table 3. FTIR identified peaks. Identified IR spectra peaks from Figure 8A using designations from Lin-Vien et al., 1991.

Frequency (cm-1)	Notes	Vibration
3376		OH
2958	shoulder	CH3 antisymmetric
2928		CH2 antisymmetric
2985		CH
2877		CH3 symmetric
2855		CH2 symmetric
2250		CO2 (atomosphere) antisymmetric
2137		CO2 (atomosphere) symmetric
1995		triple bond C
1982	? shoulder	triple bond C
1952	? shoulder	triple bond C
1875		C=O stretch
1797		C=O stretch
1689		C=C stretch
1612		C=C stretch/C=N amide?
1530		C=N
1492		ring stretch
1466	shoulder	CH2 deformation
1418		CO2 symmentric stretch
1345	? large shoulder	CH3 deformation
1298		CH deformation
1190	? shoulder	SO2 stretch
1160		SO2 symmentrical stretch
1001		ring breathing
933	wide band	ring vibration
820		C3O skeletal stretch
764		C4O skeletal stretch
700		ring vibration

Table 3. FTIR identified peaks.

Figure 9. Raman spectroscopy results of wood decay pocket. Results of screening via Raman spectroscopy to determine if specimens would yield biomarkers. Corresponding Raman spectra with area of Permian wood decay pocket examined. Scale bar=250 μm.

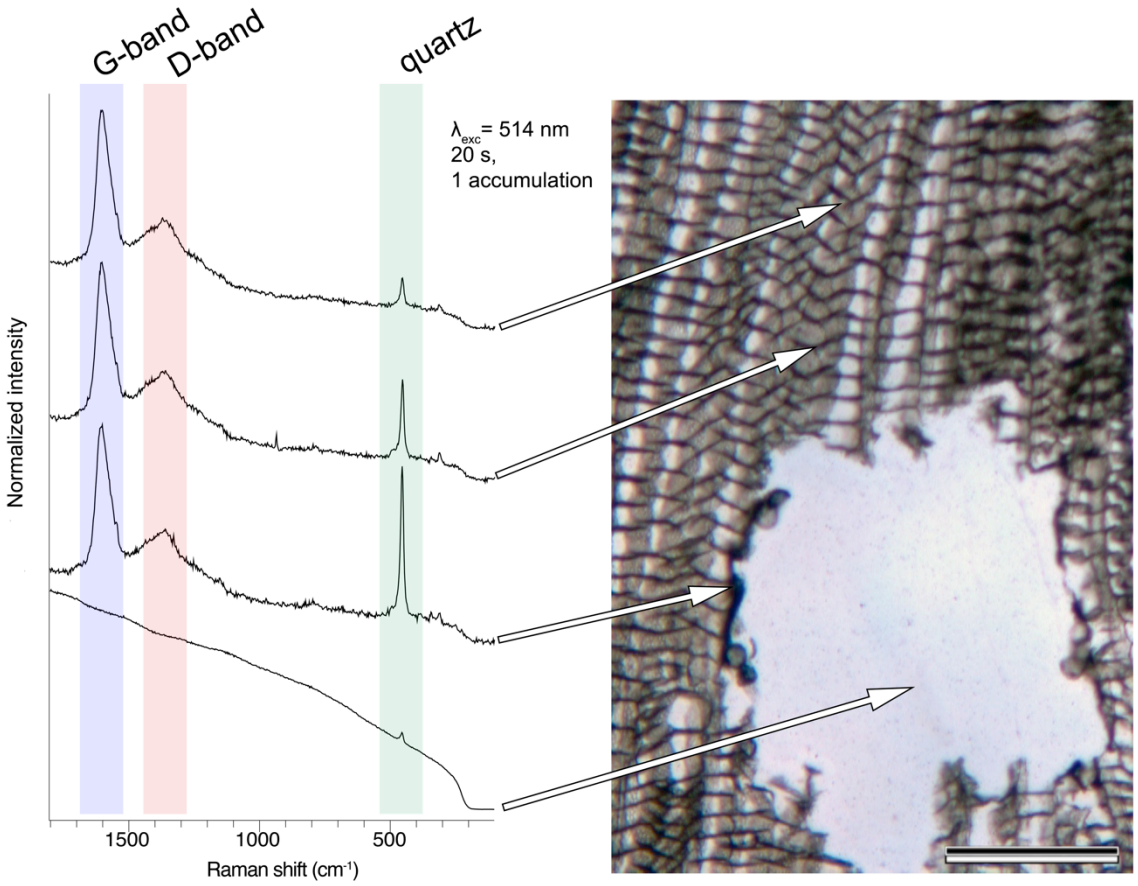

Figure 9. Raman spectroscopy results of wood decay pocket.

Figure 10. Biomarker results 1 – fluoranthene, pyrene. Results of lignin derivatives fluoranthene and pyrene in non-infected Permian wood (top) and Permian fungal infected wood (bottom). m/z value=202.

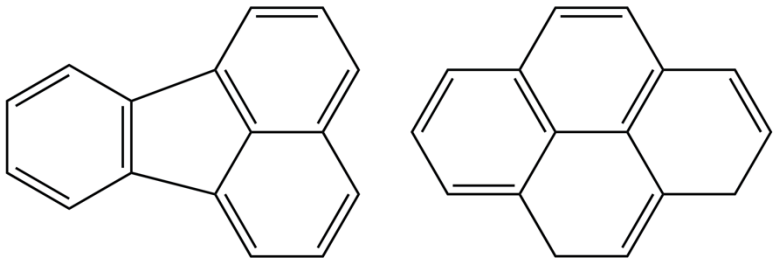

fluoranthene pyrene

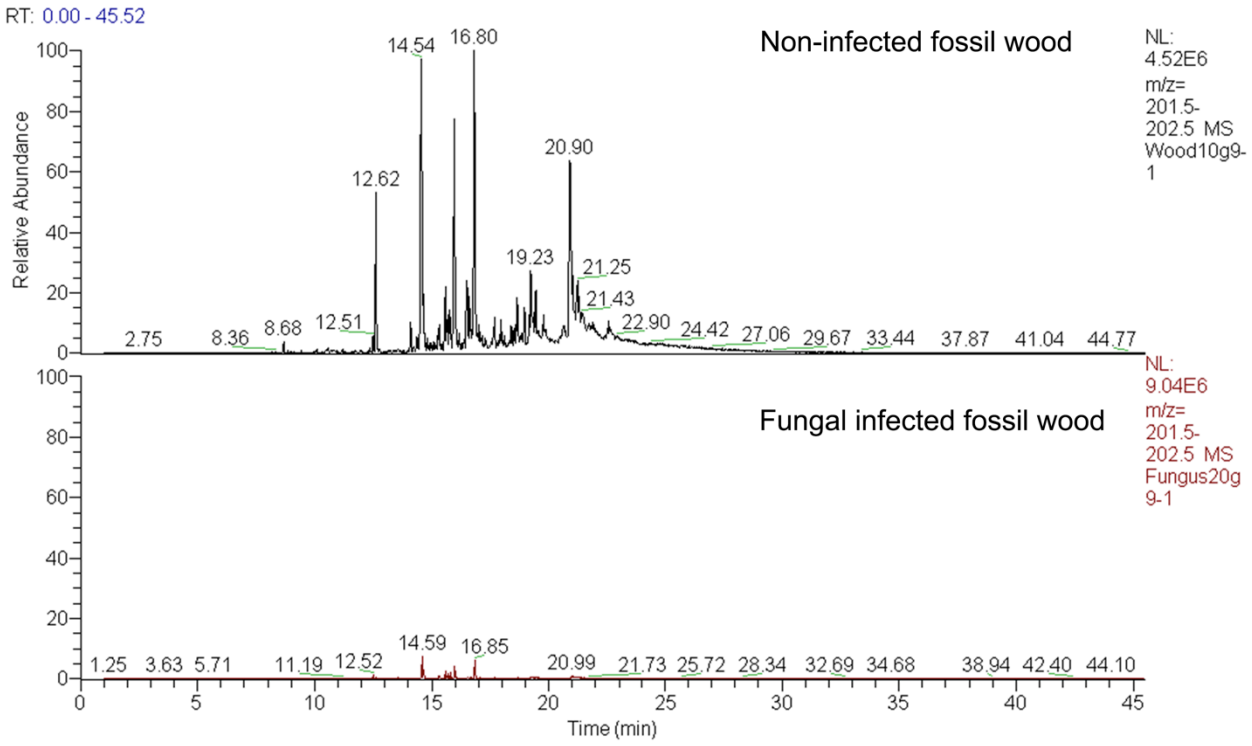

Figure 10. Biomarker results 1 – fluoranthene, pyrene.

Figure 11. Biomarker results 2 – phenanthrene. Results of lignin derivative phenanthrene in non-infected Permian wood (top) and Permian fungal infected wood (bottom). m/z value=178.

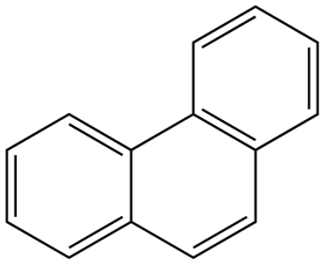

phenanthrene

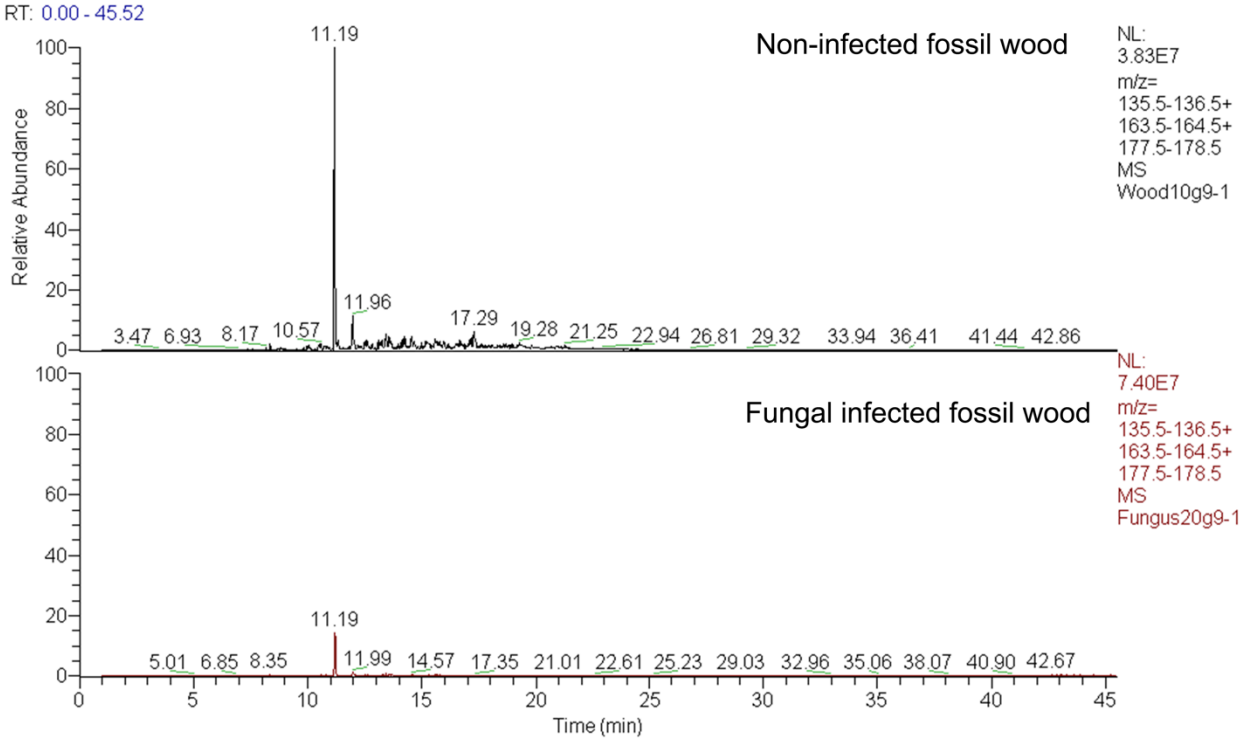

Figure 11. Biomarker results 2 – phenanthrene.

Figure 12. Biomarker results 3 – *n*-alkanes. Results of *n*-alkanes in non-infected Permian wood (top) and Permian fungal infected wood (bottom). m/z value=85.

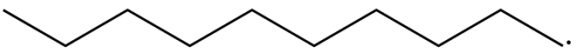

n-alkanes

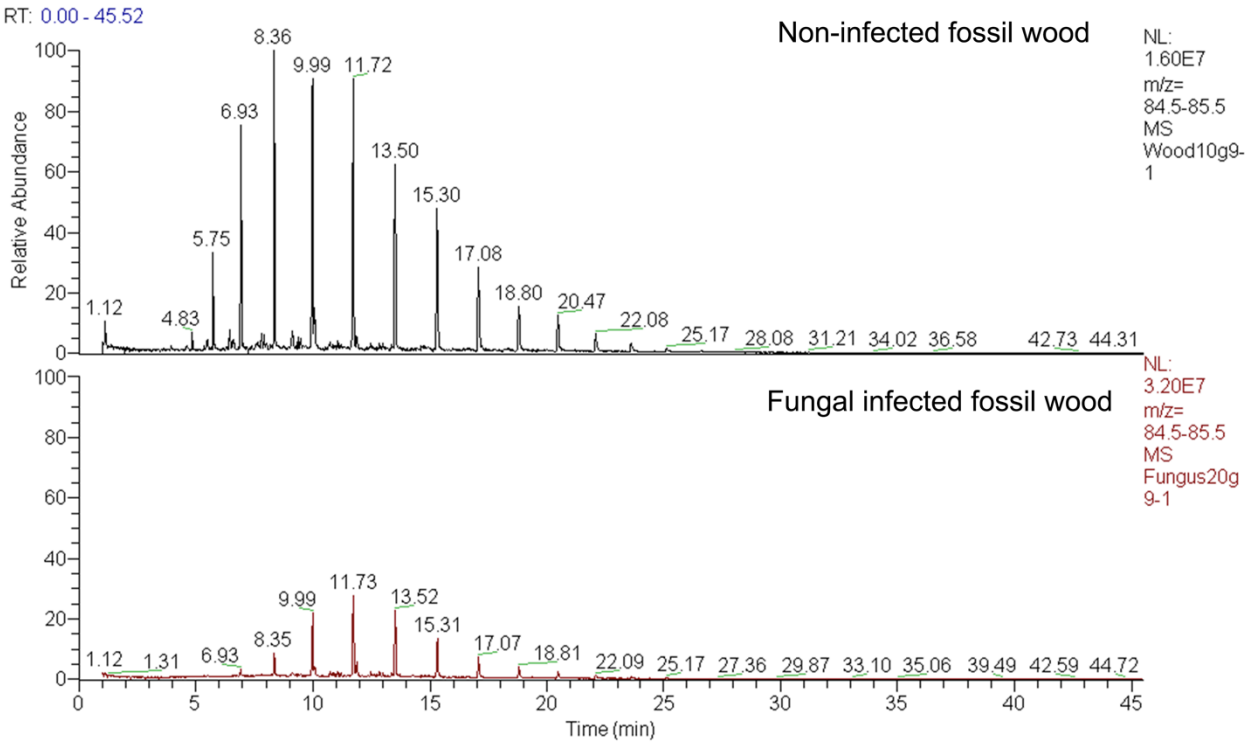

Figure 12. Biomarker results 3 – *n*-alkanes.

Figure 13. Biomarker results 4 – perylene. Results of perylene (suggested fungal biomarker) in non-infected Permian wood (top) and Permian fungal infected wood (bottom). m/z values=126 252. Results indicate absence of perylene in non-infected fossil wood and fungal infected woods.

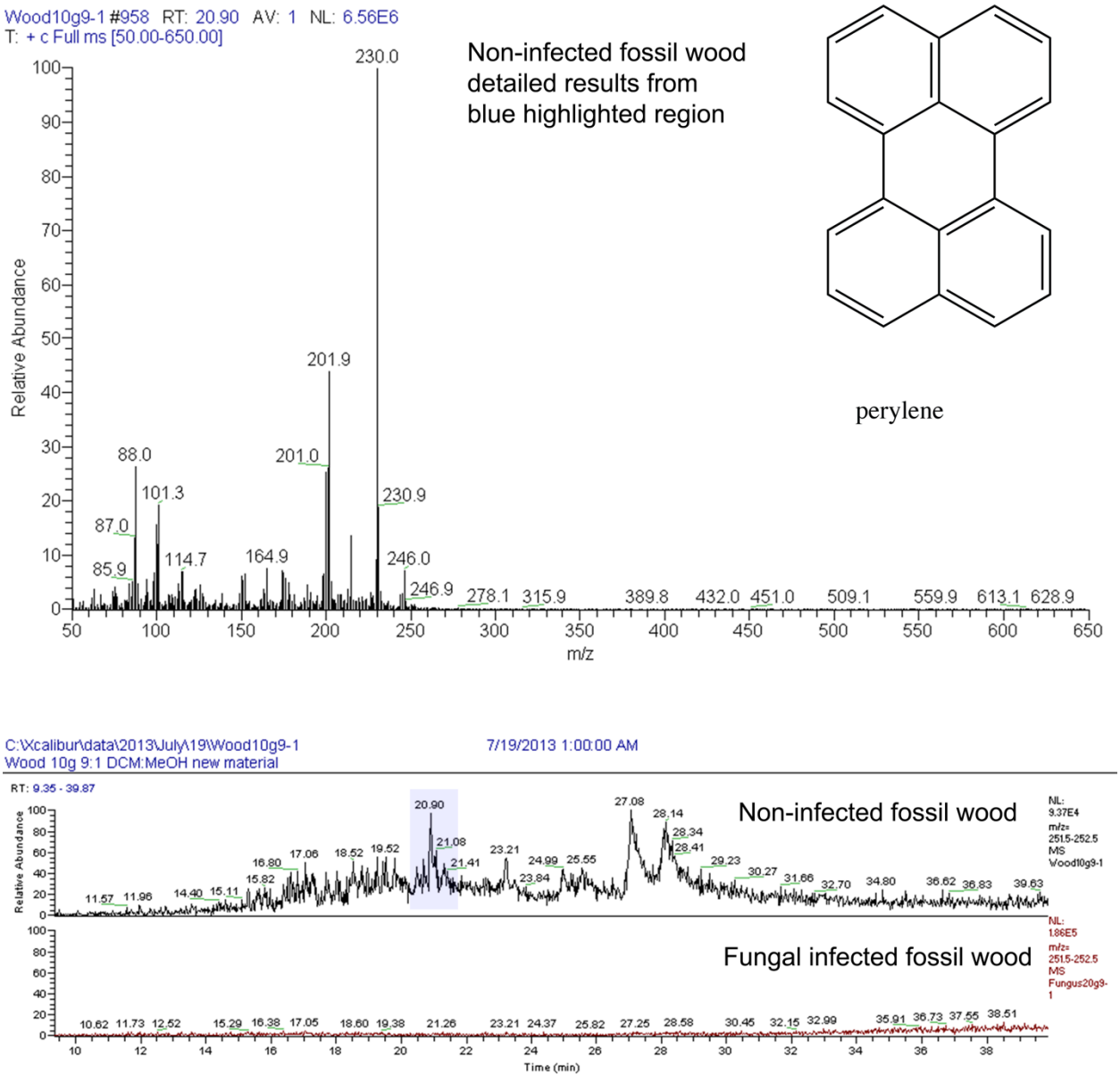

Figure 13. Biomarker results 4 – perylene.

Chapter 7. Plate 14. Overview of Jurassic wood, fungi, and tyloses

Plate 14, Figure 163. Overview of specimen with secondary xylem and phloem cells. Scale bar = 500 μm. AP-GIX-SB-007-CT2-01.

Plate 14, Figure 164. Transverse section of secondary xylem in thin section. Due to the relatively poor preservation of the wood, note the difficulty of distinguishing tracheids from rays. Scale bar = 100 μm. TS-GIX-SB-036-02.

Plate 14, Figure 165. Tangential section of secondary xylem; note narrow rays. Scale bar = 200 μm. TS-GIX-SB-036-01.

Plate 14, Figure 166. Transverse section of preserved phloem in thin section, showing large cells (#) and small cells (*). Note the hypha crossing one of the small cells and the thick, coiled contents of the larger cells. Scale bar = 25 μm. TS-GIX-SB-007-01.

Plate 14, Figure 167. Radial section of a tracheid with uniseriate circular-bordered pits. Scale bar = 25 μm. TS-GIX-SB-036-01.

Plate 14, Figure 168. Wood in transverse section showing degraded S_1–S_2 layers of the tracheid cell walls. Scale bar = 25 μm. TS-GIX-SB-036-02.

Plate 14, Figure 169. Transverse section of wood showing crushed vascular ray (dark line in center), with tyloses in adjacent tracheids. Scale bar = 25 μm. TS-GIX-SB-036-01.

Plate 14, Figure 170. Longitudinal section of wood with vascular ray (R) and tyloses in adjacent tracheids. Scale bar = 25 μm. TS-GIX-SB-036-01.

Plate 14, Figure 171. Tangential section of tracheids showing a large tylosis (center) ballooning through a cross-field pit into an adjacent tracheid. Scale bar = 25 μm. TS-GIX-SB-036-01.

Plate 14, Figure 172. Initial stage of tylosis development. Tyloses at this stage are small, bulbous protrusions with no discernable base. Scale bar = 10 µm. TS-GIX-SB-036-01.

Plate 14, Figure 173. Intermediate stage of tylosis development. Tyloses are morphologically similar to initial stage but are large and have a more distinguishable base. Scale bar = 10 µm. TS-GIX-SB-036-01.

Plate 14, Figure 174. Final stage of tylosis development. Fully developed tyloses are large bulbous structures that occlude the lumen of the tracheid and have a characteristic narrow base. Scale bar = 10 µm. TS-GIX-SB-036-01.

Plate 14, Figure 175. Tylosis with dark, filled lumen. Scale bar=25 µm. TS-GIX-SB-036-01.

Plate 14, Figure 176. Fungal hypha with a right-angled septa. Scale bar = 25 µm. TS-GIX-SB-036-01.

Plate 14, Figure 177. Longitudinal section of a tracheid with a hypha extending through its lumen (arrows). Scale bar = 25 µm. TS-GIX-SB-036-01.

Plate 14, Figure 178. High degree of hyphal knotting inside a single tylosis. Wall of tylosis indicated by arrows. Scale bar = 10 µm. Note this is a composite image. TS-GIX-SB-036-01.

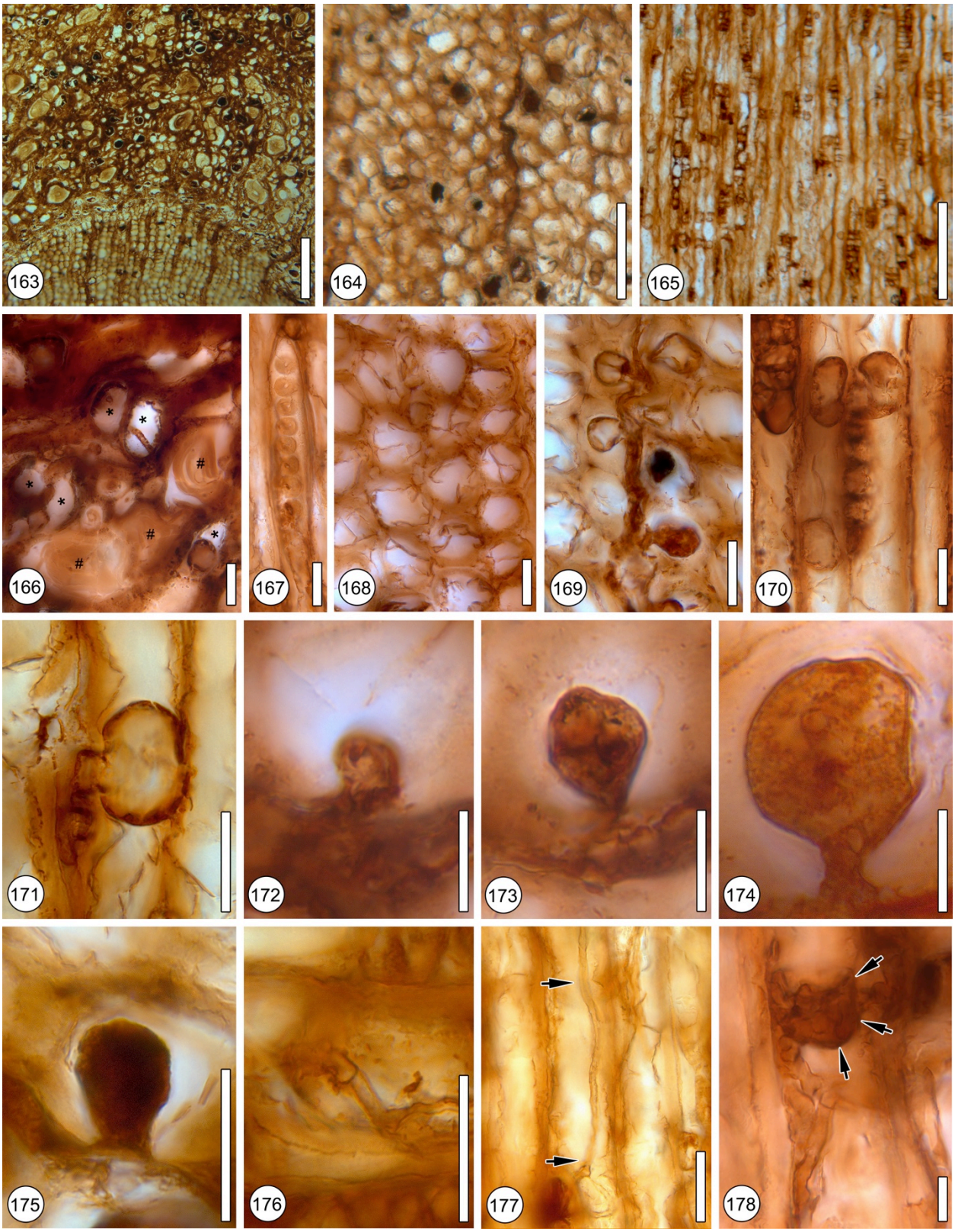

Chapter 7. Plate 14. Overview of Jurassic wood, fungi, and tyloses.

Chapter 7. Plate 15. Tylosis-fungal interaction, fungi in phloem

Plate 15, Figure 179. Knotting hyphae inside of tylosis in transverse section. Scale bar = 10 μm. TS-GIX-SB-036-02.

Plate 15, Figure 180. Hyphal (arrows) penetration of tylosis wall. Scale bar = 10 μm. TS-GIX-SB-036-01.

Plate 15, Figure 181. Y-branching hypha inside of tylosis. Wall of tylosis indicated by arrows. Scale bar = 10 μm. TS-GIX-SB-036-02.

Plate 15, Figure 182. Hypha inside lumen of smaller phloem cells. Scale bar = 25 μm. TS-GIX-SB-007-01.

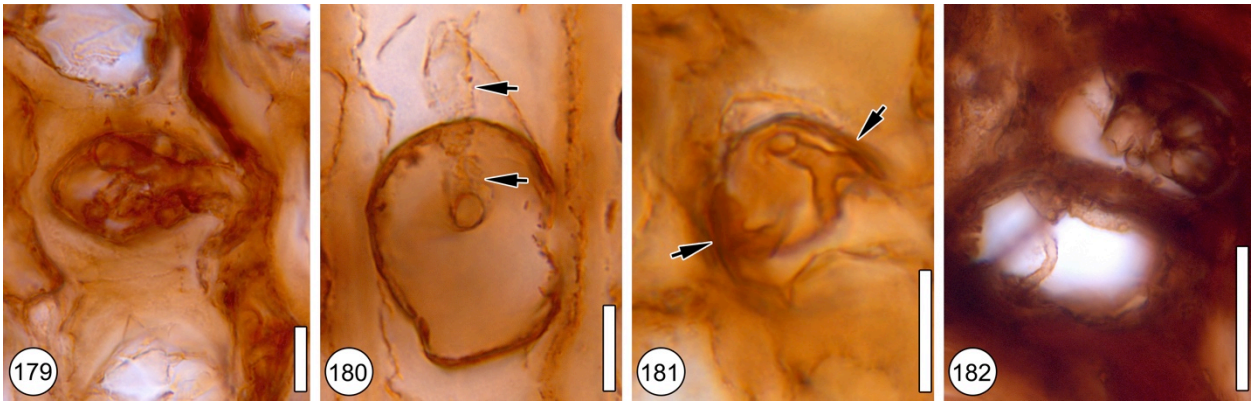

Chapter 7. Plate 15. Tylosis-fungal interaction, fungi in phloem.

Figure 14. Diagrammatic representation of the relationship between tylosis formation and fungal distribution in a three-dimensional block diagram of the wood presented in this study. (**A)**: Hyphal distribution and pattern traversing the vascular ray system. Dashed lines represent the vascular ray. (**B)**: Tyloses are often found in pairs on opposite sides of the vascular ray. (**C)**: The lumen of the tyloses can contain highly coiled hyphae. The hyphae can exit and enter through the tylosis wall, including in opposite directions. (**D)**: Hyphae that contain a high degree of dichotomies, which give the appearance of knotting structures. The knotting is often in close proximity to the tylosis, immediately outside of the tylosis wall. We hypothesize that this high degree of knotting increases the surface area of the fungus and the suberin-degrading enzymes can be concentrated and localized to the specific area. (**E)**: Highly dichotomized or knotting hyphae can also form loops adjacent to tylosis; again, we hypothesize that this can also contribute to localization of degradational enzymes. **(F)**: Hyphae travel through the ray system and enter tyloses through cross-field pits. **(G)**: Many tyloses are filled with dark material. It has been suggested that fully developed, mature tyloses contain this amorphous, likely suberized material (Chrysler, 1908).

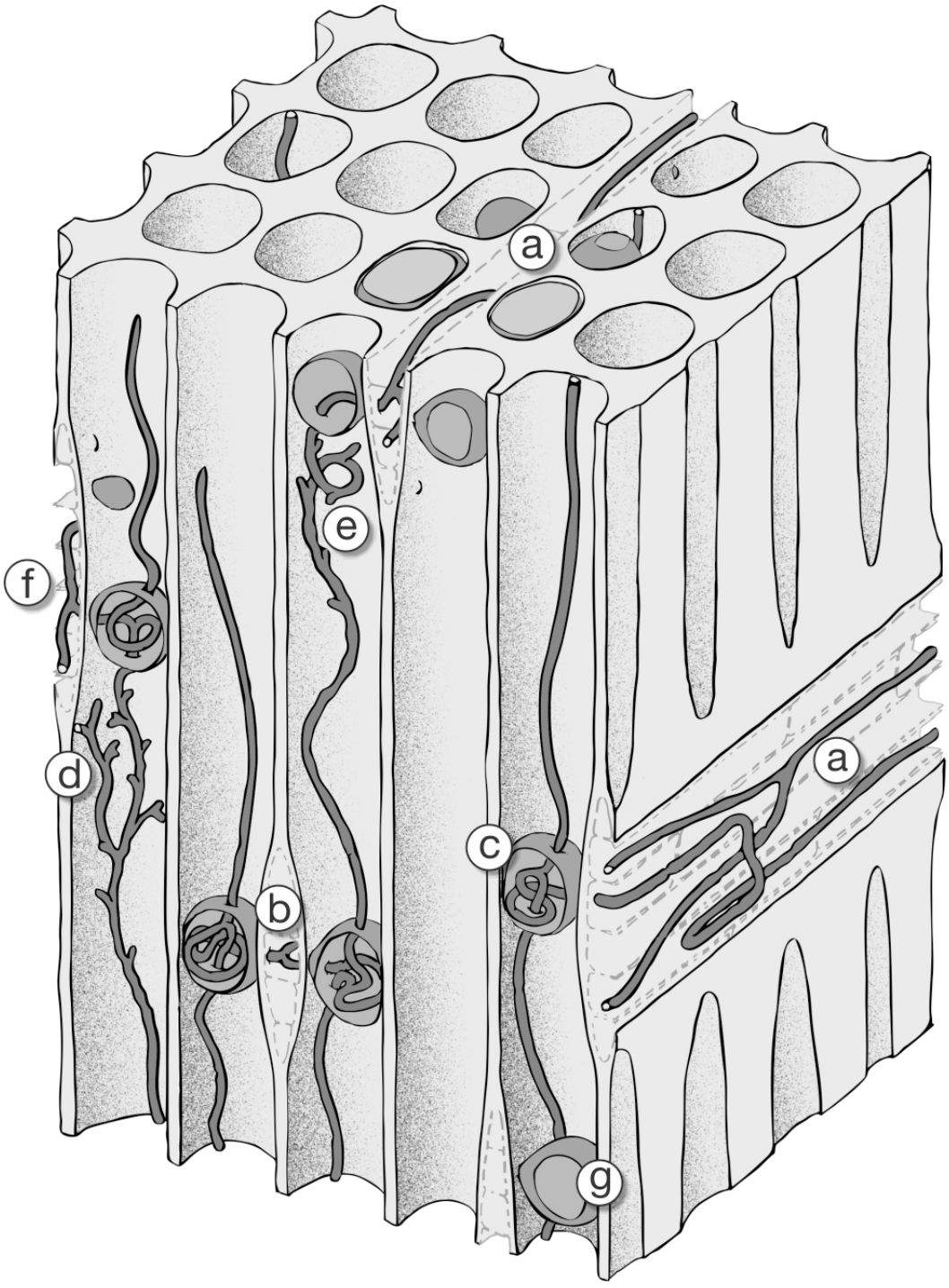

Figure 14. Diagrammatic representation of the relationship between tylosis formation and fungal distribution in a three-dimensional block diagram of the wood presented in this study.

Chapter 8. Plate 16. Fungal remains in *Glossopteris* leaves.

Plate 16, Figure 183. Leaf mat composed of highly degraded leaves (L) with discernable ends in brackets. Note that typically only parallel pattern of vascular bundles with degraded tissues surrounding them remains. Scale bar=250 μm.

Plate 16, Figure 184. Vascular bundle of *Glossopteris* with well-preserved xylem cells (X) and single septate hypha ramifying through cell. Scale bar=25 μm.

Plate 16, Figure 185. Vascular bundle of *Glossopteris* with well-preserved xylem cells and individual spherical structures occluding xylem cells (arrows). Scale bar=25 μm.

Plate 16, Figure 186. Poorly preserved mesophyll with single chytrid-like structure (arrow) within lumen of degraded cell. Scale bar=25 μm.

Plate 16, Figure 187. Degraded mesophyll with single chytrid-like structure with minute hyphal attachment (arrow). Scale bar=10 μm.

Plate 16, Figure 188. Poorly preserved mesophyll with single chytrid-like structure (arrow) below adaxial surface. Scale bar=10 μm.

Plate 16, Figure 189. Degraded mesophyll with single cross section of hyphae on surface of leaf (arrow). Scale bar=10 μm.

Plate 16, Figure 190. *Glossopteris* leaf with adaxial (Ad) and abaxial (Ab) surfaces with hyphal mycelia (arrows) ramifying mesophyll and adaxial surface. Scale bar=50 μm.

Plate 16, Figure 191. Branched hypha within mesophyll of leaf (arrow). Scale bar=25 μm.

Plate 16, Figure 192. Branched hypha with septa (arrows) within mesophyll of leaf. Scale bar=25 μm.

Plate 16, Figure 193. Individual *Glossopteris* leaf (L) with clusters of spores within mesophyll (arrow). Scale bar=250 μm.

Plate 16, Figure 194. Detail of clusters of spores (S) within mesophyll with interwoven mess of hyphae (arrow). Scale bar=25 μm.

Plate 16, Figure 195. Second example of detail of clusters of spores (S) within mesophyll with interwoven mess of hyphae (arrow). Spores in this specimen contain internal contents. Scale bar=25 μm.

Plate 16, Figure 196. Large hyphal aggregation (HA) in between *Glossopteris* leaves (L). Scale bar=100 μm.

Plate 16, Figure 197. Detail of large hyphal aggregation in between *Glossopteris* leaves. Scale bar=25 μm.

Plate 16, Figure 198. Detail of individual filament with septa (arrow) of large hyphal aggregation in between *Glossopteris* leaves. Scale bar=10 μm.

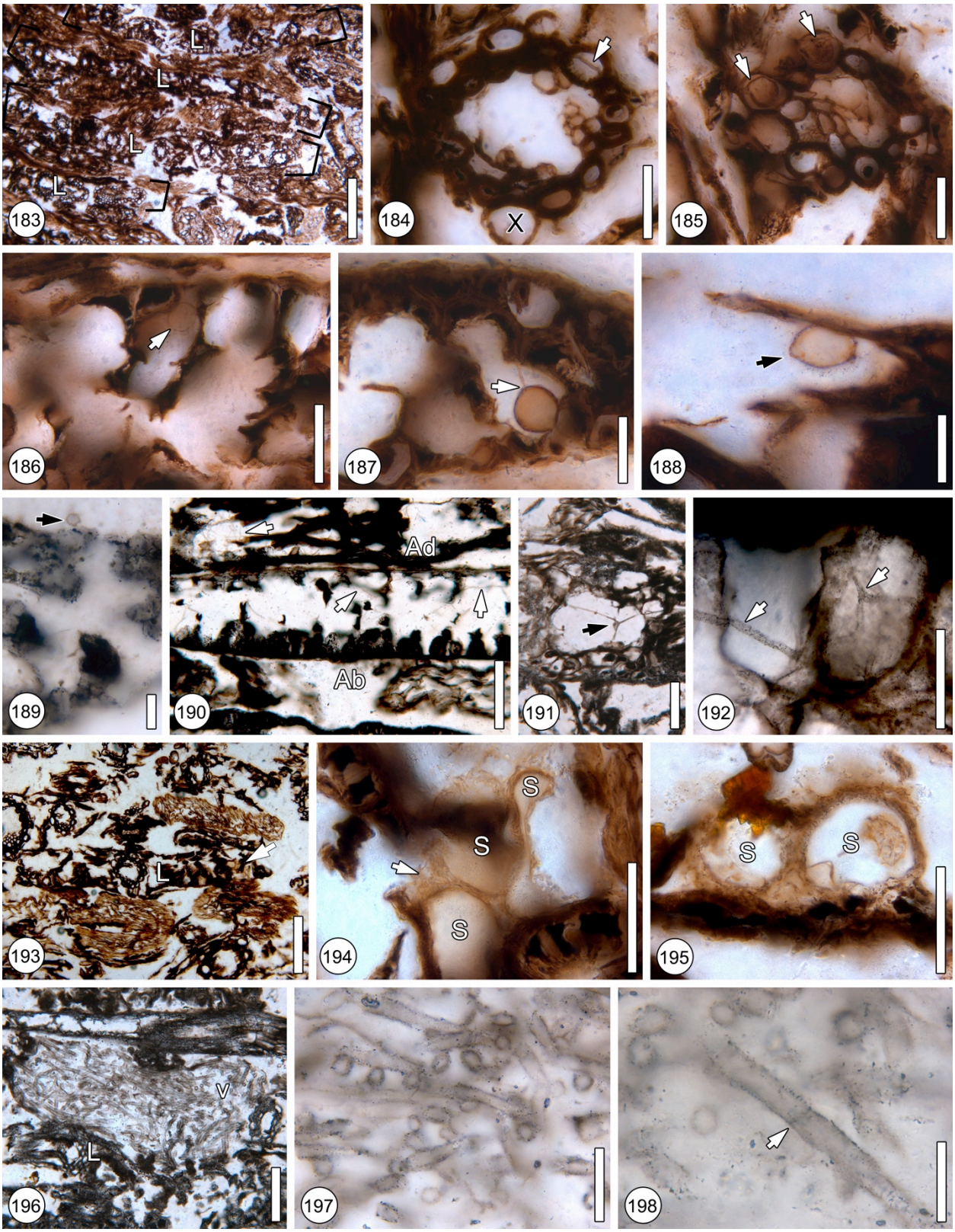

Chapter 8, Plate 16. Fungal remains in *Glossopteris* leaves.

Chapter 8, Plate 17. Fungal and fungal-like remains in *Glossopteris* leaf mats.

Plate 17, Figure 199. Spore type 1 is 40 µm in diameter and shows no discernable spore wall features (white arrow), but contains 3 partially preserved internal each spores (black arrow) approximately 10 µm in diameter. Scale bar=25 µm.

Plate 17, Figure 200. Spore type 2 is 50 µm in diameter with a spore wall of 3 µm in diameter with hyphal attachment (white arrow) that is 5 µm in diameter with internal spores (black arrow) that are 6 to 10 µm in diameter. Scale bar=25 µm.

Plate 17, Figure 201. Spore type 3 is similar to spore type 2 but lacks internal contents, is 45 µm in diameter with a 2 µm diameter spore wall and hyphal attachment (white arrow) of 5 µm in diameter, but this spore type is found within the root tissue of *Vertebraria.* Scale bar=25 mm.

Plate 17, Figure 202. Spore type 4 is slightly pyriform and is approximately 35 µm at the widest point with a 4-5 µm thickness to the cell wall, at the narrow end of the spore may represent a hyphal attachment (white arrow). Scale bar=25 µm.

Plate 17, Figure 203. Spore type 5 approximately 80 µm in diameter has a wall a 6-8 µm thick with small spherical structures in the lumen that may represent a form of mycoparasitism (black arrow). Scale bar=25 µm.

Plate 17, Figure 204. Spore type 6 (S) occurs throughout the peat that range from 15-25 µm in diameter and can occur within tissues or in the matrix, and at varying focal planes some surface ornamentation can be distinguished. Scale bar=25 µm.

Plate 17, Figure 205. Spore type 7 is a double walled (black and white arrows) spore approximately 40 µm in diameter with a 5-7 µm cell wall. Scale bar=25 µm.

Plate 17, Figure 206. is a double walled spore with a blunt attachment (arrow) point approximately 50 µm in diameter and a cell wall of 8 µm thick. Scale bar=25 µm.

Plate 17, Figure 207. Peronosporomycete type 1 is pyriform to subglobose oogonia with spiny or occasionally truncated papillations arranged regularly across the surface approximately 50 µm in diameter; papillations bear 2–3 antler-like extensions (arrow) which dichotomize once or more near their tips. Scale bar=25 µm.

Plate 17, Figure 208. Peronosporomycete type 2 is ellipsoidal to pyriform (40-60 µm in diameter) with blunt papillations with a consistent geometric surface ornament pattern (arrow) and antlers are poorly preserved or absent. Scale bar=25 µm.

Plate 17, Figure 209. Peronosporomycete type 3 is ellipsoidal to pyriform (40-60 µm in diameter) with blunt papillations with a consistent blunt projection surface ornament pattern (arrow) and antlers are poorly preserved or absent. Scale bar=25 µm.

Plate 17, Figure 209. Peronosporomycete type 4 is ellipsoidal to pyriform (40-60 µm in diameter) with blunt papillations (arrow). Scale bar=25 µm.

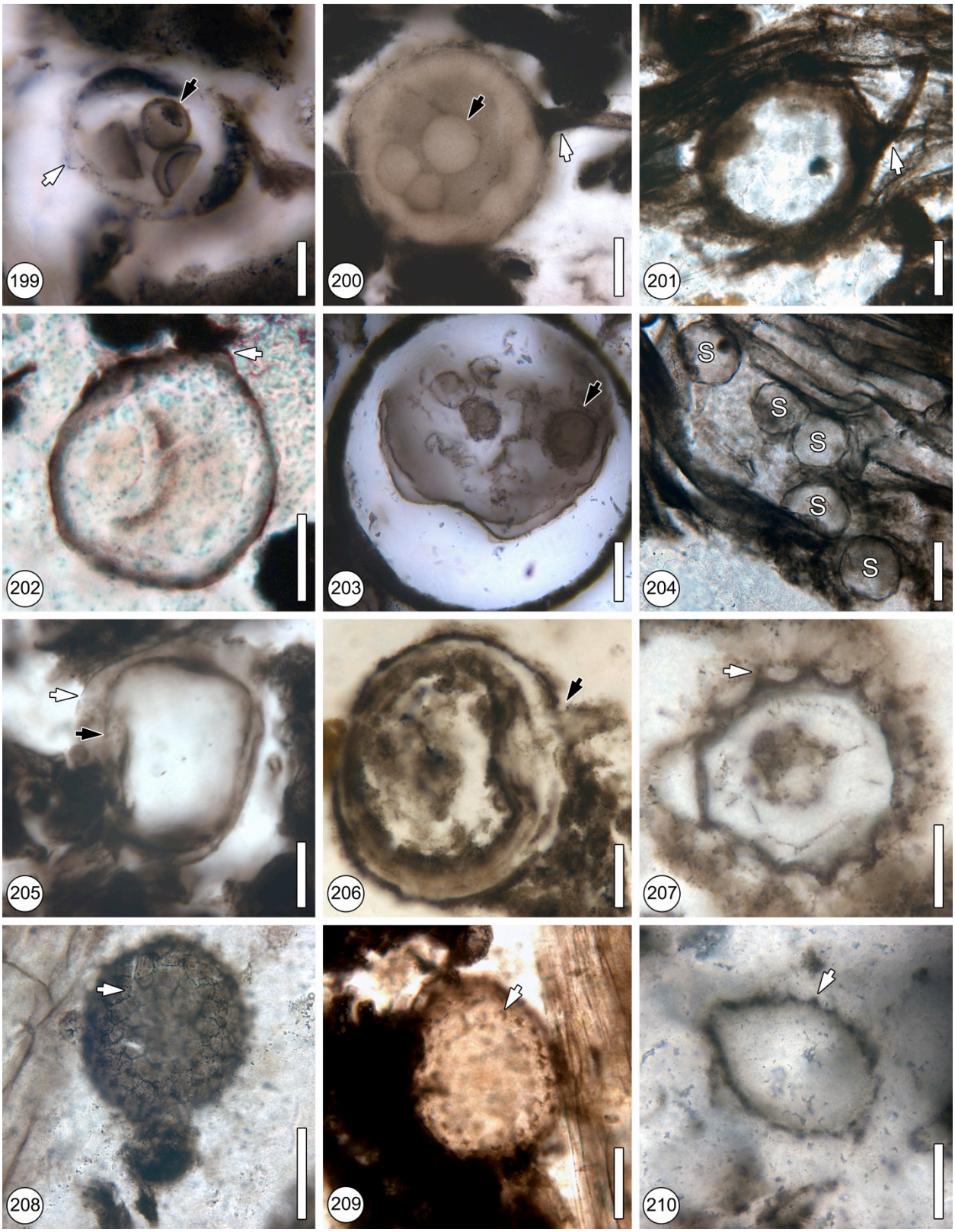

Chapter 8, Plate 17. Fungal and fungal-like remains in *Glossopteris* leaf mats.

Chapter 9. Plate 18. *Endochaetophora*-leaf litter plant associations

Plate 18, Figure 211. Isolated single *Endochaetophora* sporocarp (arrow) on epidermis of highly degraded plant axis. Scale bar=250 µm. Specimen 18084 F2 top.

Plate 18, Figure 212. Single sporocarp embedded in gleba (white matrix encasing sporocarp; arrow) in peat matrix adjacent to longitudinal section of plant cells. Scale bar=250 µm. Specimen 17779 E bot.

Plate 18, Figure 213. Transverse section of two degraded *Dicroidium* leaves (L) with two single cell wall layer sporocarps (S) within a gleba (G). Note point of possible attachment of sporocarp wall (right arrow). Isolated globose structure within white matrix adjacent to leaf, may represent an ontogenetically younger *Endochaetophora* spore (left arrow). Scale bar=250 µm. Specimen 17683 D bot.

Plate 18, Figure 214. Two sporocarps with prominent hyphal appendages extending (arrow) from cell wall within gleba. Scale bar=250 µm. Specimen 18026 F top.

Plate 18, Figure 215. Detail of gleba matrix. Note composition of hyphae, which are in multiple planes of section. Scale bar=100 µm. Specimen 18021 C top.

Plate 18, Figure 216. Gleba containing six single cell wall layered sporocarps of similar diameter surrounding an axis in oblique section. Sporocarp with internal contents (white arrow) and hyphal contents of gleba are discernable (black arrow). Scale bar=250 µm. Specimen 18026 C top.

Plate 18, Figure 217. Gleba containing six sporocarps of varying diameters, all with a single cell wall layer. Note prominent short hyphal appendages in cell wall (white arrows). One

sporocarp is at a different developmental stage than the rest, indicated by multiple cell wall layers (black arrow). Scale bar=250 µm. Specimen 18026 B bot.

Plate 18, Figure 218. Gleba containing complete and partially degraded sporocarps (arrows) surrounding transverse section of plant axis. Note well defined hyphae within gleba. Scale bar=250 µm. Specimen 18026 B bot.

Plate 18, Figure 219. Transverse section of *Dicroidium* with gleba completely surrounding the abaxial and adaxial surfaces; midvein (VB). Note varying diameters of sporocarps as well as incomplete sporocarps (arrows). Example of gleba with indiscernible hyphal mycelia composition. Scale bar=1 mm. Specimen 18026 A.

Plate 18, Figure 220. Degraded leaf in transverse section with gleba attached to single surface. Sporocarps contain contents (arrows) and development of multiple cell wall layers. Scale bars=1 mm. 17683 H bot.

Plate 18, Figure 221. Gleba containing *Endochaetophora* sporocarps surrounding two axes (A) Some sporocarps contain contents. Scale bars=1 mm. Specimen 17683 C top.

Plate 18, Figure 222. Large gleba in between matrix of degraded plant material and leaves (L). Within the gleba are multiple plant axes (A), including one that is completely degraded. Sporocarps are in various stages of development and have varying diameters. Some sporocarps contain contents (arrows) and some are incomplete. Scale bar=1 mm. Specimen 18026 C bot.

Plate 18, Figure 223. Multiple sporocarps surrounding a degraded plant axis (A). This gleba is in a matrix composed of highly degraded plant material, including leaves (VB). The vast majority of the sporocarps have multiple cell wall layers and lack contents. Additionally, the hyphae are difficult to distinguish. Scale bar=1 mm. Specimen 18026 D bot.

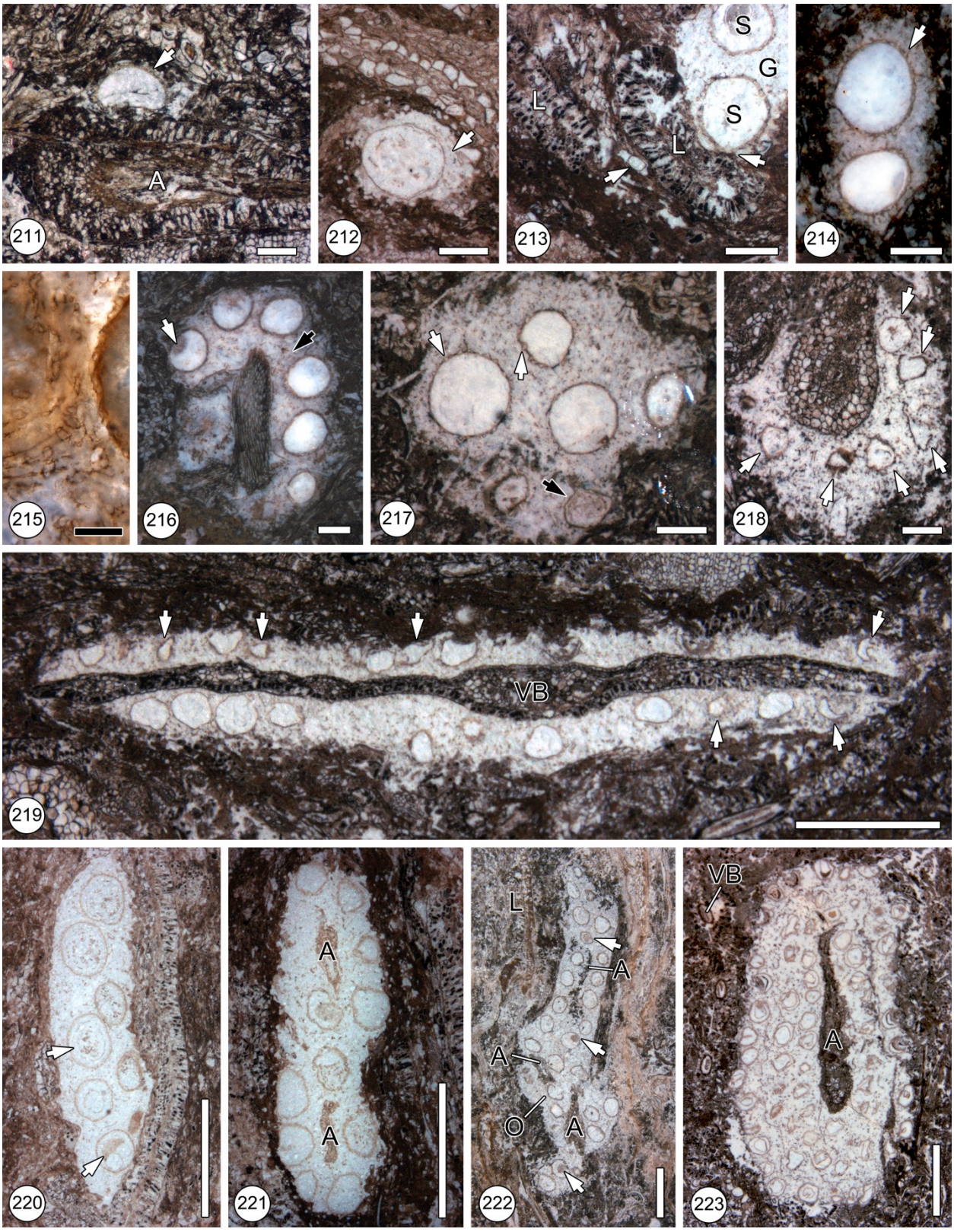

Chapter 9. Plate 18. *Endochaetophora*-leaf litter plant associations

Chapter 9. Plate 19. Tripartite cell wall *Endochaetophora*-leaf litter plant associations

Plate 19, Figure 224. Isolated, tripartite wall with no appendages, and no internal contents in the soil matrix. Scale bar=1 mm. Specimen 18026 D bot.

Plate 19, Figure 225. Isolated, tripartite wall sporocarp with no appendages in the soil matrix. Note internal contents. Scale bar=1 mm. Specimen 18026 D top.

Plate 19, Figure 226. Sporocarp with thick, tripartite wall and ostiole (arrow). Scale bar=250 µm. Specimen 18026 E top.

Plate 19, Figure 227. Sporocarp with thick, tripartite wall and visible ostiole (arrow) with prominent hyphal appendages that emerge from the sporocarp wall. Scale bar=250 µm. Specimen 17729 E bot.

Plate 19, Figure 228. Gleba containing sporocarps in multiple developmental stages and multiple planes of view. Sporocarps with thick, tripartite cell walls (TW), and thin, single cell thickness of sporocarp wall (SW), as well as a tangential, surface view of a single sporocarp (arrow). Scale bar=1 mm. Specimen 18026 C top.

Plate 19, Figure 229. Gleba containing thick walled, tripartite cell wall sporocarps. Two that are partially broken (arrows). Scale bar=500 µm. Specimen 11891 B1 base.

Plate 19, Figure 230. Gleba composed of thick, tripartite walled sporocarps (all lacking lumen contents) with hyphal appendages surrounding an axis (A). Note hyphae cannot be distinguished within gleba. Scale bar=1 mm. Specimen 18026D bot.

Plate 19, Figure 231. Multiple thick walled sporocarps at different planes of view within a gleba surrounding a partially degraded plant axis (A). *Endochaetophora* sporocarps with varying thicknesses of cell wall diameters, which may represent different ontogenetic stages of cell wall development. Isolated spherical structure that could possibly be a

developmentally immature sporocarp (arrow). Scale bar=1 mm. Specimen 18026 E top.

Plate 19, Figure 232. Detail of white matrix gleba (from Plate 19, Figure 231) showing highly degraded thick walled (arrows) and single walled sporocarps. Black areas represent highly degraded sections of hyphae. Scale bar=1 mm. Specimen 18026 D bot.

Plate 19, Figure 233. Multiple planes of section of sporocarps within single gleba. Including oblique sections (Ob), tangential section (T), radial section (R), longitudinal section (L), and a longitudinal section with contents (C). Scale bar=1 mm. Specimen 11521 D bot.

Plate 19, Figure 234. Detail of tripartite cell wall of sporocarp. Cell wall layers labeled: inner wall (I), middle wall (M), outer wall (O), sporocarp lumen (L). Opaque striations within the middle, acellular layer of the sporocarp cell wall (arrows). Scale bar=10 µm. Specimen 18026 D bot 2.

Plate 19, Figure 235. Hyphal appendages (arrows) extending from the inner wall (I), through the middle wall (M), and outside of the outer cell wall (O). Sporocarp lumen (L), and gleba matrix (G). Scale bar=25 µm. Specimen 11521 C bot 1.

Plate 19, Figure 236. Detail showing the origin of a hyphal appendage (arrows) from inner sporocarp wall (I). Acellular, middle wall layer (M). Scale bar=10 µm. Specimen 17729 E Bot.

Plate 19, Figure 237. Aggregation of woven hyphal mycelium (black arrows) outside of a sporocarp that lacks a middle wall layer. Detail of base of hyphal appendage (white arrows). Scale bar=25 µm. Specimen 18021 C top.

Plate 19, Figure 238. Detail of small branch (arrow) of hyphal appendage that is used as an additional interlocking and weaving mechanism. Scale bar=10 µm. Specimen 17729 E bot.

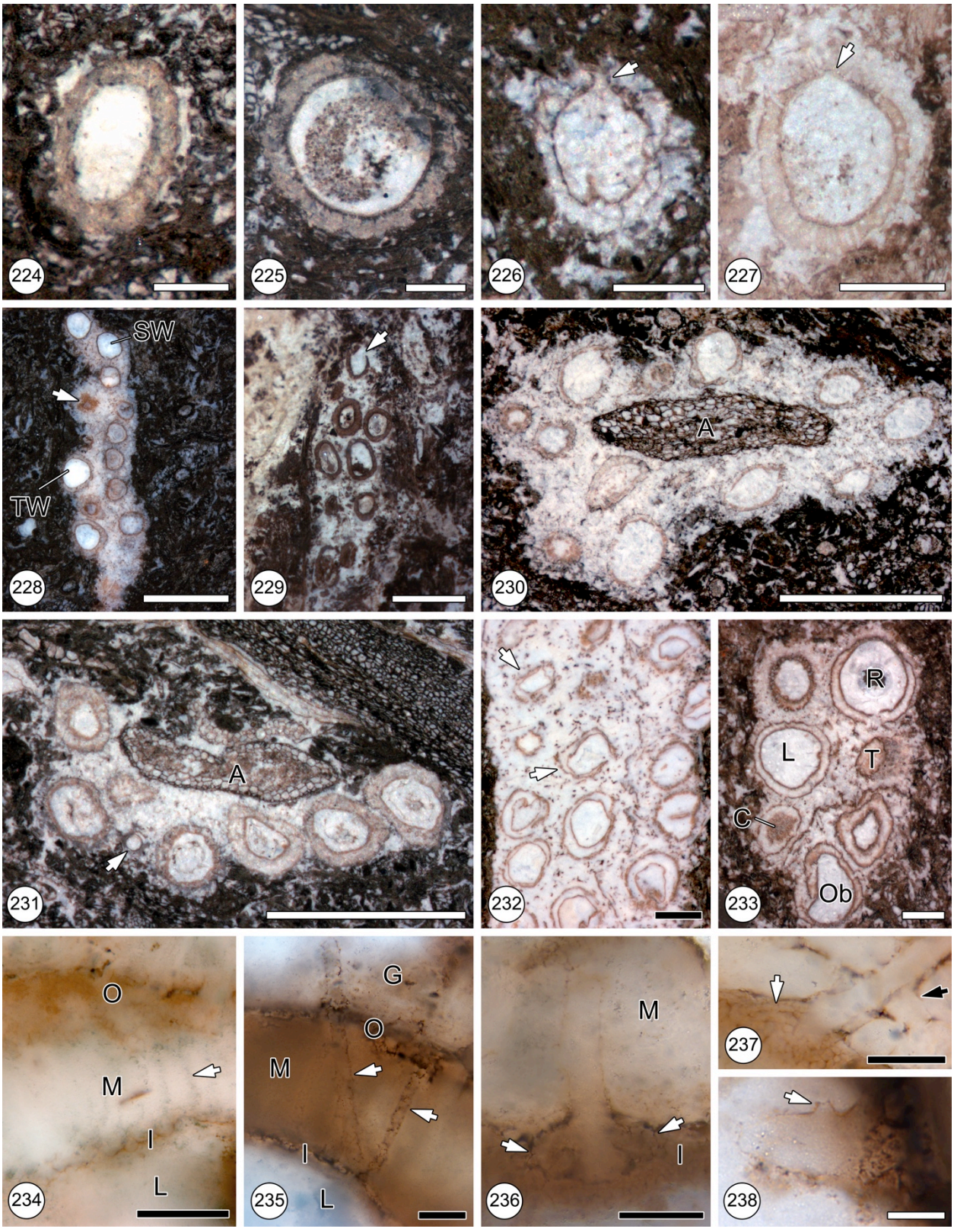

Chapter 9. Plate 19. Tripartite cell wall *Endochaetophora*-leaf litter plant associations

Chapter 9. Plate 20. Detail of *Endochaetophora* appendage development, spores, ostiole detail

Plate 20, Figure 239. Detail of single cell wall sporocarp. Developing hyphal appendages (arrows) from inner cell wall (I). Sporocarp lumen (L); gleba matrix (G). Scale bar=25 µm. Specimen 17729 E bot.

Plate 20, Figure 240. Multiple planes of sporocarps within a gleba, longitudinal section (L), tangential section (T) showing woven mesh of hyphal appendages, distal tangential section (D) indicating the cross sections of the hyphal appendages, hyphal mesh that comprises the gleba (G). Scale bar=100 µm. Specimen 17729 F top.

Plate 20, Figure 241. Detail of hyphal appendage in transverse section (arrows) on tangential section of sporocarp wall. White area is upper focal limit of sporocarp. Scale bar=25 µm. Specimen 17729 E top.

Plate 20, Figure 242. Cellular detail of area in between hyphal appendages. Location of base of hyphal appendage (arrows). Scale bar=25 µm. Specimen 18021 C top.

Plate 20, Figure 243. Sporocarps containing contents that appear to be at different ontogenetic stage of spore development. Contents occupy entire lumen (1), contents separated by membrane (2), sporocarp with contents with developed spores (3), and sporocarp with disarticulated, amorphous contents (4). Scale bar=500 µm. Specimen 17729 E bot.

Plate 20, Figure 244. Single sporocarp with amorphous, undifferentiated material. Scale bar=100 µm. Specimen 17729 F top.

Plate 20, Figure 245. Higher magnification of Plate 20, Figure 244 of amorphous, undifferentiated material within the sporocarp. Scale bar=25 µm. Specimen 17729 F top 1.

Plate 20, Figure 246. Sporocarp with well-defined internal spores, or possibly mycoparasites.

Scale bar=100 µm. Specimen 17729 F top.

Plate 20, Figure 247. Detail of spores in Plate 20, Figure 246. Note dark central contents, pattern on surface of spores that matches outer wall of parental sporocarp, and hyphal attachment point (arrows). Scale bar=25 µm. Specimen 17729 F top.

Plate 20, Figure 248. Spores with detail of spore wall with matching parental ornamentation (arrow). As well as spore lumen contents, similar to the parental sporocarp. Scale bar=10 µm. Specimen 17729 E bot.

Plate 20, Figure 249. Isolated spores within gleba. Surface ornamentation is more defined and possibly similar to parental sporocarp, and may represent the spores after being released from sporocarp or prematurely released from parental unit. Scale bar=25 µm. Specimen 18026 D bot 4.

Plate 20, Figure 250. Sporocarp with undifferentiated, amorphous material (A), as well as with developed (D1) and developing spores (D2). Scale bar=100 µm. Specimen 18021 C top.

Plate 20, Figure 251. Higher magnification of Plate 20, Figure 250 sporocarp with undifferentiated, amorphous material (A), as well as with developed (D1) and developing spores (D2). Scale bar=25 µm. Specimen 18021 C top.

Plate 20, Figure 252. Longitudinal section through sporocarp with ostiole (O), ostiole collar (C), and ostiole membrane (M). Scale bar=100 µm. Specimen 17729 F top.

Plate 20, Figure 253. Ostiole collar in upper focal plane to emphasize conical shape (arrow). Scale bar=25 µm. Specimen 17729 F top.

Plate 20, Figure 254. Lower focal plane of Plate 20, Figure 253. Medial longitudinal section through ostiole (arrow) to show 45º angle of ostiole collar wall relative to sporocarp wall. Scale bar=25 µm. Specimen 17729 F top.

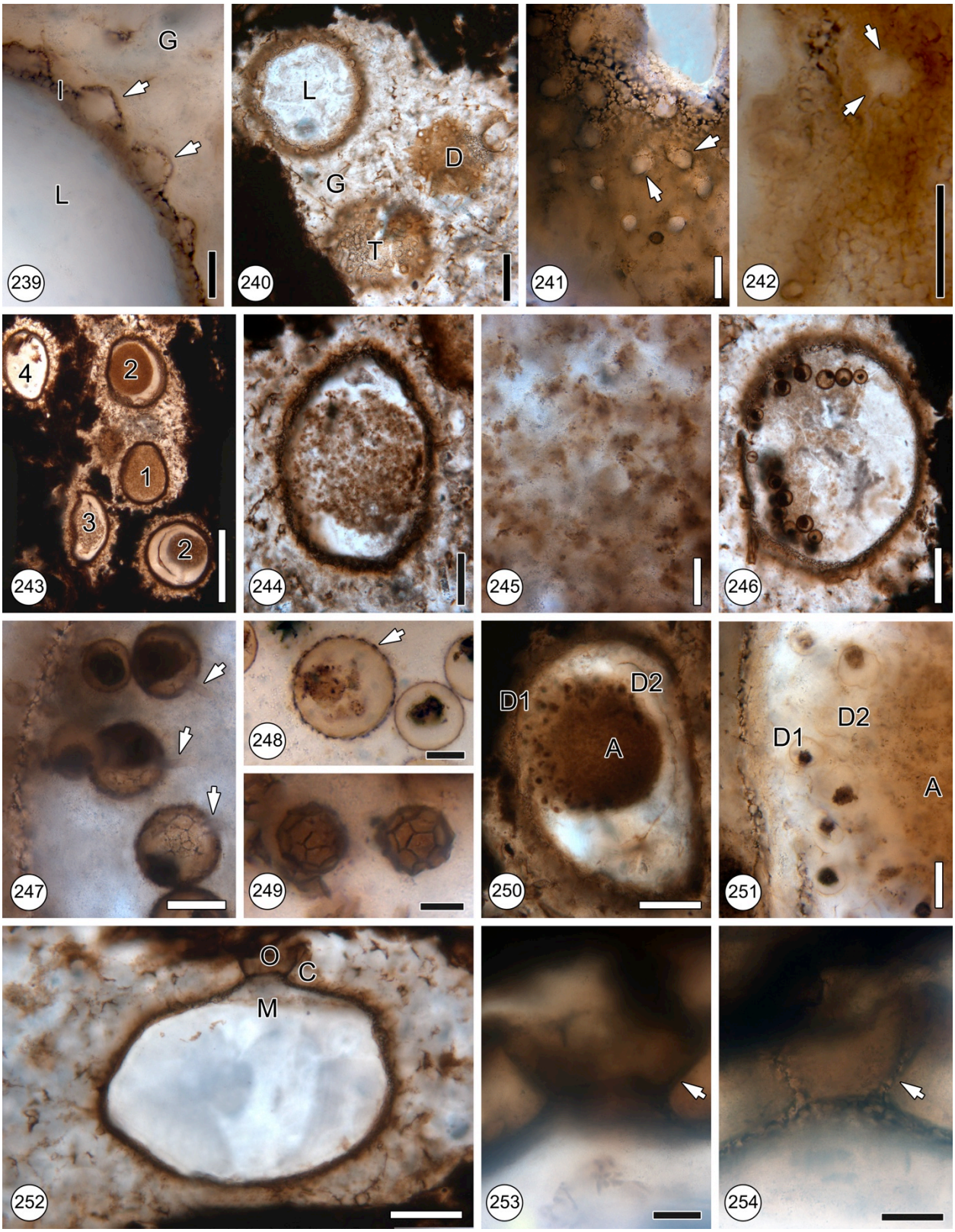

Chapter 9. Plate 20. Detail of *Endochaetophora* appendage development, spores, ostiole detail

Figure 15. Hypothesized *Endochaetophora* life cycle reconstruction.

White circles with letters denote fossil evidence is present; shaded in gray circles denote hypothesized portion of life cycle. **A.** Spores of *Endochaetophora* can either undergo sexual or asexual reproduction. **B.** Under sexual reproduction, spores will attach to the surface of either a leaf or axis within the leaf litter. **C.** After the spore attaches, mycelia are produced and the gleba forms around the leaf or axis. **D.** Based on the reproductive biology of modern zygomycetes, we hypothesize that the individual hyphal strands are either plus or minus type, and can exchange genetic material. **E.** Immature sporocarps are either borne on individual hyphae or formed within a network of mycelia. **F.** After the initial sporocarp develops, the cell walls, which characterize *Endochaetophora* develop: the initial cell wall, outer wall, and partially the acellular middle wall. **G.** The gleba forms around the leaf with the developing or immature sporocarps closest to the axis or leaf, and the more mature, fully developed sporocarps furthest or most distal from the axis. **H.** Within an individual mature sporocarp with fully developed inner and outer cell wall and appendages, spores will develop. **I.** Spores develop from an amorphous, undifferentiated material within the lumen of the sporocarp. **J.** After the spores are mature, a small portion (<45 μm) will depreciate and develop into an opening, or ostiole. **K.** Spores are released through the ostiole into the matrix. **L.** Under asexual conditions, spores will encyst and develop a thick cell wall, i.e., the inner, outer, and acellular middle layer. **M.** Appendages develop and are initiated from the inner cell wall and penetrate through cell wall layers, acting as a structural support. **N.** Spores develop within the lumen from amorphous, undifferentiated material. **O.** An ostiole develops similarly to the sexual cycle and spores are released back into the matrix.

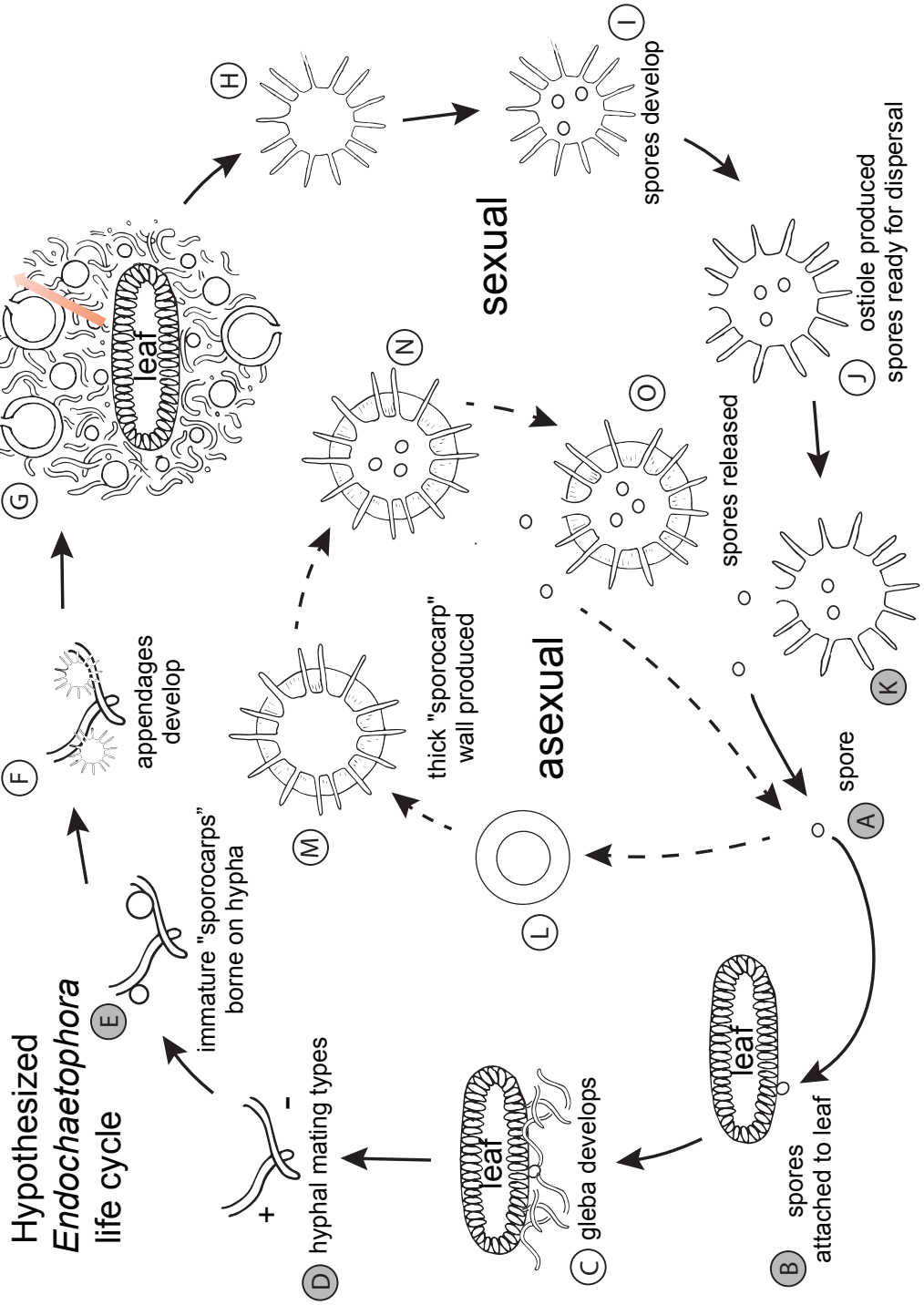

Figure 15. Hypothesized *Endochaetophora* life cycle reconstruction.

Appendix 1: Index of images, figures, and tables.